

A Supersymmetric Standard Model from a Local E_6 GUT

Dissertation
zur Erlangung des Doktorgrades
des Fachbereichs Physik
der Universität Hamburg

vorgelegt von

Felix Klaus Braam
aus Friedberg

Hamburg, 2011

Gutachter der Dissertation:	Dr. Jürgen Reuter Prof. Dr. Jan Louis
Gutachter der Disputation:	Dr. Jürgen Reuter Prof. Dr. Gudrid Moortgat-Pick
Datum der Disputation:	03. Februar 2012
Vorsitzender des Prüfungsausschusses:	Prof. Dr. Günter Sigl
Vorsitzender des Promotionsausschusses:	Prof. Dr. Peter Hauschildt
Dekan der MIN Fakultät:	Prof. Dr. Heinrich Graener

In physics, unlike mathematics, we are constantly pulled in opposite directions. At one pole, there is unification, simplicity and elegance – the Platonic ideal of nature that is created by and creates mathematics. At the other, there is the marvelous chaos of this particular world – messy, contingent, and constantly evolving with our experimental ability to probe its richness. Good physics must embrace these antipodes.

- *Howard Georgi*

Abstract

In this thesis we have investigated to what extent the exceptional Lie-group E_6 can serve as unified gauge group. In the presence of the full E_6 matter content, unification can be realized by increasing the degree of gauge symmetry above some intermediate scale. We found that a full E_6 gauge invariant theory is disfavored by phenomenological observations like proton stability and the smallness of flavor changing neutral currents. An appropriate framework to embed E_6 into a model for particle physics are higher dimensional orbifold constructions, where E_6 is the gauge group in the bulk and the intermediate symmetry group is the common subset of E_6 subgroups residing at the fixed-points of the orbifold. In this way the degree of symmetry in four space-time dimensions is reduced, such that the operators leading to the aforementioned disastrous phenomenological consequences can be forbidden independently.

In order to derive the implications of the model for the current experiments at the Large Hadron Collider (LHC), we developed an automated spectrum generator. It uses Monte-Carlo Markov-Chain techniques to cope with the high dimensionality of the space of input parameters and the complex interdependencies in the evolution of the Lagrangian parameters from the orbifold compactification scale to the TeV scale. For the spectra obtained with this program, we performed Monte-Carlo simulations of the production and decay of the Z' boson stemming from the additional $U(1)'$, using our own implementation of the model into the event generator WHIZARD.

Zusammenfassung

In der vorliegenden Arbeit haben wir untersucht, in welchem Grade die exzeptionelle Lie-Gruppe E_6 zur Beschreibung einer großen vereinheitlichten Theorie der Eichwechselwirkungen herangezogen werden kann. In Anwesenheit des vollständigen E_6 Materieinhalts an der TeV-Skala, kann die Vereinigung der Eichkopplungen durch Einführen einer zwischengelagerten Symmetriebrechung realisiert werden. Jedoch mussten wir feststellen, dass eine E_6 -invariante Theorie in der Regel phänomenologisch katastrophale Konsequenzen nach sich zieht, wie beispielsweise eine zu kurze Lebensdauer des Protons. Ein geeigneterer Rahmen ist durch eine Einbettung der E_6 Eichtheorie in eine höherdimensionale Raumzeit gegeben, die mit einer zusätzlichen Symmetry versehen ist ("Orbifold"). Die intermediäre Eichgruppe erhält man in diesem Kontext als Schnitt der Eichgruppen an den Fixpunkten der Orbifold. Auf diese Weise wird der Grad der Eichsymmetrie in vier Dimensionen hinreichend reduziert, um die Operatoren, die für die obengenannten Widersprüche verantwortlich waren, verbieten zu können.

Um Vorhersagen für das Experiment am "Large Hadron Collider" (LHC) herzuleiten, haben wir ein automatisiertes Computerprogramm namens EXSPECT geschrieben, das Teilchenspektren an der TeV-Skala aus an der Kompaktifizierungsskala der Extradimensionen gewählten Randbedingungen errechnet. Darin wird eine Monte Carlo Markov Kette verwendet, ein Algorithmus aus der Wahrscheinlichkeitstheorie, der es uns erlaubt, im hochdimensionalen Raum der freien Parametern Lösungen des komplexen Systems von Renormierungsgruppengleichungen zu finden. Für die auf diesem Wege gefundenen Spektren haben wir LHC-Observablen wie die Produktion und den Zerfall des schweren Z' Bosons, mit Hilfe von Monte Carlo Simulationen durch den Ereignisgenerator WHIZARD, berechnet.

Contents

1	Introduction	1
1.1	Supersymmetry	4
1.2	MSSM	9
1.2.1	Renormalization Group Evolution	10
1.3	NMSSM	12
1.4	E_6 Representations And Subalgebras	13
1.4.1	Subalgebras of E_6	14
1.4.2	The 27 dimensional representation of E_6	15
1.4.3	U(1) Quantum Numbers	16
1.4.4	Other Subalgebras of E_6	20
1.5	PSSSM	21
2	Local E_6 Unification with Intermediate Left-Right Symmetry	25
2.1	Gauge Coupling Unification	25
2.1.1	U(1) Mixing Below the Intermediate Scale	29
2.2	Superpotential	35
2.2.1	H -Parity and R -Parity	36
2.3	Embedding of the LR Symmetric Model into a Local E_6 GUT	37
2.3.1	Orbifold Action on E_6 Group Space	38
2.3.2	Intermediate LR symmetry from T^2/\mathbb{Z}_6 orbifold	42
2.3.3	Gauge Super-Multiplets on the T^2/\mathbb{Z}_n Orbifold	44
2.3.4	Bulk Matter and Anomalies	45
2.3.5	Local Matter Content	46
2.4	Renormalization Group Evolution	48
2.4.1	Running Gauge Couplings	48
2.4.2	Evolution of the Gaugino Masses	48
2.4.3	Evolution of the Yukawa Couplings	50
2.4.4	RGEs for Trilinear Soft SUSY Breaking Terms	52
2.4.5	RGEs for Scalar SSB masses	53
2.5	Low-Energy Spectrum	54
2.5.1	Higgs Potential Minimization	56
2.5.2	One-Loop Effective Potential	58
2.5.3	Sfermion and Leptoquark Masses	59
2.5.4	Dark Higgs Masses	59
2.5.5	Neutralino and Chargino Masses	60
2.5.6	Dark Higgsinos	61
2.5.7	$Z - Z'$ mixing	62
3	Automated Spectrum Generation	64
3.1	Initialization	65
3.1.1	Generating Renormalization Group Equations	66
3.2	Main Program	70
3.2.1	Comments	81
3.3	Random Walk	83

3.3.1	Testing the Random Walk	90
3.4	Implementation into FeynRules and WHIZARD	90
4	Phenomenology	93
4.1	TeV-Scale Spectra	93
4.2	Z' Production at the LHC	96
4.2.1	Forward-Backward Asymmetry in the Di-Muon Channel	97
5	Conclusions	104
5.1	Outlook	105
A	Orbifolds and Extended Supersymmetry	106
A.1	A toy model	106
A.2	$N = 2$ Supersymmetry in 4D	107
A.3	Conventions	109
A.4	$N = 1$ Supersymmetry in 6D	110
B	Supplements	112
B.1	Two Loop Unification	112
B.2	Dark Higgs Masses	113
B.3	Performance of the Random Walk	116
B.4	Spectra	116
B.4.1	Scenario A: EXSPECT Output	116
B.4.2	Scenario B: EXSPECT Output	124
B.4.3	Scenario C: EXSPECT Output	130
B.5	RGEs above the intermediate scale	137
B.5.1	Running of the Gauge Couplings	137
B.5.2	Running of the Gaugino Masses	137
B.5.3	Running of the Yukawa Couplings	137
B.5.4	Running of the Trilinear SSB-Terms	139
B.5.5	Running of the Scalar SSB-Masses	142
B.6	RGEs below Λ_{int}	146
B.6.1	Running of the Gauge Couplings	146
B.6.2	Running of the Gaugino Masses	147
B.6.3	Running of the Yukawa Couplings	147
B.6.4	Running of the Trilinear SSB-Terms	149
B.6.5	Running of the Scalar SSB-Masses	153

Chapter 1

Introduction

With the LHC being in operation for more than two years and accumulating more and more data every day now, not only particle physicists await some of the most interesting questions in fundamental physics to be finally answered. The current experiments at the LHC, most notably ATLAS and CMS, have been designed to probe the standard model for its last yet to be verified prediction: the Higgs boson, which so far has escaped from experimental detection. Although the standard model [1, 2, 3] has an outstanding record of successfully describing almost all experimental observations in particle physics made in the past three decades, theorists have speculated for nearly the same time span whether or not its minimal¹ Higgs sector is the true origin of electroweak symmetry breaking and the observed masses of the known heavy vector bosons Z and W^\pm .

Arguably the main, albeit rather esthetical objection is the hierarchy problem: Once the weak scale standard model is embedded into a theory involving higher scales, the value of the Higgs mass will be driven to those larger scales by quantum corrections, unless mysterious cancellations come into play. This unappealing effect originating from the trivial Lorentz representation of the Higgs particle lead theorists to investigate mechanisms setting in at scales not too far above the energy range of current experiments that either remove the ingredient of a fundamental scalar driving electroweak symmetry breaking all together (Technicolor [4]) or introduce new particles that render the quantum corrections to scalar mass terms benign (Supersymmetry [5]). More radical approaches try to explain the apparent scale hierarchy as an artifact of a transition from an underlying higher dimensional theory, with only one fundamental scale, to the effective theory in four spacetime dimensions (ADD [6]).

Technicolor is a new strong interaction which – in analogy to chiral symmetry breaking in QCD, only at the TeV scale – effects electroweak symmetry breaking through the formation of a chiral condensate of fermions. Longitudinal vector boson scattering is unitarized by Techni-meson resonances. While this ansatz can beautifully model the generation of the weak vector boson masses, it fails to implement fermion masses. Extended versions (ETC, Topcolor, TC2, . . .) [7] account for this, but all suffer from fine-tuned parameter set-ups due to electroweak precision data from the LEP and Tevatron experiments.

The motivation for building supersymmetric models in particle physics is based on the observation, that if for each particle contributing to the undesirable ultra-violet behavior of scalar masses there was an additional particle of opposite spin-statistics, the quadratic divergence would be reduced to a logarithmic one, coming exclusively from wavefunction renormalization. Unfortunately, no particle of that kind has been detected so far, implying that supersymmetry would have to be broken. In phenomenologically viable models, the breaking is usually imple-

¹ It is constructed from the minimal particle content providing a weakly interacting, renormalizable theory that incorporates electroweak symmetry breaking in a way compatible with experimental measurements.

mented explicitly via dimensionful, so-called soft supersymmetry breaking terms [8]. These terms in the Lagrangian can be numerous ($\mathcal{O}(100)$) and their precise origin remains unknown, although there are several known ways to in principle generate them appropriately (SUSY breaking mechanisms) [9]. For the most part they parametrize a lack of knowledge and it should be carefully investigated, how the physical spectrum of a supersymmetric theory is influenced by different choices.

Apart from this drawback, it was soon discovered that supersymmetry in addition to curing the hierarchy problem leads to many other spectacular predictions, most remarkably the unification of the three standard model gauge couplings at around 10^{16} GeV [10] urging theorists to speculate about a fundamental unified force at very high energies. In addition, once one disallows additional operators that potentially lead to rapid proton decay [11] (“R-Parity”) the lightest supersymmetric partner particle is stable and (if neutral) could play the role of cold dark matter in the universe, a pressing topic not addressed by the standard model. Moreover, the aforementioned electroweak precision observables, that render the models based on dynamic symmetry breaking unappealing, are for the most part in agreement with predictions from supersymmetric theories (or might even favor SUSY theories slightly [12]). If the gauge couplings unify at some energy scale, the respective interactions may be unified in the sense, that the Lie groups representing the gauge interactions below that scale can be embedded into a larger (possibly simple) Lie group. The choice of unified gauge group is not unique. Popular candidates are $SU(5)$, $SO(10)$, $SU(3)^3$ and the exceptional Lie groups E_6 and E_8 [13]. All possible choices require the introduction of extra particles at, or below the unification scale, in order to fill the irreducible representations accommodating the standard model particle content.

The topic of this work is a supersymmetric grand unified theory with an extended TeV-light particle content filling complete representations of the exceptional simple Lie algebra E_6 . In the presence of the additional particles at the TeV scale, the “simple” gauge coupling unification scenario from minimal supersymmetric models does not occur. We present a solution how unification can be restored in a multi-scale symmetry breaking scenario linked to an E_6 theory in six space-time dimensions via *orbifold compactification*. Aiming at the TeV-scale collider phenomenology of this model we present our own spectrum generator, called EXSPECT, designed to derive TeV-scale spectra from Lagrangian parameters specified at the orbifold compactification scale.

We present low-energy spectra and investigated some of their implications on collider phenomenology.

This thesis is structured as follows: We motivate the construction of our model by briefly reviewing supersymmetry and its minimal implementation in particle physics, the MSSM in sections 1.1 and 1.2. A short discussion of the μ problem substantiates the need for an extended Higgs sector as provided by the NMSSM in section 1.3. The extension of the model’s gauge group by an additional $U(1)'$ requires an extended particle content as well. Therefore we shall give some insight on the relevant irreducible representations of E_6 and their decomposition

under its maximal regular subalgebras as well as the embedding of the standard model particle content in complete E_6 multiplets in section 1.4. The study of gauge coupling unification in the $U(1)'$ -extended model, leads us to intermediate symmetry scale scenarios (PSSSM) in section 1.5. Their drawbacks motivated the use of orbifold compactification as GUT symmetry breaking mechanism. The full setup of our model will be presented in chapter 2. We start with the modification of the gauge coupling unification scenario in the four dimensional quantum field theory, such that the problems arising in the PSSSM can be circumvented.

Next, a suitable choice of a six dimensional orbifold geometry is presented which allows to embed the new gauge coupling unification scenario in an extra-dimensional setup with E_6 being the gauge group in the bulk of the extra dimensions. Within this discussion in section 2.3 it will be shown how supersymmetry can be realized in six spacetime dimensions in agreement with the orbifold boundary conditions, as well as how one can cope with gauge anomalies potentially arising from incomplete E_6 multiplets residing on the fixed points.

The parameters at the compactification scale are linked to the TeV scale via renormalization group equations (RGEs), presented in section 2.4. From the Lagrangian parameters at the TeV scale we calculate in section 2.5 all couplings, particle masses, and mixing matrices which determine the LHC phenomenology. The solution of the RGEs from section 2.4 is subject to complex boundary conditions and interdependencies. We designed an automated spectrum generator deriving TeV-scale spectra from the model's free parameters chosen at the orbifold compactification scale. The presentation of this spectrum generator in chapter 3 also entails the discussion on some additional features of our model, such as top-bottom unification.

In order to be ready to investigate the implications for TeV-scale experiments, we implemented our model in the multi-purpose event generator WHIZARD, following the steps outlined in section 3.4.

The remainder of this thesis is dedicated to the documentation of the first phenomenological studies that we conducted using the tools described in the previous chapter: Section 4.1 contains three scenarios representing how our model becomes manifest at the TeV scale. As first phenomenological implication we studied the production of the heavy Z' boson at the LHC in section 4.2.

We conclude in chapter 5 with a review of the presented model and an outlook on exciting future research projects that could fill in some interesting details left open at the current stage of investigation.

1.1 Supersymmetry

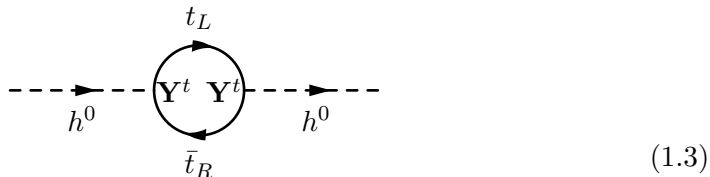
The standard model of particle physics [1, 2, 3] is in agreement with all experimental observations to an astonishing degree. However it is based upon a vacuum expectation value (vev) of the yet undiscovered Higgs field of 246 GeV, which is extremely unstable under quantum corrections. As shown e.g. in [14], the largest contribution causing the instability arises from the Yukawa interaction among Higgs and top-quark fields

$$L_{\text{Yuk}} = -\mathbf{Y}^t H^0 \bar{t}_R t_L + \dots \quad (1.1)$$

Using a momentum cutoff regularization scheme, one obtains for the top loop contribution to the Higgs mass parameter m_h^2 as illustrated in figure 1.3:

$$\delta m_h^2|_{\text{top}} = -\frac{N_c |\mathbf{Y}^t|^2}{8\pi^2} \left[\Lambda^2 - 3m_t^2 \log \frac{\Lambda^2 + m_t^2}{m_t^2} + \dots \right]. \quad (1.2)$$

Here, Λ denotes the cutoff scale, N_c the number of QCD colors and \dots hide terms being finite when Λ is taken to infinity.



From (1.2), one can conclude that having a weak scale order Higgs mass in a theory being valid up to scales $\Lambda \gg 1$ TeV requires a very precise choice of counter-terms canceling the $\mathcal{O}(\Lambda^2)$ contribution. This is commonly referred to as the “hierarchy problem”. From another point of view, one can conclude that the standard model is only an effective theory up to a few TeV of a more elaborate theory in which the the Higgs vev is (more) stable under radiative corrections. A very prominent theory of that kind is Supersymmetry (SUSY), introducing N_c pairs of scalar fields ϕ_L and ϕ_R coupling to the Higgs particle according to

$$L_{\text{scalar}} = -\frac{1}{2} |H^0|^2 (|\phi_L|^2 + |\phi_R|^2) - \frac{1}{2} \left[H^0 (\mu_L |\phi_L|^2 + \mu_R |\phi_R|^2) + h.c. \right] - m_L^2 |\phi_L|^2 - m_R^2 |\phi_R|^2. \quad (1.4)$$

As shown in [14], from these interactions arise loop contributions to the Higgs mass which itself are quadratically and logarithmically divergent. If the quartic coupling λ in (1.4) is equal to the top Yukawa coupling \mathbf{Y}^t the disastrous quadratic divergences from fermionic and scalar loops cancel. Furthermore if $m_R = m_L = m_t$ and $\mu_R^2 = \mu_L^2 = 2\mathbf{Y}^t m_t^2$, even the logarithmic contributions vanish. SUSY is a symmetry relating fermions and bosons in the precise way, guaranteeing these conditions.

Supersymmetry provides a unique non-trivial extension of the Poincaré symmetry of the S -matrix consistent with relativistic quantum field theory [15]. On top of the Poincaré generators of translations, boosts, and rotations, there are two complex, Grassmann-valued spinors Q and $\bar{Q} = Q^*$, whose anti-commutator is proportional to the generator of translations:

$$\begin{aligned} \{Q_\alpha, Q_\beta\} &= \{\bar{Q}_{\dot{\alpha}}, \bar{Q}_{\dot{\beta}}\} = 0, \\ \{Q_\alpha, \bar{Q}_{\dot{\beta}}\} &= 2\sigma_{\alpha, \dot{\beta}}^\mu P_\mu. \end{aligned} \quad (1.5)$$

The Weyl spinors Q, \bar{Q} are called SUSY generators. With the help of anti-commuting parameters $\xi^\alpha, \bar{\xi}_{\dot{\alpha}}$ (1.5) can be paraphrased in terms of commutators:

$$\begin{aligned} [\xi Q, \xi Q] &= [\bar{\xi} \bar{Q}, \bar{\xi} \bar{Q}] = 0, \\ [\xi Q, \bar{\xi} \bar{Q}] &= 2\xi\sigma^\mu\bar{\xi}P_\mu, \end{aligned} \quad (1.6)$$

allowing to view the SUSY algebra as Lie algebra with anti-commuting parameters. This allows to parametrize group elements via

$$G(a, \xi, \bar{\xi}) = \exp [i(-a \cdot P + \xi Q + \bar{\xi} \bar{Q})]. \quad (1.7)$$

Superfields are defined as functions $\mathbf{F}(x, \theta, \bar{\theta})$ of spacetime coordinates x_μ and the anti-commuting spinor components θ^α and $\bar{\theta}_{\dot{\alpha}}$ that transform according to

$$\mathbf{F}(x, \theta, \bar{\theta}) \longrightarrow \mathbf{F}(x', \theta', \bar{\theta}') = G(a, \xi, \bar{\xi}) \mathbf{F}(x, \theta, \bar{\theta}) G(a, \xi, \bar{\xi})^\dagger, \quad (1.8)$$

with

$$\begin{aligned} x'_\mu &= x_\mu + a_\mu + i\xi\bar{\sigma}_\mu\bar{\theta} - i\bar{\xi}\sigma_\mu\theta, \\ \theta' &= \theta + \xi, \quad \bar{\theta}' = \bar{\theta} + \bar{\xi}. \end{aligned} \quad (1.9)$$

From an infinitesimal variation

$$\begin{aligned} \delta\mathbf{F}(x, \theta, \bar{\theta}) &= \mathbf{F}(x', \theta', \bar{\theta}') - \mathbf{F}(x, \theta, \bar{\theta}) \\ &= \left[\underbrace{-ia^\mu}_{P_\mu} \underbrace{i\partial_\mu}_{P_\mu} - i\xi^\alpha \underbrace{i(\partial_{\theta^\alpha} + i\bar{\sigma}_{\alpha\dot{\alpha}}^\mu \bar{\theta}^{\dot{\alpha}} \partial_\mu)}_{Q_\alpha} - i\bar{\xi}_{\dot{\alpha}} \underbrace{i(\partial_{\bar{\theta}_{\dot{\alpha}}} + i\sigma^{\mu\dot{\alpha}\alpha} \theta_\alpha \partial_\mu)}_{\bar{Q}^{\dot{\alpha}}} \right] \mathbf{F}(x, \theta, \bar{\theta}) \end{aligned} \quad (1.10)$$

one can find the indicated representation of the SUSY generators in terms of differential operators on the superspace, which indeed satisfies the SUSY algebra (1.5). We note that linear combinations, complex conjugates and products of superfields are again superfields as the representation is linear and unitary and can be build from differential operators of order one.

There is another important set of differential operators

$$D_\alpha \equiv i(\partial_{\theta^\alpha} - i\bar{\sigma}_{\alpha\dot{\alpha}}^\mu \bar{\theta}^{\dot{\alpha}} \partial_\mu),$$

$$\bar{D}^{\dot{\alpha}} \equiv i (\partial_{\bar{\theta}_{\dot{\alpha}}} - i\sigma^{\mu\dot{\alpha}\alpha}\theta_{\alpha}\partial_{\mu}) \quad (1.11)$$

which when applied to a superfield \mathbf{F} yield again superfields $D_{\alpha}\mathbf{F}$ and $\bar{D}^{\dot{\alpha}}\mathbf{F}$ and are therefore denoted as SUSY covariant derivatives.

A *component representation* of a general superfield $\mathbf{F}(x', \theta', \bar{\theta}')$ can be found via a Taylor-expansion in θ and $\bar{\theta}$. This expansion is truncated after finitely many terms due to the Grassmann properties of θ^{α} and $\bar{\theta}_{\dot{\alpha}}$. Yet, the general form of the superfield from (1.8) is highly reducible. It can be shown, that all renormalizable SUSY Lagrangians can be constructed from two types of irreducible superfield representations, *vector* and *chiral* superfields. By definition, we call a superfield $\Phi(x, \theta, \bar{\theta})$ obeying

$$\bar{D}^{\dot{\alpha}}\Phi = 0 \quad [D_{\alpha}\Phi = 0] \quad (1.12)$$

a *right-chiral* [*left-chiral*] superfield. In a suitable basis for the spacetime coordinate $y^{\mu} \equiv x^{\mu} - i\theta\bar{\sigma}^{\mu}\bar{\theta}$ one finds

$$\bar{D}^{\dot{\alpha}} = i\partial_{\bar{\theta}_{\dot{\alpha}}}, \quad (1.13)$$

yielding a very simple form for the Taylor-expansion in the anti-commuting superspace coordinates of a right-chiral superfield:

$$\Phi(x, \theta, \bar{\theta}) = \Phi(y, \theta) = \phi(y) + \sqrt{2}\theta\psi(y) + \theta\theta F(y). \quad (1.14)$$

The *component fields* transform under infinitesimal SUSY transformations according to

$$\begin{aligned} \delta_{\xi}\phi &= \sqrt{2}\xi\psi, \\ \delta_{\xi}\psi_{\alpha} &= -\sqrt{2}F\xi_{\alpha} - i\sqrt{2}\bar{\sigma}_{\alpha\dot{\alpha}}^{\mu}\bar{\xi}^{\dot{\alpha}}\partial_{\mu}\phi, \\ \delta_{\xi}F &= i\sqrt{2}\bar{\xi}\sigma^{\mu}\partial_{\mu}\psi. \end{aligned} \quad (1.15)$$

As suggested by the notation, we can identify ϕ as scalar, ψ as spinor, and F as field of mass-dimension two if we assign the mass dimension $-1/2$ to the spinors of Grassmann parameters ξ . The expansion of a left handed superfield into component fields and their behavior under infinitesimal SUSY transformations can be obtained in a similar fashion, or simply by complex conjugation of (1.14) and (1.15). A crucial observation from (1.15) is that the highest component F of the superfield transforms into a total spacetime derivative, which will become the key ingredient to construct SUSY Lagrangians.

First, let us study the second class of irreducible superfields. A *vector* superfield is real scalar superfield

$$\mathbf{V}(x, \theta, \bar{\theta}) = \mathbf{V}^{\dagger}(x, \theta, \bar{\theta}). \quad (1.16)$$

An expansion in the spinor parameters leads to

$$\mathbf{V}(x, \theta, \bar{\theta}) = -\theta\bar{\sigma}^{\mu}\bar{\theta}A_{\mu}(x) - i\theta\theta\bar{\theta}\bar{\lambda} + i\bar{\theta}\bar{\theta}\theta\lambda - \frac{1}{2}\bar{\theta}\bar{\theta}\theta\theta D(x) + \dots, \quad (1.17)$$

where A_μ is a Lorentz vector, λ and $\bar{\lambda}$ can be assembled into a Majorana spinor and D is again a field of mass dimension two. There are finitely many additional terms in the expansion of a general vector superfield which have been omitted, as in physical theories they can be eliminated in the so-called Wess-Zumino gauge [15]. As in the case of the chiral superfield the highest component D transforms into a total spacetime derivative. With this knowledge, one can construct a supersymmetric theory, by choosing the Lagrangian density to be the sum of the projections on the respective highest component of a vector and chiral superfield²

$$S = \exp \left[-i \int d^4x L \right] = \exp \left[-i \int d^4x \left(\Phi \Big|_{\theta\theta} + \Phi^\dagger \Big|_{\bar{\theta}\bar{\theta}} + \mathbf{V} \Big|_{\theta\theta\bar{\theta}\bar{\theta}} \right) \right]. \quad (1.18)$$

In order to understand what can be gained from this realization, let us summarize the highest components of the following products of chiral superfields:

$$\Phi_i \Phi_j \Big|_{\theta\theta} = \phi_i F_j + \phi_j F_i - \psi_i \psi_j, \quad (1.19a)$$

$$\Phi_i \Phi_j \Phi_k \Big|_{\theta\theta} = F_i \phi_j \phi_k + F_j \phi_k \phi_i + F_k \phi_i \phi_j - \psi_i \psi_j \phi_k - \psi_j \psi_k \phi_i - \psi_k \psi_i \phi_j, \quad (1.19b)$$

$$\Phi_i^\dagger \Phi_j \Big|_{\theta\theta\bar{\theta}\bar{\theta}} = \partial^\mu \phi^* \partial_\mu \phi + i \bar{\psi} \bar{\sigma}^\mu \partial_\mu \psi + F^* F + \dots, \quad (1.19c)$$

where in the last line total spacetime derivatives have been abbreviated by dots. In the highest component of the vector superfield from (1.19c), one can identify the kinetic terms for scalars ϕ and Weyl fermions ψ . A general renormalizable, interacting supersymmetric Lagrangian (without gauge interactions) is constructed from linear combinations of the terms from (1.19) and the $\theta\theta$ component from (1.14) and the respective Hermitian conjugates. This becomes more clear realizing that there appear no derivatives of the dimension two *auxiliary* fields F and F^* , rendering their equations of motion purely algebraic. Integrating out those unphysical degrees of freedom we obtain

$$\begin{aligned} \int d^4x L &= -i \int d^4x \left[\Phi_i^\dagger \Phi_j \Big|_{\theta\theta\bar{\theta}\bar{\theta}} + \left(W(\Phi) \Big|_{\theta\theta} + h.c. \right) \right] \\ &= -i \int d^4x \left[\partial^\mu \phi_j^* \partial_\mu \phi^j + i \bar{\psi}^j \bar{\sigma}^\mu \partial_\mu \psi_j \right. \\ &\quad \left. - \frac{1}{2} \left(W_{ik} \psi^j \psi^k + W_{ik}^* \bar{\psi}^j \bar{\psi}^k \right) - W^j W_j^* \right], \end{aligned} \quad (1.20)$$

where we have introduced the notion of the *superpotential*

$$W = E^j \Phi_j + \frac{1}{2!} M^{ij} \Phi_i \Phi_j + \frac{1}{3!} y^{ijk} \Phi_i \Phi_j \Phi_k \quad (1.21)$$

²The projection is often written as integration over the Grassmann-valued superspace components [16]. The meaning is identical to our notation.

and the derivatives of the superpotential understood as a function of the scalar fields

$$W^i \equiv \frac{\partial W}{\partial \phi^i}, \quad W^{ij} \equiv \frac{\partial^2 W}{\partial \phi^i \partial \phi^j}. \quad (1.22)$$

Note, that the superpotential W has to be a *holomorphic function* in the complex superfields in order to be a chiral superfield itself, as required by the construction (1.19).

Gauge theories can be implemented in SUSY introducing a vector superfield V^a as in (1.17), which transforms under the SUSY-extended gauge symmetry as

$$V^a \longrightarrow V^a + \Lambda^a + \Lambda^{a\dagger} + \dots, \quad (1.23)$$

where Λ is a chiral superfield. A *supergauge* transformation of a chiral superfield is given by

$$\Phi \longrightarrow \exp[-gT^a \Lambda^a] \Phi. \quad (1.24)$$

The Lagrangian of a gauge theory with minimal coupling to chiral superfields then reads

$$\begin{aligned} L &= \Phi^\dagger e^{gT^a V^a} \Phi \Big|_{\theta\theta\bar{\theta}\bar{\theta}} \\ &= \sqrt{2}g [(\phi^* T^a \psi)\lambda^a + \bar{\lambda}^a (\bar{\psi} T^a \phi)] + g(\phi^* T^a \phi) D^a. \end{aligned} \quad (1.25)$$

The SUSY Yang-Mills action can be written as

$$\begin{aligned} \int d^4x L_{\text{SYM}} &= \frac{1}{4} \int d^4x \left(W^{a\alpha} W_\alpha^a \Big|_{\theta\theta\bar{\theta}\bar{\theta}} + h.c. \right) \\ &= \int d^4x \left(-\frac{1}{4} F_{\mu\nu}^a F^{a\mu\nu} + i\bar{\lambda}^a \bar{\sigma}^\mu \partial_\mu \lambda + \frac{1}{2} D^a D^a \right), \end{aligned} \quad (1.26)$$

where the chiral *field-strength* superfield W_α^a in the first line is defined via

$$T^a W_\alpha^a \equiv -\frac{1}{4} \bar{D}_{\dot{\alpha}} \bar{D}^{\dot{\alpha}} \exp[-T^a V^a] D_\alpha \exp[T^a V^a], \quad (1.27)$$

with the SUSY covariant derivatives from (1.11). In the Lagrangian containing all gauge interactions, the dimension two field D^a is an auxiliary field obeying algebraic equations of motion

$$D^a = -g\phi^* T^a \phi. \quad (1.28)$$

The scalar potential in an unbroken supersymmetric theory is obtained by replacing the auxiliary fields with their equations of motion:

$$V_{\text{scalar}} = F_i^* F^i + \frac{1}{2} D^a D^a = W_i^* W^i + \frac{1}{2} g^2 (\phi^* T^a \phi)^2, \quad (1.29)$$

leading to the categorization of scalar interactions of *F-terms* and *D-terms*.

Obviously, SUSY is not an intact symmetry in the real world, which means that it can only be of use to the description of TeV-scale physics if it is broken. If SUSY was broken spontaneously [17], the center of mass of any supermultiplet would be equal to the fermion mass parameter, so there would have to be scalars, lighter than their fermionic superpartners, which is excluded by the experiment. The common approach is to introduce dimensionful couplings, lifting the scalar mass spectrum to higher scales, in order to have eluded experiments so far, but maintaining the SUSY relations among dimensionless couplings, in order not to re-introduce the disastrous quadratic divergencies in the scalar mass parameters. This is referred to as *soft-supersymmetry breaking* (SSB). Without specifying a theory generating SSB, we can parametrize our lack of knowledge in the following form:

$$L_{\text{SSB}} = -\frac{1}{2}(M_\lambda \lambda^a \lambda^a + h.c.) - m_{ij}^2 \phi_i^* \phi_j - \left(\frac{1}{2!} b_{ij} \phi_i \phi_j + \frac{1}{3!} a_{ijk} \phi_i \phi_j \phi_k + \frac{1}{2!} c_{ijk} \phi_i^* \phi_j \phi_k + e_i \phi_i + h.c. \right). \quad (1.30)$$

The terms c_{ijk} may introduce quadratic divergencies again, and are omitted in most SUSY models. In a realistic model the scalar terms from (1.30) have to be added to the scalar potential (1.29).

A strong corollary in at most softly broken SUSY theories is the so-called *non-renormalization theorem* stating that scale dependence of the superpotential parameters can be entirely expressed in terms of the wave function renormalizations of the chiral superfields (see e.g. [16] and the references therein).

1.2 MSSM

Having sketched the general formalism for the construction of a supersymmetric quantum field theory in the previous section, we can use it to derive the minimal supersymmetric version of the standard model (MSSM): The gauge interactions can be rendered supersymmetric in a straightforward manner, whereas the Yukawa potential requires some consideration. The minimal superpotential containing all terms necessary to provide standard model-like fermion masses reads

$$W_{\text{MSSM}} = \mu H_u H_d + \mathbf{Y}_{ij}^e e_i^c L_j H_d + \mathbf{Y}_{ij}^d d_i^c Q_j H_d + \mathbf{Y}_{ij}^u u_i^c H_u Q_j, \quad (1.31)$$

where all group indices have been suppressed. Note, that since the superpotential has to be a holomorphic function of chiral superfields, a second Higgs superfield H_u is required in order to provide masses for up- and down-type fermions at the same time. The geometric mean of the vevs of the two Higgs fields is fixed via M_W , but their relative size is a free parameter in the MSSM:

$$\langle H_u \rangle = \frac{v_u}{\sqrt{2}} \quad \langle H_d \rangle = \frac{v_d}{\sqrt{2}}$$

Q	$(\mathbf{3}, \mathbf{2})$	$\frac{1}{6}$	L	$(\mathbf{1}, \mathbf{2})_{-\frac{1}{2}}$	H_d	$(\mathbf{1}, \mathbf{2})_{-\frac{1}{2}}$
d^c	$(\bar{\mathbf{3}}, \mathbf{1})$	$\frac{1}{3}$	e^c	$(\mathbf{1}, \mathbf{1})_1$	H_u	$(\mathbf{1}, \mathbf{2})_{\frac{1}{2}}$
u^c	$(\bar{\mathbf{3}}, \mathbf{1})$	$\frac{1}{3}$	$[\nu^c$	$(\mathbf{1}, \mathbf{1})_0]$		

Table 1.1: The MSSM particle content categorized according to the representations under the SM gauge group (1.33).

$$v_u^2 + v_d^2 = (246 \text{ GeV})^2 \quad \tan \beta \equiv \frac{v_u}{v_d} \quad (1.32)$$

The superfields appearing in (1.31) transform under the standard model gauge group

$$SU(3) \times SU(2) \times U(1) \quad (1.33)$$

according to table 1.1. The superpotential from (1.31) is not the most general one containing the particles from table 1.1: Terms that would either violate baryon- or lepton-number by one unit could be added:

$$\mathcal{W}_{\text{dis}} = \alpha_{ijk} Q_i L_j d_k^c + \beta_{ijk} L_i L_j e_k^c + \gamma_i L_i H^u + \delta_{ijk} d_i^c d_j^c u_k^c, \quad (1.34)$$

which would lead to rapid proton decay [14]. Setting these undesirable couplings to zero renders (1.31) invariant under a Z_2 symmetry commonly referred to as matter- (or R - on component fields) parity. This parity implies that the supersymmetric partners of standard model fermions and scalar components of the Higgs superfields are always produced in pairs, which means that the lightest superpartner is stable and hence a potential candidate for cold dark matter if electrically neutral.

In the superpotential (1.31), there is no term trilinear in the Higgs superfields. Therefore all quartic scalar terms originate from D -terms, restricting the lightest Higgs mass to be less than the Z -boson mass at the tree-level. Depending on the superpartner spectrum, there may be sizable quantum corrections lifting the Higgs mass to higher values [18].

The appearance of the superpartners (above a certain threshold) also changes the *running of the gauge couplings*.

1.2.1 Renormalization Group Evolution

In high energy physics, dealing predominately with weakly coupled theories the path integral of an interacting quantum field theory is expanded as a perturbative series in the coupling constants. Unfortunately this series leads to infinities beyond zeroth order, calling for a *regularization* and *renormalization* procedure to render the predictions for physical observables finite. This procedure is far from unique, but results obtained in different renormalization schemes at n -th order in perturbation theory differ only by order $(n + 1)$ contributions. Part of the choice of the renormalization scheme is that of an unphysical scale parameter

μ . The physical predictions of the theory remain independent of μ , if changing it is accompanied by a suitable change of the renormalized parameters, in that context thought of as μ -dependent. This transformation of the parametrization is - somewhat misleadingly - called a renormalization group transformation. The renormalization group evolution (*running* of the parameters) in terms of a differential equation can be calculated using the independence of the *bare* parameters of the theory of μ . Usually by setting μ to some scale intrinsic to the process under investigation, potentially large logarithms in μ in the chosen and higher orders in the perturbative series are tamed, which leads to the widely accepted interpretation of the renormalization group evolution reflecting the dependence of the parameters on physical energy scales. For a thorough introduction to the field of renormalization consult e.g. [19, 16].

For a the coupling constant g of an arbitrary gauge group coupled to fermions and scalars the renormalization group equation (RGE) at the one-loop level reads:

$$\frac{dg}{d(\log(\mu/\mu_0))} = \frac{1}{16\pi^2} \left[-\frac{11}{3}C(G) + \frac{2}{3} \sum_f S(R_f) + \frac{1}{3} \sum_s S(R_s) \right] g^3, \quad (1.35)$$

where $C(G)$ represents the quadratic Casimir of the gauge group, and $S(R_f), S(R_s)$ the representation constants of the representation R_f, R_s according to which the fermion f or the scalar s transform under, respectively. μ_0 is a reference scale fixed to some arbitrary value. Imposing supersymmetry on (1.35), i.e. synchronizing the two sums over scalars and fermions as well as adding the gaugino, a Majorana spinor transforming according to the adjoint representation of the gauge group, we obtain with $S(R_{\text{adj}}) = C(G)$

$$\frac{dg}{d(\log(\mu/\mu_0))} = \frac{1}{16\pi^2} \left[-3C(G) + \sum_i S(R_i) \right] g^3, \quad (1.36)$$

with i running over all chiral superfields.

Solving the RGEs for the standard model gauge couplings for a) the standard model particle content and b) for its supersymmetrized version from table 1.1, one obtains the striking result shown in figure 1.1: The additional particles that have to be added to the loop in transition from the standard model to the MSSM are all fermions and scalars, hence thwarting the tendency of the gauge bosons self-interactions to asymptotic freedom, in precisely such a manner that the coupling constants unify at around 10^{16} GeV.

This surprising discovery fanned the flames of speculations about so-called Grand Unified Theories (GUTs), where the standard model gauge group is viewed as the unbroken remnant of a larger (possibly simple) unified gauge group. In fact, in most of today's discussions about supersymmetry, the TeV-scale theory is implicitly understood to originate from a unified theory valid above the unification scale.

There are two major problems to this notion:

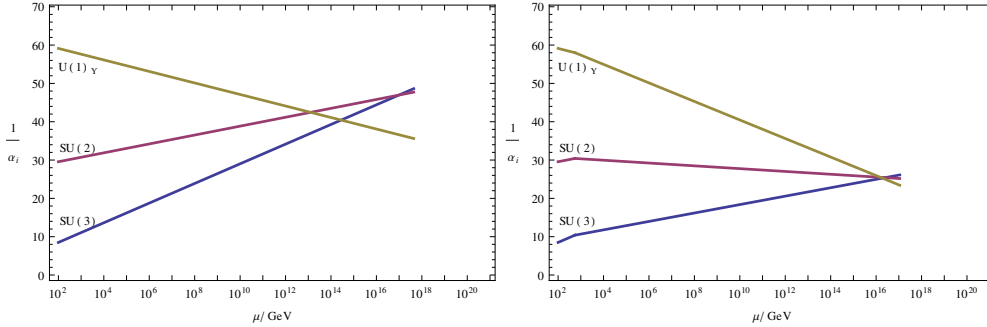


Figure 1.1: One-loop running of the gauge couplings in the standard model (left), and its minimal supersymmetric extension (right).

- Within the context of the MSSM being the low-energy limit of a GUT with intrinsic scale $\Lambda \sim 10^{16}$ GeV it is not plausible why the μ -parameter from (1.31) should be of the order of the weak scale, as demanded by phenomenology.
- There is no set of irreducible representations of a simple Lie algebra solely containing the (MS-)SM matter content, which means that there has to exist some additional particle content, in order to fill the GUT multiplets. If these particles were present below Λ , they would alter the running of the couplings and spoil gauge unification. Therefore, the additional particles which are combined with some or all MSSM-particles to form an irreducible GUT representation have to acquire masses of order Λ , while the MSSM-share of the GUT multiplet has to remain massless. This is commonly referred to as *doublet-triplet splitting-problem* as mechanisms that can facilitate the splitting are prone to fine-tuning [20].

1.3 NMSSM

The next-to-minimal supersymmetric version of the standard model (NMSSM)[21] was designed to eliminate the μ -problem by introducing an additional superfield S transforming trivially under the standard model gauge group. The MSSM-superpotential (1.31) is modified to take the following form:

$$\mathcal{W}_{\text{NMSSM}} = \mathbf{Y}^S S^3 + \mathbf{Y}^{\text{SH}} S H_u H_d + \mathbf{Y}_{ij}^e e_i^c L_j H_d + \mathbf{Y}_{ij}^d d_i^c Q_j H_d + \mathbf{Y}_{ij}^u u_i^c H_u Q_j, \quad (1.37)$$

equipped with a symmetry that forbids linear and quadratic terms in S , which would re-introduce TeV-sized dimensionful superpotential parameters contradicting the ansatz of the NMSSM. There is then no dimensionful parameter left in the superpotential, but in the course of electroweak symmetry breaking the scalar

component of S acquires a non-trivial vev

$$\langle S \rangle = v_s / \sqrt{2}, \quad (1.38)$$

generating an effective μ -term dynamically:

$$\mu_{\text{eff}} = \mathbf{Y}^{\text{SH}} \frac{v_s}{\sqrt{2}}. \quad (1.39)$$

The S^3 term in (1.37) has to be present in order to render the Higgs potential bounded from below. This also lifts the tree-level Higgs mass bound [16] to

$$m_{h_1}^2 \leq M_Z^2 \left[\cos^2 2\beta + \frac{2(\mathbf{Y}^{\text{SH}})^2}{g_2^2 + g_Y^2} \sin^2 2\beta \right]. \quad (1.40)$$

The discrete Z_3 symmetry of the superpotential of the NMSSM and the singlet field S may cause cosmologically unacceptable domain-walls [22]. Historically, this was one of the motivations to study the NMSSM with an $U(1)'$ -extended gauge sector [24]. The NMSSM S field is charged under the extra $U(1)'$, which disallows all polynomial terms in S . The quartic terms in S in the scalar potential are generated from $U(1)'$ D -terms. The requirement of anomaly freedom limits the number of possible $U(1)'$ groups and is generally accompanied by the introduction of extra field content [23]. In order to understand where the additional particles come from, we shall dedicate the next section to representation theory of Lie groups, with a focus on the rank six exceptional Lie group E_6 .

1.4 E_6 Representations And Subalgebras

The minimal particle content for an anomaly-free, generation-universal $U(1)'$ -extended version of the NMSSM forms a **27** dimensional irreducible representation (irrep) of the rank six exceptional Lie group E_6 [25]. In this section we will illustrate how E_6 can be decomposed into the relevant subalgebras using *Dynkin diagrams*. Irreducible representations will be constructed using *weight-space diagrams*. In order to calculate $U(1)$ charges, we will introduce a general technique, mapping the elements of the weight-space onto the corresponding $U(1)$ quantum numbers. As we do not give a general introduction to group theory, we refer the interested reader to the standard literature [25, 26] and the references therein.

1.4.1 Subalgebras of E_6

E_6 is the rank six Lie group represented by the Cartan matrix ³

$$A_{E_6} = \begin{pmatrix} 2 & -1 & 0 & 0 & 0 & 0 \\ -1 & 2 & -1 & 0 & 0 & 0 \\ 0 & -1 & 2 & -1 & 0 & -1 \\ 0 & 0 & -1 & 2 & -1 & 0 \\ 0 & 0 & 0 & -1 & 2 & 0 \\ 0 & 0 & -1 & 0 & 0 & 2 \end{pmatrix} \quad (1.41)$$

which can be represented graphically by the diagram in figure 1.2 (lhs) .

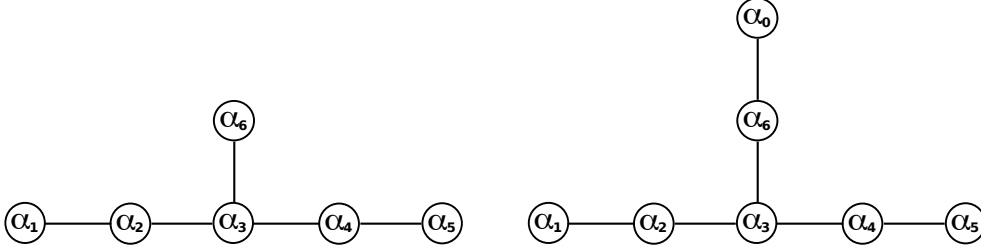


Figure 1.2: The Dynkin diagram of E_6 and its extension, obtained by adding α_0 as given in (1.42).

First we shall study the *maximal regular subalgebras* of E_6 , i.e. the subalgebras of the same rank. Adding the *smallest root* of the adjoint representation to the Dynkin diagram yields the the so-called extended diagram, from which the semi-simple maximal regular subalgebras are obtained by removing one root. In addition, any simple root can be reduced to an Abelian generator by disconnecting it from the rest of the diagram. This represents removing the raising/lowering operators of the associated $SU(2)$ algebra, while leaving the Cartan generator intact.

In the case of E_6 , the smallest root α_0 is given as the following linear combination of the simple roots:

$$\alpha_0 = -\alpha_1 - 2\alpha_2 - 3\alpha_3 - 2\alpha_4 - \alpha_5 - 2\alpha_6. \quad (1.42)$$

The extended Dynkin diagram of the E_6 algebra is displayed in figure 1.2 (rhs). The most relevant subalgebras of E_6 within this work read

$$E_6 \supset SU(6) \times SU(2)_L \quad (1.43a)$$

$$\supset SU(4) \times SU(2)_R \times U(1)_\chi \times SU(2)_L \quad (1.43b)$$

³The ordering of the rows and columns in the Cartan matrix, and correspondingly in the Dynkin diagrams throughout this work is chosen by convention. The results that we present here do not depend on this choice.

$$\supset SU(3) \times SU(2)_R \times U(1)_{B-L} \times U(1)_\chi \times SU(2)_L \quad (1.43c)$$

$$\supset SU(3) \times U(1)_Y \times SU(2)_L [\times U(1)']. \quad (1.43d)$$

Provided the identification of $SU(2)_{L/R}$ as in the above equations (which is not unique), all $U(1)$ groups can be embedded into $SU(6)$. This notion will be used later in this chapter, when calculating the $U(1)$ quantum numbers. Furthermore, note that the standard model from the last line (1.43d) is not a maximal subalgebra of E_6 as the rank has been reduced. The decomposition from (1.43) in terms of Dynkin diagrams is displayed in figure 1.3.

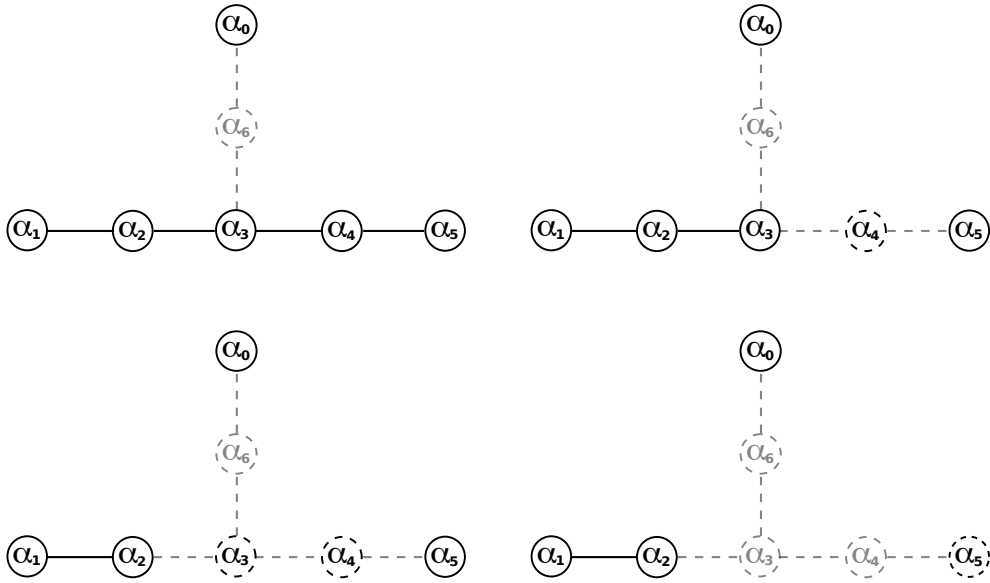


Figure 1.3: Subsequent decomposition of E_6 into the subalgebras from (1.43). The roots that have been completely removed from the diagram are indicated in gray. Those reduced to their Abelian generator are displayed in dashed black circles. In the last picture $U(1)_Y$ would actually correspond to a linear combination of α_3 and α_5 .

1.4.2 The 27 dimensional representation of E_6

The weight space diagram of the **27** is shown in figure 1.4. We observe that the **27** of E_6 decomposes under $SU(6) \times SU(2)$ into

$$(\mathbf{6}, \mathbf{2}) \oplus (\mathbf{15}, \mathbf{1}). \quad (1.44)$$

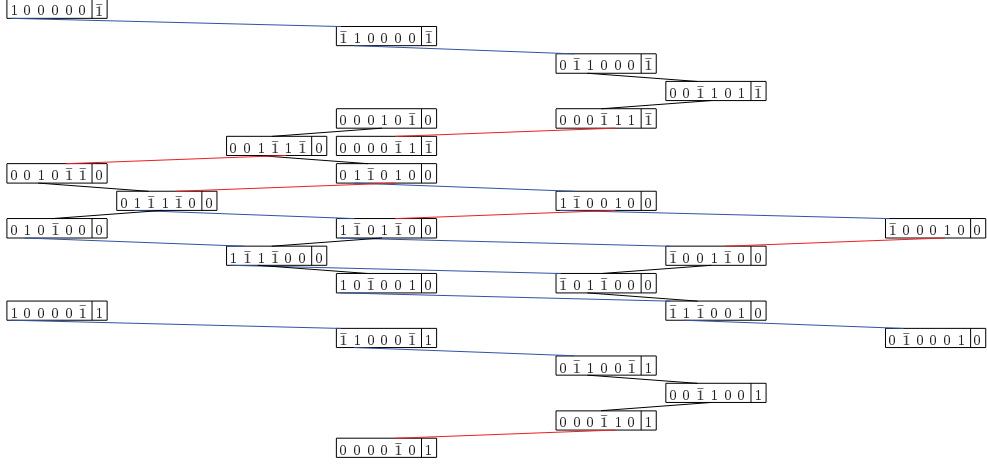


Figure 1.4: Weight space diagram of $\mathbf{27}$ of E_6 in terms of Dynkin coefficients. Negative values are represented with overbars. The weights are ordered consistent with figure 1.2. The lines indicate changes in α_1, α_2 (blue), α_3, α_4 (black), and α_5 (red). The lines corresponding to α_6 have been suppressed for readability. The separated seventh entry labels the Dynkin coefficients corresponding to the smallest root α_0 from (1.42).

Omitting the α_6 entry, we identify (using overbars to abbreviate negative entries)

$$\begin{array}{ll}
 1, 0, 0, 0, 0, \bar{1} & 1, 0, 0, 0, 0, 1 \\
 \bar{1}, 1, 0, 0, 0, \bar{1} & \bar{1}, 1, 0, 0, 0, 1 \\
 0, \bar{1}, 1, 0, 0, \bar{1} & 0, \bar{1}, 1, 0, 0, 1 \\
 0, 0, \bar{1}, 1, 0, \bar{1} & 0, 0, \bar{1}, 1, 0, 1 \\
 0, 0, 0, \bar{1}, 1, \bar{1} & 0, 0, 0, \bar{1}, 1, 1 \\
 0, 0, 0, 0, \bar{1}, \bar{1} & 0, 0, 0, 0, \bar{1}, 1
 \end{array} \tag{1.45}$$

as $(\mathbf{6}, \mathbf{2})$ of $SU(6) \times SU(2)$ at the top and bottom of figure 1.4.

All further decomposition under the semi-simple parts of the regular subalgebras (1.43) can be obtained analogously, by tracing which weights are connected through the respective roots. A summary is given in table 1.2. The $U(1)$ quantum numbers therein will be derived in the following.

1.4.3 $U(1)$ Quantum Numbers

The embedding of the Abelian groups into E_6 can be understood most easily by realizing that with the identification of the $SU(2)_L$ according to (1.43a), all $U(1)$ generators appearing in (1.43) can be embedded into $SU(6)$. We can construct all $U(1)$ charges of the maximal regular subalgebras from the following three requirements: a) commutativity with the semi-simple remainder of the respective gauge groups, b) normalization, and c) that the charges summed over $SU(6)$ multiplets vanish. Condition c) accounts for the fact that each $U(1)$ generator is

E_6	$SU(6) \times SU(2)$	$SU(4) \times SU(2)^2 \times U(1)$	$SU(3) \times SU(2)^2 \times U(1)^2$
27	$(\bar{\mathbf{15}}, \mathbf{1})$	$(\bar{\mathbf{4}}, \mathbf{1}, \mathbf{2})_1$	$(\bar{\mathbf{3}}, \mathbf{1}, \mathbf{2})_{(\bar{\mathbf{1}}, \mathbf{1})}$ $(\mathbf{1}, \mathbf{1}, \mathbf{2})_{(3, \mathbf{1})}$
		$(\mathbf{6}, \mathbf{1}, \mathbf{1})_{\bar{2}}$	$(\bar{\mathbf{3}}, \mathbf{1}, \mathbf{1})_{(\bar{2}, \bar{2})}$ $(\mathbf{3}, \mathbf{1}, \mathbf{1})_{(\bar{2}, \bar{2})}$
		$(\mathbf{1}, \mathbf{1}, \mathbf{1})_4$	$(\mathbf{1}, \mathbf{1}, \mathbf{1})_{(0, 4)}$
	$(\mathbf{6}, \mathbf{2})$	$(\mathbf{4}, \mathbf{2}, \mathbf{1})_1$	$(\mathbf{3}, \mathbf{2}, \mathbf{1})_{(1, \mathbf{1})}$ $(\mathbf{1}, \mathbf{2}, \mathbf{1})_{(\bar{3}, \mathbf{1})}$
		$(\mathbf{1}, \mathbf{2}, \mathbf{2})_{\bar{2}}$	$(\mathbf{1}, \mathbf{2}, \mathbf{2})_{(0, \bar{2})}$

Table 1.2: Subsequent branching rules of the **27** of E_6 into representations of the maximal regular subalgebras from (1.43). The subscripts denote the $U(1)$ quantum numbers $2\sqrt{6}Q_\chi$ and $(2\sqrt{6}Q_{B-L}, 2\sqrt{6}Q_\chi)$, respectively.

a linear combination of traceless diagonal generators of $SU(6)$. We choose the conventional normalization

$$\text{tr}[T^a T^a] = \frac{1}{2} \tag{1.46}$$

for all $SU(N)$ generators, which leaves the E_6 generators normalized to three. In the subsequent decomposition of the E_6 algebra (1.43), $U(1)_\chi$ first appears in (1.43b). We now construct pseudo-projection matrices,⁴ such that they map the weights of $SU(6) \times SU(2)_L$ onto the weights of $SU(4) \times SU(2)_R \times SU(2)_L \times U(1)_\chi$

$$\begin{pmatrix} 1 & 0 & 0 & 0 & 0 & \bar{1} \\ \bar{1} & 1 & 0 & 0 & 0 & \bar{1} \\ 0 & \bar{1} & 1 & 0 & 0 & \bar{1} \\ 0 & 0 & \bar{1} & 1 & 0 & \bar{1} \\ 0 & 0 & 0 & \bar{1} & 1 & \bar{1} \\ 0 & 0 & 0 & 0 & \bar{1} & \bar{1} \end{pmatrix} \cdot \mathbf{P}_1 = \begin{pmatrix} 1 & 0 & 0 & 0 & \bar{1} & n_1 \\ \bar{1} & 1 & 0 & 0 & \bar{1} & n_1 \\ 0 & \bar{1} & 1 & 0 & \bar{1} & n_1 \\ 0 & 0 & \bar{1} & 0 & \bar{1} & n_1 \\ 0 & 0 & 0 & 1 & \bar{1} & n_2 \\ 0 & 0 & 0 & \bar{1} & \bar{1} & n_2 \end{pmatrix}. \tag{1.47}$$

The Dynkin coefficients of the $U(1)_\chi$ (quantum numbers) leave $SU(4) \times SU(2)^2$ invariant. From normalization according to (1.46) and the vanishing trace, we

⁴These matrices are introduced in [25] as “projection” matrices, although they are neither quadratic nor idempotent.

obtain $n_1 = 1/(2\sqrt{6})$, $n_2 = -1/\sqrt{6}$, yielding

$$\mathbf{P}_1 = \begin{pmatrix} 1 & 0 & 0 & 0 & 0 & \frac{1}{2\sqrt{6}} \\ 0 & 1 & 0 & 0 & 0 & \frac{1}{\sqrt{6}} \\ 0 & 0 & 1 & 0 & 0 & \frac{3}{2\sqrt{6}} \\ 0 & 0 & 0 & 0 & 0 & \frac{2}{\sqrt{6}} \\ 0 & 0 & 0 & 1 & 0 & \frac{1}{\sqrt{6}} \\ 0 & 0 & 0 & 0 & 1 & 0 \end{pmatrix}. \quad (1.48)$$

The same procedure can be repeated in the next step (1.43c) of the decomposition of the E_6 algebra in order to obtain the $U(1)_{B-L}$ charges. The pseudo projection matrix from the weights of $SU(4) \times SU(2)_R \times SU(2)_L \times U(1)_\chi$ onto those of $SU(3) \times SU(2)_R \times SU(2)_L \times U(1)_{B-L} \times U(1)_\chi$ reads

$$\mathbf{P}_2 = \begin{pmatrix} 1 & 0 & 0 & 0 & \frac{1}{2\sqrt{6}} & 0 \\ 0 & 1 & 0 & 0 & \frac{1}{\sqrt{6}} & 0 \\ 0 & 0 & 0 & 0 & \frac{3}{2\sqrt{6}} & 0 \\ 0 & 0 & 1 & 0 & 0 & 0 \\ 0 & 0 & 0 & 1 & 0 & 0 \\ 0 & 0 & 0 & 0 & 0 & 1 \end{pmatrix}. \quad (1.49)$$

The matrix mapping the weights of $SU(6) \times SU(2)_L$ directly onto the $SU(3) \times SU(2)_R \times SU(2)_L \times U(1)_{B-L} \times U(1)_\chi$ weights can be obtained from the composition of the pseudo-projection matrices:

$$\mathbf{P} \equiv \mathbf{P}_1 \mathbf{P}_2 = \begin{pmatrix} 1 & 0 & 0 & 0 & \frac{1}{2\sqrt{6}} & \frac{1}{2\sqrt{6}} \\ 0 & 1 & 0 & 0 & \frac{1}{\sqrt{6}} & \frac{1}{\sqrt{6}} \\ 0 & 0 & 0 & 0 & \frac{3}{2\sqrt{6}} & \frac{3}{2\sqrt{6}} \\ 0 & 0 & 0 & 0 & 0 & \frac{2}{\sqrt{6}} \\ 0 & 0 & 1 & 0 & 0 & \frac{1}{\sqrt{6}} \\ 0 & 0 & 0 & 1 & 0 & 0 \end{pmatrix}. \quad (1.50)$$

We define the $U(1)$ pseudo-projectors \mathbf{P}_{B-L} and \mathbf{P}_χ acting on the weight space of E_6 as the fifth and sixth column of \mathbf{P} from (1.50), respectively.

The $U(1)_{B-L}$ and $U(1)_\chi$ charges of all weights of E_6 representations (decomposed into $SU(6) \times SU(2)_L$ irreps) can be calculated using the above pseudo-projection matrices. The results for the **27** dimensional fundamental representation from figure 1.4 are summarized in table 1.3.

Looking at the $U(1)_{B-L}$ charges, we note that one can indeed consistently identify the charges with the difference of baryon and lepton number up to a normalization if the embedding of the particles is chosen accordingly. With the embedding

α_1	α_2	α_3	α_4	α_5	α_0	$\sqrt{\frac{8}{3}}Q_{B-L}$	$\sqrt{6}Q_\chi$	T_R^3	T_L^3	
1	0	0	0	0	-1	$\frac{1}{3}$	$\frac{1}{2}$	0	$-\frac{1}{2}$	Q_L
1	0	0	0	0	1	$\frac{1}{3}$	$\frac{1}{2}$	0	$\frac{1}{2}$	
-1	1	0	0	0	-1	$\frac{1}{3}$	$\frac{1}{2}$	0	$-\frac{1}{2}$	
-1	1	0	0	0	1	$\frac{1}{3}$	$\frac{1}{2}$	0	$\frac{1}{2}$	
0	-1	1	0	0	-1	$\frac{1}{3}$	$\frac{1}{2}$	0	$-\frac{1}{2}$	
0	-1	1	0	0	1	$\frac{1}{3}$	$\frac{1}{2}$	0	$\frac{1}{2}$	
0	0	-1	1	0	-1	-1	$\frac{1}{2}$	0	$-\frac{1}{2}$	L_L
0	0	-1	1	0	1	-1	$\frac{1}{2}$	0	$\frac{1}{2}$	
0	0	0	-1	1	-1	0	-1	$\frac{1}{2}$	$-\frac{1}{2}$	H^u
0	0	0	-1	1	1	0	-1	$\frac{1}{2}$	$\frac{1}{2}$	
0	0	0	0	-1	-1	0	-1	$-\frac{1}{2}$	$-\frac{1}{2}$	H^d
0	0	0	0	-1	1	0	-1	$-\frac{1}{2}$	$\frac{1}{2}$	
1	0	-1	0	0	0	$-\frac{2}{3}$	-1	0	0	D^c
-1	1	-1	0	0	0	$-\frac{2}{3}$	-1	0	0	
0	-1	0	0	0	0	$-\frac{2}{3}$	-1	0	0	
0	1	0	-1	0	0	$\frac{2}{3}$	-1	0	0	D
1	-1	1	-1	0	0	$\frac{2}{3}$	-1	0	0	
-1	0	1	-1	0	0	$\frac{2}{3}$	-1	0	0	
0	0	1	-1	1	0	1	$\frac{1}{2}$	$\frac{1}{2}$	0	e^c
0	1	-1	0	1	0	$-\frac{1}{3}$	$\frac{1}{2}$	$\frac{1}{2}$	0	d^c
1	-1	0	0	1	0	$-\frac{1}{3}$	$\frac{1}{2}$	$\frac{1}{2}$	0	
-1	0	0	0	1	0	$-\frac{1}{3}$	$\frac{1}{2}$	$\frac{1}{2}$	0	
0	0	1	0	-1	0	1	$\frac{1}{2}$	$-\frac{1}{2}$	0	ν^c
0	1	-1	1	-1	0	$-\frac{1}{3}$	$\frac{1}{2}$	$-\frac{1}{2}$	0	u^c
1	-1	0	1	-1	0	$-\frac{1}{3}$	$\frac{1}{2}$	$-\frac{1}{2}$	0	
-1	0	0	1	-1	0	$-\frac{1}{3}$	$\frac{1}{2}$	$-\frac{1}{2}$	0	
0	0	0	1	0	0	0	2	0	0	S

Table 1.3: Weights of the **27** of E_6 with $U(1)$ - and $T_3^{L/R}$ -charges obtained by projection with \mathbf{P} from (1.50). In the last column, the weights have been labeled by the corresponding particle names, based on the identification of $\sqrt{8/3}Q_{B-L}$ as baryon-lepton number and their $SU(2)$ quantum numbers. In the $SU(2)_R$ doublets up- and down-type fermions have been reversed corresponding to a standard model hypercharge operator $Y \propto \sqrt{\frac{3}{4}}Q_{B-L} + T_3^R$.

of the standard model particles into the **27** of E_6 from table 1.3, we find that there appears a vector-like pair of exotic particles that transform as triplets under $SU(3)$ while being singlets under $SU(2)_{L/R}$. Furthermore, we can identify a right-

handed neutrino ν^c . In addition, as Higgs and matter fields are unified in one representation, the accommodation of three generations of SM matter requires three $\mathbf{27}$'s, leading to three generations of NMSSM-like Higgs sectors, unless an additional mechanism is invoked that allows for a splitting into incomplete representations.

At this stage in the decomposition of the E_6 algebra (1.43c), the only additional contribution apart from $U(1)_{B-L}$ and $U(1)_\chi$ to the Abelian groups in the $U(1)'$ -extended NMSSM can arise from the diagonal operator T_3^R of $SU(2)_R$. On doublets under $SU(2)_R$ we are free to define whether up- or down-type fields have $T_3^R = +1/2$. We choose $T_3^R(d^c, e^c) = 1/2(d^c, e^c)$ which allows to identify the standard model hypercharge operator as:

$$Y_{\text{SM}} = \sqrt{\frac{3}{4}}Q_{B-L} + T_3^R \quad \Rightarrow \quad Y_{\text{GUT}} \equiv Y = \sqrt{\frac{3}{5}} \left(\sqrt{\frac{2}{3}}Q_{B-L} + T_3^R \right), \quad (1.51)$$

where Y_{GUT} denotes the hypercharge operator GUT-normalized according to (1.46). It is obvious from table 1.3, that the hypercharge cannot involve the $U(1)_\chi$ generator, as the NMSSM singlet S only carries $U(1)_\chi$ charge. On the other hand it is clear that the additional $U(1)'$ in (1.43d) has to include a share of $U(1)_\chi$ in order to fulfill the requirements formulated in the previous section. The values of the $U(1)'$ charges will generally be dependent on the symmetry breaking scenario, i.e. on the size of the gauge couplings⁵ as we shall develop in the following chapter.

1.4.4 Other Subalgebras of E_6

The above procedure of removing simple roots from the extended Dynkin diagram (figure 1.2) and eliminating the corresponding connections in the weight space diagram can be used to study the branching rules of the $\mathbf{27}$ of E_6 under arbitrary subalgebras. Two other maximal subalgebras of E_6 which will become relevant later in this work, when studying the extra-dimensional UV completion of our model, are $SU(3) \times SU(3) \times SU(3)$ and $SO(10) \times U(1)$. Their Dynkin diagrams are shown in figure 1.5. The decomposition of the $\mathbf{27}$ under these subalgebras is

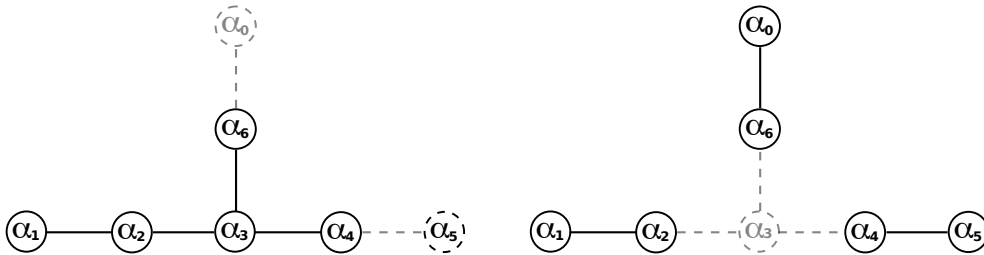


Figure 1.5: Dynkin diagrams of the maximal regular subalgebras $SO(10) \times U(1)_\chi$ (lhs) and $SU(3)^3$ (rhs) of E_6 .

⁵As it is the case in the standard model for the coupling of the Z -Boson to fermions.

summarized in table 1.4. Note, that the common subset of these two algebras is

$SO(10) \times U(1)_\chi$		$SU(3)^3$	
$\mathbf{16}_1$	$Q \oplus u^c \oplus d^c \oplus L \oplus \nu^c \oplus e^c$	$(\mathbf{3}, \bar{\mathbf{3}}, \mathbf{1})$	$Q \oplus D^c$
$\mathbf{10}_{\bar{2}}$	$H^u \oplus H^d \oplus D \oplus D^c$	$(\bar{\mathbf{3}}, \mathbf{1}, \mathbf{3})$	$u^c \oplus d^c \oplus D$
$\mathbf{1}_4$	S	$(\mathbf{1}, \mathbf{3}, \bar{\mathbf{3}})$	$H^u \oplus H^d \oplus L \oplus \nu^c \oplus e^c$

Table 1.4: Branching rules of the $\mathbf{27}$ of E_6 into representations of the maximal regular subalgebras $SO(10) \times U(1)_\chi$ and $SU(3)^3$. The subscripts denote $2\sqrt{6}Q_\chi$.

the *left-right* (LR) group from (1.43c). This can easily be verified by folding the Dynkin diagrams from figure 1.5⁶.

1.5 PSSSM

In the previous section, we investigated the extension of the particle spectrum that goes hand in hand with the $U(1)'$ -extended gauge sector, as required by anomaly cancellation. The additional particles contribute to the RG evolution of the coupling constants (1.36), unfortunately not preserving the beautiful unification of all couplings as in the (N)MSSM (figure 1.1). The RG evolution of the gauge couplings with supersymmetric E_6 particle content is shown in figure 1.6. In [27] it was proposed and in [28, 29] realized that gauge coupling unifica-

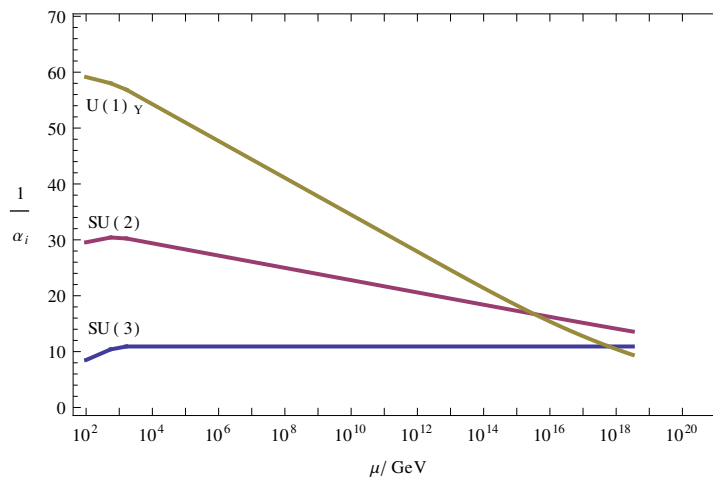


Figure 1.6: RG evolution of the gauge couplings with matter filling three generations of $\mathbf{27}$ dimensional representations of E_6 .

⁶The assignment of the simple roots generating $SU(2)$ algebras then differs from the choice in figure 1.3, but this amounts only to a basis change, which leaves all derived quantities such as $U(1)$ quantum numbers unchanged.

tion can be restored if the gauge interactions underwent a phase transition at an intermediate scale Λ_{int} to a Pati-Salam (PS) [30] symmetric phase

$$SU(4) \times SU(2)_L \times SU(2)_R \times U(1)_\chi. \quad (1.52)$$

The intermediate gauge symmetry implies the unification of quarks and leptons into one four dimensional representation of $SU(4)$, which we denote as $Q_{L/R}$.⁷ The exotic color triplet fields D and D^c are assembled to form a single real representation $\mathbf{6}$ of $SU(4)$, which we simply call D . In addition $SU(2)_R$ requires the unification of the right-handed matter fields into doublets, analogous to the left-handed standard model doublets,⁸ as well as the integration of the MSSM Higgs doublets into a $(\mathbf{2}, \mathbf{2})$ representation H under the two $SU(2)$ groups.

The unification scenario is based on the observation that the hypercharge generator (1.51) is contained in $SU(4) \times SU(2)_R$, as T_{B-L} is among the Cartan generators of $SU(4)$. Hence, when extending the standard model symmetry group to the PS group at a scale where the resulting coupling g_{2R} of $SU(2)_R$ equals the weak coupling g_{2L} , only two couplings g_4 of $SU(4)$ and $g_2 \equiv g_{2L} \equiv g_{2R}$ will have independent RG evolutions. The two couplings unify close to the Planck scale as can be seen in figure 1.7. Note, that $U(1)_\chi$ is orthogonal to all standard model gauge groups (in the sense of the argumentation at the end of the previous section) and hence does not interfere with their running at leading order. The RG flow for the coupling constant of the additional Abelian gauge groups $U(1)_\chi, U(1)'$ is determined by matching the coupling constants at Λ_{E_6} and Λ_{int} , respectively. This was done in [28, 29], but at this point the details are not relevant to our argumentation. We only keep in mind that there is an additional $U(1)'$ providing the quartic D -term of the standard model singlet S , stabilizing the Higgs potential.

At the intermediate scale a vev in the direction of the right-handed neutrino in group space of some vector like pair of fields $H_{\text{int}}, \bar{H}_{\text{int}}$ transforming as $\mathbf{27}$ and $\bar{\mathbf{27}}$, breaks the intermediate PS symmetry to the standard model. As the right-handed neutrino does not feel any gauge interactions below Λ_{int} , a Majorana mass term $m_{\nu^c} \sim \Lambda_{\text{int}}$ could trigger a *see-saw mechanism* [31] effecting the light neutrino masses. Unfortunately, the intermediate scale in these scenarios turns out to be so large (see figure 1.7) that the neutrino masses would become too small [32].

The minimal superpotential in the E_6 symmetric phase above Λ_{E_6} including all interactions required to yield a viable phenomenology is contained in a single term (per matter generation)

$$W_{E_6} = \mathbf{Y}^{E_6} \mathbf{1}_s \subset \mathbf{Y}^{E_6} \mathbf{27} \otimes \mathbf{27} \otimes \mathbf{27}. \quad (1.53)$$

The singlet from the above tensor product can be decomposed under the inter-

⁷We will try to always clarify the context in which fields with non-unique denotations appear.

⁸This implies the presence of a right-handed neutrino field.

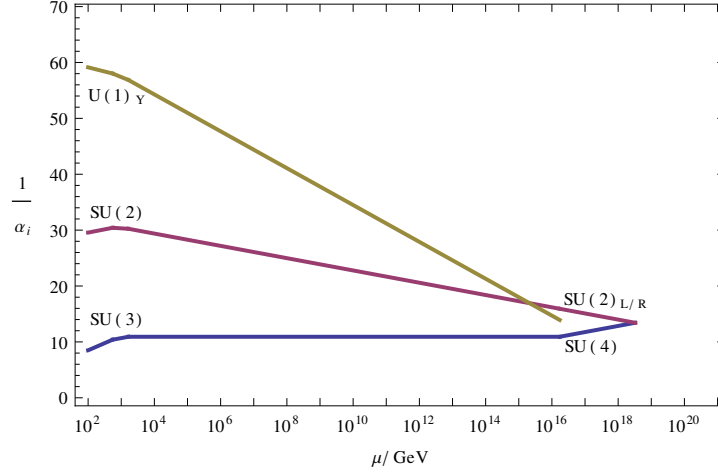


Figure 1.7: Gauge unification in the PSSSM. Above $\Lambda_{\text{int}} \approx 10^{16}$ GeV the gauge symmetry is extended to the Pati-Salam group (1.52). The couplings unify at $\Lambda_{E_6} \approx 3.3 \times 10^{18}$ GeV.

mediate PS symmetry (1.52) into

$$\begin{aligned}
 W_{\text{PS}} = & \mathbf{Y}^Q Q_L H Q_R \\
 & + \mathbf{Y}^{DQ_R} D Q_R Q_R + \mathbf{Y}^{DQ_L} D Q_L Q_L \\
 & + \mathbf{Y}^{SD} S D D + \mathbf{Y}^{SH} S H H.
 \end{aligned} \tag{1.54}$$

The E_6 -invariant superpotential is determined by only one coupling constant, which determines the size of the Yukawa couplings in (1.54) at the scale where E_6 is broken to the intermediate symmetry. In terms of the representations of the standard model gauge group the superpotential reads (with an appropriate re-definition of the Yukawa couplings absorbing possible signs and rational factors from the Clebsch-Gordan decomposition)

$$\begin{aligned}
 W_{\text{PSSSM}} = & \mathbf{Y}^u u^c H^u Q + \mathbf{Y}^d d^c Q H^d + \mathbf{Y}^e e^c L H^d [+ \mathbf{Y}^{\nu^c} \nu^c H^u L] \\
 & + \mathbf{Y}_1^{D^c} D^c d^c u^c + \mathbf{Y}_1^D D u^c e^c [+ \mathbf{Y}_2^D D d^c \nu^c] + \mathbf{Y}_3^D D Q Q + \mathbf{Y}_2^{D^c} D^c L Q \\
 & + \mathbf{Y}^{SD} S D^c D + \mathbf{Y}^{SH} S H^u H^d.
 \end{aligned} \tag{1.55}$$

Terms involving the right-handed neutrino superfield ν^c are integrated out below the intermediate scale and hence do not contribute to the superpotential interactions at the TeV scale.

There are various points that need to be addressed regarding (1.55):

- Terms of the form $u^c d^c d^c$, $Q L d^c$, $L L e^c$, or $H^u L$ which in the (N)MSSM have to be forbidden by means of the additional R -parity in order to render the proton stable, are automatically absent from the superpotential in this theory. These terms are not contained in the singlet from (1.53) and as

SUSY prevents new superpotential terms to get introduced by means of the RG flow they are absent at all scales in this theory.

- There are leptoquark and diquark couplings \mathbf{Y}_i^D and $\mathbf{Y}_i^{D^c}$ present in the superpotential (1.55), which in combination introduce rapid proton decay, as they would allow the proton to decay into a meson and a lepton. At the level of the intermediate gauge symmetry, quarks and leptons are contained in the same multiplets Q_L and Q_R , which implies that at this stage there is no distinction among the lepto- and di-quark couplings in \mathbf{Y}^{DQ_R} and \mathbf{Y}^{DQ_L} . Hence, neither one of them can be set to zero independent from the other. Requiring them both to vanish would render the exotic particles stable, resulting in baryonic dark matter [33]. Both couplings could be chosen to be sufficiently small to insure proton stability [28]

$$\mathbf{Y}_i^D \sim \mathbf{Y}_i^{D^c} \sim 10^{-14}, \quad \forall i, \quad (1.56)$$

but it is not plausible how these couplings could unify with e.g. the top-Yukawa coupling $\mathbf{Y}^t \sim 1$ at the Λ_{E_6} as required by E_6 invariance of (1.53).

- So far we have not addressed the fact that the superpotential has to accommodate three generations of matter, which according to E_6 -invariance also implies the presence of three Higgs field generations. Although the Higgs fields can be rotated in family space that only one generation acquires vevs, the other two generations generally couple to the matter fields as well, which would cause dangerous flavor-changing neutral currents (FCNC) as discussed in [34]. Forbidding the couplings of the non-vev Higgs generations renders the theory invariant under a Z_2 -symmetry, denoted as H -parity [34].

Unfortunately this not compatible with the E_6 symmetric superpotential: The singlet in the tensor product from (1.53) is completely symmetric in all three $\mathbf{27}$'s, meaning that if the undesired terms are forbidden, the entire superpotential has to vanish.

In the light of the above arguments, it is clear that the unification to E_6 within this model, although nicely bringing together a $U(1)'$ -extension of the standard model gauge group with supersymmetric gauge coupling unification, comes at the price of severe inconsistencies with established experimental observations, namely the proton stability and the absence of sizable flavor-changing neutral currents.

Chapter 2

Local E_6 Unification with Intermediate Left-Right Symmetry

The lesson learned in the studies presented in the previous chapter is that it is unclear, how a viable TeV-scale phenomenology could originate from an E_6 invariant superpotential (1.53), although the unification to E_6 can be realized in the gauge sector [27, 28, 29]. Furthermore, the expedience of the Pati-Salam gauge group (1.52) serving as intermediate symmetry group is dubious in this setting: The dangerous co-existence of leptoquark- (2.1a) and diquark-like (2.1b) couplings of the color-triplet exotics D, D^c

$$\mathbf{Y}_1^D D u^c e^c, \quad \mathbf{Y}_2^D D d^c \nu^c, \quad \mathbf{Y}_2^{D^c} D L Q, \quad (2.1a)$$

$$\mathbf{Y}_1^{D^c} D^c d^c u^c, \quad \mathbf{Y}_3^D D Q Q \quad (2.1b)$$

leading to unacceptable decay channels of the proton into light mesons and leptons, cannot be inhibited at the stage of the PS-invariant superpotential¹ (1.54). In the remainder of the work presented here, we shall therefore abandon the notion of E_6 as unified gauge group in the context of a quantum field theory in four spacetime dimensions and the Pati-Salam group as intermediate symmetry group.

Instead, we will first develop a gauge coupling unification scenario based on

$$SU(3) \times SU(2)_L \times SU(2)_R \times U(1)_{B-L} \times U(1)_\chi \quad (2.2)$$

as intermediate symmetry [35],² allowing to include leptoquark couplings (2.1a) while suppressing the diquark interactions (2.1b) in this phase (or vice versa). Furthermore, the corresponding superpotential can be chosen in a way consistent with an H -parity, effecting the absence of FCNC at the tree-level.

After the presentation of the unification of the gauge couplings in four spacetime dimensions we shall present a six-dimensional *orbifold* setting suited to produce the 4D scenario after compactification of the additional two dimensions. The gauge group in the *bulk* of the extra dimensions will again be E_6 .

2.1 Gauge Coupling Unification

Having chosen a reduced degree of symmetry in the intermediate phase, namely $SU(3)$ instead of $SU(4)$ does not allow to reduce the number of independently running couplings above the intermediate scale, as in the PSSSM. The Cartan

¹See the discussion at the end of the previous chapter.

²There are also ways to accomplish gauge coupling unification in $U(1)$ -extended SUSY models, that do not involve an intermediate symmetry breaking scale in the context of E_6 as GUT group [36]. These models require the presence of incomplete E_6 vector-like representations at the TeV scale in order to compensate the malign effects of the matter from the **27** (see figure 1.6.).

generator of $SU(4)$ not contained in its $SU(3)$ subgroup has to be added to the gauge group in terms of $U(1)_{B-L}$. We shall at first ignore the Abelian groups $U(1)'$ and $U(1)_\chi$ as we do not know the boundary condition at any low scale to RG evolve the respective coupling constants up to high scales. But, since we still expect gauge coupling unification at some scale Λ_{uni} , the size of the additional couplings will be determined by their RG evolution down from that scale.

The couplings of the remaining low energy gauge groups have to be matched to the coupling constants of the intermediate group at some scale Λ_{int} via

$$\begin{aligned} g_{B-L} \Big|_{\Lambda_{\text{int}}} &= \frac{\sqrt{2}g_2g_Y}{\sqrt{5g_2^2 - 3g_Y^2}} \Big|_{\Lambda_{\text{int}}} \\ g_{2R} \Big|_{\Lambda_{\text{int}}} &= g_2 \Big|_{\Lambda_{\text{int}}}. \end{aligned} \quad (2.3)$$

The matching conditions of the strong coupling and g_2 , denoted as g_{2L} above Λ_{int} are trivial. The RG evolution above that scale is dependent on the choice of the particle content that is responsible for the breaking of the intermediate symmetry. In the case of the PSSSM, a vector-like pair of $\mathbf{27}, \overline{\mathbf{27}}$ could account for this. Unfortunately, this is not the case for the LR gauge group (2.2) anymore: As shown in figure 2.1 (top), the introduction of intermediate matter $H_{\text{int}}, \overline{H}_{\text{int}}$ filling a $\mathbf{27}, \overline{\mathbf{27}}$ of E_6 , causes the strong coupling constant to become non-perturbative below a possible unification scale. In the absence of intermediate matter, the gauge couplings would unify far above the Planck-scale, as can be seen in the second plot of figure 2.1.³

At this stage, we make use of the freedom to introduce intermediate matter forming incomplete E_6 representations, in order to accomplish gauge coupling unification. The intermediate matter must contain the fields transforming as the right-handed neutrino to effect a suitable breaking mechanism as in the PSSSM. Furthermore, it should be left-right symmetric, in order to preserve the identical running of g_{2L} and g_{2R} above Λ_{int} . The minimal choice meeting these criteria is

$$H_{\text{int}} \sim (\mathbf{1}, \mathbf{2}, \mathbf{1})_{(\overline{\mathbf{3}}, \mathbf{1})} \oplus (\mathbf{1}, \mathbf{1}, \mathbf{2})_{(\mathbf{3}, \mathbf{1})} \sim L \oplus e^c \oplus \nu^c, \quad (2.4a)$$

where the bold-face entries denote the transformation behavior under $SU(3) \times SU(2)_L \times SU(2)_R$ and the subscripts the Abelian charges $2\sqrt{6}Q_{B-L}, 2\sqrt{6}Q_\chi$, respectively. Alternatively, one can also include the remaining color-singlets contained in the $\mathbf{27}$ (including colored particles usually drives the strong coupling into a Landau pole, before unification can occur):

$$\begin{aligned} H_{\text{int}} &\sim (\mathbf{1}, \mathbf{1}, \mathbf{2})_{(Q_\chi^L, Q_{B-L}^L)} \oplus (\mathbf{1}, \mathbf{2}, \mathbf{1})_{(Q_\chi^L, Q_{B-L}^L)} \\ &\oplus (\mathbf{1}, \mathbf{2}, \mathbf{2})_{(Q_\chi^H, Q_{B-L}^H)} \oplus (\mathbf{1}, \mathbf{1}, \mathbf{1})_{(Q_\chi^S, Q_{B-L}^S)} \\ &\sim L \oplus e^c \oplus \nu^c \oplus H^u \oplus H^d \oplus S \sim (\mathbf{1}, \overline{\mathbf{3}}, \overline{\mathbf{3}}) \quad \text{of } SU(3)^3. \end{aligned} \quad (2.4b)$$

³The meaning of the unification without having additional matter to provide the vev breaking the intermediate symmetry remains unclear, irrespective of whether or not the couplings unify below the Planck-scale.

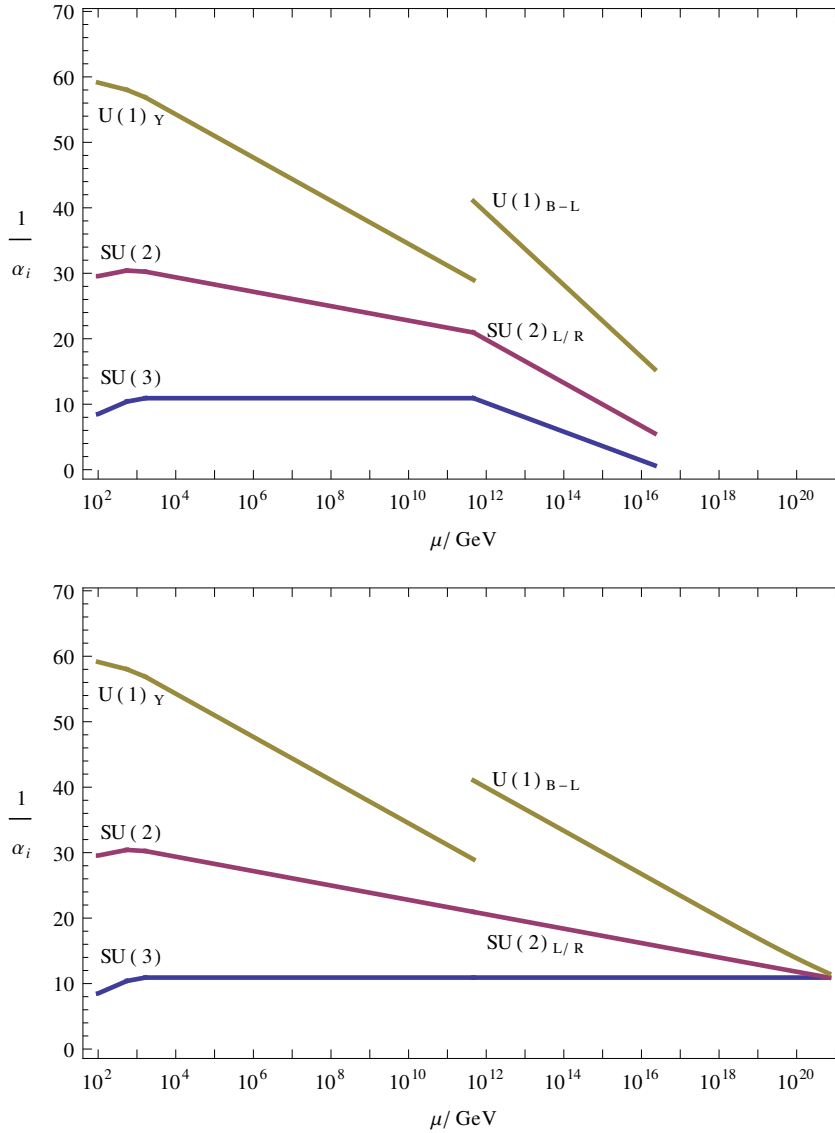


Figure 2.1: The gauge coupling RG flow featuring three full $\mathbf{27}$ multiplets of E_6 , with intermediate LR symmetry (2.2). The intermediate particle content furnishes a $\mathbf{27}, \overline{\mathbf{27}}$ (top), or is absent (bottom) altogether.

Unlike in the PSSSM, the matching conditions (2.3) do not over-constrain the couplings at the intermediate scale, leaving Λ_{int} a free parameter to play with in order to achieve unification of g_3, g_{2L} determining Λ_{uni} . An optimization algorithm starts from an initial guess for Λ_{int} , running up the couplings constants until $g_3 = g_{2L/R}$ which occurs for any choice of intermediate particle content from (2.4) eventually, yielding a guess for Λ_{uni} . Then $g_{B-L}|_{\Lambda_{\text{uni}}}$ is evaluated and optimized to $g_{B-L} = g_3 = g_{2L/R} \equiv g_{\text{uni}}$ iteratively. The resulting unification sce-

narios for both choices of intermediate matter are displayed in figure 2.2. At this

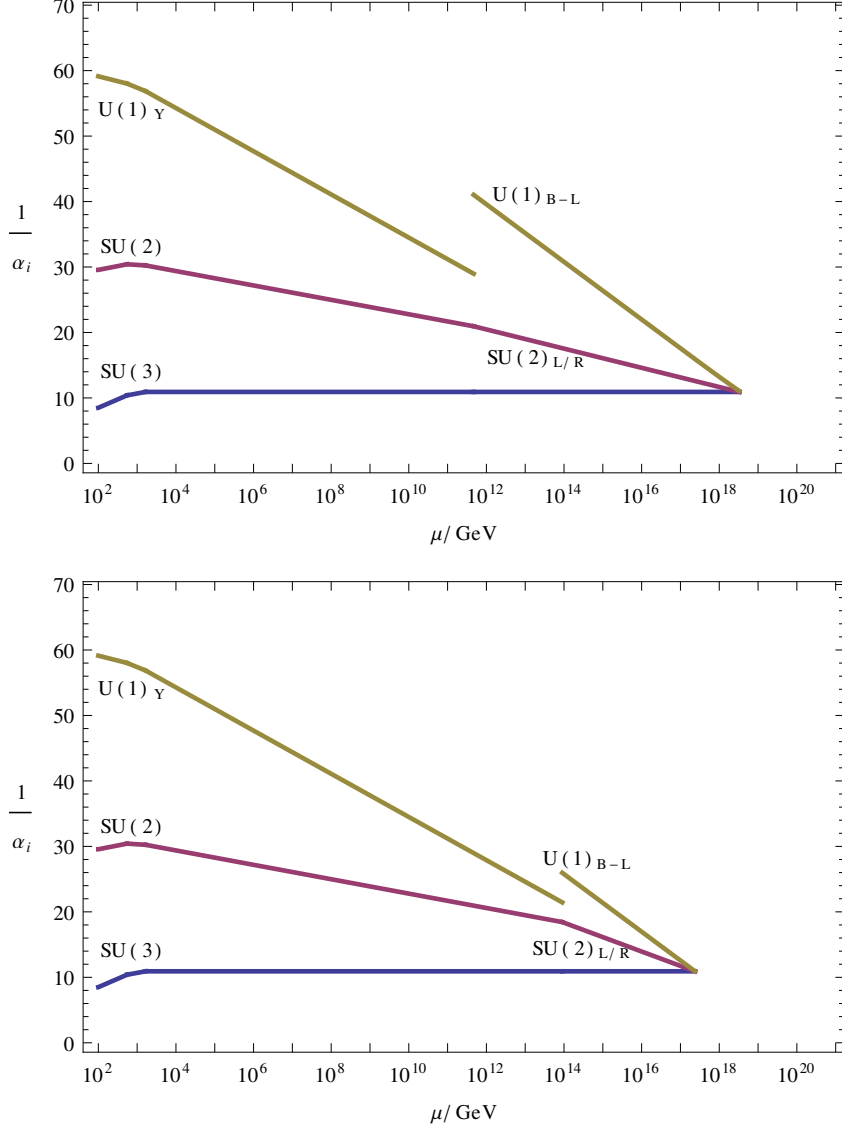


Figure 2.2: Unification scenarios at 1-loop with matter in complete E_6 multiplets and intermediate breaking with combinations of incomplete vector-like Higgs representations (2.4a) (top) and (2.4b) (bottom). The scale hierarchy is: $\Lambda_{\text{int}} = 5.35 \times 10^{11}\text{GeV}$, $\Lambda_{\text{uni}} = 3.38 \times 10^{18}\text{GeV}$ (top) and: $\Lambda_{\text{int}} = 9.91 \times 10^{13}\text{GeV}$, $\Lambda_{\text{uni}} = 2.49 \times 10^{17}\text{GeV}$ (bottom).

point, one can set $g_\chi|_{\Lambda_{\text{uni}}} = g_{\text{uni}}$ and run the couplings down to the intermediate scale, where – in addition to (2.3) – one needs the matching condition for the second $U(1)$ gauge group below Λ_{int} . Conventionally, one would diagonalize the (intermediate) gauge boson mass term

$$|(D_\mu H_{\text{int}})|^2, \quad (2.5a)$$

where

$$\langle D_\mu H_{\text{int}} \rangle \equiv -i (g_{2R} Q_R^{\nu c} A_\mu^R + g_{B-L} Q_{B-L}^{\nu c} A_\mu^{B-L} + g_\chi Q_\chi^{\nu c} A_\mu^\chi) \langle H_{\text{int}} \rangle, \quad (2.5b)$$

setting one of the massless modes to be A_μ^Y and choosing the other A'_μ orthogonal such that mixing gauge kinetic terms vanish (at the tree-level):

$$F'^{\mu\nu} F_{\mu\nu}^Y = 0. \quad (2.5c)$$

In this basis however, the particles charged under both $U(1)'$ and $U(1)_Y$ re-introduce a mixing of gauge kinetic terms through quantum corrections, originating from diagrams like

$$\text{Diagram} \propto g_Y g' \text{tr}[Q' Q_Y] \quad (2.6)$$

at the one-loop level. This is a general phenomenon, whenever there are several $U(1)$ groups involved: Unless the particle content running in the loop furnishes complete representations of a simple Lie-algebra, a mixing occurs already at the one-loop level. From the two-loop level on, the Yukawa couplings contribute to the beta function of gauge bosons. These have an independent algebraic structure, causing mixing among wave-function renormalizations proportional to the differences of the involved Yukawa couplings.

Note, that above Λ_{int} there is no mixing among the gauge kinetic terms of the two $U(1)$ gauge bosons at the one-loop level: The matter is assembled into complete E_6 representations, and neither of the two choices of intermediate particle content from (2.4) gives rise to mixing as

$$\text{tr}_R[Q_{B-L} Q_\chi] = 0. \quad (2.7)$$

The left- and right-handed doublets are oppositely charged under $U(1)_{B-L}$ and they carry the same $U(1)_\chi$ charge, resulting in (2.7). The inclusion of Higgs and/or singlet components into the intermediate particle content does not alter this result, since these fields carry neither lepton nor baryon number.

2.1.1 $U(1)$ Mixing Below the Intermediate Scale

The general concept dealing with the loop-induced appearance of off-diagonal gauge kinetic terms [37] introduces off-diagonal $U(1)$ coupling constants g^{ab} , such that contributions as in figure B.1 determine the RG evolution of g^{ab} .

At the one-loop level however, it is possible in our case to avoid the introduction of off-diagonal couplings by choosing a suitable basis for the two $U(1)$ generators in group space [38].

Before we engage in constructing the correct basis, where no mixing terms appears at the one-loop level, we shall briefly review the scheme that we had introduced

in [35], in order to underline the significance of the construction we will use here: In our previous work the second $U(1)$ group was defined according to (2.5) at the intermediate scale and then an orthogonal matrix O was introduced such that

$$O^T \begin{pmatrix} g_Y g_Y \text{tr}[Q_Y Q_Y] & g_Y g' \text{tr}[Q_Y Q'] \\ g' g_Y \text{tr}[Q' Q_Y] & g' g' \text{tr}[Q' Q'] \end{pmatrix} O \equiv \begin{pmatrix} g_A^2 \text{tr}[Q_A^2] & 0 \\ 0 & g_B^2 \text{tr}[Q_B^2] \end{pmatrix}. \quad (2.8)$$

This notion is somewhat misleading, as the charges Q' defined at Λ_{int} do not correspond to the charges of the heavy gauge boson from the additional $U(1)$ broken around the TeV scale (independent of whether or not one neglects its mixing with the Z -Boson after electroweak symmetry breaking). This can be traced most easily in the picture using a third coupling constant, that parametrizes the mixing of the un-rotated $U(1)$ factors: After the couplings evolved down to the $U(1)'$ breaking scale from the intermediate scale, there would be a kinetic mixing term proportional to g_{YX} . When a field with non-zero charge under $U(1)'$ and vanishing hypercharge (as the NMSSM-like S -field in our scenario) acquires a vev, $U(1)_Y \times U(1)'$ is broken to $U(1)_Y$, but the orthogonal (then massive) state cannot be $U(1)'$ as the basis has to be changed in order to rotate the mixing ($\propto g_{YX}$) away.

Therefore, we technically abandon the notion of the intermediate LR symmetry (1.43c) being broken at Λ_{int} to

$$SU(3) \times SU(2)_L \times U(1)_Y \times U(1)' \quad (2.9)$$

and introduce a symmetry breaking scenario that actually works in three steps

$$\begin{array}{l} SU(3) \times SU(2)_L \times SU(2)_R \times U(1)_{B-L} \times U(1)_\chi \\ \xrightarrow{\Lambda_{\text{int}}} SU(3) \times SU(2)_L \times U(1)_A \times U(1)_B \\ \xrightarrow{M_{Z'}} SU(3) \times SU(2)_L \times U(1)_Y \quad [\times U(1)'], \end{array} \quad (2.10)$$

where in the last step $U(1)'$ denotes the broken gauge group corresponding to the heavy extra Z' boson. At this point we have to specify the construction of the bases for $U(1)_{A/B}$. The charges Q_A and Q_B will turn out to be dependent on the values of the coupling constants g_{2R} , g_{B-L} , and g_χ at the intermediate scale and therefore do not take rational values. The new basis for the $U(1)$ -generators in group space can be most easily found using the projection matrices introduced in (1.50). Let us define \mathbf{P}_{B-L} , \mathbf{P}_χ and $2\mathbf{P}_R$ (normalizing the eigenvalues of T_R^3 to $\pm 1/2$) as the fifth, sixth, and third column of \mathbf{P} . Then the projectors acting on the weight space of $\mathbf{27}$ onto the new $U(1)$ charges have to satisfy⁴

$$\begin{aligned} g_A \mathbf{P}_A &= \kappa_{B-L}^A g_{B-L} \mathbf{P}_{B-L} + \kappa_\chi^A g_\chi \mathbf{P}_\chi + \kappa_R^A g_{2R} \mathbf{P}_R \\ g_B \mathbf{P}_B &= \kappa_{B-L}^B g_{B-L} \mathbf{P}_{B-L} + \kappa_\chi^B g_\chi \mathbf{P}_\chi + \kappa_R^B g_{2R} \mathbf{P}_R \\ g_C \mathbf{P}_C &= \kappa_{B-L}^C g_{B-L} \mathbf{P}_{B-L} + \kappa_\chi^C g_\chi \mathbf{P}_\chi + \kappa_R^C g_{2R} \mathbf{P}_R, \end{aligned} \quad (2.11a)$$

⁴This is equivalent to the condition of continuity of the covariant derivative at Λ_{int} .

where C labels the neutral current part of the gauge bosons that are rendered heavy in the course of symmetry breaking at the intermediate scale. In order to determine \mathbf{P}_A , \mathbf{P}_B , and \mathbf{P}_C , we have to eliminate the twelve free parameters $\{\kappa_j^i\}$, g_A, g_B, g_C from (2.11a). We again make use of the fact that all the $U(1)$ factors appearing at different stages of our model can be embedded into $SU(6)$ via the construction shown in chapter 1.4. For normalization, we use the weight space representation of the fundamental representation of $SU(6)$ from (1.45). The constraints applied to (2.11a) then read:

1. The right-handed neutrino is not charged under the unbroken $U(1)$ factors:

$$(0, 0, 1, 0, -1, 0) \cdot \mathbf{P}_i = 0 \quad i = A, B; \quad (2.11b)$$

2. GUT normalization:

$$\left| \left(\mathbf{6} \right)_{SU(6)} \cdot \mathbf{P}_i \right|^2 = \frac{1}{2} \quad i = A, B, C; \quad (2.11c)$$

3. Vanishing mixing at the one-loop level:

$$\begin{aligned} \text{tr}[Q_A Q_B] &= 0 \\ \Leftrightarrow \left(\left(\mathbf{6} \right)_{SU(6)} \cdot \mathbf{P}_A \right) \cdot \left(\left(\mathbf{6} \right)_{SU(6)} \cdot \mathbf{P}_B \right) &= 0 \end{aligned} \quad (2.11d)$$

4. Orthogonal transformations of the gauge fields

$$(A_\mu^A, A_\mu^B, A_\mu^C) = (A_\mu^{B-L}, A_\mu^X, A_\mu^R) \kappa^T, \quad \text{with } \kappa_j^i \kappa_j^k = \delta^{ik} \quad (2.11e)$$

Solving the above equations (numerically) yields the matching conditions of couplings at the intermediate scale and provides the projectors to calculate the charges of the matter from table 1.3 under $U(1)_A$ and $U(1)_B$, enabling us to evolve the gauge coupling constants from Λ_{int} to the scale $\langle S \rangle$, where the gauge group is broken to the standard model as in the last step of (2.10). The requirement that the S -field carries zero charge under the remaining unbroken $U(1)$ uniquely determines that group (up to a sign) to be the linear combination of $U(1)_A$ and $U(1)_B$ that is identical to the standard model hypercharge as given in (1.51) in terms of $U(1)_{B-L}$ and T_R^3 . The matching conditions at the scale where the additional $U(1)$ gauge group is broken read

$$\begin{aligned} g_Y \mathbf{P}_Y &= \kappa_A^Y g_A \mathbf{P}_A + \kappa_B^Y g_B \mathbf{P}_B \\ g' \mathbf{P}' &= \kappa_A' g_A \mathbf{P}_A + \kappa_B' g_B \mathbf{P}_B. \end{aligned} \quad (2.12a)$$

Here \mathbf{P}' denotes the pseudo-projector on the broken $U(1)'$ charges, determining the coupling strength of matter to the heavy Z' boson. There are in total six free parameters in (2.12a). These are eliminated by applying the following set of constraints:

1. The standard model singlet S is not charged under the unbroken $U(1)$:

$$(0, 0, 0, 1, 0, 0) \cdot \mathbf{P}_Y = 0 \quad (2.12b)$$

2. GUT normalization:

$$\left| \left| (\mathbf{6})_{SU(6)} \cdot \mathbf{P}_i \right| \right|^2 = \frac{1}{2} \quad i = Y, t; \quad (2.12c)$$

3. Orthogonal transformation of the gauge fields

$$(A_\mu^Y, A'_\mu) = (A_\mu^A, A_\mu^B) \kappa^T, \quad \text{with } \kappa_j^i \kappa_j^k = \delta^{ik} \quad (2.12d)$$

After matching g_Y at the $U(1)'$ breaking scale (for this scale, we made the ansatz $M_{Z'} = 1.5$ TeV for the gauge unification scenario, in order to match the constraints from electroweak precision data [39] and collider searches [40]; the quantities derived from gauge coupling unification, such as Q' -charges and the g' -coupling only exhibit a very weak dependence on the choice of the Z' scale), the couplings can be evolved down to M_Z , where we note, that the value of $g_Y|_{M_Z}$ has been altered compared to the value we originally started from in figure 2.2, due to the mixing of the $U(1)$ groups between Λ_{int} and $M_{Z'}$. This means that the intermediate and the unification scale have to be adjusted such that $g_Y|_{M_Z}$ agrees with its experimentally measured value. This is done by an iteration that defines Λ_{uni} as the crossing of g_3 and $g_{2L/R}$ while running up and evolves all coupling constants down from that value, optimizing g_Y as a function of the intermediate scale. The full coupling unification scenario is displayed in figure 2.3 for the two choices of intermediate matter (2.4). We can see that size of the intermediate and unification scale differs for the two unification scenarios: With intermediate particle content from (2.4a) the scale hierarchy is (see figure 2.3 (top))

$$\Lambda_{\text{int}} = 2.34 \times 10^{11} \text{GeV}, \quad \Lambda_{\text{uni}} = 2.75 \times 10^{18} \text{GeV} \quad (2.13a)$$

whereas the extension of the intermediate particle content including a set of NMSSM-like Higgs fields (2.4b) reduces the distance between the two scales and lowers the absolute value of the unification scale:

$$\Lambda_{\text{int}} = 3.63 \times 10^{13} \text{GeV}, \quad \Lambda_{\text{uni}} = 1.51 \times 10^{17} \text{GeV}. \quad (2.13b)$$

The two choices of matter that breaks the intermediate symmetry which were presented in (2.4) are not unique. In fact, combinations of them lead to viable unification scenarios as well, as we had shown in [35]. Generally, a larger intermediate particle content pulls the intermediate and unification scale closer together.

The charges of all particles under $U(1)_A, U(1)_B$ and $U(1)'$ for the two unification scenarios are given in table 2.1. The $U(1)_{A,B}$ charges therein are not of great physical importance, but as argued at the beginning of this section they are

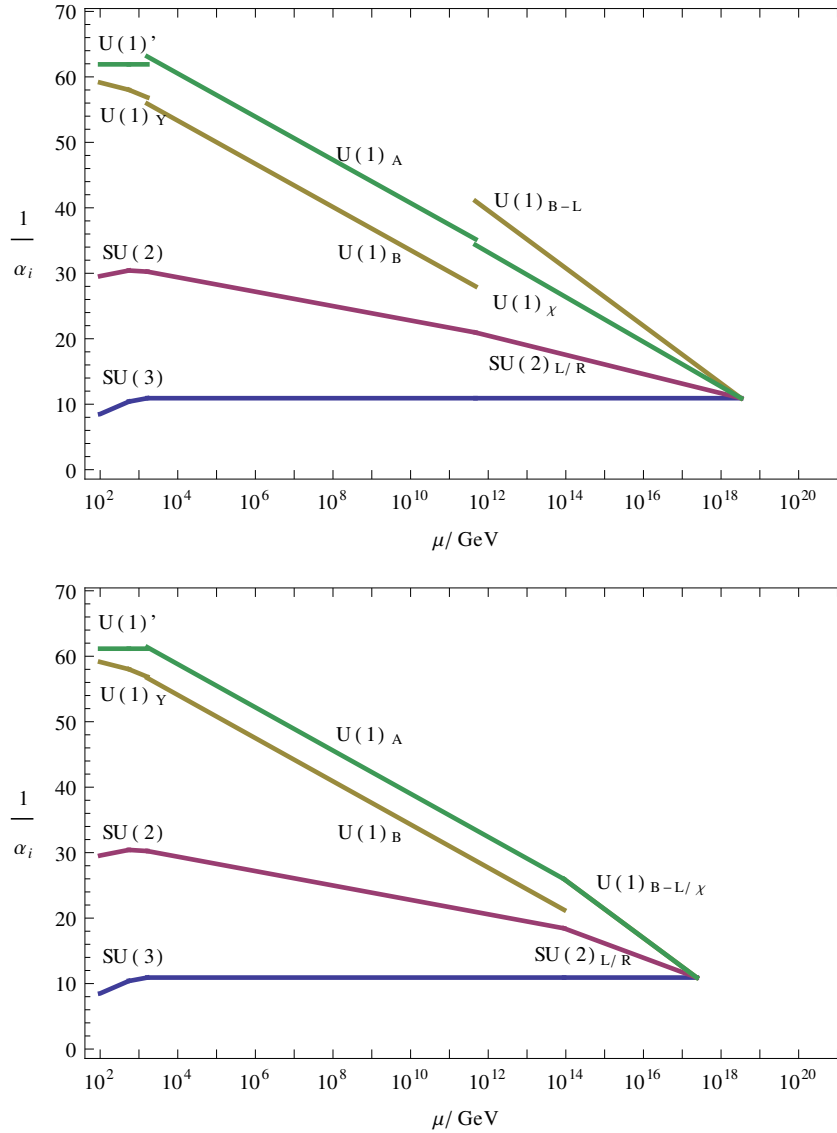


Figure 2.3: Full unification scenarios at one-loop with matter in complete E_6 multiplets and intermediate breaking vector-like Higgs representations $H_{\text{int}}, \bar{H}_{\text{int}}$ according to (2.4a) and (2.4b) at the top and bottom, respectively.

essential for the correct determination of the $U(1)'$ charges of the Z' boson to all matter.

For completeness, we also summarize the rotation matrices parametrizing the change of $U(1)$ basis according to (2.11) at the intermediate scale (κ_{int}) and (2.12) at the Z' -scale ($\kappa_{M_{Z'}}$). These, of course, depend on the form of the intermediate

	(i)			(ii)		
	Q_A	Q_B	Q'	Q_A	Q_B	Q'
Q_L	0.100	-0.178	-0.164	0.129	-0.158	-0.160
u^c	0.336	0.422	-0.136	0.258	0.474	-0.150
d^c	0.200	-0.356	-0.327	0.258	-0.316	-0.320
L_L	0.436	0.244	-0.299	0.387	0.316	-0.310
e^c	-0.137	-0.779	-0.191	0.000	-0.791	-0.171
ν^c	0.000	0.000	0.000	0.000	0.000	0.000
D	-0.536	-0.066	0.463	-0.516	-0.158	0.470
D^c	-0.200	0.356	0.327	-0.258	0.316	0.320
H^d	-0.299	0.534	0.491	-0.387	0.474	0.481
H^u	-0.436	-0.244	0.299	-0.387	-0.316	0.310
S	0.736	-0.290	-0.790	0.775	-0.158	-0.790

Table 2.1: Unification scheme dependent $U(1)$ charges.

particle content. For H_{int} from (2.4a), they read

$$\begin{aligned} \kappa_{\text{int}} &= \begin{bmatrix} -0.445 & -0.106 & 0.889 \\ -0.626 & -0.673 & -0.393 \\ -0.640 & 0.732 & -0.233 \end{bmatrix}, \\ \kappa_{M_{Z'}} &= \begin{bmatrix} -0.922 & 0.386 \\ -0.386 & -0.922 \end{bmatrix}, \end{aligned} \quad (2.14)$$

while in the second unification scenario with intermediate particle content from (2.4b) they are given by

$$\begin{aligned} \kappa_{\text{int}} &= \begin{bmatrix} -0.316 & 0. & 0.949 \\ -0.642 & -0.736 & -0.214 \\ -0.698 & 0.677 & -0.233 \end{bmatrix}, \\ \kappa_{M_{Z'}} &= \begin{bmatrix} -0.978 & 0.208 \\ -0.208 & -0.978 \end{bmatrix}. \end{aligned} \quad (2.15)$$

Another characteristic feature of the unification scenarios presented in figure 2.3 is the trivial RG flow of the strong coupling constant at scales where the full **27**-like matter content contributes. In order to ensure that our unification scenario at the one-loop level gives a realistic picture, we investigated the RG evolution of the gauge couplings at the two-loop level. The results can be found in appendix B.1.

2.2 Superpotential

Now that we have verified that the unification of the gauge couplings in a $U(1)'$ -extended supersymmetric standard model can be restored with the left-right symmetry group (2.2) in the intermediate phase, we can construct a superpotential that does not lead to the severe problems of the PSSSM as discussed at the end of the previous chapter:

1. The simultaneous presence of lepto- and di-quark couplings for the colored exotics endangering proton stability.
2. Couplings of all three generations of Higgs fields to matter leading to flavor changing neutral currents at the tree-level.

Under the intermediate LR symmetry, we can write down a superpotential circumventing these problems:

$$\begin{aligned}
 W_{\text{LR}} &= \mathbf{Y}^Q Q_L H Q_R + \mathbf{Y}^L L_L H L_R \\
 &\quad + \mathbf{Y}^D D Q_R L_R + \mathbf{Y}^{D^c} D^c Q_L L_L \\
 &\quad + \mathbf{Y}^{SD} S D^c D + \mathbf{Y}^{SH} S H H,
 \end{aligned} \tag{2.16a}$$

where no diquark terms are included.⁵ Rewriting this superpotential in terms of the fields as representations of the TeV-scale gauge symmetry

$$SU(3) \times SU(2)_L \times U(1)_Y \left[\times U(1)' \right], \tag{2.16b}$$

yields

$$\begin{aligned}
 W_{\text{LRSSM}} &= \mathbf{Y}^u u^c H^u Q + \mathbf{Y}^d d^c Q H^d + \mathbf{Y}^e e^c L H^d \left[+ \mathbf{Y}^{\nu^c} \nu^c H^u L \right] \\
 &\quad + \mathbf{Y}^D D u^c e^c \left[+ \mathbf{Y}_2^D D d^c \nu^c \right] + \mathbf{Y}^{D^c} D^c L Q \\
 &\quad + \mathbf{Y}^{SD} S D^c D + \mathbf{Y}^{SH} S H^u H^d.
 \end{aligned} \tag{2.16c}$$

The terms in brackets contain couplings involving the right-handed neutrinos, which will not be contained in the low-energy theory, as they are assumed to acquire Majorana masses in the course of the intermediate symmetry breaking of the order Λ_{int} . For readability, we have omitted all generation indices, but we implicitly require the fields H (H^u, H^d) and S in (2.16) to be charged under an H -parity, such that all but the generation that acquires vacuum expectation values are odd.

It should be noted, that such a superpotential cannot be embedded into an E_6 symmetric superpotential of the form of (1.53), as we had discussed in section 1.5.

⁵Alternatively one could require that the theory only contains diquark couplings of the exotic in the absence of leptoquark couplings, but in this work, we will not pursue this scenario.

2.2.1 H -Parity and R -Parity

In this section we briefly discuss some general implications of the implementation of an H -parity Z_2^H [34] into our model. With the assignment of charges under H -parity as mentioned in the previous paragraph, it follows, that the two Higgs generations with trivial vevs only appear in the last term of the superpotential from (2.16a). As they do not couple to ordinary matter, we will call them *dark Higgs* fields (or *un-Higgs* [41] fields). The parity forces them to be only produced in pairs, which renders their lightest mass eigenstate (LHP) stable. The two generations of dark Higgs fields will be denoted as H_i, S_i with the subscript $i = 1, 2$. From this point on, the Higgs fields H, S without subscripts shall denote the Higgs fields that obtain vevs in the course of EWSB. Accounting explicitly for the three generations of Higgs fields, the last term in the superpotential from (2.16a) and (2.16c) read

$$W_{\text{LR}}^{\text{H}} = \mathbf{Y}_{3ij}^{\text{SH}} S H_i H_j + \mathbf{Y}_{i3j}^{\text{SH}} S_i H H_j \quad (2.17)$$

and

$$W_{\text{LRSSM}}^{\text{H}} = \mathbf{Y}_{3ij}^{\text{SH}} S H_i^d H_j^u + \mathbf{Y}_{i3j}^{\text{SH}} S_i H^d H_j^u + \mathbf{Y}_{ij3}^{\text{SH}} S_i H_j^d H^u, \quad (2.18)$$

respectively.

Regarding the particle spectra of this model, H -parity forbids mixing mass terms among the scalar dark Higgs fields and the Higgs fields, as well as mass terms that couple neutralinos to dark Higgsinos. The details of the mass spectra will be given in section 2.5.

Note, that the superpotential (2.16) already incorporates R -Parity as $U(1)_{B-L}$ is contained in the intermediate symmetry group (2.2).

Even though the investigation of cosmological implications following from this model is beyond the scope of the work presented here, it is worth noticing, that there are generally at least two kinds of dark matter in models of this kind, namely the lightest H -odd (LHP) and the lightest R -odd (LSP) state. In principle there could even be a third type of dark matter in the following constellation: If the lightest particle, with odd charges under both parities is too light to decay into the two lightest singly odd-charged states, it would be stable as well.

2.3 Embedding of the LR Symmetric Model into a Local E_6 GUT

The obvious question – after having developed the gauge coupling unification scenario in section 2.1 while stressing the incompatibility of the superpotential required by phenomenology (2.16a) with an embedding into a simple Lie-group – is why one would bother finding a unification scheme that cannot be completed by a grand unified theory.⁶ It is difficult to exclude that there is a way of a sensible *ad hoc* formulation of an E_6 -GUT yielding the left-right symmetric model or the PSSSM as low energy theory, but especially the inconsistency of H -parity with the E_6 -symmetric superpotential leads us to pursue a different strategy of finding a UV-completion for the LR symmetric SUSY model, namely *orbifold* or *local* GUTs.

Orbifold GUTs provide an elegant framework in which a gauge theory in four spacetime dimensions can be interpreted as the low energy limit of a higher dimensional theory with a larger gauge group:⁷

The d extra dimensions are understood as being compactified which we implement via the identification

$$x_i \longleftrightarrow x_i + 2\pi R_i \quad i = 1, \dots, d, \quad (2.19)$$

such that R_i becomes the radius of the i -th extra dimension. $1/R_i$ is denoted as the *compactification scale* as the propagation in the extra dimensions requires the excitation of modes (in Fourier-expansion) with energies $E > 1/R_i$.

Starting from a quantum field theory in $4+d$ dimensional spacetime, we assume the extra-dimensions M , as well as the QFT, to exhibit a symmetry under a discrete group \mathcal{G} :

$$\mathcal{G} : y \longrightarrow \theta(y) \quad y \in M. \quad (2.20)$$

If the (non-trivial) action θ of \mathcal{G} on the extra dimensions has *fixed points* i.e.

$$\exists y \in M : \theta(y) = y \quad (2.21)$$

we call the resulting (quotient) space M/\mathcal{G} an orbifold. The action of the symmetry group \mathcal{G} on the field space can have non-trivial embeddings in all the symmetries of the QFT. We consider embeddings in these symmetries that yield (commuting) phase rotations of the fields: The embedding into the gauge symmetry of the theory we denote as *gauge twist*. Non-trivial representations G_θ on the group space can lead to a reduced degree of gauge symmetry below the compactification scale of the extra dimensions (see appendix A).

In supersymmetric theories, there is an additional freedom to implement the orbifold action: The $N = 1$ SUSY algebra in higher dimensions can be re-cast in

⁶Note, that in addition to the hurdles discussed in section 1.5 the unification scenario in the LR model depends on the presence of incomplete E_6 representations constituting the intermediate particle content.

⁷An exemplary toy model is studied in appendix A, for further reference consult, e.g. [42, 43].

terms of extended $N > 1$ SUSY algebras in 4D (see [44, 45] and references therein, as well as appendix A.4). The action in these theories is invariant under rotations among the fermionic components of its symmetry algebra commonly referred to as R -symmetry [44].⁸ It will be demonstrated in section 2.3.3, how the orbifold action can be implemented into R -symmetry. This does not affect the resulting 4D gauge group but influences which 4D fields originating from higher dimensional *hypermultiplets* have (massless) zero modes in their Fourier-expansion on the compact extra dimensions and hence appear in the low energy spectrum at $E \ll 1/R$. In particular, a non-trivial embedding in the R -symmetry will be required to ensure 4D $N = 1$ supersymmetry below the orbifold compactification scale.

Our goal is to find an orbifold setup with E_6 being the gauge symmetry in the bulk of the extra dimensions⁹ with reduced symmetries at the fixed points, such that their common subset is the LR symmetric group which constitutes the intermediate symmetry group in our gauge coupling unification scenario. In [35], the limitations of 5D orbifold constructions were discussed and it was shown that they are not suited to yield $SU(3) \times SU(2)^2 \times U(1)^2$ as a four dimensional remnant of E_6 living in the bulk. Therefore, we will focus on 6D orbifolds, meaning the 4D Minkowski spacetime times an orbifold torus T^2/Z_n : First, we will discuss the implementation of gauge twists in E_6 group space, and give examples G_θ for how all subgroups of E_6 containing the LR group (1.43c) can be obtained at the fixed points. Next, an orbifold is presented on which gauge twists leading to the desired 4D symmetry can be realized. The discussion proceeds with the choice of an R_θ -symmetry on the $N = 2$ SUSY generators associated with the orbifold action θ . In order to ensure the consistency of our construction, we present a suitable choice of additional matter placed in the bulk of the extra-dimensional spacetime canceling bulk and localized anomalies on the orbifold. We conclude with the placement of 4D matter located at the fixed points.

2.3.1 Orbifold Action on E_6 Group Space

The orbifold action θ is defined as a symmetry acting on the extra-dimensional space. As shown explicitly in the next section, fields pick up a phase Λ^θ under these symmetry transformations according to their respective Lorentz representations. Additionally, a gauge twist G^θ – a simultaneous rotation of the fields depending on their embedding into the gauge group – can be superimposed.

Since we wish to break E_6 down to the intermediate symmetry group (1.43c) by orbifold compactification, we shall first investigate gauge twists that preserve rank 6 without an a priori specification of the orbifold geometry on which the symmetry can be realized. Restricting the orbifold symmetries to rotations, we bear in mind that, according to the crystallographic restriction theorem [46], only

⁸This is conceptionally independent from the R -parity, introduced to suppress proton decay in the MSSM.

⁹Since it is the smallest simple Lie algebra that can accommodate LR symmetric intermediate gauge group (including $U(1)_\chi$).

rotations of order 2, 3, 4, and 6 can be realized on the torus.¹⁰ In order not to break any of the Cartan generators H and hence reducing the rank, we require the gauge twist to be generated by the Cartan generators: Let θ be a generator of an orbifold rotation.¹¹ We parametrize the associated action in group space by a shift vector V_θ acting on the roots E_α of E_6 [47]. The roots are the weights of the adjoint representation [26], which is the **78** dimensional representation in case of E_6 . In terms of the the construction scheme sketched in section 1.4, the graphical representation in weight space, labeled by the Dynkin coefficients $\Delta(\alpha)$ can be obtained by starting from the highest weight $\Delta(\mu_{\max}) = (0, 0, 0, 0, 0, 1)$ provided that the ordering of the simple roots is chosen according to (1.41). The roots thus transform as

$$G^\theta E_\alpha = \exp [2\pi i V_\theta \cdot H] E_\alpha = \exp [2\pi i V_\theta \cdot \alpha] E_\alpha \quad (2.22)$$

where we demand that V_θ is chosen such that the gauge twist respects the multiplication law of the orbifold space group, i.e.

$$G(\theta)^n = \exp [2n\pi i V_\theta \cdot H] = 1 \quad (2.23)$$

for \mathbb{Z}_n . This is equivalent to

$$\forall \alpha : V_\theta \cdot \alpha = \bar{V} \cdot \Delta(\alpha) \in \mathbb{Z}/n. \quad (2.24)$$

In the expression on the right hand side, \bar{V} denotes V in the dual basis such that the roots can be conveniently represented by their Dynkin coefficients. The unbroken subgroup which survives under such an orbifold action is given by the set of generators (the Cartan subalgebra and roots) left invariant under the action of $G(\theta)$ from (2.22), i.e. for which holds

$$V_\theta \cdot \alpha = \bar{V} \cdot \Delta(\alpha) \in \mathbb{Z}. \quad (2.25)$$

The procedure shall be illustrated in the following example: Consider the shift vector

$$\bar{V}_\theta = 1/6(1, 5, 4, 3, 5, 0), \quad (2.26)$$

generating an action in group space consistent with a \mathbb{Z}_6 symmetry (2.24). In table 2.2 the shift vector is applied to all positive roots of the **78**. The unbroken roots are those fulfilling (2.25). There are in total 16 of them: The five listed in table 2.2, the corresponding negative roots, as well as the six-fold degenerate entry in the weight space diagram with Dynkin coefficients $(0, 0, 0, 0, 0, 0)$ corresponding to the Cartan generators. This tells us that the sum of the dimensions of the respective adjoint representations of the resulting group is 16. For the identification of the this group it is useful to construct the Cartan matrix of

¹⁰On the 1-sphere there is essentially only $S^1/(\mathbb{Z}_2)$ and $S^1/(\mathbb{Z}_2 \times \mathbb{Z}'_2)$, covered by the rotations of order 2.

¹¹The procedure could be generalized to translations, reflections, and glide reflections in a straightforward manner, but for our purposes focusing on rotations is sufficient.

$\Delta(\alpha)$	$V_\theta \cdot \alpha$	$\Delta(\alpha)$	$V_\theta \cdot \alpha$	$\Delta(\alpha)$	$V_\theta \cdot \alpha$
(0, 0, 0, 0, 0, 1)	0	(1, 0, $\bar{1}$, 1, $\bar{1}$, 1)	-5/6	(0, $\bar{1}$, 0, 1, $\bar{1}$, 1)	-7/6
(0, 0, 1, 0, 0, $\bar{1}$)	2/3	($\bar{1}$, 0, 1, 0, $\bar{1}$, 0)	-1/3	(1, 1, $\bar{1}$, 0, 0, 0)	1/3
(0, 1, $\bar{1}$, 1, 0, 0)	2/3	($\bar{1}$, 1, $\bar{1}$, 0, 1, 1)	5/6	($\bar{1}$, 1, 1, $\bar{1}$, 0, $\bar{1}$)	5/6
(0, 1, 0, $\bar{1}$, 1, 0)	7/6	(1, 0, 0, 1, $\bar{1}$, $\bar{1}$)	-1/6	(0, $\bar{1}$, 1, 1, $\bar{1}$, $\bar{1}$)	-1/2
(1, $\bar{1}$, 0, 1, 0, 0)	-1/6	(1, 0, 0, $\bar{1}$, 0, 1)	-1/3	(0, $\bar{1}$, 1, $\bar{1}$, 0, 1)	-2/3
(0, 1, 0, 0, $\bar{1}$, 0)	0	($\bar{1}$, 1, 0, 0, 1, $\bar{1}$)	3/2	(0, 0, $\bar{1}$, 1, 1, 0)	2/3
(1, $\bar{1}$, 1, $\bar{1}$, 1, 0)	1/3	($\bar{1}$, 1, $\bar{1}$, 1, $\bar{1}$, 1)	-1/3	(2, $\bar{1}$, 0, 0, 0, 0)	-1/2
($\bar{1}$, 0, 0, 1, 0, 0)	1/3	(0, $\bar{1}$, 0, 0, 1, 1)	0	($\bar{1}$, 2, $\bar{1}$, 0, 0, 0)	5/6
(1, $\bar{1}$, 1, 0, $\bar{1}$, 0)	-5/6	(1, 0, 1, $\bar{1}$, 0, $\bar{1}$)	1/3	(0, $\bar{1}$, 2, $\bar{1}$, 0, $\bar{1}$)	0
(1, 0, $\bar{1}$, 0, 1, 1)	1/3	($\bar{1}$, 1, 0, 1, $\bar{1}$, $\bar{1}$)	1/3	(0, 0, $\bar{1}$, 2, $\bar{1}$, 0)	-1/2
($\bar{1}$, 0, 1, $\bar{1}$, 1, 0)	5/6	($\bar{1}$, 1, 0, $\bar{1}$, 0, 1)	1/6	(0, 0, 0, $\bar{1}$, 2, 0)	7/6
(1, 0, 0, 0, 1, $\bar{1}$)	1	(0, $\bar{1}$, 1, 0, 1, $\bar{1}$)	2/3	(0, 0, $\bar{1}$, 0, 0, 2)	-2/3

Table 2.2: The positive roots of the **78** of E_6 , and their scalar products with the shift vector $\bar{V}_\theta = 1/6(1, 5, 4, 3, 5, 0)$, generating a Z_6 orbifold action on the group space.

its semi-simple constituents: First, we identify a set of simple roots, i.e. positive roots¹² that cannot be written as a linear combination with only positive or vanishing coefficients of other unbroken positive roots:

$$\begin{pmatrix} 0 & 1 & 0 & 0 & -1 & 0 \\ 1 & 0 & 0 & 0 & 1 & -1 \\ 0 & -1 & 0 & 0 & 1 & 1 \\ 0 & -1 & 2 & -1 & 0 & -1 \end{pmatrix}. \quad (2.27)$$

From here we note that there are only four simple roots corresponding to non-Abelian gauge groups left. As our implementation of the orbifold action in group space does not allow for a reduction of the rank six, the remaining two ranks have to be preserved in terms of $U(1)$ factors, which span the null-space of the 6×4 matrix in (2.27). The angles among the simple roots as well as their lengths can be calculated via [25]

$$A_{ij} = \alpha_i \cdot \alpha_j = \sum_{k,l} \Delta^k(\alpha_i) A_{E_6}^{kl} \Delta^l(\alpha_j), \quad (2.28)$$

where A_{E_6} denotes the Cartan matrix of E_6 from (1.41). The resulting A_{ij} then is

¹² $E_\alpha^\dagger = E_{-\alpha}$ ensures that the choice of positiveness made in assigning the roots of the parent group remains a valid choice.

the Cartan matrix which encodes the semi-simple part of the remaining subgroup:

$$A = \begin{pmatrix} 2 & -1 & 0 & 0 \\ -1 & 2 & 0 & 0 \\ 0 & 0 & 2 & 0 \\ 0 & 0 & 0 & 2 \end{pmatrix}, \quad (2.29)$$

which corresponds to

$$SU(3) \times SU(2) \times SU(2). \quad (2.30)$$

Together with the additional two unbroken Cartan generators corresponding to Abelian groups, we obtain the left-right symmetric group that serves as intermediate gauge group in the unification scenario.

This procedure was applied repeatedly for various shift vectors parametrizing all possible kinds of rotations on two-dimensional orbifolds. The resulting subgroups with corresponding shift vectors are listed in table 2.3. We have already

\mathbb{Z}_2	Subgroup H	Shift $2\bar{V}$
	$SO(10) \times U(1)_\chi$	(1, 1, 0, 1, 1, 0)
	$SU(6) \times SU(2)_R$	(0, 0, 1, 0, 0, 0)
	$SU(6) \times SU(2)_L$	(1, 1, 1, 1, 1, 0)
\mathbb{Z}_3	Subgroup H	Shift $3\bar{V}$
	$SU(3)_C \times SU(3)_L \times SU(3)_R$	(1, 2, 1, 0, 2, 0)
\mathbb{Z}_4	Subgroup H	Shift $4\bar{V}$
	$SU(5) \times U(1) \times SU(2)_L$	(3, 1, 3, 1, 1, 0)
	$SU(5) \times U(1) \times SU(2)_R$	(2, 2, 1, 0, 2, 0)
	$SU(4)_C \times SU(2)_L \times SU(2)_R \times U(1)_\chi$	(3, 1, 2, 3, 1, 0)
	$SU(3)_C \times SU(3)_L \times SU(2)_R \times U(1)$	(0, 0, 1, 2, 0, 0)
	$SU(3)_C \times SU(3)_R \times SU(2)_L \times U(1)$	(3, 1, 1, 1, 1, 0)
\mathbb{Z}_6	Subgroup H	Shift $6\bar{V}$
	$SU(3)_C \times SU(3)_L \times SU(2)_R \times U(1)$	(4, 2, 1, 0, 2, 0)
	$SU(3)_C \times SU(3)_R \times SU(2)_L \times U(1)$	(5, 1, 5, 3, 1, 0)
	$SU(3)_C \times SU(2)_L \times SU(2)_R \times U(1)_{B-L} \times U(1)_\chi$	(1, 5, 4, 3, 5, 0)

Table 2.3: The subgroups of E_6 that contain the LR group which can be obtained from gauge twists corresponding to \mathbb{Z}_2 , \mathbb{Z}_3 , \mathbb{Z}_4 and \mathbb{Z}_6 rotations. Sample shift vectors for each case are given in the dual basis.

demonstrated that in the case of \mathbb{Z}_6 one can realize the LR group as residual symmetry on an orbifold fixed point directly. Alternatively, various combinations of

$\mathbb{Z}_2, \mathbb{Z}_3, \mathbb{Z}_4$ and \mathbb{Z}_6 lead to symmetry groups with the common subgroup being the LR group. These are enclosed in table 2.4. The simplest construction is based upon two independent gauge twists corresponding to \mathbb{Z}_2 and \mathbb{Z}_3 rotations, which can effect a breaking of E_6 to $SO(10) \times U(1)_\chi$ and $SU(3)^3$, respectively (compare with table 2.3 and section 1.4.4). Note, that the choice of V_θ is not uniquely

$\mathbb{Z}_2 \times \mathbb{Z}_2$	$SU(4)_C \times SU(2)_L \times SU(2)_R \times U(1)_\chi$
$\mathbb{Z}_2 \times \mathbb{Z}_3$	$SU(3)_C \times SU(2)_L \times SU(2)_R \times U(1)_{B-L} \times U(1)_\chi$ $SU(3)_C \times SU(3)_L \times SU(2)_R \times U(1)$ $SU(3)_C \times SU(3)_R \times SU(2)_L \times U(1)$
$\mathbb{Z}_2 \times \mathbb{Z}_4$	$SU(4)_C \times SU(2)_L \times SU(2)_R \times U(1)_\chi$ $SU(3)_C \times SU(2)_L \times SU(2)_R \times U(1)_{B-L} \times U(1)_\chi$
$\mathbb{Z}_3 \times \mathbb{Z}_4$	$SU(3)_C \times SU(3)_L \times SU(2)_R \times U(1)$ $SU(3)_C \times SU(3)_R \times SU(2)_L \times U(1)$ $SU(3)_C \times SU(2)_L \times SU(2)_R \times U(1)_{B-L} \times U(1)_\chi$
$\mathbb{Z}_4 \times \mathbb{Z}_4$	$SU(4)_C \times SU(2)_L \times SU(2)_R \times U(1)_\chi$ $SU(3)_C \times SU(2)_L \times SU(2)_R \times U(1)_{B-L} \times U(1)_\chi$

Table 2.4: The nontrivial ($H_i \not\subseteq H_j$) common invariant subgroups $H_i \cap H_j$ under combinations of two shifts.

determined by the orbifold action on spacetime θ as for each orbifold action θ there is a countable number of shift vectors V_θ respecting (2.24).

2.3.2 Intermediate LR symmetry from T^2/\mathbb{Z}_6 orbifold

The simplest 6D orbifold geometry on which both a \mathbb{Z}_2 and \mathbb{Z}_3 shift can be realized is a torus T^2 equipped with a \mathbb{Z}_6 invariance, as shown in figure 2.4. In orbifold notation [48], it corresponds to $\mathbb{R}^2/\mathbf{632}$, i.e. the plane with $\mathbb{Z}_6, \mathbb{Z}_3$, and \mathbb{Z}_2 fixed points. These are indicated in figure 2.4, as well. In the T^2/\mathbb{Z}_6 picture, we can regard the order 2 and 3 rotations as effects induced by the order 6 rotation and translations

$$r_2 = t_1 r_6^3, \quad r_3 = t_1 r_6^2. \quad (2.31)$$

Recall that the gauge twists (2.22) lead by construction only to (commuting) phase rotations of the roots. Hence, the gauge twists associated with (2.31) obey

$$G(r_2) = G(t_1) G(r_6)^3, \quad G(r_3) = G(t_1) G(r_6)^2, \quad (2.32)$$

implying

$$G(t_1)^2 = G(t_1)^3 = \mathbb{1} \quad \Rightarrow \quad G(t_1) = \mathbb{1}. \quad (2.33)$$

This means that we cannot assign a non-trivial gauge twist with the translations on the torus (which is commonly referred to as *discrete Wilson line* [49]). At the

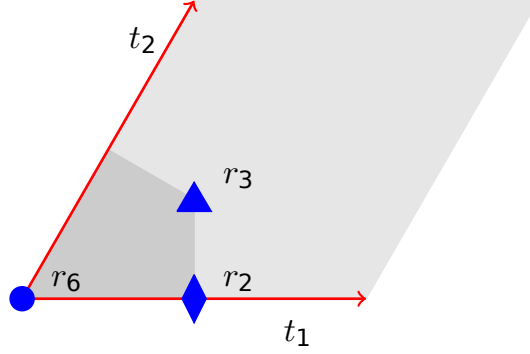


Figure 2.4: The $\mathbb{R}^2/\mathbf{632}$ orbifold which is one of the T^2/\mathbb{Z}_6 orbifolds. The blue circle, triangle and diamond indicate the fixed points under the 60° , 120° and 180° rotations respectively, while the red arrows are the translations which span the torus. The light shaded area indicates the torus, the dark shaded area corresponds to the fundamental domain of the orbifold.

respective fixed points the roots of the gauge group then transform according to

$$\begin{aligned} G(r_2)E_\alpha &= G(r_6)^3 E_\alpha \in \{1, -1\}E_\alpha \\ G(r_3)E_\alpha &= G(r_6)^2 E_\alpha \in \{1, e^{2\pi i/3}, e^{4\pi i/3}\}E_\alpha, \\ G(r_6)E_\alpha &= G(r_2)G(r_3)^{-1}E_\alpha \in \{1, e^{\pi i/3}, e^{2\pi i/3}, -1, e^{4\pi i/3}, e^{5\pi i/3}\}E_\alpha. \end{aligned} \quad (2.34)$$

With an appropriate choice of the orbifold action on the group space, we can achieve a breaking of E_6 to the LR symmetry group, with reduced symmetry groups at the fixed points (figure 2.4) of the $\mathbb{R}^2/\mathbf{632}$ orbifold as depicted in figure 2.5. In order to illustrate this, we choose the gauge twist at the \mathbb{Z}_6 fixed

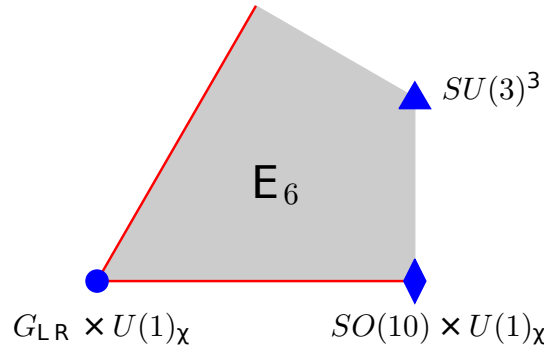


Figure 2.5: An $E_6 \rightarrow G_{LR} \times U(1)_\chi$ breaking scenario on the $\mathbb{R}^2/\mathbf{632}$ orbifold and the local gauge groups at the \mathbb{Z}_6 , \mathbb{Z}_3 and \mathbb{Z}_2 fixed points which are shown as blue circle, triangle and diamond. The shaded area shown is the fundamental domain only, and long (red) and short sides are identified.

point such that the gauge group is broken to the LR symmetry

$$\bar{V}_6 = \frac{1}{6}(1, 5, 4, 3, 5, 0) \quad (2.35)$$

(see the last line in table 2.3 and the example given in section 2.3.1). Then (2.34) requires the gauge twist at the \mathbb{Z}_3 and \mathbb{Z}_2 fixed points to be generated by the shift vectors $2\bar{V}_6$ and $3\bar{V}_6$, respectively. One can see that the roots of E_6 transform under gauge twist generated by $2\bar{V}_6$ and $3\bar{V}_6$ precisely as they would transform under

$$\bar{V}_3 = \frac{1}{3}(1, 2, 1, 0, 2, 0) \quad \text{and} \quad \bar{V}_2 = \frac{1}{2}(1, 1, 0, 1, 1, 0), \quad (2.36)$$

respectively: The entries of \bar{V}_3 [\bar{V}_2] differ from $2\bar{V}_6$ [$3\bar{V}_6$] only by integers, which amounts to a phase rotation by 2π according to (2.22) and hence does not alter the action of the gauge twist on the roots. According to table 2.3, the shift vector \bar{V}_3 [\bar{V}_2] breaks the E_6 gauge group to $SU(3)^3$ [$SO(10) \times U(1)$], leading to the situation depicted in figure 2.5. The gauge group in the four dimensional theory emerging at energies below the compactification scale is the common subset of the gauge groups located at the fixed points of the orbifold, which is indeed the desired LR symmetric group (2.2).

2.3.3 Gauge Super-Multiplets on the T^2/\mathbb{Z}_n Orbifold

The compactification of the extra dimensions breaks the 6D Lorentz group to

$$SO(1, 5) \longrightarrow SO(1, 3) \times U(1). \quad (2.37)$$

The orbifold space group is then a subgroup of the $SO(2) \sim U(1)$ symmetry on the extra dimensions $\mathbb{Z}_n \subset U(1)$. In $U(1)$ language the \mathbb{Z}_n rotations act on the extra dimensions as

$$x_5 - ix_6 \longrightarrow e^{-2\pi i/n}(x_5 - ix_6). \quad (2.38)$$

A 6D gauge field is then split into a 4D vector A_μ and a complex scalar in the adjoint representation of the gauge group

$$\Sigma = \frac{1}{\sqrt{2}}(A_6 + iA_5). \quad (2.39)$$

If one assigns a gauge twist to the orbifold action as in (2.22), the 6D vector components associated with the root E_α transform according to

$$A_\mu^\alpha \longrightarrow e^{2\pi i V \cdot \alpha} A_\mu^\alpha, \quad \Sigma^\alpha \longrightarrow e^{2\pi i V \cdot \alpha} e^{-2\pi i/n} \Sigma^\alpha. \quad (2.40)$$

This implies that there can only appear scalar massless modes in the low energy theory if their corresponding roots are broken by the gauge twist on all fixed points of the orbifold (as the massless modes have constant wavefunctions in the extra dimensions) in such a way that the two transformations from (2.40) cancel.

A supersymmetric action in 6D spacetime can be formulated in terms of $N = 1$ superfields [45], which has a field content that is equivalent to 4D $N = 2$ supersymmetry [44]. Some aspects of this equivalence have been summarized in appendix A.2 and A.4.

In terms of 4D $N = 1$ superfields, the 6D gauge hypermultiplets consists of a vector superfield \hat{V} and a chiral superfield $\hat{\chi}$, both transforming under the adjoint representation of the gauge group. The extra-dimensional components of the 6D gauge fields Σ from (2.39) are contained in $\hat{\chi}$. The supersymmetric action written in terms of the component fields of \hat{V} and $\hat{\chi}$ can be re-written into a form invariant under an internal $SU(2)$ symmetry under which the two spinor components of \hat{V} and $\hat{\chi}$ transform as doublets [44] (see also appendix A.2). This is denoted as R -symmetry. The off-shell version also contains three auxiliary real scalar fields transforming as triplets under $SU(2)^R$.

The chiral fermionic SUSY parameters can be parametrized as eight component 6D spinor $\xi \equiv (\xi_1, \xi_2, 0, 0)^T$. Their transformations under the \mathbb{Z}_n orbifold rotations (with trivial embedding into R -symmetry) are given by

$$\Lambda_{\frac{1}{2}}^{56} = \exp \left[\frac{2\pi}{n} \frac{1}{4} [\Gamma^5, \Gamma^6] \right], \quad (2.41)$$

where Γ^M denote the 6D Dirac matrices as defined in appendix A.3. This would result in a non-supersymmetric theory at energies below the compactification scale as neither of the two SUSY generators ξ_1, ξ_2 is invariant under (2.41) and $(S_\theta^{56})^n \neq 1$.

Fortunately, we are free to assign an embedding of the \mathbb{Z}_n rotations in I^{3R} of the R -symmetry to the 6D chiral spinors

$$\Lambda_{\frac{1}{2}}^R = \exp [a_R I^{3R}], \quad (2.42)$$

where the constant a_R can be chosen such that the 4D theory is $N = 1$ supersymmetric, i.e. the transformation behavior of the spinors (the product of (2.41) and (2.42)) contained in \hat{V} and $\hat{\chi}$ is aligned to the transformation of the respective bosonic degrees of freedom (2.40). Then the superfields transform coherently as a whole, generalizing the transformations from (2.40) to

$$\hat{V}^\alpha \longrightarrow e^{2\pi i V \cdot \alpha} \hat{V}^\alpha, \quad \hat{\chi}^\alpha \longrightarrow e^{2\pi i V \cdot \alpha} e^{-2\pi i/n} \hat{\chi}^\alpha. \quad (2.43)$$

Note, that $N = 2$ SUSY in 4D cannot be preserved in the course of orbifold compactification as the SUSY algebra in 6D (A.27) generates translations in the extra dimensions, which are not a symmetry of the orbifold [45].

2.3.4 Bulk Matter and Anomalies

The achievement of preserving $N = 1$ 4D SUSY with the embedding of the superfields according to (2.43) has the undesirable consequence that zero modes from the 4D chiral part of the 6D gauge hypermultiplet $\hat{\chi}^\alpha$ appear corresponding

to roots that are broken at all fixed points. Moreover, they cause anomalies which would break gauge symmetry at the level of quantum corrections. In the context of orbifolded extra-dimensional theories, there are two types of anomalies: bulk and localized (at the orbifold's fixed points) anomalies [50, 51].

The bulk anomalies are independent from the orbifold structure (apart from the dimension, of course, as chiral anomalies only appear in even dimensions) [51]. In the 6D notation the fermionic components of the gauge hypermultiplet (V, χ) form a chiral spinor (see appendix A.4 and [44]), which would cause bulk anomalies. To cancel these, we introduce a hypermultiplet of opposite 6D chirality in the adjoint representation of the gauge group. In terms of 4D superfields the 6D chiral multiplet decomposes into (Φ, Φ_c) [45]. Regarding the local anomalies, we note that the invariance of the 6D kinetic term of the hypermultiplet

$$\int d^6x (\Phi_c \partial \Phi + h.c.)|_{\theta\theta}, \quad (2.44)$$

where – in analogy to the extra-dimensional components of the gauge field (2.40)

$$\partial \equiv \frac{1}{\sqrt{2}} (\partial_5 - i\partial_6) \quad \longrightarrow \quad e^{\frac{-2\pi i}{6}} \partial \quad (2.45)$$

under orbifold rotations, requires a transformation behavior of the hypermultiplet of the form

$$\begin{aligned} \Phi^\alpha &\longrightarrow e^{2\pi i V \cdot \alpha} e^{\frac{-2\pi i}{6} a_+} \Phi^\alpha \\ \Phi_c^{-\alpha} &\longrightarrow e^{-2\pi i V \cdot \alpha} e^{\frac{-2\pi i}{6} a_-} \Phi_c^{-\alpha}, \end{aligned} \quad (2.46)$$

with $a_+ + a_- = 5 \pmod{6}$. Choosing $a_+ = 5, a_- = 0$ has the consequence that with each invariant mode $\chi^{-\alpha}$ a corresponding invariant mode from Φ^α and the zero modes from the two superfields appear in mutually complex conjugate representations, which ensures the cancellation of localized 4D anomalies [51]. Analogously, the invariant modes of Φ_c^α furnish an adjoint representation of the gauge group, nicely canceling the local anomalies of the 4D gaugino contained in V . The additional bulk matter is assumed to acquire masses at the orbifold compactification scale (the zero modes of Φ_c and the combination of Φ, χ form vector-like representations under the 4D gauge group), hence not affecting the unification scenario (2.10) in the emerging 4D theory.

2.3.5 Local Matter Content

The matter content of the low-energy theory can be placed on the fixed points of the orbifold (in terms of an appropriate generalization of (A.7)) in complete representations of the respective gauge groups (see figure 2.5). The distribution of the three generations of matter over the fixed points is not unique. With exact localization, there are no superpotential interactions possible involving fields living at distinct fixed points. However it is clear that the degree of symmetry (compared to E_6) is sufficiently reduced at the fixed points such that a superpotential

discriminating lepto- from di-quark couplings and incorporating H -Parity (2.16a) can be realized in this setting. Note, that the matter content (including the additional matter breaking the intermediate LR symmetry) does not introduce any kind of anomalies, as the matter comes in complete $\mathbf{27}$'s and the intermediate matter is chosen to be vector-like (2.4).

This concludes the discussion of how the extra-dimensional setup allows to view our gauge coupling unification scenario (figure 2.3) in the context of (local) unification into the simple Lie-group E_6 .

In the remainder of this work we document our efforts to derive the implications of the model for TeV-scale collider physics.

2.4 Renormalization Group Evolution

Now that we have specified a gauge coupling unification scenario along with a suitable orbifold setup which can facilitate the breaking of the bulk GUT group, we aim at the investigation of the model's impact on TeV-scale physics with a focus on the LHC phenomenology.

As in the case of the gauge couplings, we can link the theory's remaining parameters specified at the orbifold compactification scale to the Lagrangian parameters at the TeV scale by means of the renormalization group equations (RGEs).

As we wish to investigate the behavior of the coupling constants over a wide energy range (from nearly the Planck scale, down to the TeV scale), it is suitable to re-express the RGEs in terms of a log-scaled variable $t = \log \mu/\mu_0$, where μ_0 denotes an arbitrary reference scale.

The RGEs for all parameters of a general supersymmetric theory, only subject to the constraint that there is at most one $U(1)$ gauge group, where given in [52]. For completeness, we repeat their results and in the cases of the SSB parameters present our generalization that allows us to treat the case where two Abelian groups come into play [38]. The generalization is only valid in combination with the particular choice of basis presented in section 2.1.1 and cannot be extended to the two-loop level (or beyond).

Furthermore, we will give the matching conditions determining the parameters in the $SU(3) \times SU(2) \times U(1)^2$ phase in terms of the LR symmetric parameters at the intermediate scale .

2.4.1 Running Gauge Couplings

According to [52] and references therein, the gauge coupling evolution at the one-loop level is given by

$$\frac{d}{dt}g_a = \frac{1}{16\pi^2} \beta_a g_a^3. \quad (2.47)$$

The so-called beta-function β_a collects the contributions of gauge self-interactions, as well as fermion and scalar loops. In a (at most softly broken) supersymmetric theory it reads

$$\beta_a = S(R) - 3\mathcal{C}(G), \quad (2.48)$$

where $S(R)$ is the Dynkin index summed over all chiral multiplets and $\mathcal{C}(G)$ the quadratic Casimir of the adjoint representation. Even in the presence of a radiative mixing among two $U(1)$ gauge groups we can maintain the correctness of these results, employing the formalism that we introduced in section 2.1.1.

2.4.2 Evolution of the Gaugino Masses

In the absence of $U(1)$ mixing the one-loop RGEs for the soft-breaking gaugino masses are given by

$$\frac{d}{dt}M_a = \frac{2}{16\pi^2} \beta_a g_a^2 M_a, \quad (2.49)$$

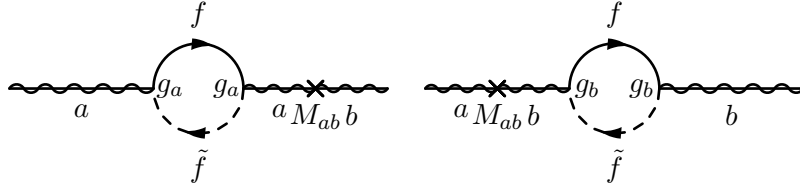
with the same beta-coefficients as in (2.48). In the model under investigation, one has to take the mixing of the $U(1)_Y$ with $U(1)'$ into account by rotating into a new basis $U(1)_{A/B}$ with some orthogonal matrix O . Looking at the gaugino mass term in the Lagrangian, it is obvious that this rotation does not yield a diagonal mass term unless the two gaugino masses are degenerate

$$\mathcal{L}_{M_g} = \bar{\chi}_a M_{aa} \tilde{\chi}_a = \bar{\chi}'_a \underbrace{O_{ab} M_{bc} O_{cd}^T}_{\equiv M'_{ad}} \tilde{\chi}'_d. \quad (2.50)$$

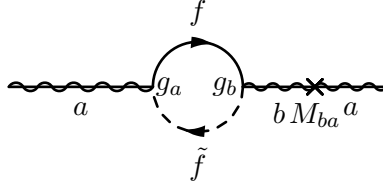
In the present scenario it is highly unnatural to assume the $U(1)$ gaugino masses being equal at the intermediate breaking scale, as they evolve independently from Λ_{E6} to Λ_{int} . Therefore (2.49) has to be extended to include the running of off-diagonal gaugino mass terms [38]

$$\frac{d}{dt} M_{ab} = \frac{1}{16\pi^2} (\beta_a g_a^2 M_{ab} + \beta_b g_b^2 M_{ab}). \quad (2.51)$$

These contributions arise from the following diagrams



Note, that the running of the diagonal entries in the gaugino mass matrix are not altered in the presence of mixed mass terms, as diagrams like



are by construction canceled out after rotating to the $U(1)_{A/B}$ basis. The input parameters at the intermediate scale are obtained from the following matching conditions:

$$\left(\begin{array}{ccc} M_{AA} & M_{AB} & M_{AC} \\ M_{BA} & M_{BB} & M_{BC} \\ M_{CA} & M_{CB} & M_{CC} \end{array} \right) \Bigg|_{\Lambda_{\text{int}} - \epsilon} = \mathbf{O} \left(\begin{array}{ccc} M_{B-L} & 0 & 0 \\ 0 & M_\chi & 0 \\ 0 & 0 & M_R \end{array} \right) \mathbf{O}^T \Bigg|_{\Lambda_{\text{int}} + \epsilon}, \quad (2.52)$$

where \mathbf{O} denotes the orthogonal matrix rotating the $U(1)$ gauge kinetic terms into the diagonal basis (corresponding to κ in (2.11e)). The third row and column on the left-hand side of (2.52) contain the mass terms involving the gaugino corresponding to $U(1)_C$ which is broken at the intermediate scale. Hence, this gaugino acquires mass of the order $\Lambda_{\text{int}} \gg M$ and is integrated out from the theory below Λ_{int} . The matching conditions for the two remaining $U(1)$ gauginos

are given by the upper left 2×2 block matrix in (2.52). At the Z' -scale the soft SUSY breaking contribution to the neutralino (λ^Y, λ') masses is obtained by rotating the $U(1)$ gaugino masses into the $U(Y) \times U(1)'$ basis:

$$\left(\begin{array}{cc} M_Y & M'_Y \\ M'_Y & M' \end{array} \right) \Big|_{M_{Z'} - \epsilon} = \mathbf{O} \left(\begin{array}{cc} M_{AA} & M_{AB} \\ M_{BA} & M_{BB} \end{array} \right) \mathbf{O}^T \Big|_{M_{Z'} + \epsilon}, \quad (2.53)$$

where the rotation matrix \mathbf{O} is given in (2.12d).

2.4.3 Evolution of the Yukawa Couplings

In a supersymmetric theory, according to the non-renormalization theorem [16], at the one-loop level, the running of the Yukawa couplings arises solely from wave function renormalization and gauge contributions:

$$\frac{d}{dt} \mathbf{Y}^{ijk} \propto \text{[Diagrams]} + \text{[Diagrams]} + (i \leftrightarrow k) + (j \leftrightarrow k) + \text{supersymmetrized diagrams} .$$

The renormalization group equations read [52]

$$\frac{d}{dt} \mathbf{Y}^{ijk} = \frac{1}{16\pi^2} Y^{ijl} \left[\frac{1}{2} \mathbf{Y}_{lpq} \mathbf{Y}^{kpq} - 2\delta_l^k g_a^2 C_a(l) \right] + (k \leftrightarrow i) + (k \leftrightarrow j), \quad (2.54)$$

where the Yukawa couplings are taken to be completely symmetrized in all three indices. As the Yukawa couplings do not receive radiative corrections involving SSB parameters, (2.54) can be applied to our model, when working in the $U(1)$ -basis from section 2.1.1.

In the introduction to our model we discussed the need to be able to choose the values of the Yukawa couplings at the unification scale independently, in order not to run into problems with proton decay through lepto- and di-quarks. Furthermore we needed to impose H-Parity, allowing for only one generation of Higgs fields to couple to matter fields, to avoid FCNC in the Higgs sector. In addition we make the following simplifying assumptions:

- The leptoquark Yukawa couplings are diagonal in all three generation indices, as they would otherwise contribute to EWP observables such as

$K^0 - \bar{K}^0$ mixing.

- The Yukawa couplings of Higgs to dark-Higgs fields are taken to be diagonal in the generation indices of the dark-Higgs fields. When investigating the dark-Higgs phenomenology in the future, this constraint will be relaxed.
- The MSSM-like Yukawa couplings of Higgs to light matter fields (e, μ, τ, u, d, c, s) are neglected all-together.

Under these assumptions we obtain the following set of Yukawa couplings consistent with $SU(3) \times SU(2)_L \times SU(2)_R \times U(1)_{B-L} \times U(1)_\chi$ above the intermediate scale

$$\begin{aligned} & \mathbf{Y}_{333}^Q, \mathbf{Y}_{111}^D, \mathbf{Y}_{222}^D, \mathbf{Y}_{333}^D, \mathbf{Y}_{111}^{Dc}, \mathbf{Y}_{222}^{Dc}, \mathbf{Y}_{333}^{Dc}, \\ & \mathbf{Y}_{113}^{SD}, \mathbf{Y}_{223}^{SD}, \mathbf{Y}_{333}^{SD}, \mathbf{Y}_{311}^{SH}, \mathbf{Y}_{322}^{SH}, \mathbf{Y}_{131}^{SH}, \mathbf{Y}_{232}^{SH}, \mathbf{Y}_{333}^{SH}. \end{aligned} \quad (2.55)$$

Below the intermediate scale, the right-handed matter superfields are no longer assembled into $SU(2)_R$ doublets, leading to independent Yukawa couplings for the top- and bottom-superfields. Furthermore, the two MSSM $SU(2)_L$ -doublet Higgs fields H^d and H^u arise from the splitting of the of H -field transforming as $(\mathbf{2}, \mathbf{2})$ under $SU(2)_L \times SU(2)_R$ above Λ_{int} .

The set of Yukawa couplings from above the intermediate scale (2.55) then transforms into

$$\begin{aligned} & \mathbf{Y}_{333}^d, \mathbf{Y}_{333}^u, \mathbf{Y}_{111}^D, \mathbf{Y}_{222}^D, \mathbf{Y}_{333}^D, \mathbf{Y}_{111}^{Dc}, \mathbf{Y}_{222}^{Dc}, \mathbf{Y}_{333}^{Dc}, \\ & \mathbf{Y}_{113}^{SD}, \mathbf{Y}_{223}^{SD}, \mathbf{Y}_{333}^{SD}, \mathbf{Y}_{311}^{SH}, \mathbf{Y}_{322}^{SH}, \mathbf{Y}_{131}^{SH}, \mathbf{Y}_{232}^{SH}, \mathbf{Y}_{113}^{SH}, \mathbf{Y}_{223}^{SH}, \mathbf{Y}_{333}^{SH}, \end{aligned} \quad (2.56)$$

via the following *matching conditions* for the Yukawa couplings at the intermediate scale:

$$\begin{aligned} \mathbf{Y}_{ijk}^Q \Big|_{\Lambda_{\text{int}}+\epsilon} &= \mathbf{Y}_{ijk}^u \Big|_{\Lambda_{\text{int}}-\epsilon} = \mathbf{Y}_{ijk}^d \Big|_{\Lambda_{\text{int}}-\epsilon}, \\ \mathbf{Y}_{ijk}^L \Big|_{\Lambda_{\text{int}}+\epsilon} &= \mathbf{Y}_{ijk}^e \Big|_{\Lambda_{\text{int}}-\epsilon} \left[= \mathbf{Y}_{ijk}^\nu \Big|_{\Lambda_{\text{int}}-\epsilon} \right], \\ \mathbf{Y}_{ijk}^D \Big|_{\Lambda_{\text{int}}+\epsilon} &= \mathbf{Y}_{ijk}^D \Big|_{\Lambda_{\text{int}}-\epsilon} \left[= \mathbf{Y}_{ijk}^{D'} \Big|_{\Lambda_{\text{int}}-\epsilon} \right], \\ \mathbf{Y}_{ijj}^{SH} \Big|_{\Lambda_{\text{int}}+\epsilon} &= \frac{1}{2} \mathbf{Y}_{ijj}^{SH} \Big|_{\Lambda_{\text{int}}-\epsilon} \end{aligned} \quad (2.57)$$

where the terms in brackets belong to operators containing the right-handed neutrino, which is integrated out at the intermediate scale. The factor $1/2$ in the last line arises from the decomposition of the tensor product

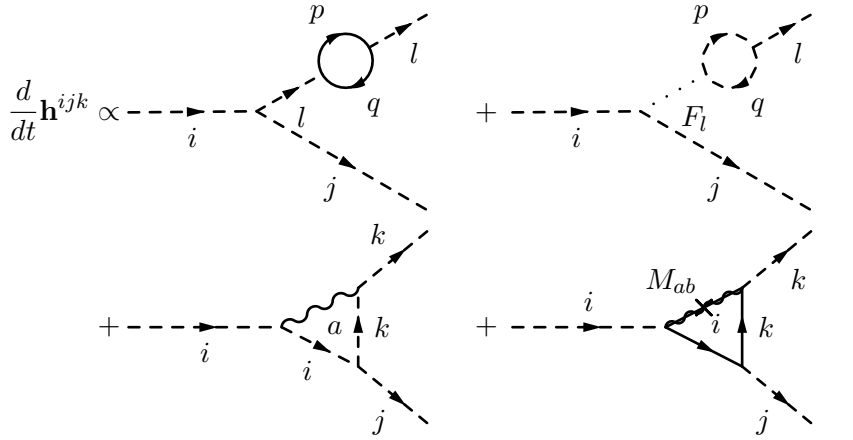
$$(\mathbf{1}, \mathbf{2}, \mathbf{2}) \sim \epsilon_{ab} \epsilon_{ij} H^{ai} H^{bj} = 2 \epsilon_{ab} H^{a1} H^{b2}. \quad (2.58)$$

For the rest of the Yukawa couplings, the matching is trivial, and the nomenclature below Λ_{int} remains the same as above.

The explicit set of renormalization group equations for the Yukawa couplings above (2.55) and below (2.55) the intermediate scale can be found in appendix B.5.3 and B.6.3, respectively.

2.4.4 RGEs for Trilinear Soft SUSY Breaking Terms

The diagrams contributing to the running of the trilinear SSB terms can be obtained in a straightforward way from (2.4.2):



where in the second term of the first line, the auxiliary field F_l of the superfield \hat{l} has been used in order to sketch where this contribution arises from. Note, that again in the presence of two mixing $U(1)$ gauge groups, there is a contribution involving the mixing parameter, as shown in the last diagram. The corresponding renormalization group equations read

$$\frac{d\mathbf{h}^{ijk}}{dt} = \frac{1}{16\pi^2} \left[\frac{1}{2} \mathbf{h}^{ijl} \mathbf{Y}^{lpq} \mathbf{Y}^{pqk} + \mathbf{Y}^{ijl} \mathbf{Y}^{lpq} \mathbf{h}^{pqk} + 2 \left(\mathbf{h}^{ijk} - 2M_{ab} \mathbf{Y}^{ijk} \right) g_a g_b \mathcal{C}_{ab}(k) \right], \quad (2.59)$$

with

$$\mathcal{C}_{ab}(k) = \begin{cases} \mathcal{C}_a(k) & \text{if } a = b \\ Q_a^k Q_b^k & \text{if } a \neq b \end{cases}. \quad (2.60)$$

The latter case only applies for mixing $U(1)$ factors.

The RGEs for the trilinear SSB couplings above and below the intermediate scale are given in appendix B.5.4 and B.6.4, respectively. Unless there are trilinear SSB couplings not having an analogous superpotential term (i.e. the corresponding Yukawa coupling is set to zero at all scales and does not appear in the set of the Yukawa RGEs appendix B.5.3 and B.6.3), the matching conditions of the trilinear couplings are identical to those of the corresponding Yukawa couplings given in (2.57).

2.4.5 RGEs for Soft SUSY Breaking Scalar Mass Squared Terms

For the scalar mass squared terms the generalization of the result from [52], adjusted to take $U(1)$ mixing into account read:

$$\begin{aligned} \frac{d}{dt}(\mathbf{m}^2)_j^i = \frac{1}{16\pi^2} & \left[\frac{1}{2} \mathbf{Y}_{j pq} \mathbf{Y}^{pq n} (\mathbf{m}^2)_n^i + \frac{1}{2} \mathbf{Y}^{ip q} \mathbf{Y}_{pq n} (\mathbf{m}^2)_j^n + 2 \mathbf{Y}_{j pq} \mathbf{Y}^{ip n} (\mathbf{m}^2)_n^q \right. \\ & \left. \mathbf{h}_{j pq} \mathbf{h}^{ip q} - 8 \delta_j^i |M_{ab}|^2 g_a g_b \mathcal{C}_{ab}(j) + 2 g_\beta^2 \delta_j^i Q_\beta^j \left(\delta_k^l Q_\beta^k (\mathbf{m}^2)_l^i \right) \right]. \end{aligned} \quad (2.61)$$

In the last term, the index β runs over all $U(1)$ factors. The explicit expressions for above and below the intermediate scale are given in appendix B.5.5 and B.6.5, respectively.

The matching between the two RGE sets at the intermediate scale, accounting for the splitting of $SU(2)_R$ multiplets, is altered by a D -term contribution generated in the course of the intermediate symmetry breaking [53]. In order not to break SUSY at scales much larger than the weak scale ~ 1 TeV, we use two fields H_{int} and \bar{H}_{int} [54], as outlined in section 2.1. Along the direction in field space where $H_{\text{int}} = \bar{H}_{\text{int}}$, the D -term vanishes exactly. If a symmetry is broken by $\langle H_{\text{int}} \rangle = \langle \bar{H}_{\text{int}} \rangle$ one therefore speaks of a breaking in a D -flat direction. It was found in [53], that in softly-broken SUSY scenarios, a symmetry breaking originating from a scalar potential with non-trivial minima, requires a breaking in an *almost* D -flat direction. That is, the symmetry breaking is triggered by the SSB mass squared term of H_{int} becoming negative, such that

$$\mathbf{m}_{H_{\text{int}}}^2 + \mathbf{m}_{\bar{H}_{\text{int}}}^2 < 0. \quad (2.62)$$

This situation is not unrealistic as $H_{\text{int}} \in \mathbf{27}$ can have superpotential interactions with the ordinary matter fields, driving its SSB mass term to negative values. In this way, the vacuum expectation value may be of the order of the intermediate scale, while the D -term in the potential is of the order of the SSB terms [53]:

$$\frac{1}{2} g_C^2 (Q_{H_{\text{int}}}^C)^2 \left(\langle H_{\text{int}} \rangle^2 - \langle \bar{H}_{\text{int}} \rangle^2 \right) \simeq \mathbf{m}_{H_{\text{int}}}^2 - \mathbf{m}_{\bar{H}_{\text{int}}}^2. \quad (2.63)$$

In our unification scenario, we assumed H_{int} to acquire a vev in the direction of the right-handed neutrino. Therefore, we use in the following $Q_{\nu^c}^C = Q_{H_{\text{int}}}^C$ to denote the charge of the intermediate vev under the broken gauge group. As we did not specify the exact symmetry breaking mechanism at the intermediate scale, we follow the notation from [55] and introduce a parameter M_Δ^2 containing the D -term (2.63) at the intermediate scale. Its effect on the SSB mass parameter (compare with the D -term contributions to the sfermion masses generated in the course of EWSB) of a particle i at the intermediate scale is given by:

$$\Delta \mathbf{m}_i^2 = - \frac{Q_i^C}{Q_{\nu^c}^C} M_\Delta^2. \quad (2.64)$$

Taking this effect into account, the matching conditions at the intermediate scale for the scalar mass terms become

$$\begin{aligned}
\mathbf{m}_{e^c}^2|_{\Lambda_{\text{int}}-\epsilon} &= \mathbf{m}_{LR}^2|_{\Lambda_{\text{int}}+\epsilon} - \frac{Q_{\nu^c}^C}{Q_{\nu^c}^C} M_\Delta^2, \\
\mathbf{m}_{LL}^2|_{\Lambda_{\text{int}}-\epsilon} &= \mathbf{m}_{LL}^2|_{\Lambda_{\text{int}}+\epsilon} - \frac{Q_{\nu^c}^C}{Q_{\nu^c}^C} M_\Delta^2, \\
\mathbf{m}_{u^c}^2|_{\Lambda_{\text{int}}-\epsilon} &= \mathbf{m}_{QR}^2|_{\Lambda_{\text{int}}+\epsilon} - \frac{Q_{\nu^c}^C}{Q_{\nu^c}^C} M_\Delta^2, \\
\mathbf{m}_{d^c}^2|_{\Lambda_{\text{int}}-\epsilon} &= \mathbf{m}_{QR}^2|_{\Lambda_{\text{int}}+\epsilon} - \frac{Q_{\nu^c}^C}{Q_{\nu^c}^C} M_\Delta^2, \\
\mathbf{m}_{QL}^2|_{\Lambda_{\text{int}}-\epsilon} &= \mathbf{m}_{QL}^2|_{\Lambda_{\text{int}}+\epsilon} - \frac{Q_{\nu^c}^C}{Q_{\nu^c}^C} M_\Delta^2, \\
\mathbf{m}_{D^c}^2|_{\Lambda_{\text{int}}-\epsilon} &= \mathbf{m}_{D^c}^2|_{\Lambda_{\text{int}}+\epsilon} - \frac{Q_{\nu^c}^C}{Q_{\nu^c}^C} M_\Delta^2, \\
\mathbf{m}_D^2|_{\Lambda_{\text{int}}-\epsilon} &= \mathbf{m}_D^2|_{\Lambda_{\text{int}}+\epsilon} - \frac{Q_D^C}{Q_{\nu^c}^C} M_\Delta^2, \\
\mathbf{m}_{H^d}^2|_{\Lambda_{\text{int}}-\epsilon} &= \mathbf{m}_H^2|_{\Lambda_{\text{int}}+\epsilon} - \frac{Q_{\nu^c}^C}{Q_{\nu^c}^C} M_\Delta^2, \\
\mathbf{m}_{H^u}^2|_{\Lambda_{\text{int}}-\epsilon} &= \mathbf{m}_H^2|_{\Lambda_{\text{int}}+\epsilon} - \frac{Q_{\nu^c}^C}{Q_{\nu^c}^C} M_\Delta^2, \\
\mathbf{m}_S^2|_{\Lambda_{\text{int}}-\epsilon} &= \mathbf{m}_S^2|_{\Lambda_{\text{int}}+\epsilon} - \frac{Q_S^C}{Q_{\nu^c}^C} M_\Delta^2.
\end{aligned} \tag{2.65}$$

2.5 Low-Energy Spectrum

In this section, we summarize the explicit analytical expressions for the mass matrices of the TeV-scale spectrum (below the $U(1)'$ scale). The major part of the discussion of general phenomenological aspects of the model will be postponed until chapter 3 and chapter 4.

For simplicity we split up the superpotential (1.55) into three parts which describe Higgs-matter, Higgs-exotics and Higgs self-interactions W_M , matter-exotics interactions W_D , and the dark Higgs sector W_H , respectively:

$$W_M = \mathbf{Y}^u u^c Q_L H^u + \mathbf{Y}^d d^c Q_L H^d + \mathbf{Y}^e e^c L_L H^d + \mathbf{Y}^{SD} D^c D S + \mathbf{Y}^{SH} S H^d H^u. \tag{2.66}$$

Note, that all group-theoretical indices are suppressed in this notation. Furthermore, neglecting CKM mixing, we take all Higgs-matter Yukawa couplings to be 3×3 diagonal matrices in family space.

In the leptoquark sector, we will assume a simplified scenario: The leptoquark Yukawa couplings are taken to be completely diagonal tensors in $3 \times 3 \times 3$ dimen-

sional family space:

$$W_D = \sum_{i=1}^3 (\mathbf{Y}_i^D D_i Q_{L_i} L_{L_i} + \mathbf{Y}_i^{D^c} D_i^c u_i^c e_i^c) \quad (2.67)$$

This choice is made in the logic of dedicating this work to the implications of our model on collider physics, as it implies that there are no contributions from the leptoquarks to the mixing of neutral mesons (see [56] and references therein¹³).

The masses of scalars receive contributions from three sources: the soft supersymmetry breaking terms, and the so-called D - and F -terms, which are quadrilinear scalar terms arising when writing out the gauge and superpotential Lagrangian in component fields (see (1.29) and (1.30)).

The auxiliary gauge (D) field obeys an algebraic equation of motion

$$D^a = - \sum_i (\phi_i^* T^a \phi_i). \quad (2.68)$$

After inserting the above identity into the Lagrangian it becomes:

$$- \mathcal{L}_D = \frac{g^2}{2} D^a D^a. \quad (2.69)$$

In order to yield a mass term, there have to be involved two fields, which have a non-trivial vacuum expectation value (vev). In our scenario H_3^d , H_3^u , and S_3 ¹⁴ acquire vevs. All scalars with vanishing vacuum expectation values receive D -term contributions to their masses of the form:

$$\begin{aligned} \mathcal{D}_Y(\tilde{f}) &\equiv \frac{g_Y^2}{2} Q_{\tilde{f}}^Y (Q_{H^u}^Y v_u^2 + Q_{H^d}^Y v_d^2), \\ \mathcal{D}'(\tilde{f}) &\equiv \frac{g'^2}{2} Q'_{\tilde{f}} (Q'_{H^u} v_u^2 + Q'_{H^d} v_d^2 + Q'_S v_s^2). \\ \mathcal{D}_2(\tilde{f}) &\equiv \frac{g_2^2}{8} T_{\tilde{f}}^3 (v_d^2 - v_u^2). \end{aligned} \quad (2.70)$$

In the last expression the scalar field is understood as component of an $SU(2)_L$ doublet, with $T_{\tilde{f}}^3$ yielding 1 or -1 for up- and down-type fields, respectively.

The F -terms denote the scalar potential originating from the superpotential W :

$$- \mathcal{L}_F = \left| \frac{\partial W}{\partial \phi_i} \right|^2. \quad (2.71)$$

¹³As shown there, such contributions might in some cases even be desirable from a phenomenological point of view, but their analysis exceeds the scope of this thesis.

¹⁴From now on we keep in mind that we identify the NMSSM-like Higgs sector with the third generation of H^u , H^d , and S particles and suppress the generation index, unless it is needed to avoid ambiguities.

2.5.1 Higgs Potential Minimization

The potential for the neutral fields of the Higgs-sector is given by

$$\begin{aligned}
V_{\text{Higgs}} &= (\mathbf{Y}^{SH})^2 [|H_d^0|^2 |H_u^0|^2 + |H_d^0|^2 |S|^2 + |S|^2 |H_u^0|^2] \\
&+ \frac{1}{2} g_Y^2 [Q_{H^u}^Y |H_u^0|^2 + Q_{H^d}^Y |H_d^0|^2]^2 + \frac{1}{8} g_2^2 [|H_u^0|^2 - |H_d^0|^2]^2 \\
&+ \frac{1}{2} g'^2 [Q'_{H^u} |H_u^0|^2 + Q'_{H^d} |H_d^0|^2 + Q'_S |S|^2]^2 \\
&+ \mathbf{m}_{H^d}^2 |H_d^0|^2 + \mathbf{m}_{H^u}^2 |H_u^0|^2 + \mathbf{m}_S^2 |S|^2 - (\mathbf{h}^{SH} S H_d^0 H_u^0 + h.c.). \quad (2.72)
\end{aligned}$$

In the course of electroweak symmetry breaking, all three neutral fields receive non-trivial vacuum expectations values, by which we shift the fields

$$H_0^d = \frac{1}{\sqrt{2}}(v_d + h^d + iA^d), \quad H_0^u = \frac{1}{\sqrt{2}}(v_u + h^u + iA^u), \quad S = \frac{1}{\sqrt{2}}(v_s + h^s + iA^s). \quad (2.73)$$

At its extrema the Higgs potential satisfies

$$\begin{aligned}
0 &\stackrel{!}{=} \left. \frac{\partial V}{\partial h_d} \right|_{\min} = \mathbf{m}_{H^d}^2 v_d - \frac{1}{\sqrt{2}} \mathbf{h}^{SH} v_s v_u + \frac{1}{2} \mathbf{Y}^{\text{SH}^2} v_d (v_s^2 + v_u^2) \\
&+ \frac{1}{8} g_2^2 v_d (v_d^2 - v_u^2) + \frac{1}{2} g'^2 Q'_{H^d} v_d (Q'_{H^u} v_u^2 + Q'_{H^d} v_d^2 + Q'_S v_s^2) \\
&+ \frac{1}{2} g_Y^2 Q_{H^d}^Y v_d (Q_{H^u}^Y v_u^2 + Q_{H^d}^Y v_d^2) \\
0 &\stackrel{!}{=} \left. \frac{\partial V}{\partial h_u} \right|_{\min} = \mathbf{m}_{H^d}^2 v_d - \frac{1}{\sqrt{2}} \mathbf{h}^{SH} v_s v_d + \frac{1}{2} \mathbf{Y}^{\text{SH}^2} v_u (v_s^2 + v_d^2) \\
&+ \frac{1}{8} g_2^2 v_u (v_u^2 - v_d^2) + \frac{1}{2} g'^2 Q'_{H^u} v_u (Q'_{H^u} v_u^2 + Q'_{H^d} v_d^2 + Q'_S v_s^2) \\
&+ \frac{1}{2} g_Y^2 Q_{H^u}^Y v_u (Q_{H^u}^Y v_u^2 + Q_{H^d}^Y v_d^2) \\
0 &\stackrel{!}{=} \left. \frac{\partial V}{\partial h_s} \right|_{\min} = \mathbf{m}_S^2 v_s - \frac{1}{\sqrt{2}} \mathbf{h}^{SH} v_u v_d + \frac{1}{2} \mathbf{Y}^{\text{SH}^2} v_s (v_d^2 + v_u^2) \\
&+ \frac{1}{2} g'^2 Q'_{H^u} v_u (Q'_{H^u} v_u^2 + Q'_{H^d} v_d^2 + Q'_S v_s^2) \quad (2.74)
\end{aligned}$$

As the geometric mean of v_d and v_u is related at the tree level to the very precisely measured mass of the Z -boson via

$$M_Z = \frac{\sqrt{g_Y^2 + g_2^2}}{2} v, \quad \text{where } v \equiv \frac{v_u}{\sin \beta} = \frac{v_d}{\cos \beta}, \quad (2.75)$$

is convenient to fix the vacuum expectation values and adjust the scalar soft breaking masses instead to satisfy the extremalization condition (2.74):

$$\mathbf{m}_{H^d}^2 = -\frac{1}{8} g_2^2 (v_d^2 - v_u^2) - \frac{1}{2} g'^2 Q'_{H^d} (Q'_{H^d} v_d^2 + Q'_{H^u} v_u^2 + Q'_S v_s^2)$$

$$\begin{aligned}
& -\frac{1}{2}g_Y^2 Q_{H^d}^Y (Q_{H^d}^Y v_d^2 + Q_{H^u}^Y v_u^2) - \frac{1}{2}(\mathbf{Y}^{SH})^2 (v_u^2 + v_s^2) \\
& + \frac{1}{\sqrt{2}} \mathbf{h}^{SH} \frac{v_s v_u}{v_d} \\
\mathbf{m}_{H^u}^2 = & -\frac{1}{8}g_2^2 (v_u^2 - v_d^2) - \frac{1}{2}g'^2 Q_{H^u}' (Q_{H^d}' v_d^2 + Q_{H^u}' v_u^2 + Q_S' v_s^2) \\
& -\frac{1}{2}g_Y^2 Q_{H^u}^Y (Q_{H^d}^Y v_d^2 + Q_{H^u}^Y v_u^2) - \frac{1}{2}(\mathbf{Y}^{SH})^2 (v_d^2 + v_s^2) \\
& + \frac{1}{\sqrt{2}} \mathbf{h}^{SH} \frac{v_s v_d}{v_u} \\
\mathbf{m}_S^2 = & -\frac{1}{2}g'^2 Q_S' (Q_{H^d}' v_d^2 + Q_{H^u}' v_u^2 + Q_S' v_s^2) \\
& -\frac{1}{2}(\mathbf{Y}^{SH})^2 (v_u^2 + v_d^2) + \frac{1}{\sqrt{2}} \mathbf{h}^{SH} \frac{v_d v_u}{v_s}
\end{aligned} \tag{2.76}$$

In the absence of CP-violating terms in the Lagrangian, the Higgs-sector can be decomposed into scalar, pseudo-scalar and charged Higgs-fields. The entries of the mass-squared matrix for the CP-even Higgs fields are given by

$$\begin{aligned}
m_{h^{dd}}^2 &= \mathbf{h}^{SH} \frac{v_s v_u}{\sqrt{2} v_d} + g_Y^2 (Q_{H^d}^Y)^2 v_d^2 + g'^2 (Q_{H^d}')^2 v_d^2 + \frac{g_2^2}{4} v_d^2 \\
m_{h^{uu}}^2 &= \mathbf{h}^{SH} \frac{v_s v_d}{\sqrt{2} v_u} + g_Y^2 (Q_{H^u}^Y)^2 v_u^2 + g'^2 (Q_{H^u}')^2 v_u^2 + \frac{g_2^2}{4} v_u^2 \\
m_{h^{ss}}^2 &= \mathbf{h}^{SH} \frac{v_d v_u}{\sqrt{2} v_s} + g'^2 (Q_S')^2 v_s^2 \\
m_{h^{du}}^2 &= (\mathbf{Y}^{SH})^2 v_u v_d - \mathbf{h}^{SH} \frac{v_s}{\sqrt{2}} + g_Y^2 Q_{H^d}^Y Q_{H^u}^Y v_u v_d + g'^2 Q_{H^d}' Q_{H^u}' v_u v_d - \frac{g_2^2}{4} v_u v_d \\
m_{h^{ds}}^2 &= (\mathbf{Y}^{SH})^2 v_d v_s - \mathbf{h}^{SH} \frac{v_u}{\sqrt{2}} + g'^2 Q_{H^d}' Q_S' v_s v_d \\
m_{h^{us}}^2 &= (\mathbf{Y}^{SH})^2 v_u v_s - \mathbf{h}^{SH} \frac{v_d}{\sqrt{2}} + g'^2 Q_{H^u}' Q_S' v_s v_u
\end{aligned} \tag{2.77}$$

Correspondingly, the pseudo-scalar mass matrix reads in the basis (A_d, A_u, A_s) :

$$m_A^2 = \frac{\mathbf{h}^{SH}}{\sqrt{2}} \begin{pmatrix} \frac{v_u v_s}{v_d} & v_s & v_u \\ v_s & \frac{v_d v_s}{v_u} & v_d \\ v_u & v_d & \frac{v_d v_u}{v_s} \end{pmatrix}, \tag{2.78}$$

which yields one physical pseudo-scalar with mass

$$M_A = \mathbf{h}^{SH} \frac{v_d^2 v_s^2 + v_u^2 v_s^2 + v_u^2 v_d^2}{\sqrt{2} v_d v_u v_s} \tag{2.79}$$

and two massless Goldstone modes providing masses for the Z and Z' bosons. The mass matrix of the charged Higgs particles takes the form

$$m_{H^\pm}^2 = \left(\mathbf{h}^{SH} \frac{v_s}{\sqrt{2}} + \frac{v_u v_d}{4} (g_2^2 - 2(\mathbf{Y}^{SH})^2) \right) \begin{pmatrix} \frac{v_u}{v_d} & 1 \\ 1 & \frac{v_d}{v_u} \end{pmatrix}, \quad (2.80)$$

yielding one physical charged Higgs boson of mass

$$M_{h^\pm}^2 = \mathbf{h}^{SH} v_s \frac{v_d^2 + v_u^2}{\sqrt{2} v_u v_d} + \frac{1}{4} g_2^2 (v_d^2 + v_u^2) - \frac{1}{2} (\mathbf{Y}^{SH})^2 (v_u^2 + v_d^2) \quad (2.81)$$

2.5.2 One-Loop Effective Potential

The masses of the lightest Higgs particles receive significant contributions from their couplings to the other particles in the theory at the quantum level. To calculate them, we use the *effective potential* approach [57] at the one-loop level. The radiative corrections to the Higgs potential (2.72) are given by

$$V_{rad}^{(1)} = \sum_p \text{tr} \left[\frac{N_p \mathcal{M}_p^4}{64\pi^2} \left(\log \frac{\mathcal{M}_p^2}{\Lambda^2} - \frac{3}{2} \right) \right]. \quad (2.82)$$

Here, \mathcal{M}_p^2 denotes the field dependent mass matrix (where the Higgs fields are not set to their vevs) of the particle p and N_p counts the degrees of freedom. The one-loop correction to the mass matrix M_{ij}^2 , is given by

$$\delta M_{ij}^2 = \left. \frac{\partial^2 V_{rad}^{(1)}}{\partial \phi_i \partial \phi_j} \right|_{vevs}. \quad (2.83)$$

As we chose to eliminate the SSB Higgs mass terms via (2.74), the above equation has to be modified in order to account for the shift in the \mathbf{m}_i^2 parameters arising from the extremalization of the full one-loop potential [58]:

$$\delta M_{ij}^2 = \left. \frac{\partial^2 V_{rad}^{(1)}}{\partial \phi_i \partial \phi_j} \right|_{vevs} - \frac{\delta_{ij}}{\sqrt{2} v_i} \left. \frac{\partial V_{rad}^{(1)}}{\partial \phi_i} \right|_{vevs}. \quad (2.84)$$

The analytical expressions for the radiative corrections at one-loop order to the Higgs masses in a $U(1)'$ extended MSSM originating from top- and bottom-quarks, as well as the colored exotics and their respective superpartners were given in [59]. Although these corrections are weighted by a color factor of 3 compared to the $SU(3)$ singlets, the contributions from the Higgs and dark Higgs sectors may be sizable, depending on the values of the respective Yukawa couplings. These can not be expressed analytically as the corresponding mass matrices are often of rank ≥ 5 (see the subsequent discussion in this section). The contributions to the Higgs mass matrix from (2.84) are evaluated numerically using the following identities, where the trace from (2.82) over the mass matrix \mathcal{M}_p^2 has been replaced

by the sum over its eigenvalues $m_{p,\alpha}^2$ [58]:

$$\begin{aligned} \frac{\partial V_{rad}^{(1)}}{\partial \phi_i} \Big|_{vevs} &= \frac{1}{32\pi^2} \sum_{p,\alpha} m_{p,\alpha}^2 \frac{\partial m_{p,\alpha}^2}{\partial \phi_i} \left(\log \frac{m_{p,\alpha}^2}{\Lambda^2} - 1 \right) \Big|_{vevs}, \\ \frac{\partial^2 V_{rad}^{(1)}}{\partial \phi_i \partial \phi_j} \Big|_{vevs} &= \frac{1}{32\pi^2} \sum_{p,\alpha} \left[\frac{\partial m_{p,\alpha}^2}{\partial \phi_i} \frac{\partial m_{p,\alpha}^2}{\partial \phi_j} \log \frac{m_{p,\alpha}^2}{\Lambda^2} + \frac{\partial^2 m_{p,\alpha}^2}{\partial \phi_i \partial \phi_j} \left(\log \frac{m_{p,\alpha}^2}{\Lambda^2} - 1 \right) \right] \Big|_{vevs}. \end{aligned} \quad (2.85)$$

2.5.3 Sfermion and Leptoquark Masses

The structure of the sfermion and leptoquark masses is the same for all three generations and hence the generation index shall be omitted in the subsequent discussion.¹⁵ The scalar mass-squared matrices are given in the basis $(\tilde{f}_L, \tilde{f}_R)$ with the D -terms defined in (2.70).

$$\begin{aligned} m_{\tilde{u}}^2 &= \begin{pmatrix} \mathbf{m}_{Q_L}^2 + (\mathbf{Y}^u)^2 \frac{v_u^2}{2} + \mathcal{D}_Y(\tilde{u}_L) + \mathcal{D}'(\tilde{u}_L) + \mathcal{D}_2(\tilde{u}_L), & \mathbf{h}^u \frac{v_u}{\sqrt{2}} - \mathbf{Y}^u \mathbf{Y}^{SH} \frac{v_s v_d}{2} \\ \mathbf{h}^u \frac{v_u}{\sqrt{2}} - \mathbf{Y}^u \mathbf{Y}^{SH} \frac{v_s v_d}{2}, & \mathbf{m}_{u^c}^2 + (\mathbf{Y}^u)^2 \frac{v_u^2}{2} + \mathcal{D}_Y(\tilde{u}_R) + \mathcal{D}'(\tilde{u}_R) \end{pmatrix} \\ m_{\tilde{d}}^2 &= \begin{pmatrix} \mathbf{m}_{Q_L}^2 + (\mathbf{Y}^d)^2 \frac{v_d^2}{2} + \mathcal{D}_Y(\tilde{d}_L) + \mathcal{D}'(\tilde{d}_L) + \mathcal{D}_2(\tilde{d}_L), & \mathbf{h}^d \frac{v_d}{\sqrt{2}} - \mathbf{Y}^d \mathbf{Y}^{SH} \frac{v_s v_u}{2} \\ \mathbf{h}^d \frac{v_d}{\sqrt{2}} - \mathbf{Y}^d \mathbf{Y}^{SH} \frac{v_s v_u}{2}, & \mathbf{m}_{d^c}^2 + (\mathbf{Y}^d)^2 \frac{v_d^2}{2} + \mathcal{D}_Y(\tilde{d}_R) + \mathcal{D}'(\tilde{d}_R) \end{pmatrix} \\ m_{\tilde{e}}^2 &= \begin{pmatrix} \mathbf{m}_{L_L}^2 + (\mathbf{Y}^e)^2 \frac{v_d^2}{2} + \mathcal{D}_Y(\tilde{e}_L) + \mathcal{D}'(\tilde{e}_L) + \mathcal{D}_2(\tilde{e}_L), & \mathbf{h}^e \frac{v_d}{\sqrt{2}} - \mathbf{Y}^e \mathbf{Y}^{SH} \frac{v_s v_u}{2} \\ \mathbf{h}^e \frac{v_d}{\sqrt{2}} - \mathbf{Y}^e \mathbf{Y}^{SH} \frac{v_s v_u}{2}, & \mathbf{m}_{e^c}^2 + (\mathbf{Y}^e)^2 \frac{v_d^2}{2} + \mathcal{D}_Y(\tilde{e}_R) + \mathcal{D}'(\tilde{e}_R) \end{pmatrix} \end{aligned} \quad (2.86)$$

The leptoquark masses in the basis (D_L, D_R) take the form

$$m_{\tilde{D}}^2 = \begin{pmatrix} \mathbf{m}_D^2 + (\mathbf{Y}^{SD})^2 \frac{v_s^2}{2} + \mathcal{D}_Y(D) + \mathcal{D}'(D), & \mathbf{h}^{SD} \frac{v_s}{\sqrt{2}} - \mathbf{Y}^{SD} \mathbf{Y}^{SH} \frac{v_d v_u}{2} \\ \mathbf{h}^{SD} \frac{v_s}{\sqrt{2}} - \mathbf{Y}^{SD} \mathbf{Y}^{SH} \frac{v_d v_u}{2}, & \mathbf{m}_{D^c}^2 + (\mathbf{Y}^{SD})^2 \frac{v_s^2}{2} + \mathcal{D}_Y(D^R) + \mathcal{D}'(D^R) \end{pmatrix}. \quad (2.87)$$

2.5.4 Dark Higgs Masses

The first two generations of Higgs particles do not couple to matter, due to a Z_2 symmetry, requiring the so-called dark Higgs particles to be produced in pairs. These particles are nonetheless subject to gauge interactions and Yukawa interactions stemming from the superpotential:

$$\begin{aligned} W_H &= \mathbf{Y}_{113}^{SH} S_1 H_1^d H_3^u + \mathbf{Y}_{123}^{SH} S_1 H_2^d H_3^u + \mathbf{Y}_{213}^{SH} S_2 H_1^d H_3^u + \mathbf{Y}_{223}^{SH} S_2 H_2^d H_3^u \\ &\quad + \mathbf{Y}_{131}^{SH} S_1 H_3^d H_1^u + \mathbf{Y}_{132}^{SH} S_1 H_3^d H_2^u + \mathbf{Y}_{231}^{SH} S_2 H_3^d H_1^u + \mathbf{Y}_{232}^{SH} S_2 H_3^d H_2^u \end{aligned}$$

¹⁵This only works when neglecting a CKM-like mixing among particle generations.

$$+ \mathbf{Y}_{311}^{SH} S_3 H_1^d H_1^u + \mathbf{Y}_{312}^{SH} S_3 H_1^d H_2^u + \mathbf{Y}_{321}^{SH} S_3 H_2^d H_1^u + \mathbf{Y}_{322}^{SH} S_3 H_2^d H_2^u. \quad (2.88)$$

The entries of the 6×6 mass matrices for the CP-even, CP-odd and charged dark Higgs particles can be found in appendix B.2.

2.5.5 Neutralino and Chargino Masses

The Lagrangian describing a generic interaction of gauginos λ^a and chiral matter ϕ has the form

$$\mathcal{L}_{\lambda\tilde{h}} = -\sqrt{2}g_\alpha(T_\alpha^a)_{ij}\lambda^a\tilde{\phi}_j\phi_i + h.c.,$$

where ϕ and $\tilde{\phi}$ denote the scalar and fermionic component of a chiral superfield, respectively. This interaction causes a mixing of the gaugino and the fermionic chiral field when the scalar components of the chiral field condenses. In our model there is, apart from the five NMSSM fields, the $U(1)'$ gaugino contributing to the neutralino sector.

$$\begin{aligned} \mathcal{L}_{\lambda^0\tilde{h}}|_{\text{vevs}} = & -\frac{g_2}{2}\lambda^3\left(\tilde{h}_d^0v_d - \tilde{h}_u^0v_u\right) - g_Y\lambda^Y\left(Q_{H^d}^Y\tilde{h}_d^0v_d + Q_{H^u}^Y\tilde{h}_u^0v_u\right) \\ & - g'\lambda'\left(Q'_{H^d}\tilde{h}_d^0v_d + Q'_{H^u}\tilde{h}_u^0v_u + Q'_S\tilde{h}_s v_s\right) + h.c. \end{aligned} \quad (2.89)$$

In addition, there are soft supersymmetry breaking gaugino masses, as well as the Higgs-Higgsino self-interaction terms originating from the superpotential, contributing to the neutralino masses:

$$\mathcal{L}_{\text{SSB}} = -\frac{1}{2}M_2\lambda^3\lambda^3 - \frac{1}{2}M_Y\lambda^Y\lambda^Y - \frac{1}{2}M'\lambda'\lambda' - M'_Y\lambda'\lambda^Y + h.c., \quad (2.90)$$

$$\mathcal{L}_W = \mathbf{Y}^{SH}\left(v_s\tilde{h}_d^0\tilde{h}_u^0 + v_d\tilde{h}_s\tilde{h}_u^0 + v_u\tilde{h}_s\tilde{h}_d^0\right) + h.c. \quad (2.91)$$

Note, that in the first equation, we introduced a term accounting for the mixing among the $U(1)'$ and $U(1)_Y$ gauginos.

At this point, the Lagrangian is conventionally re-arranged in the following way:

$$\mathcal{L}_m^n = -\frac{1}{2}\psi_0^T\mathcal{M}_0\psi_0 + h.c., \quad (2.92)$$

with $\psi = (\lambda^3, \lambda^Y, \lambda', \tilde{h}_d^0, \tilde{h}_u^0, \tilde{h}_s)^T$ and

$$\mathcal{M}_0 = \begin{pmatrix} M_2 & 0 & 0 & g_2\frac{v_d}{2} & -g_2\frac{v_u}{2} & 0 \\ 0 & M_Y & M'_Y & g_Y Q_{H^d}^Y v_d & g_Y Q_{H^u}^Y v_u & 0 \\ 0 & M'_Y & M' & g' Q'_{H^d} v_d & g' Q'_{H^u} v_u & g' Q'_S v_s \\ g_2\frac{v_d}{2} & g_Y Q_{H^d}^Y v_d & g' Q'_{H^d} v_d & 0 & -\mathbf{Y}^{SH}\frac{v_s}{\sqrt{2}} & -\mathbf{Y}^{SH}\frac{v_u}{\sqrt{2}} \\ -g_2\frac{v_u}{2} & g_Y Q_{H^u}^Y v_u & g' Q'_{H^u} v_u & -\mathbf{Y}^{SH}\frac{v_s}{\sqrt{2}} & 0 & -\mathbf{Y}^{SH}\frac{v_d}{\sqrt{2}} \\ 0 & 0 & g' Q'_S v_s & -\mathbf{Y}^{SH}\frac{v_u}{\sqrt{2}} & -\mathbf{Y}^{SH}\frac{v_d}{\sqrt{2}} & 0 \end{pmatrix}. \quad (2.93)$$

The chargino mass terms are equivalent to the NMSSM (which corresponds to the MSSM chargino mass, upon a replacement $\mu \rightarrow \mathbf{Y}^{SH} \frac{v_s}{\sqrt{2}}$):

$$\mathcal{L}_m^c = (\psi^-)^T \mathcal{M}_\pm \psi^+ + h.c., \quad (2.94)$$

where

$$\psi^- = \begin{pmatrix} \lambda^- \\ \tilde{h}_d^- \end{pmatrix}, \quad \psi^+ = \begin{pmatrix} \lambda^+ \\ \tilde{h}_u^+ \end{pmatrix}, \quad \text{and } \mathcal{M}_\pm = \begin{pmatrix} M_2 & g_2 \frac{v_u}{\sqrt{2}} \\ g_2 \frac{v_d}{\sqrt{2}} & \mathbf{Y}^{SH} \frac{v_s}{\sqrt{2}} \end{pmatrix}. \quad (2.95)$$

2.5.6 Dark Higgsinos

As the dark Higgs fields all have trivial vacuum expectation values, their fermionic superpartners do not mix with the gaugino fields. The mass matrix of these neutral dark Higgsinos reads in the basis $(\tilde{h}_d^1, \tilde{h}_u^1, \tilde{h}_s^1, \tilde{h}_d^2, \tilde{h}_u^2, \tilde{h}_s^2)$:

$$\mathcal{M}_0 = -\frac{1}{\sqrt{2}} \begin{pmatrix} 0 & \mathbf{Y}_{311}^{SH} v_s & \mathbf{Y}_{113}^{SH} v_u & 0 & \mathbf{Y}_{312}^{SH} v_s & \mathbf{Y}_{213}^{SH} v_u \\ \mathbf{Y}_{311}^{SH} v_s & 0 & \mathbf{Y}_{131}^{SH} v_d & \mathbf{Y}_{321}^{SH} v_s & 0 & \mathbf{Y}_{231}^{SH} v_d \\ \mathbf{Y}_{113}^{SH} v_u & \mathbf{Y}_{131}^{SH} v_d & 0 & \mathbf{Y}_{123}^{SH} v_u & \mathbf{Y}_{132}^{SH} v_d & 0 \\ 0 & \mathbf{Y}_{321}^{SH} v_s & \mathbf{Y}_{123}^{SH} v_u & 0 & \mathbf{Y}_{322}^{SH} v_s & \mathbf{Y}_{223}^{SH} v_u \\ \mathbf{Y}_{312}^{SH} v_s & 0 & \mathbf{Y}_{132}^{SH} v_d & \mathbf{Y}_{322}^{SH} v_s & 0 & \mathbf{Y}_{232}^{SH} v_d \\ \mathbf{Y}_{213}^{SH} v_u & \mathbf{Y}_{231}^{SH} v_d & 0 & \mathbf{Y}_{223}^{SH} v_u & \mathbf{Y}_{232}^{SH} v_d & 0 \end{pmatrix} \quad (2.96)$$

This mass-matrix generically has two very light eigenstates (~ 1 GeV). In order to understand whether they contradict the results from experimental searches like $e^+e^- \rightarrow Z \rightarrow inv$, we have to trace back, where they originate from. Assuming the Yukawa couplings mixing both generations of dark Higgs superfields to vanish, renders (2.96) block-diagonal. In the limit $v_s \gg v_u, v_d$, the upper 3×3 block has eigenvalues

$$\begin{aligned} m_1 &= \sqrt{2} \frac{\mathbf{Y}_{131}^{SH} \mathbf{Y}_{113}^{SH} v_u v_d}{\mathbf{Y}_{311}^{SH} v_s}, & m_2 &= \frac{\mathbf{Y}_{311}^{SH} v_s}{\sqrt{2}} + \frac{(\mathbf{Y}_{131}^{SH} v_d - \mathbf{Y}_{113}^{SH} v_u)^2}{\sqrt{2} \mathbf{Y}_{311}^{SH} v_s} \\ m_3 &= -\frac{\mathbf{Y}_{311}^{SH} v_s}{\sqrt{2}} - \frac{(\mathbf{Y}_{131}^{SH} v_d + \mathbf{Y}_{113}^{SH} v_u)^2}{\sqrt{2} \mathbf{Y}_{311}^{SH} v_s}. \end{aligned} \quad (2.97)$$

The physical state corresponding to the lightest eigenvalue m_1 is

$$-\mathbf{Y}_{131}^{SH} \frac{v_d}{M} \tilde{h}_d^1 - \mathbf{Y}_{113}^{SH} \frac{v_u}{M} \tilde{h}_u^1 + \mathbf{Y}_{311}^{SH} \frac{v_s}{M} \tilde{h}_s^1, \quad (2.98)$$

where M denotes the geometric mean of the three vacuum expectation values, weighted with the dark Higgs Yukawa couplings:

$$M \equiv \sqrt{(\mathbf{Y}_{131}^{SH} v_d)^2 + (\mathbf{Y}_{113}^{SH} v_u)^2 + (\mathbf{Y}_{311}^{SH} v_s)^2}.$$

From this, we conclude that the two extremely light dark neutralinos consist predominantly of dark singlinos, relaxing the LEP-bounds $Z \rightarrow inv$ significantly, as they do not couple to standard model gauge bosons. In the course of investigating the phenomenology of this model in chapter 4, we shall briefly sketch possible issues regarding the cosmological impact of dark Higgsinos.

The Lagrangian containing the mass terms of the charged dark Higgsinos has the following form:

$$\begin{aligned} \mathcal{L}_{\tilde{\chi}_{\alpha,\beta}^\pm} &= \tilde{\chi}_\alpha^- (M_{\tilde{\chi}^\pm})_{\alpha\beta} \tilde{\chi}_\beta^+ + h.c., & \tilde{\chi}^+ &\equiv (\tilde{h}_{u_1}^+, \tilde{h}_{u_2}^+), & \tilde{\chi}^- &\equiv (\tilde{h}_{d_1}^-, \tilde{h}_{d_2}^-), \\ \text{and} & & (M_{\tilde{\chi}^\pm})_{\alpha\beta} &= \mathbf{Y}_{3\alpha\beta}^{SH} \frac{v_s}{\sqrt{2}}. \end{aligned} \quad (2.99)$$

2.5.7 $Z - Z'$ mixing

The gauge covariant derivative in the $SU(2)_L \times U(1)_Y \times U(1)'$ basis reads:

$$D_\mu = \partial_\mu + ig_2 T^3 W_\mu^3 + i \underbrace{\left(g_Y \sqrt{\frac{3}{5}} \right)}_{=g_{SM}^Y} \underbrace{\left(Q^Y \sqrt{\frac{5}{3}} \right)}_{=Q_{SM}^Y} B_\mu^Y + ig' Q' B'_\mu. \quad (2.100)$$

After electroweak symmetry breaking, the coupling of the gauge fields W_μ^3, B_μ^Y, B'_μ to the vacuum expectation value of the Higgs fields renders the gauge fields massive. As in the standard model, after diagonalization of the gauge boson mass matrix, there is one massless gauge boson, which we identify with the photon. With this in mind, it is convenient to re-write (2.100) in terms of the standard model mass eigenstates

$$\begin{aligned} Z_\mu &= \frac{g_2}{\sqrt{(g_{SM}^Y)^2 + g_2^2}} W_\mu^3 - \frac{g_{SM}^Y}{\sqrt{(g_{SM}^Y)^2 + g_2^2}} B_\mu^Y, \\ A_\mu &= \frac{g_{SM}^Y}{\sqrt{(g_{SM}^Y)^2 + g_2^2}} W_\mu^3 + \frac{g_2}{\sqrt{(g_{SM}^Y)^2 + g_2^2}} B_\mu^Y, \\ \text{and} \quad Z'_\mu &= B'_\mu. \end{aligned} \quad (2.101)$$

as the coupling of the photon to all the Higgs fields H_0^d, H_0^u, S vanishes. The gauge covariant derivative as it acts on electrically neutral fields then becomes:

$$D_\mu|_{Q^e=0} = \partial_\mu + \frac{i}{\sqrt{(g_{SM}^Y)^2 + g_2^2}} (g_2^2 T_3 - (g_{SM}^Y)^2 Q_{SM}^Y) Z_\mu + ig' Q' Z'_\mu \quad (2.102)$$

yielding the $Z - Z'$ mass matrix:

$$\begin{aligned} M_{ZZ'}^2 &= \begin{pmatrix} M_Z^2 & \delta M_{ZZ'}^2 \\ \delta M_{ZZ'}^2 & M_{Z'}^2 \end{pmatrix}, & \text{with} \\ M_Z^2 &= \frac{1}{4} (g_2^2 + (g_{SM}^Y)^2) (v_u^2 + v_d^2), \end{aligned}$$

$$\begin{aligned}
M_{Z'}^2 &= g'^2 \left(Q'_{H^d}{}^2 v_d^2 + Q'_{H^u}{}^2 v_u^2 + Q'_S{}^2 v_s^2 \right) \\
\delta M_{ZZ'}^2 &= \frac{1}{2} g' \sqrt{g_2^2 + (g^Y_{\text{SM}})^2} (Q'_{H^d} v_d^2 + Q'_{H^u} v_u^2)
\end{aligned}
\tag{2.103}$$

The mixing mass term $\delta M_{ZZ'}^2$ of the additional neutral heavy gauge boson with the SM's Z is of great importance to the consistency of any $U(1)'$ -extension of the standard model with electroweak precision (EWP) data: The light eigenvalue of the mass matrix (2.103) is numerically set equal to the observed Z mass, which amounts to a shift in the couplings of the Z -boson (mass eigenstate) due to the admixture of the (gauge eigenstate) Z' .

The coupling of the Z -boson to the standard model fermions was very precisely measured [60], and puts very stringent bounds on the maximal mixing of the additional Z' with the Z which is obtained from (2.103) to be of the order

$$Z_\mu^{\text{new}} = Z_\mu^{\text{SM}} - \frac{\delta M_{ZZ'}^2}{M_{Z'}^2} Z'_\mu.
\tag{2.104}$$

As we aim at the collider phenomenology and do not wish to re-calculate all the EWP observables, we will simply assume the Z' to be sufficiently heavy ($\gtrsim 1.5$ TeV) not to have left a noticeable trace in the Z coupling to the SM fermions ($\Rightarrow 10^{-3} \gtrsim \delta M_{ZZ'}^2/M_{Z'}^2$) at LEP. This also corresponds roughly to the current bound from direct searches at the LHC [40]. With this strategy, we assume that all possible malign contributions to EWP-observables from our model are rendered sufficiently small and the general good agreement of SUSY models with EWP data [12] is restored.

Chapter 3

Automated Spectrum Generation

After having presented the general structure of our model in the previous chapters, we now aim at investigating the model's implications on TeV-scale collider physics.

We wish to specify the free parameters at the orbifold compactification scale. In a first step all TeV-scale Lagrangian parameters have to be derived by solving the renormalization group equations linked via matching conditions at the symmetry breaking scales accounting for the gauge structure in the respective energy ranges, as discussed in section 2.4. In a subsequent step the full TeV-scale spectrum including all particle masses, mixing matrices and couplings are derived from the Lagrangian parameters according to the formulas from section 2.5.

This calls for a numerical evaluation using a so-called *spectrum generator*. As TeV-scale SUSY is commonly placed in the context of grand unification, there are many programs available [61], that allow to derive (N)MSSM spectra from input parameters chosen at the GUT scale. Unfortunately, there are many non-standard SUSY features inherent to our model which would have required substantial modifications within any of the pre-existing programs. The multi-stepped unification scenario, the $U(1)$ -mixing yielding off-diagonal gaugino masses within our prescription, the extended particle content leading to new kinds of interactions, motivated us to write our own spectrum generator – called **EXSPECT**, especially designed to account for the new features of our model.

As much of the physics and the technical point of its handling is incorporated in the structure and the usage of this program, we give a detailed documentation of its design here.

The development of the current version of **EXSPECT** was oriented at the following guidelines:

- As we did not specify a soft SUSY breaking mechanism in our model, the SSB terms should be regarded as a parametrization of our lack of knowledge. Hence, the program should be able to handle a large number of independent input parameters, in order not to overly constrain the SSB sector (without physical motivation).
- We wish to analyze the entire space of free input parameters of our model. Therefore the program should be fast regarding runtime. In turn, we accept some loss in precision (by only using one-loop RGEs).
- The program is aimed at the investigation of the collider phenomenology of our model, so far omitting its cosmological implications. That is, the program computes the masses and couplings of the dark matter candidates, but further derivations of the cosmological observables such as relic densities are not provided at this stage of development.
- For extended future investigations it is desirable to use general structures: The renormalization group equations for example can be generated from

within the program, in order to be ready to investigate other setups as modified leptoquark couplings, off-diagonal dark-Higgs couplings, etc.

Disclaimer: The program presented here should be understood as the first stage of an ongoing development. We will present in the following the structures that have been realized so far and also comment on the potential future development later in this work.

EXSPECT is structured in the following way: The installing routine a) computes the gauge coupling unification scenario and b) generates the full set of one-loop renormalization group equations for the remaining parameters of the model. The main program runs all RGEs from the unification scale down to the TeV scale and translates the numerical values of the Lagrangian parameters into a spectrum. The main program is embedded into a Monte-Carlo Markov-Chain algorithm used to search the parameter space. In the remainder of this chapter we shall discuss each of the above parts of EXSPECT in detail. While reviewing the steps that lead from a specification of the free parameters in our theory at the orbifold compactification scale to the TeV-scale spectrum, we will encounter some additional features of the model, which follow from the structure of the RGEs and the phase transition at the intermediate symmetry breaking scale (e.g. top-bottom Yukawa unification), but have not been in the focus of our attention so far.

3.1 Initialization: Gauge Unification and Auto-Generation of RGEs

As the RGEs are solved at the one-loop level, we see from the formulas in section 2.4 that they decouple into the subsets displayed in table 3.1, with minimal interdependencies. The fact that the RGEs describing the running of the gauge

RGEs	dependencies				
	g	\mathbf{Y}	M_g	\mathbf{h}	\mathbf{m}^2
g	+				
\mathbf{Y}	+	+			
M_g	+		+		
\mathbf{h}	+	+	+	+	
\mathbf{m}^2	+	+	+	+	+

Table 3.1: The dependencies of the RGEs for gauge- (g), Yukawa- (\mathbf{Y}), and trilinear SSB couplings (\mathbf{h}), as well as SSB mass terms for gauginos (M_g) and scalars (\mathbf{m}^2) on each other at the one-loop level.

couplings at the one-loop level do not depend on the evolution of other Lagrangian parameters allows us to solve them once, prior to the solution of the remaining RGEs (they solely depend on the choice of the intermediate particle content from (2.4) and lead to the distinct unification scenarios shown in figure

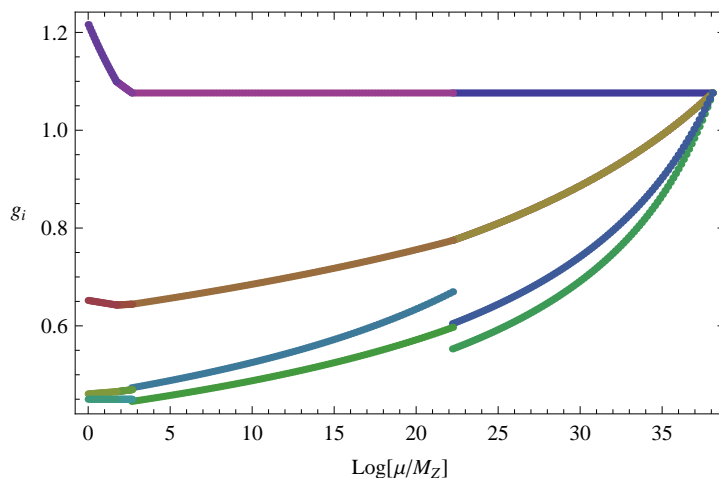


Figure 3.1: Numerical output of `mathematica_files/run_couplings.m` for the running of the gauge couplings.

2.3). The gauge coupling unification is calculated by a Mathematica [62] routine `./mathematica_files/run_couplings.m` which is called in the first step of the `install.sh`-script. It follows the steps discussed in detail in section 2.1 (the reasons to invoke Mathematica at this stage are mainly of historical origin; a future version of `EXSPECT` should integrate this part into the C++ program). The running of the gauge couplings is evaluated at a discrete number of scales and written to files. A sample is plotted in figure 3.1. Furthermore, all charges (table 2.1) and mixing matrices for the gauge bosons at the symmetry breaking scales (2.15) are calculated and stored in files as well.

In the second step the `install.sh`-script calls a C++ program `./RGEgenerator/RGEgenerator.cpp` that derives the full set of RGEs for the remaining Lagrangian parameters and writes them to files which can later be included into the main program using the `#include <.>` directive. Furthermore, there is the possibility to generate `LATEX` code for documentation. In the following subsection we give detailed information on the algorithms generating the RGEs.

3.1.1 Generating Renormalization Group Equations

After the RGEs for the gauge couplings have already been solved, the remaining RGEs for the Yukawa couplings and the soft SUSY breaking parameters (gaugino mass terms, trilinear scalar couplings and scalar mass terms) can be derived from a minimal set of specifications (for each phase of the symmetry breaking pattern separately):

- The gauge group is specified in an array of class `CGauge` (there is currently no interface synchronizing the routine calculating the gauge coupling unification with this program. The gauge groups have to be ordered according to the charges outputted by `run_couplings.m`).

- All particles in the spectrum with their charges under all gauge groups stored in `gauge_group` have to be specified in an array of the type `CParticle`. (the ordering has to follow the output of `run_couplings.m` again).
- All Yukawa couplings have to be given as objects of type `CYukawa` in the form

$$\mathbf{Y}_{gen_i, gen_j, gen_k}^{i,j,k}, \quad (3.1)$$

where i, j, k denote particle types and gen_i the generation.

- The set of gaugino mass terms is derived from the specified gauge groups. The formulas are corrected for mixing mass terms among $U(1)$ gauginos below the intermediate scale.
- Trilinear and scalar mass-squared SSB terms can either be specified explicitly as objects of the classes `CYukawa` and `CMass`, respectively, or can be generated automatically from the array containing all Yukawa couplings:

The function `autocreate_SSB` simply returns a trilinear SSB coupling for each Yukawa coupling. `autocreate_SSB_mass` checks for each pair of particles (i, j) if they can be connected through a loop of the form $\mathbf{Y}^{ipq} \mathbf{Y}_{pqj}$ and if so, creates a corresponding `CMass` object m_{ij} .

This procedure ensures that one cannot specify a set of soft SUSY breaking parameters without having included all terms that would receive radiative contributions even if they vanish at the input scale.

On the other hand, one has to manually add SSB parameters if one neglects Yukawa couplings (e.g. for the light matter content) and still have corresponding trilinear couplings and/or masses for the corresponding sfermions.

- The group theoretical factors for non-Abelian gauge groups are hard-coded (independent of the unification scenario), whereas the Abelian factors are calculated from the charges outputted by `run_couplings.m`.

The results obtained with this code have been compared to the RGEs for the MSSM as given in [52] and double-checked with explicit calculations for particularly complicated set-ups as non-diagonal wave-function renormalization in the dark Higgs sector. The case of couplings involving the $(\mathbf{1}, \mathbf{2}, \mathbf{2})$ Higgs fields under $SU(3) \times SU(2)_L \times SU(2)_R$ was compared to [63].¹

In the remainder of this section we show schematically how the algorithms generating the RGEs for Yukawa couplings, SSB gaugino masses, trilinear SSB, and scalar mass-squared SSB work.

¹Bare in mind the different convention used to normalize the superpotential terms.

Generation of the Yukawa RGEs

Let i, j, k, \dots denote objects of type `CParticle`, \mathbf{Y}_{ijk} a Yukawa coupling (of type `CYukawa`) involving the particles i, j, k and $\{\mathbf{Y}\}$ the list of all specified Yukawa couplings.

- The gauge contribution to the running of the Yukawa coupling \mathbf{Y}_{ijk} corresponding to the diagrams in (2.4.2) can simply be calculated from the charges under each gauge group of the particles involved in the coupling according to (2.54). It is always proportional to the \mathbf{Y}_{ijk} .
- The cubic Yukawa terms in (2.54) are created using the following functions:
 - `two_in_common` maps k , \mathbf{Y}_{ijk} , and $\{\mathbf{Y}\}$ onto a list of all Yukawa couplings involving the other two particles i, j from \mathbf{Y}_{ijk} and the respective third particles.

$$\begin{array}{c} k \\ \diagup \\ \text{---} \\ \diagdown \\ j \end{array} \quad \longrightarrow \quad \left\{ \begin{array}{c} l \\ \diagup \\ \text{---} \\ \diagdown \\ j \end{array}, l, \forall l \right\}.$$

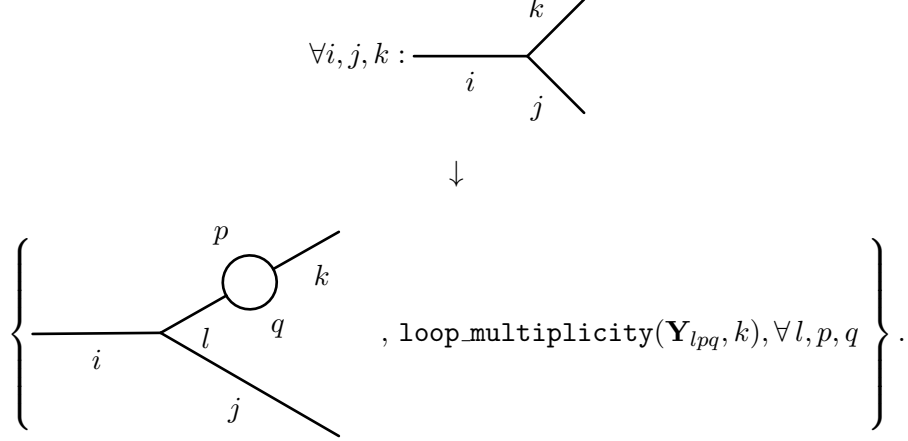
- The function `loops_xy` creates an array containing all pairs of Yukawa couplings that connect a given pair of particles through a loop:

$$\{i, j\} \longrightarrow \left\{ \begin{array}{c} q \\ \diagup \\ \text{---} \\ \diagdown \\ p \end{array}, \begin{array}{c} q \\ \diagup \\ \text{---} \\ \diagdown \\ p \end{array}, \forall p, q \right\}.$$

- As particles in this case are understood as entire multiplets under the respective gauge groups, one has to insert multiplicities as they are not automatically accounted for by the summation over inner particles, as it is understood in [52]. The multiplicity of a loop, represented by a pair of Yukawa couplings and two external particles, is calculated in two steps: `mult_yuk` evaluates how many terms the tensor product of either of the two Yukawa couplings contains. Then this result is divided by `particle_multiplicity` of the external particles, which is just the product of the dimensions of the representations of non-Abelian gauge groups the particle transforms under. If there are two identical particles running in the loop, the result is divided by two. Within our model the latter becomes relevant for \mathbf{Y}^{SH} above the intermediate scale.
- The function `vertices` takes as arguments a Yukawa coupling \mathbf{Y}_{ijk} and the list of all Yukawa couplings.

For each particle k involved in \mathbf{Y}_{ijk} the array `two_in_common` is built. Then for each entry in that array, it takes the particle l and creates all loops that connect k and l and calculates the multiplicity for each loop. In the

end, an array of triples of Yukawa couplings ($\mathbf{Y}_{ijl}, \mathbf{Y}_{lpq}, \mathbf{Y}_{pqk}$) and the loop multiplicity is returned:



Generating the RGEs for the h-Terms

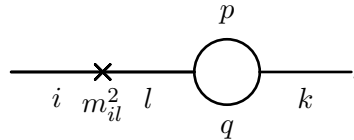
The terms $\mathbf{h}^{ijl} \mathbf{Y}^{lpq} \mathbf{Y}^{pqk}$ and $\mathbf{Y}^{ijl} \mathbf{Y}^{lpq} \mathbf{h}^{pqk}$ in the beta function of \mathbf{h}^{ijk} (2.59) have exactly the same structure as the cubic terms in the Yukawa RGE. Therefore, they can be obtained from the same function `vertex` where in each vertex the first or last Yukawa is replaced by its corresponding trilinear coupling, respectively.

The contributions from gauge and gaugino interactions are again proportional to \mathbf{h}^{ijk} . Their coefficients are calculated from the particles coupled by \mathbf{h}^{ijk} . In case that $U(1)_{A/B}$ are part of the gauge group, the contribution from the mixing of the off-diagonal gaugino masses is added in a hard-coded fashion.

Generating RGEs for the Scalar SSB Masses

The beta functions of \mathbf{m}_{ij}^2 from (2.61) are generated in the following steps:

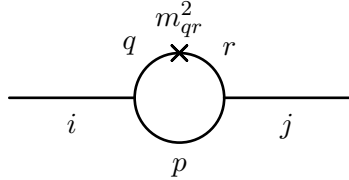
- The terms $\mathbf{h}^{ipq} \mathbf{h}^{pqj}$ have the structure of loops connecting the particles i and j . The function `loops_xy` is now used to return all pairs of trilinear couplings with external particles i, j .
- The contributions $\mathbf{Y}^{ipq} \mathbf{Y}^{pql} \mathbf{m}_{lj}$ and $\mathbf{Y}^{j pq} \mathbf{Y}^{pql} \mathbf{m}_{li}$ correspond to diagrams like



In order to build them, the function `one_in_common` takes a particle i and returns an array of all masses $\{\mathbf{m}_{il}^2\}$ containing this particle and the respective other particles l . This array is created for both particles in \mathbf{m}_{ij}^2 and

for each entry \mathbf{m}_{il}^2 all loops connecting the particles l and j are created by `loops_xy`.

- The term $\mathbf{Y}^{ipq}\mathbf{Y}^{jpr}\mathbf{m}_{qr}$ has the diagrammatic form



The function `four_vertex` builds an array of all quadruples of particles that can be connected through two Yukawa couplings linked at tree level. In addition it returns the respective Yukawa couplings.

Given a mass \mathbf{m}_{ij}^2 , the array of four-vertices is scanned for whether the particles i, j can be attached to opposite sides of the vertex. If so, all masses are investigated for if they can connect the remaining two loose ends of the vertex.

- The gaugino mass contribution is calculated from the charges of the particles connected through each mass. It only contributes if the two particles are identical.
- The last contribution in (2.61) comes from the D -terms of the $U(1)$ gauge groups. First, the function `diag_masses` sets up a list of all mass terms connecting the same particles. Then, the D -term contribution of the $U(1)$ groups is generated on the fly (i.e. while executing the write statement). If the mass term is (generation-) diagonal (which may not be the case for dark Higgs masses, or in the case where CMK mixing is taken into account), for which the RGE is currently written, all $U(1)$ groups are checked for whether they are in effect, and if the mass' particle is charged under them. If so, all diagonal masses from the list whose particle carries charge under the respective group are inserted in the D -term.

3.2 Main Program: Running the Remaining RGEs

The centerpiece of `EXSPECT` is a C++ program called `RGERunner/main.cpp` which solves the RGEs for the Yukawa couplings, and all soft SUSY breaking parameters from the GUT scale, where all input parameters are specified, to the TeV scale (or M_Z in the case of the Yukawa couplings). At all symmetry breaking scales in between, the number of independently running parameters may change, as symmetry constraints are relaxed and particles may be integrated out, effectively removing the corresponding operators from the theory below that scale. This is accounted for via the matching conditions (2.57). The RGEs are solved subsequently in an order consistent with table 3.1. `EXSPECT` uses the `gsl_odeiv`

routines from the `Gnu Scientific Library` [64] to solve the RGEs, storing the result as arrays `gsl_matrix`. The discrete values are interpolated and supplied to subsequent routines as `gsl_spline` objects.

The `RGERunner/main.cpp` program is structured as follows:

0. The running of the gauge couplings is read in (as arrays) from the files written during the execution of the `install.sh` script. The discrete data is interpolated using the tools provided by the `Gnu Scientific Library` [64] in order to be supplied to the routine solving the remaining RGEs.
1. The RGEs for the Yukawa couplings are solved within an iteration loop that varies the unified Yukawa coupling of the third generation quark superfields to the Higgs fields and optimizes $\tan\beta = v_u/v_d$ until the top and bottom quark masses agree with their experimentally determined values (at M_Z). The running of the couplings from the final step in the above iteration is interpolated to be available for the routines solving the RGEs of the trilinear and mass squared scalar SSB terms in the following.
2. The running of the SSB gaugino mass terms is calculated, accounting for the mixing of the $U(1)$ gauge groups below the intermediate scale and the result is interpolated.
3. The RGEs for the trilinear SSB parameters are solved and stored in an interpolation object.
4. The Higgs potential is minimized. As described in section 2.5, we choose to eliminate the soft breaking masses of the three Higgs fields H^d , H^u , and S via the extremalization condition (2.74). Therefore the minimization of the Higgs potential is independent of the running of the scalar mass squared SSB parameters (at the tree-level).
5. The RGEs for the scalar mass squared SSB terms are solved, monitoring whether there appear unwanted negative values (for non-Higgs mass terms), that would lead to breaking of QCD or electromagnetism.
6. The results for $\mathbf{m}_{H^d}^2$, $\mathbf{m}_{H^u}^2$, and \mathbf{m}_S^2 from the RG evolution are compared to their values obtained from the Higgs potential minimization (2.76).
7. From the TeV-scale parameters calculated in the above steps of the program, the full mass spectrum is calculated, using the formulas given in section 2.5.
8. The spectrum, as well as a minimal set of coupling parameters are written to disk in `SINDARIN` format for `WHIZARD` input.

In each step of the program, there is a monitoring system invoking an exception handling routine unless the respective step has been passed successfully. In the following, we shall give detailed information on each of the steps in the above list.

Running of the Yukawa Couplings and Top-Bottom Unification

The set of Yukawa couplings in the energy range $[\Lambda_{\text{GUT}}, \Lambda_{\text{int}}]$, as well their RGEs can be found in appendix B.5.3.

With the matching conditions from (2.57) yielding the input parameters at Λ_{int} , the Yukawa couplings can be RG-evolved down to the TeV scale. For the set of RGEs in the energy range $[\Lambda_{\text{int}}, \Lambda_{Z'}]$ consult appendix B.6.3.

As the Yukawa couplings of the top and bottom quarks are subject to experimental constraints, they are evolved down to M_Z using a set of MSSM-like RGEs to 500 GeV and assuming the sparticles to be heavy, a two-Higgs doublet model RGE set below (given in appendix B.6.3 as well). The dependence on the exact choice of scales where the rest of the spectrum (but the standard model fermions and the two Higgs doublets) become heavy and hence do not contribute to the RGE evolution at lower scales is not very strong. Therefore, we fix these scales to $M_{Z'} = 1.5$ TeV and $M_{\text{SSM}} = 500$ GeV, accepting a slight loss in precision in favor of runtime. The RGEs used in this energy regime are listed at the bottom of appendix B.6.3.

At the Z boson mass, $\tan \beta$ is calculated from the top quark mass relation:

$$m_{t_{\text{exp}}} = \mathbf{Y}_{333}^u \frac{v_u}{\sqrt{2}} = \mathbf{Y}_{333}^u \frac{v \sin \beta}{\sqrt{2}}. \quad (3.2)$$

If $\sin \beta \in (0, 1)$ the bottom quark mass

$$m_{b_{\text{run}}} = \mathbf{Y}_{333}^d \frac{v \cos \beta}{\sqrt{2}}. \quad (3.3)$$

can be calculated and compared to its experimentally measured value $m_{b_{\text{exp}}}$. As $m_{b_{\text{run}}}$ and $m_{b_{\text{exp}}}$ rarely agree, an algorithm optimizing the unified quark Yukawa coupling \mathbf{Y}_{333}^Q and $\tan \beta$ is invoked. The running of the quark Yukawa couplings is very sensitive to the values of the other Yukawa couplings, which makes it difficult to predict a good starting value for \mathbf{Y}_{333}^u . Furthermore, if \mathbf{Y}_{333}^u at M_Z is too small, the corresponding bottom mass $m_{b_{\text{run}}}$ becomes imaginary. The running of the top and bottom Yukawa couplings starting from a common value at Λ_{int} is almost identical, as only the small $U(1)$ gauge contributions and those proportional to $(\mathbf{Y}^D)^2$ drive the couplings apart. Therefore in our model essentially the entire mass splitting among the top and bottom quarks has to originate from the hierarchy of the Higgs vevs (in contrast to models without unification in the Yukawa sector):

$$\tan \beta = \frac{v_u}{v_d} \approx \frac{m_t}{m_b} \approx 40. \quad (3.4)$$

In turn, this implies $\sin \beta$ to be close to unity, hence close to the unphysical region, in order not to yield too large bottom masses. The situation is illustrated in figure 3.2, where the difference $m_{b_{\text{run}}} - m_{b_{\text{exp}}}$ is plotted over \mathbf{Y}_{333}^Q at Λ_{GUT} for some sample set of Yukawa couplings. Within the algorithm we artificially defined

$$m_{b_{\text{run}}} - m_{b_{\text{exp}}} \equiv -5 \text{ (GeV)} \quad \text{if } \sin \beta > 1. \quad (3.5)$$

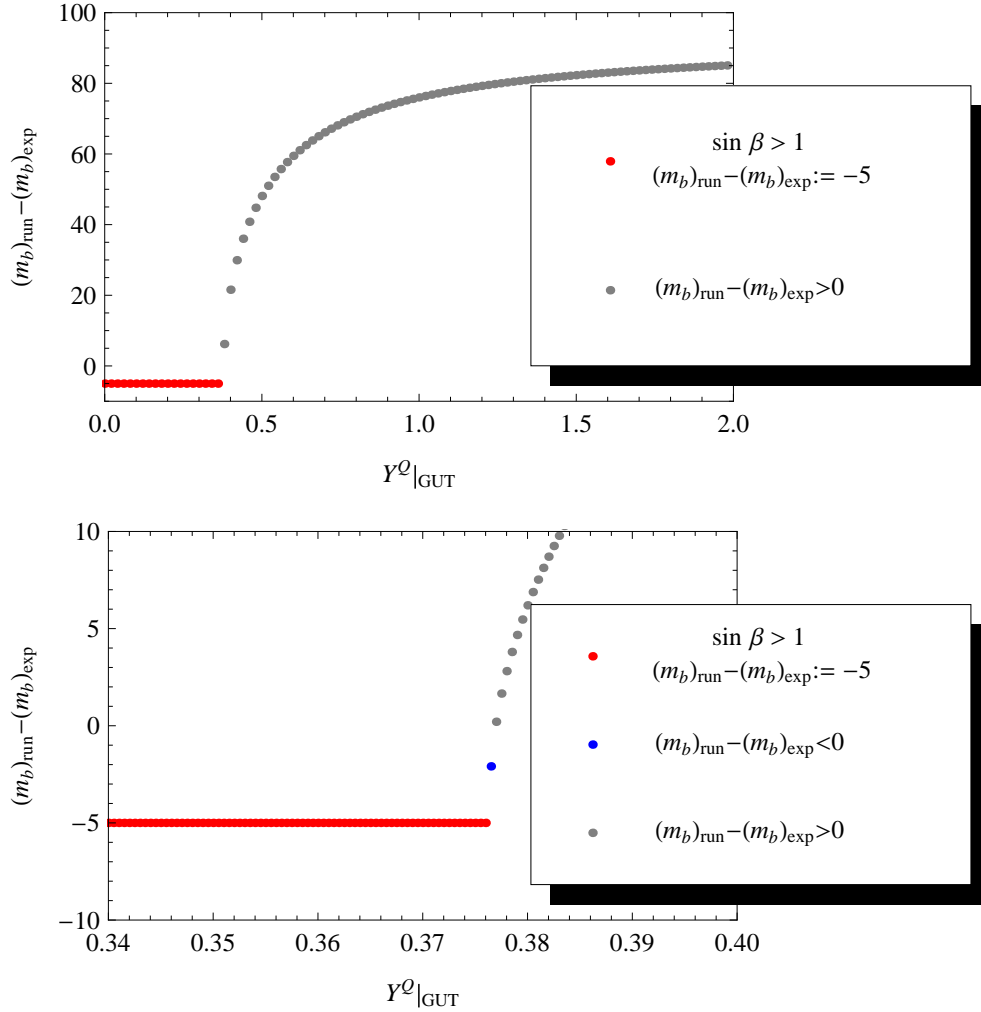


Figure 3.2: The difference of $m_{b_{\text{run}}}$ and $m_{b_{\text{exp}}}$ as a function of the unified quark Yukawa coupling \mathbf{Y}_{333}^Q . The other Yukawa couplings in this example are: $\mathbf{Y}^D = 0.04$, $\mathbf{Y}^{Dc} = 0.15$, $\mathbf{Y}^{SD} = 0.08$, $\mathbf{Y}^{SH} = 0.89$, and $\mathbf{Y}_{333}^{SH} = 1.51$.

As one can see from figure 3.2, the region where $m_{b_{\text{run}}}$ is close to the experimental value is very narrow. In order to efficiently search for a consistent unified quark coupling, we developed the following algorithm, which is a combination of a random search and nested intervals.

- The initial domain of \mathbf{Y}_{333}^Q is $[y_{\text{min}}^Q, y_{\text{max}}^Q] \equiv [0, 2]$.
- We generate uniformly distributed values for $y_i^Q \in [y_{\text{min}}^Q, y_{\text{max}}^Q]$ and calculate $m_{b_{\text{run}}} - m_{b_{\text{exp}}}$.

$$\text{If } m_{b_{\text{run}}} - m_{b_{\text{exp}}} < 0 \Rightarrow y_{\text{min}}^Q = y_i^Q$$

$$\text{Else } m_{b_{\text{run}}} - m_{b_{\text{exp}}} > 0 \Rightarrow y_{max}^Q = y_i^Q, \quad (3.6)$$

with the interval $[y_{min}^Q, y_{max}^Q]$ already being narrowed.

- The loop is interrupted once two values y_i^Q, y_j^Q have been found with the corresponding bottom mass differences having opposite signs.
- At this point, we know that the solution resides in $[y_{min}^Q, y_{max}^Q]$.
- Now the nested intervals start, by evaluating $m_{b_{\text{run}}} - m_{b_{\text{exp}}}$ at the center of the interval $y_{1/2}^Q$ and assigning y_{min}^Q or y_{max}^Q according to (3.6).
- The algorithm exits the loop, once $4.13 \text{ GeV} < m_{b_{\text{run}}} < 4.37 \text{ GeV}$ and the running of all Yukawa couplings from the orbifold compactification scale down to the Z' -scale is returned in an array containing 200 evaluations for each coupling.
- The algorithm typically converges quickly ($\lesssim 15$ iterations).

The result of the Yukawa RG evolution is interpolated in order to be re-used in the subsequent steps of the program.

Running of the SSB Gaugino Masses and Trilinear Couplings

The RGEs of the gaugino masses at the one-loop level depend on the running of the gauge couplings only. At the intermediate scale the matching conditions (2.52) are applied, where the rotation matrices were calculated in the course of gauge unification during the install routine and written to files. The result is interpolated.

The RG evolution of the trilinear SSB terms depends on the running of the gauge- and Yukawa couplings, as well as on the evolution of the gaugino masses, which are supplied in terms of interpolation functions. The result of the RG evolution of the trilinear SSB couplings is stored as interpolation functions, to be later supplied to the routine solving the RGEs of the scalar mass squared SSB terms.

Higgs potential minimization

At this stage, all parameters appearing in the Higgs potential (2.72) are known, if the scalar mass terms $\mathbf{m}_{H^d}^2, \mathbf{m}_{H^u}^2$ and \mathbf{m}_S^2 are eliminated via (2.76) in favor of the three vacuum expectation values. The latter in turn can be re-parametrized in terms of $v, \tan \beta$, and v_s . The first two are fixed in our model via the mass of the weak W boson and by the requirement of top-bottom Yukawa unification (3.4). The vev of the standard model singlet S is in principle a free parameter, apart from constraints on the masses of heavy Z' bosons and leptoquarks requiring $v_s \gtrsim 2.5 \text{ TeV}$. On the other hand we do not wish to introduce arbitrarily large fine-tuning in the Higgs potential minimization, by making v_s too large. In

addition to the extremalization condition (2.74), the Hesse matrix of the Higgs potential evaluated at the vevs has to be positive definite

$$\left. \frac{\partial^2 V_{\text{Higgs}}}{\partial \phi_i \partial \phi_j} \right|_{\text{vevs}} > 0. \quad (3.7)$$

This is the case if and only if all sub-determinants of the Hesse matrix are positive. As all the gauge couplings and charges are fixed by the gauge coupling unification (calculated during the installing routine described in section 3.1), the Hesse matrix becomes a function of the Higgs Yukawa coupling \mathbf{Y}^{SH} , the corresponding trilinear SSB coupling \mathbf{h}^{SH} and the yet undetermined v_s . The first two parameters \mathbf{Y}^{SH} and \mathbf{h}^{SH} were obtained through RG evolution during the previous steps of the program. A nested intervals algorithm then checks whether there are values for $v_s \in [2, 7]$ TeV for which (3.7) holds, and returns the interval $[v_s^{(min)}, v_s^{(max)}] \subset [2, 7]$ TeV where this is true. The algorithm is based on three functions²

- `max_still_good` searches for the maximal value $v_s^{(max)}$ yielding (3.7), given that this is true for some value $v_s^{(0)}$ and not true for a supremum $v_s^{(sup)} > v_s^{(0)}$. It calculates (3.7) for the center $v_s^{(1/2)}$ of the interval $[v_s^{(0)}, v_s^{(sup)}]$ and depending on the output re-assigns $v_s^{(0)} = v_s^{(1/2)}$ or $v_s^{(sup)} = v_s^{(1/2)}$ until the required resolution (currently set to 10 GeV) is reached.
- `min_still_good` works analogously, only using an infimum $v_s^{(inf)} < v_s^{(0)}$ to determine $v_s^{(min)}$.
- If at neither $v_s = 2$ TeV nor $v_s = 7$ TeV (3.7) is fulfilled, a function `inf_hit_sup` is called, searching for a set of values $v_s^{(0)} \in [v_s^{(inf)}, v_s^{(sup)}] \in [2, 7]$ TeV, as sketched in figure 3.3.
- The values $(v_s^{(0)}, v_s^{(sup)})$ and $(v_s^{(inf)}, v_s^{(0)})$ are then supplied to `max_still_good` and `min_still_good`, respectively.

The use of having an interval of possible values for v_s yielding a minimum of the Higgs potential will become obvious, when comparing the scalar mass squared parameters obtained from the extremalization of the Higgs potential to the results from the RG evolution after the next stage of the `main.cpp` program.

Determination of the Higgs mass parameters from potential minimization

With our choice made in section 2.5.1 of eliminating the three scalar Higgs mass squares in favor of the corresponding vevs, the mass squared parameters (m_i^2) are determined by (2.76). As they are calculated at the tree-level, only gauge,

²Provided that there is one and only one continuous interval of this kind. This has been verified with a scan in the two possible input parameters \mathbf{Y}^{SH} and \mathbf{h}^{SH} .

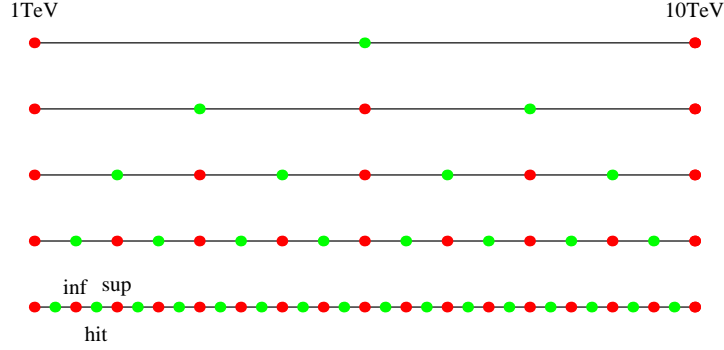


Figure 3.3: Sketch of the algorithm `inf_hit_sup`. After not having found a v_s such that (3.7) holds at a given resolution (green points within a layer), the resolution is doubled (one layer down) investigating the values for v_s marked by green values again. If a value is found (“hit”) the adjacent red points are returned as a supremum “sup” and infimum “inf” to be supplied to `max_still_good` and `min_still_good`, respectively.

Yukawa, and trilinear SSB couplings, as well as the three vevs enter (2.76), allowing the (m_i^2) to be determined at this stage in the program. A future version of `EXSPECT` should account for the corrections arising in the one-loop effective potential approach used for the calculations of the scalar Higgs masses (discussed at the end of this section), in order to provide a more consistent treatment.

At least one of the mass squared parameters must be negative in order to prevent the Higgs potential to have a stable minimum at the origin. Recall, that as our model does not have a MSSM-like μ parameter, leaving the SSB scalar masses the only terms in the potential that are bilinear in the Higgs fields.

$$\Rightarrow \left. \frac{\partial^2 V_{\text{Higgs}}}{\partial \phi_i \partial \phi_j} \right|_{\phi=0} = \text{diag}(\mathbf{m}_{H^d}^2, \mathbf{m}_{H^u}^2, \mathbf{m}_S^2) \not\geq 0. \quad (3.8)$$

As a test for the complete Higgs potential minimization routine, we performed a scan over the parameter space at the TeV scale

$$[-10, 10]_{\mathbf{h}^{SH}/\text{TeV}} \times [1, 10]_{v_s/\text{TeV}} \times [0, 2]_{\mathbf{Y}^{SH}} \times [37, 44]_{\tan \beta}. \quad (3.9)$$

The results for $\tan \beta = 40$ with the additional requirement of $\mathbf{m}_{H^d}^2 < (2000 \text{ GeV})^2$ are plotted in figure 3.4. We note, that \mathbf{m}_S^2 is always negative as long as $v_s > 1 \text{ TeV}$, so (3.8) is automatically fulfilled if there is a minimum at the non-trivial vevs (3.7).

The restriction of $\mathbf{m}_{H^d}^2$ may appear rather unmotivated at this point in the discussion of our program. It was introduced after not having found agreement among Higgs potential minimization and the RG evolution of the corresponding scalar mass terms in the initial runs of the complete program.

This accounts for the fact, that due to the large value of $\tan \beta$ required by the Yukawa unification, (2.76) tends to yield a large splitting among $\mathbf{m}_{H^d}^2$ and $\mathbf{m}_{H^u}^2$, as well as very large positive values for $\mathbf{m}_{H^d}^2 \sim (10000 \text{ GeV})^2$ for non-vanishing

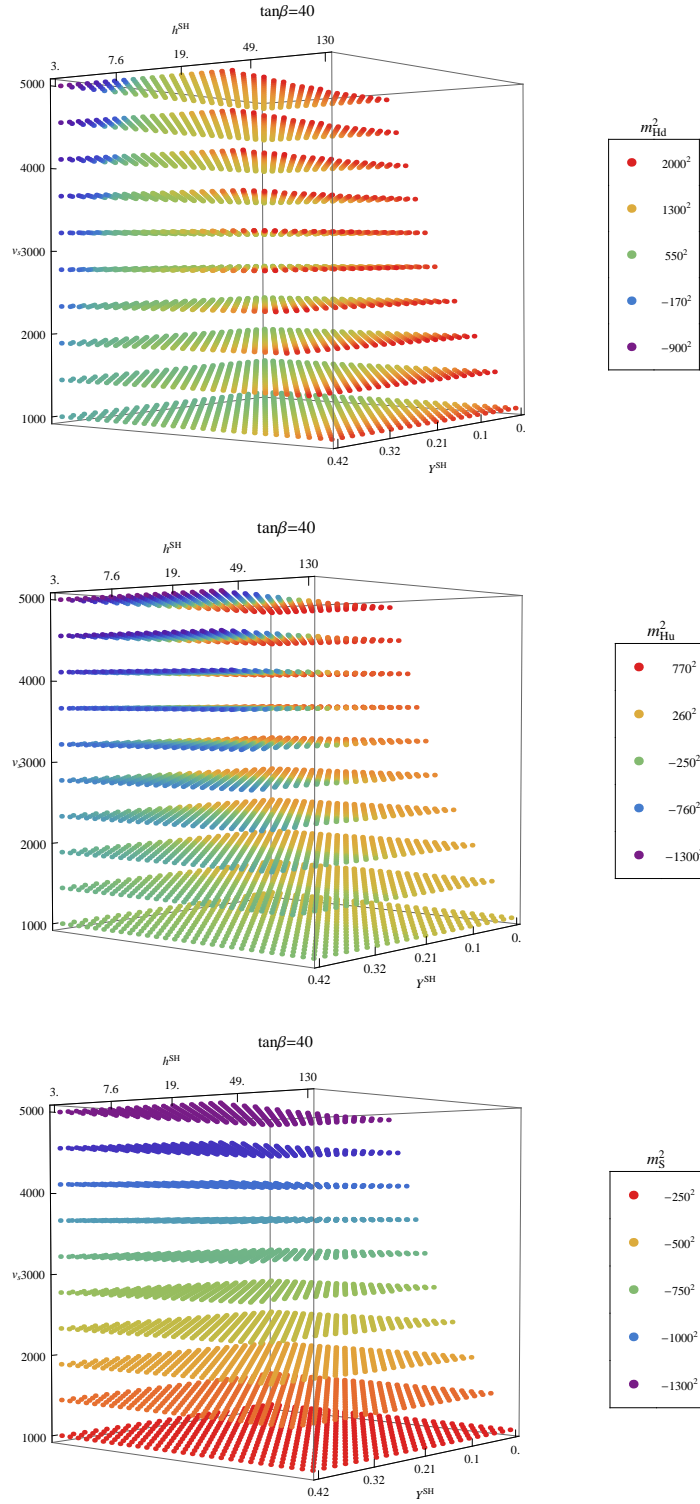


Figure 3.4: The scalar mass squared parameters of the Higgs fields (in GeV²) as a function of the values of $(v_s/\text{GeV}, \mathbf{h}^{SH}/\text{GeV}, \mathbf{Y}^{SH})$ allowed by the potential extremalization (2.76) and minimization conditions (3.7). The set of plotted values was further restricted to $m_{Hd}^2 < (2000 \text{ GeV})^2$.

\mathbf{h}^{SH} . The splitting is generally not reflected in the corresponding RG evolution of the parameters (see the next paragraph). Therefore, we added a second screening routine restricting the interval $[v_s^{(min)}, v_s^{(max)}]$ to values of v_s where $\mathbf{m}_{H^d}^2 < (2000 \text{ GeV})^2$. This severely constrains the possible values of the trilinear SSB Higgs coupling at the minimization scale as can be seen in figure 3.4

Constraining the Higgs mass terms at this stage has proved to be a very crucial handle in the course of finding physical spectra using random walk techniques, which will be the topic of section 3.3.

Running of the scalar mass squared SSB terms

The scalar mass terms at the TeV scale are obtained by evolving them according to the RGEs in appendix B.5.5 and B.6.5 down from the compactification scale via the intermediate scale, where they are linked using (2.65). As we have not specified the breaking mechanism at the intermediate scale, which would allow for the calculation of the splitting parameter M_Δ^2 in (2.65) through the RG evolution of the SSB masses of the intermediate particle $\mathbf{m}_{H_{int}}^2, \mathbf{m}_{\tilde{H}_{int}}^2$ from (2.4), we keep $M_\Delta^2|_{\Lambda_{int}}$ as a free input parameter.

During the entire evolution the program monitors whether masses other than those of the third Higgs generation become negative, in order not to have unwanted symmetry breaking. If the RG evolution has been successful, the values of the three Higgs mass terms at the Z' scale $(m'_i)^2$ are compared to the values (m_i^2) obtained from the potential minimization as outlined in the previous paragraph. The latter are functions of v_s which was restricted to lie within the interval $[v_s^{min}, v_s^{max}]$ from the previous steps of the program, by the requirement of having a true minimum at v_d, v_u, v_s and reasonably sized Higgs mass parameters. The value of $v_s \in [v_s^{min}, v_s^{max}]$ yielding the best agreement among the parameters from RG evolution and potential minimization is evaluated using an optimization algorithm provided by the `Gnu Scientific Library` that maximizes a *goodness* function g . It maps the agreement among the values on the interval $[0, 1]$, with 1 signifying perfect agreement according to a user-defined precision p . First we define a distance measure on a space with mass dimension one. The m^2 values are mapped onto that space using a `signed_sqrt` function (and `signed_square` for the inverse operation defined analogously):

$$m = \begin{cases} \sqrt{m^2}, & \text{if } m^2 > 0 \\ -\sqrt{m^2}, & \text{if } m^2 < 0 \end{cases} \quad (3.10)$$

On the interval $m_i \pm m_i * p/2$ the distance is defined to be zero. Away from the lower (upper) bounds of the interval, the normalized distance (as we are predominantly interested in relative deviations) is defined by

$$d(m', m) = \frac{(m - m * p/2) - m'}{|m - m * p/2|} \quad \left(= \frac{m' - (m + m * p/2)}{|m + m * p/2|} \right). \quad (3.11)$$

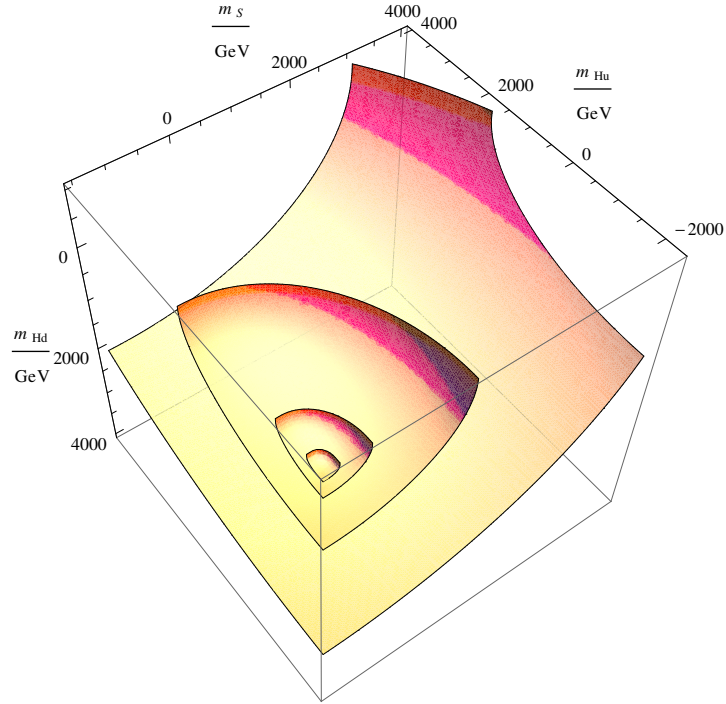


Figure 3.5: The contours of the goodness function from (3.13) with $\alpha = 1$ for $g = .9, .7, .4$, and $g = .2$ from the inner to the outer layer. The central point is $\{m_{H^d}, m_{H^u}, m_S\} = \{-1000, -2300, -1500\}$ which corresponds to $\{\mathbf{m}_{H^d}^2, \mathbf{m}_{H^u}^2, \mathbf{m}_S^2\} = \{-(1000)^2, -(2300)^2, -(1500)^2\}$ in terms of Lagrangian parameters.

To combine the deviations among each of the three pairs of m_i values we use the Euclidean norm of the vector

$$\mathbf{d} \equiv \left\| \left\{ d(m'_{H^d}, m_{H^d}), d(m'_{H^u}, m_{H^u}), d(m'_S, m_S) \right\} \right\|_2. \quad (3.12)$$

As the goodness g we define

$$g(\mathbf{d}) \equiv \frac{1 - g_{\min}}{(\mathbf{d} + 1)^\alpha} + g_{\min}, \quad (3.13)$$

with $\alpha > 0$ parametrizing the slope of the curve falling off asymptotically to the minimal value g_{\min} of g . An exemplary plot illustrating the functionality of the goodness g on the space with mass dimension one is shown in figure 3.5. The best value for v_s in the sense of the above goodness function is returned. If the goodness signals agreement among the scalar mass terms from the RG evolution and the potential minimization, we have verified that all TeV-scale Lagrangian parameters can be derived from the input parameters specified at the orbifold compactification scale in a consistent way.

Calculation of the Spectrum

The TeV-scale Lagrangian parameters are translated into mass matrices using the explicit expressions given in section 2.5. In case of the Higgs masses, the program evaluates the one-loop corrected values using (2.84). In order to avoid numerical instabilities in this case, approximations for the eigenvalues of the field-dependent pseudo-scalar and charged Higgs mass matrices have been used: Due to the strong hierarchy in the Higgs vevs (from the exclusion limits on the Z' mass and the requirement of top bottom Yukawa unification)

$$v_s \gg v_u \gg v_d, \quad (3.14)$$

the non-vanishing eigenvalues of m_A^2 (2.78) and $m_{H^\pm}^2$ (2.80) belong to eigenvectors that correspond (up to very small admixtures of the other Higgs field(s) of the order $\lesssim 10^{-4}$) to A_u and H_u^+ , respectively. Therefore, `EXSPECT` only includes the contributions $m_{A^{uu}}^2$ and $m_{H_u^\pm}^2$ instead of the full set of eigenvalues in the calculation of the sum from (2.84).

Generally, a mass (squared) matrix $\{\mathcal{M}_{ij}\}$ is represented in `EXSPECT` as an object of type `CMass_Matrix` containing the information of $\{\mathcal{M}_{ij}\}$ in a one-dimensional array as

$$M_{i*n+j} \equiv M_{ij}, \quad \text{with } i, j = 0, \dots, n-1,$$

its eigenvectors and eigenvalues in a `gsl_matrix` and `gsl_vector`, respectively. The chargino mass matrix (2.95) has to be treated separately, as there are two rotation matrices U, V necessary to rotate it into a diagonal basis (singular value decomposition). The corresponding structure is called `Chargino_mass` containing U, V in two separate members of type `gsl_matrix`.

In either case, the mass matrices are calculated first and then the diagonalization is executed, with the masses (eigenvalues) ordered ascending in size, apart from the neutralino masses, which are ordered ascending in their absolute values. In this way, only the first entry of each set of eigenvalues has to be checked for positiveness in order to guarantee a physical spectrum.

In case of the latter, the eigenvalues of the scalar mass squared matrices are replaced by their square roots, i.e. the physical masses.

In the last step, the spectrum of physical masses is compared to experimental bounds taken from the PDG [39]. This is considered to be a pre-selectional step only. In order to thoroughly test the compatibility of one of our spectra, we will have to simulate observables and compare them to the respective experimental analysis, as most of the SUSY exclusion bounds depend on (MSSM) assumptions about branching ratios and coupling constants. In many cases, such as the dark Higgs fields appearing in our model there are no suitable exclusion bounds. In this case we have oriented our choices at the values given for searches for other hypothetical particles (in this case: heavy leptons). In the case of the lightest dark neutralino, where we expect masses as light as 1 GeV and below (see section 2.5.6), we did not set any bound, as the discussion of its implications on collider phenomenology and cosmology is beyond the scope of this thesis. The values

currently used by `EXSPECT` can be found in table 3.2. The full mass spectrum

$\frac{m}{\text{GeV}} >$	h_1^0	A^0	h^\pm	$\tilde{\chi}^0$	$\tilde{\chi}^\pm$	\tilde{l}	\tilde{q}	D	\tilde{D}
	90	90	130	60	130	200	500	500	500
$\frac{m}{\text{GeV}} >$	h'^0	A'^0	$\tilde{\chi}'^0$	$\tilde{\chi}'^\pm$	Z'	\tilde{g}	$\frac{\delta M_{ZZ'}^2}{M_{Z'}^2} < 10^{-3}$		
	100	100	–	120	1500	600			

Table 3.2: Values of the lower mass bounds used by `EXSPECT` in a pre-selection step to estimate whether a given spectrum roughly agrees with the exclusion limits on new particles as provided in [39].

and a consistent (non-minimal) set of coupling constants and mixing matrices is written into a `SINDARIN` file, in order to be able to directly feed it to the event generator `WHIZARD` [65]. Further information on the current status of the implementation of our model into `WHIZARD` will be given in section 3.4 and sample output files of `EXSPECT` in the `SINDARIN` format can be found in appendix B.4.

3.2.1 Comments on the workflow of `EXSPECT`'s main program

The program can calculate spectra from parameters specified at the orbifold compactification scale. It incorporates all features of the model that so far have been worked out. All input parameters that have not been constrained by some mechanism can in principle be handled as independent.

The model itself is not suited to define *constrained* versions with only a handful of parameters, as there are many new superpotential terms. Requiring them to have unified values would contradict the spirit of the orbifold construction: It was motivated by the necessity to be able to choose independent Yukawa couplings at the gauge coupling unification scale in order to forbid diquark couplings while allowing for non-vanishing leptoquark couplings.

In the following, we will give a brief summary of all steps within the main leading from a set of input parameters at the orbifold compactification scale to a TeV-scale spectrum. Whenever – at any of the following steps – the input parameters fail to pass any of the applied consistency checks, an exception handler using the C++ `throw/catch` routines to skip the rest of the running evaluation:

- Throughout the top-bottom Yukawa coupling unification, we require all Yukawa couplings to lie within $(0, 3]$ to be consistent with the conventions used in section 2.5 and to assure perturbativity.

This requirement is unproblematic: the algorithm presented in the previous section usually converges within the maximal iteration depth (< 40 iterations).

- The running of the gaugino mass and trilinear SSB parameters at that stage is unconstrained.

- The requirement of a successful Higgs potential minimization is not automatically fulfilled. Although this already constrains the parameter space (at the TeV scale) significantly (especially \mathbf{h}^{SH} , see figure 3.4), it is hard to trace the failure back to a corresponding region in the input parameter space, due to the complicated set of coupled differential equations linking the free parameter space to the boundary conditions.
- It appears that asking for a true minimum at the vevs (3.7) implies a saddle point or a maximum at the origin in the space of Higgs fields, satisfying (3.8) automatically.

In addition, we introduce a (optional) selection criterion, checking whether $\mathbf{m}_{H^d}^2 < (2000 \text{ GeV})^2$. If this is not the case, the algorithm may anticipate the irreconcilability of the (m_i^2) with the RG evolution reducing the runtime.

- The RG evolution of the SSB scalar mass terms is a critical step as well: The mass squares of scalar fermions, leptoquarks, and dark Higgs particles are often driven to negative values, causing unwanted symmetry breakings.

The RG evolution is highly sensitive to all input values at the orbifold compactification scale, not only to the mass-squared values.

- The requirement of “accidental” agreement (up to tunability of v_s) among the results for the Higgs mass squares from RG evolution and potential minimization is very strong.

There are several options within **EXSPECT** to approach the complicated issue of solving the RGEs for the SSB scalar mass terms and the subsequent matching to the results from the Higgs potential minimization:

- a) An iteration varying the three free input parameters $\mathbf{m}_H^2, \mathbf{m}_S^2, \mathbf{m}_\Delta^2$ using the Nelder-Simplex algorithm [66] provided by the **Gnu Scientific Library** to find agreement among the potential minimization (independent of the parameters of the iteration) and the RG flow in the sense of the goodness function as defined in (3.13).
 - b) A Monte-Carlo Markov Chain, as introduced in the following section, trying to optimize the same setting as the iteration from a).
 - c) A Monte-Carlo Markov Chain with all SSB scalar masses handled as free parameters, also maximizing the goodness from (3.13). This version does not allow the user to specify the SSB scalar masses (which are apart from the Higgs terms free parameters of the theory, within our conventions). On the other hand it allows for a broader search always using the same input parameters for the Yukawa and trilinear SSB couplings that have already proved to yield a successful Higgs potential minimization.
- The spectrum calculation first checks for the positiveness of the eigenvalues of the scalar mass matrices and compares the resulting spectrum to the pre-defined bounds specified in table 3.2.

The major hurdle when comparing the computed spectrum to the experimental bounds appears to be the lightest Higgs mass, which in many cases turns out to be as low as 20 GeV (at the tree-level). Even though we anticipate sizable one-loop corrections to lift this value significantly (see section 2.5.2), we decided to require at least the 90 GeV at the tree-level to safely assume consistency with the direct searches [39]. This (rather than comparing the one-loop level Higgs mass to exclusion limits) is chosen to be the current setting, as it provides a way of exploring our model’s capacity to accommodate tree-level Higgs masses above the theoretical upper limit of the MSSM (which is known to be lifted in $U(1)'$ -extended versions of the MSSM [59]).

All routines encoding the above steps in `EXSPECT`’s main program have been tested for memory corruption using `Valgrind`.

The difficulties of passing all the hurdles mentioned in this section motivated the embedding of the main program into a Monte-Carlo Markov Chain, which provides a very powerful framework to optimize problems on high-dimensional configuration spaces.

3.3 Random Walk

A widely used approach to explore high-dimensional configuration spaces is a Markov-Chain Monte Carlo (MCMC). It consists of a random walk equipped with features that anticipate being stuck in local extrema of the “landscape” under investigation. In our case the “landscape” would correspond to some *goodness*, expressing how well a spectrum matches our criteria, as a function of the model’s free parameters.

The basic setup is the following:

- (i) Definition of the goodness function

$$g : x \longrightarrow \mathbb{R} \tag{3.15}$$

measuring the “relevance” of a certain point x from the configuration space. Suppose for simplicity that g grows monotonously with increasing relevance.

- (ii) g is evaluated at some point x_i .
- (iii) A new point x_{i+1} is generated from some distribution centered at x_i .
- (iv) g is evaluated at x_{i+1} .
- (v) If $g(x_{i+1}) > g(x_i) : x_i \longrightarrow x_{i+1}$ in step (iii).
Else there is a finite probability p associated with taking the x_{i+1} to be the new center of the distribution from which the next point will be sampled, even though $g(x_{i+1}) < g(x_i)$. With probability $1 - p$ the algorithm jumps back to step (iii), sampling from the same distribution centered at x_i .

There are many aspects within the above scheme, which have to be adjusted to the specific problem under investigation. First of all the configuration space in our case is given by the space of the free parameters at the orbifold compactification scale supplemented by the splitting mass term at the intermediate scale M_Δ from (2.65). This space is compact, as we aim at generating spectra yielding a TeV-scale phenomenology (i.e. excluding unphysical and/or arbitrarily large input parameters).

The relevance function g will be a goodness function in our MCMC, quantifying how many of the criteria discussed at the end of the previous subsection are met. The choice of distribution from which the next step in the random walk is sampled, is a trade-off between acceptance rate and exploration depth: If the standard deviation of the distribution is small, the next step will most likely be within a small distance from center, resulting in a large likelihood to yield comparable results, hence being accepted as the new center of the distribution. On the other hand, the average distance covered by the MCMC per time is small. In `EXSPECT`, we use a probability function for sampling whose standard deviation may depend on the goodness evaluated at its center: The better the current point is, the more profoundly its close vicinity may be investigated if this feature is enabled. In the following, we shall give detailed information of how the above concepts are realized in `EXSPECT`.

Configuration Space (Free Parameters)

The total number of free parameters in our model, as in any softly broken SUSY model, is very large $\mathcal{O}(100)$. Given the complex interdependencies outlined in the discussion of the main program and the expectedly very narrow regions in the parameter space actually leading to physical spectra, it would clearly overstrain our computational resources to treat all these parameters as independent. Keep in mind, that within conventional scanning algorithms with n points being evaluated for each of d free parameters, the number of total evaluations grows as

$$\#(\text{evaluations}) \sim n^d. \quad (3.16)$$

Therefore, we start from the set of 18 input parameters shown in table 3.3, restricted to the intervals specified therein. The (compact) *parameter space* is then given by the product of the intervals listed in table 3.3. Its dimensionality ($d = 18$) is still large in the context of (3.16), rendering systematic scans unfeasible.

Sampling Function

The random numbers generally have to be limited to a given interval $[a, b]$ in order to avoid unphysical input parameters. This is accounted for by the function `limited_random`, depending on a random number generator (rng),³ a central

³The variable `rng_type` selects the random number generator. Currently the `gs1` implementation of the `taus` algorithm is employed, as it is very fast and reasonably stable. Note, that

y_lq	[0, 1.]	\mathbf{Y}_{ii}^D	$i = 1, 2, 3$
y_lqc	[0, 1.]	\mathbf{Y}_{ii}^{Dc}	$i = 1, 2, 3$
y_sd	[0, 1.]	\mathbf{Y}_{3ii}^{SD}	$i = 1, 2, 3$
y_sh	[0, 1.]	\mathbf{Y}_{3ij}^{SH}	$i, j = 1, 2$
y_nmssm	[0, 1.]	\mathbf{Y}_{333}^{SH}	$i, j = 1, 2$
M_g	[-1500, 1500]	M_g^i	$i \neq 3$
M_gluino	\pm [800, 1500]	M_g^3	
h_sm	[-1500, 1500]	\mathbf{h}_{333}^Q	
h_lq	[-1500, 1500]	\mathbf{h}_{ii}^D	$i = 1, 2, 3$
h_lqc	[-1500, 1500]	\mathbf{h}_{ii}^{Dc}	$i = 1, 2, 3$
h_sd	[-1500, 1500]	\mathbf{h}_{3ii}^{SD}	$i = 1, 2, 3$
h_sh	[-1500, 1500]	\mathbf{h}_{3ij}^{SH}	$i, j = 1, 2$
h_nmssm	[-1500, 1500]	\mathbf{h}_{333}^{SH}	$i, j = 1, 2$
m_sfer	[800, 2000]	$\mathbf{m}_{ii}^{\tilde{f}}$	$i = 1, 2, 3$
m_dh	[800, 2000]	$\mathbf{m}_{ii}^H \equiv \mathbf{m}_{ii}^S$	$i = 1, 2$
m_H	[-2000, 2000]	\mathbf{m}_{33}^H	
m_D	[800, 2000]	\mathbf{m}_{ii}^D	$i = 1, 2, 3$
m_S	[-2000, 2000]	\mathbf{m}_{33}^S	
m_int	[-2000, 0]	$\mathbf{M}_{\Delta}(\text{at}\Lambda_{\text{int}})$	

Table 3.3: The free input parameters of the random walk. All values are given at the orbifold compactification scale, unless indicated otherwise. The dimensionful parameters are understood to have the dimension GeV. The scalar mass values are translated into mass squared parameters using `signed_square`, the inverse of `signed_sqrt` from (3.10).

value μ , the interval $[a, b]$, and a width parameter α . At first, a random number is generated from the so-called logistic distribution

$$p(x) dx = \frac{\exp(-x/\alpha)}{\alpha (1 + \exp(-x/\alpha))^2}, \quad (3.17)$$

with central value zero. This distribution has broader tails than a Gaussian and hence makes it more likely to escape from an extremum, assuming that there can be several local extrema of the goodness function on the parameter space.

In the second step this random number is rescaled to half of the width of the

we do not use the random number generator in a context of probabilistic measures. As a safety measure, the random generator is re-seeded using the system time after $\sim 1.6 \times 10^6$ random numbers have been generated.

interval $[a, b]$ and shifted to the mean value μ

$$x \rightarrow \mu + x \frac{a-b}{2} \quad (3.18)$$

If the now rescaled random number x does not fall in $[a, b]$ it is discarded and a new one is generated. This design is aimed at producing scale invariant random numbers on any interval $[a, b]$. In figure 3.6 the results of the function `limited_random` on two intervals differing by a scale-factor of 100 is shown.

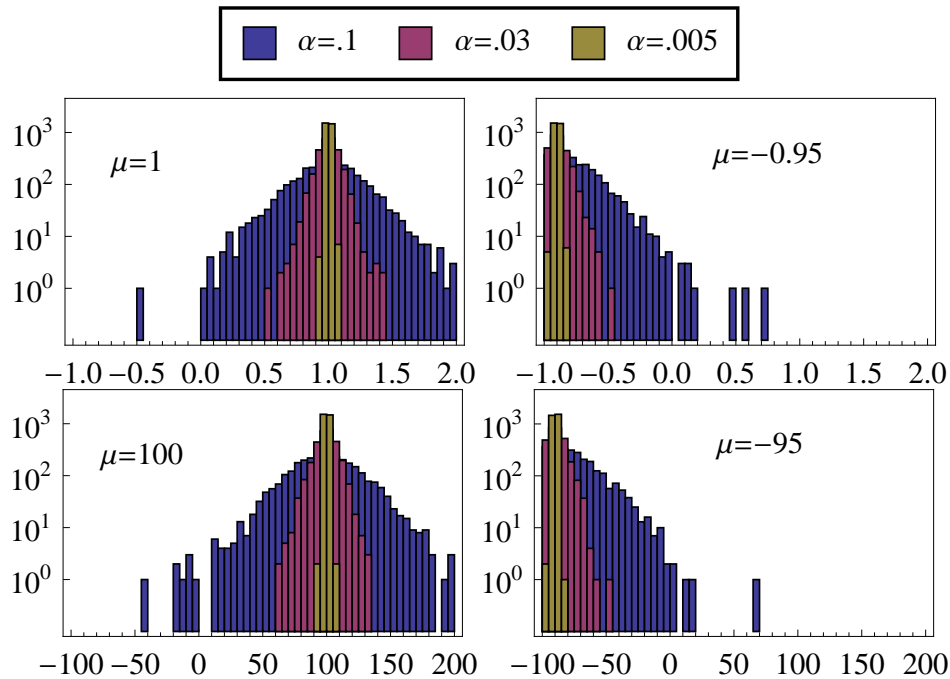


Figure 3.6: 3000 calls of the function `limited_random` on $[-1, 2]$ and the same interval up-scaled by a factor 100, for varying mean values μ and width parameters α .

Goodness Function

The choice of the goodness function is the most crucial step in the process of designing the random walk routine: It has to map the relevance of a given parameter space point, which is by no means uniquely defined. The only measure for the quality of a particular choice of goodness function is how well does a random walk based on it perform. Unfortunately, the latter is not well defined either: We do not have any a priori knowledge about the density of points leading to physical spectra on our parameter space – for quite some time, we did not even know if there are any points that lead to consistent spectra in the sense of our requirements.

The performance of the other functions constituting the random walk can be tested on a *test landscape* (see section 3.3.1) with known extrema, but the goodness function has to be chosen based on the specific problem under investigation. It has to define the landscape (solely based on knowing the requirements that have to be met in order to yield its maximum value) such that the random walk can find the maxima.

The goodness function used in EXSPECT's random walk keeps track of how many of the steps listed in section 3.2.1 in the process of generating a spectrum from a given point in the parameter space have been passed successfully until the first failure occurs. It is defined to return values on the interval $[g_{\min}, 1]$, where $g_{\min} \equiv .01$ in the current setting and 1 corresponding to consistency with all applied constraints.

Its rather complicated structure, which will be presented in detail in the following, is aimed at reflecting how important the achievement of having passed the respective step in the evaluation is in order to yield a physical spectrum. This is obviously not a well defined quantity, hence the design of the goodness function is based on the experience we gained during the process of setting up the current version of the random walk (as of this writing, we have investigated over 10^7 points in parameter space at all the stages of the development, including several definitions of the goodness function itself, combined).

There are seven “check points” in the main program where individual goodness functions g_i (with values on $[g_{\min}, 1]$ as well) are evaluated, encoding whether or not the point in the parameter space has passed the respective criterion (and in some cases how close it came to passing), contributing to the overall goodness. All the individual g_i are initialized to $g_i = g_{\min}$. Recall, that all remaining evaluations in the program are skipped once one criterion is not met. The g_i monitor the following steps.

1. Top-bottom Yukawa unification: $g_1 = 1$ if it can be achieved with all Yukawa couplings remaining perturbative and in agreement with our superpotential conventions i.e. $\mathbf{Y}^i \in [0, 3]$.
2. Higgs potential minimization: $g_2 = 1$ if (3.7) holds true.
3. Higgs mass parameters from potential minimization: $g_3 = 1$ if there is no stable minimum at the origin and $\mathbf{m}_{H^d}^2 < (2 \text{ TeV})^2$.
4. RGEs for the SSB scalar mass terms:

$$g_4(\mu^c) \equiv (1 - g_{\min}) \left(\frac{\mu_{\text{GUT}} - \mu^c}{\mu_{\text{GUT}} - \mu_{Z'}} \right)^2 + g_{\min}, \quad (3.19)$$

where μ^c is the scale where any of the mass squared terms not corresponding to third generation Higgs fields first becomes negative. The μ^i denote log scaled quantities in this context

$$\mu^i = \log \left(\frac{\Lambda_i}{M_Z} \right). \quad (3.20)$$

5. Consistency of potential minimization with RG evolution: g_5 maps the best agreement of the values obtained from (2.76) with the results from the RG evolution on $[g_{\min}, 1]$ according to (3.13).

6. Positive (physical) scalar mass terms: If all scalar mass terms are physical

$$m_i^2 > 0 \quad \forall i \quad \Rightarrow \quad g_6 = 1. \quad (3.21)$$

7. Consistency of the spectrum with experimental constraints: Each bound from table 3.2 is compared to the result of the spectrum calculation using the one-dimensional version of the goodness measuring the distance from the desired interval according to (3.13). The individual results g_7^i are combined into g_7 such that the result is not dominated by the worst agreement as in the multi-dimensional interpretation of (3.13):

$$g = \left(\frac{1}{n} - g_{\min} \right) \frac{g^1 - g_{\min}}{1 - g_{\min}} + \sum_{i=2}^n \frac{1}{n} \frac{g^i - g_{\min}}{1 - g_{\min}} + g_{\min}, \quad (3.22)$$

where n counts the number of individual values of goodness functions (each on $[g_{\min}, 1]$) to be combined. The idea behind this particular design will be commented in the following.

We use the function defined in (3.22) to combine g_1 through g_7 to the overall goodness associated with the parameter space point under investigation. According to (3.22) it returns g_{\min} if the point fails to meet the first criterion. If it fails in the j^{th} out of a total of n steps, the result is $(j-1)/n$ (or smaller than j/n if the j^{th} goodness function can measure by how much the criterion is missed, such as g_4, g_5 and g_7). The different criteria can be weighted individually, by simply including them several times in sum in (3.22). In our random walk routine, the individual results from steps 4, 5 and 7 are weighted doubly compared to the others, as these are the most critical steps in the course of the spectrum calculation (based on our experience). The behavior of the step-wise goodness function from (3.22) is sketched in figure 3.7.

Acceptance Function

In the general remarks at the beginning of this section, we stated that the idea of the MCMC is based on “eventually taking a step down”. By this, we mean that with a finite probability the next point x_{i+1} is generated from the sampling function being centered at the current point x_i even if its goodness turned out to be lower than the goodness of the previously investigated point x_{i-1} . In contrast, a conventional (Newton) multi-dimensional optimization would only accept steps in directions with positive gradient. This feature enables the MCMC to escape from local maxima.

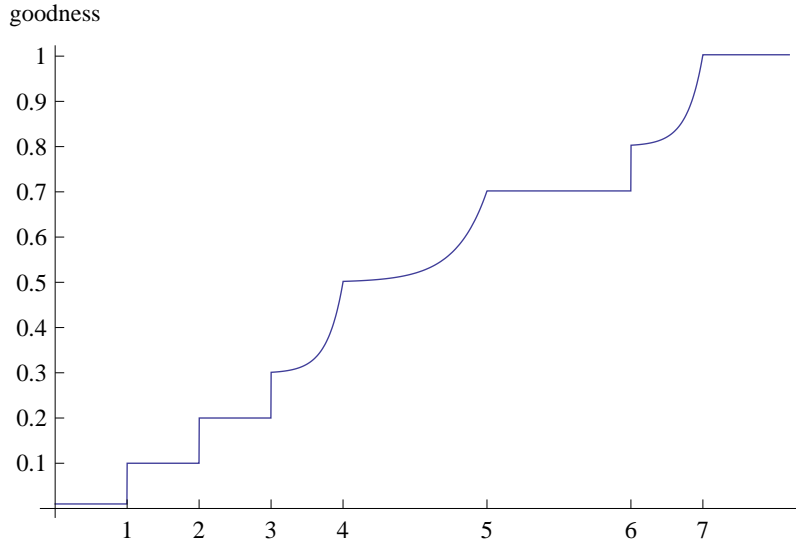


Figure 3.7: Sketch of the step-wise goodness function from (3.22) plotted over the number of subsequently passed criteria. The continuous growth to step 4,5 and 7 symbolizes that g_4, g_5 and g_7 can measure by how much the respective criterion has been missed.

In EXSPECT this step is implemented as follows: In the style of the simulated annealing algorithm [67] we define the probability to accept x_i as the new center of the sampling function via

$$p_s(x_i, x_{i-1}) \equiv \begin{cases} e^{(g(x_i)-g(x_{i-1}))/T} & g(x_i) < g(x_{i-1}) \\ 1 & g(x_i) \geq g(x_{i-1}) \end{cases} \quad (3.23)$$

In the above equation, g denotes the goodness function from the previous paragraph and T is a tunable parameter corresponding to the temperature in the simulation of physical systems, such as the Ising model [68]. In the current version $T = .1$, a choice which turned out to yield a good performance of the random walk (in principle, one could slowly decrease T with the number of evaluated points leading to a so-called “freeze out”, that is rendering the probability of stepping down smaller over time, forcing the algorithm to investigate the closest extremum).

The decision is made by generating a uniformly distributed random number `fate` $\in [0, 1]$.

Width of the Sampling Function

The remaining task is to translate the goodness $g \equiv g(x_i)$ of the center $\mu = x_i$ of the sampling function into the width $\alpha(g)$ of the corresponding distribution. The width should become smaller with increasing goodness, in order to investigate

the vicinity of interesting points profoundly. We chose $\alpha(g)$ to return pre-defined values at the boundaries of the range of values of the goodness function:

$$\alpha(g_{\min}) = \alpha_{\max}, \quad \alpha(1) = \alpha_{\min}. \quad (3.24)$$

The width function in EXSPECT is given by

$$\begin{aligned} \alpha(g) &= \alpha_{\max} \exp(a(g - g_{\min})), \\ \text{where} \quad a &= \log\left(\frac{\alpha_{\min}}{\alpha_{\max}}\right) \frac{1}{(1 - g_{\min})}, \end{aligned} \quad (3.25)$$

The extremal values of the width function are set to $\alpha_{\min} = 10^{-4}$ and $\alpha_{\max} = 0.1$.

3.3.1 Testing the Random Walk

The general setup of EXSPECT's random walk – i.e. the sampling, the acceptance, and the width function – was tested using a five-dimensional test-parcours given by

$$\begin{aligned} f(x_1, x_2, x_3, x_4, x_5) &= \exp\left(-\left|\frac{x_1^2 + x_2^2}{a^2} - 1\right|\right) \left(\sqrt{x_3^2 + x_4^2 + b^2} - \sqrt{x_3^2 + x_4^2}\right) \\ &\times \left[\left(\frac{\pi}{2} + \arctan\frac{x_5 - c}{c}\right) + 3 \exp\left(-\frac{(x_5 - 500)^2}{25}\right)\right], \end{aligned} \quad (3.26)$$

$$\text{with} \quad a = 400 \quad b = 500 \quad c = 250.$$

(3.27)

This function originally served as a test-landscape for an application of the VEGAS algorithm [69] to high-dimensional optimization problems [70], which allowed us to compare the performance of our algorithm (see appendix B.3) to their results (see <http://omnibus.uni-freiburg.de/~ob76/adScan/>). The test confirmed that our random walk indeed performs very well (the maxima were more carefully investigated, leading to the discovery of higher peaks than found by the VEGAS routine with the same number of calls).

In addition the test function from (3.27) proved to be very valuable in providing some insights on the effect of tuning of the random walk's free parameters α_{\min} , α_{\max} and T . The values for these parameters stated in the preceding paragraphs were obtained from a systematic scan (in those parameters), where in each step the average of the highest value of ten independent random walk runs à 40,000 calls was recorded. The result of this scan is plotted in figure 3.8.

3.4 Implementation into FeynRules and WHIZARD

The phenomenology of the model under investigation is expected to be rich in spectacular new signals of collider physics. Clearly, the heavy Z' would give

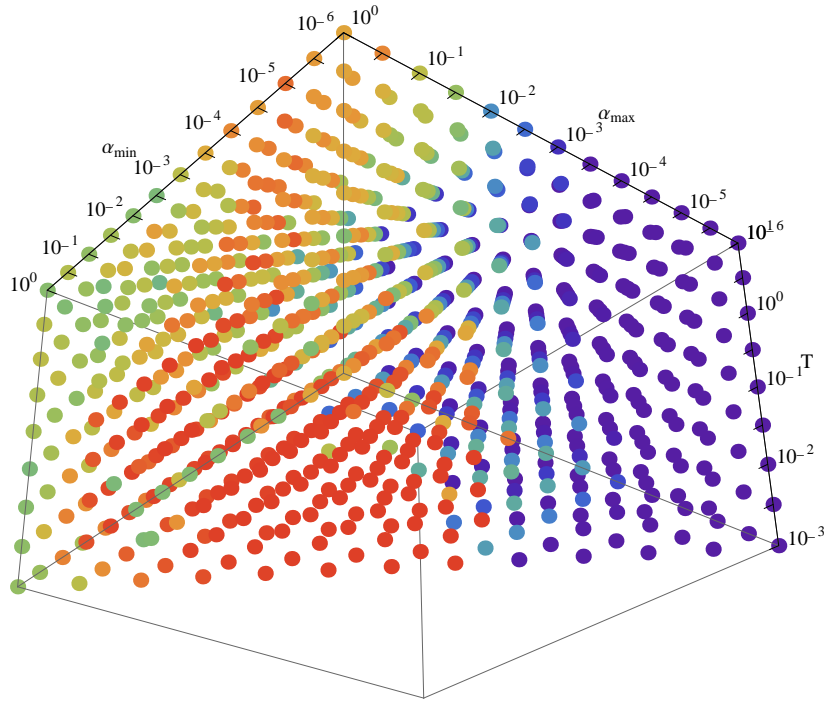


Figure 3.8: The result of the scan in the tunable parameters of the random walk. The quality of the performance increases from purple to red, i.e. for the triples $\{\alpha_{\min}, \alpha_{\max}, T\}$ with red dots, the maxima of (3.27) were found.

the most obvious channel to look for, if its mass lies within the range of the LHC. Nonetheless, there are other striking signals whose theoretical description is more cumbersome. Therefore it is desirable to have an automatized tool for the calculation of cross sections and event generation at hand. We implemented our model in the event generator WHIZARD [65].

WHIZARD provides a powerful tool to calculate matrix elements, cross sections, and generate events from the Feynman rules of almost any model. The extensive particle zoo as well as the large number of interactions result in $\mathcal{O}(10000)$ Feynman Rules, most of them describing the scalar D - and F -term interactions (1.29), to be implemented accompanied by difficult combinatorics.⁴

Fortunately, FeynRules [72], a Mathematica-based tool, allows to calculate the Feynman rules from particle definitions and the Lagrangian. Recently an interface [73] to WHIZARD was provided that creates all necessary WHIZARD model-files from FeynRules output.

⁴During the work on my thesis, I implemented the NMSSM into WHIZARD [71], based on the pre-existing MSSM implementation. The introduction by hand of only one additional field and a handful of new vertices became quite cumbersome.

The calculation of the full Lagrangian in terms of superfield component fields was done in a semi-automatized way, using Mathematica's analytic and pattern-matching features to derive it from the list of all particles, the gauge groups, the superpotential, the soft supersymmetry breaking Lagrangian, and the gauge kinetic terms. The fermionic component fields then have to be translated into Dirac and Majorana spinors, using the following formalism: All Dirac fermions are built from two Weyl spinors that in general can have different quantum numbers before electroweak symmetry breaking, but transform identically under $SU(3) \times U(1)_e$:

$$\psi_f \equiv \begin{pmatrix} f_L \\ \bar{f}^c \end{pmatrix}, \quad (3.28)$$

provides a unique translation rule within the naming convention of this work for all fermionic fields, except for the leptoquarkinos and charginos. In these cases we identify

$$\psi_{\tilde{D}} \equiv \begin{pmatrix} \tilde{D} \\ \bar{\tilde{D}}^c \end{pmatrix}, \quad \lambda^+ \equiv \begin{pmatrix} \psi^+ \\ \bar{\psi}^- \end{pmatrix}. \quad (3.29)$$

Majorana fermions, such as neutral Higgsinos and Gauginos are defined via

$$\lambda_{\tilde{h}} \equiv \begin{pmatrix} \tilde{\chi}_h \\ \bar{\tilde{\chi}}_h \end{pmatrix}. \quad (3.30)$$

The Lorentz-dual spinors of Dirac and Majorana spinors are given by

$$\bar{\psi}_f \equiv \psi_f^\dagger \gamma^0 = (f^c, \bar{f}_L), \quad (3.31)$$

$$\bar{\lambda}_h \equiv \lambda_h^\dagger \gamma^0 = \lambda^T. \quad (3.32)$$

respectively. As the charge-conjugate of a Dirac spinor we shall use

$$\psi_f^c \equiv \begin{pmatrix} f^c \\ \bar{f}_L \end{pmatrix}. \quad (3.33)$$

The Majorana spinors are self-conjugate.

There are three types of couplings involving two Dirac fermions relevant to our model:

$$f^{1c} f_L^2 = \bar{\psi}_1 P_L \psi_2, \quad f^{1c} f^{2c} = \bar{\psi}_1 P_L \psi_2^c, \quad f_L^1 f_L^2 = \bar{\psi}_1^c P_L \psi_2, \quad (3.34)$$

where the projection operator is given by

$$P_L = \frac{1}{2}(1 - \gamma_5), \quad \left[P_R = \frac{1}{2}(1 + \gamma_5) \right].$$

Chapter 4

First Phenomenological Results

In this section we present the first viable TeV-scale spectra of our model that were found using **EXSPECT**, our automated spectrum generator, embedded in the random walk routine that was described in the previous chapter. For these spectra we have – as a first step – investigated the phenomenology of the heavy Z' boson: We numerically calculated its width at leading order (LO) for each spectrum depending on the kinematically accessible decay channels, and simulated events for

$$pp \longrightarrow \mu^- \mu^+ \quad (4.1)$$

at a center of mass energy of 14 TeV using WHIZARD. Furthermore the forward-backward asymmetry in the di-muon final state was calculated analytically and compared to the result obtained in a numerical analysis using WHIZARD.

4.1 TeV-Scale Spectra

The tension within our model of the LR symmetry above Λ_{int} on the one side and the requirement of a Higgs potential leading to the correct EWSB on the other is very strong: That is, in large regions of the space of free parameters (table 3.3) there is either no minimum of the Higgs potential according to (3.8), the scalar SSB mass terms of fields other than the Higgs fields become negative in the course of the RG evolution, or the scalar Higgs mass terms determined from the potential minimization (2.76) do not coincide with their RG evolution.

Nonetheless, the MCMC implemented in **EXSPECT** discovered (small) areas in the parameter space leading to physical spectra which pass the abovementioned hurdles. We present here three scenarios which are representative for these areas found at this (early) stage of our investigation.¹ In the close vicinity of the input parameters of these three scenarios the random walk discovers many suitable sets of input parameters leading to essentially identical physical spectra. The input parameters for these cases are listed in table 4.1. The TeV-scale mass spectra derived from the input parameters in table 4.1 are plotted in figure 4.1. The complete sets of masses, mixing matrices, and coupling constants for scenario A, B, and C can be found in appendix B.4.1, B.4.2, and B.4.3, respectively. Although the plots of the mass spectra in figure 4.1 only have a low resolution, they provide a nice overview over the TeV-scale spectra:

All three spectra are clearly shaped by the large values of v_s

$$\text{Scenario A and B: } v_s = 7 \text{ TeV}, \quad \text{Scenario C: } v_s = 5.9 \text{ TeV}. \quad (4.2)$$

Note, that the parameter v_s is not given explicitly in the **EXSPECT** output (section B.4.1-B.4.3). Within the implementation of our model into WHIZARD it is cal-

¹All three spectra presented here correspond to the first of the two gauge coupling unification scenarios presented in figure 2.3.

	Scenario A	Scenario B	Scenario C
y_lq	0.106	0.145	0.210
y_lqc	0.082	0.075	0.230
y_sd	0.397	0.856	0.655
y_sh	0.214	0.321	0.052
y_nmssm	0.173	0.145	0.150
M_g	1105	-1452	-1359
M_gluino	-820	-875	-841
h_sm	-764	-1261	-749
h_lq	372	-446	-376
h_lqc	-224	-0.9	-897
h_sd	-264	500	307
h_sh	351	-767	19
h_nmssm	22.5	-185	73
m_sfer	1689	814	1690
m_dh	1234	1154	1936
m_H	1959	1921	1465
m_D	816	805	826
m_S	1201	1921	1357
m_int	-1459	-1050	-845

Table 4.1: The input parameters of the three scenarios A,B, and C at the orbifold compactification scale. The meaning of the parameters in the first column within EXSPECT was explained in table 3.3.

culated from the effective μ parameter and the Higgs Yukawa coupling according to (1.39).

Most notably, the exotic leptoquarks D and their fermionic superpartners \tilde{D} are very heavy $\gtrsim 2$ TeV. The sfermions are consequently quite heavy as well, the lightest having masses around 1 TeV (as they receive D -term contributions of the order $g'v_s$ according to (2.70)). They are therefore in agreement with the current exclusion limits set by the LHC.

In the Higgs sector, we find a very large splitting among light mass eigenstates which up to very small admixtures from the SM-singlet S correspond to H^d and H^u , whereas the heaviest CP-even Higgs is almost a pure singlet state (compare with the mixing matrices given in section B.4.1-B.4.3). The masses of the lightest CP-even Higgs particles evaluated in the one-loop effective potential approxima-

tion are

$$\text{Scenario A and C: } m_h = 110 \text{ GeV,} \quad \text{Scenario B: } m_h = 107 \text{ GeV.} \quad (4.3)$$

Although we collected all contributions arising in the one-loop effective potential (accounting for the full extended particle content including the D -terms contributions) in our numerical analysis, one should bare in mind, that the corrections at higher orders in perturbation theory [74] may be sizable ($\sim 5 \text{ GeV} - 15 \text{ GeV}$). Furthermore, it is worth noticing that the tree-level Higgs masses in all three scenarios are above 90 GeV, hence exceeding the theoretical upper limit on the MSSM's lightest Higgs mass (at the tree-level).

The dark Higgs sectors of the spectra A and C are both very heavy, whereas spectrum B features one light CP-even, CP-odd and charged dark Higgs state, respectively.

The mass of the heavy Z' is practically identical in the scenarios A and B

$$\text{Scenario A and B: } M_{Z'} \approx 2480 \text{ GeV.} \quad (4.4)$$

In scenario C the Z' mass is about 400 GeV lighter, which greatly affects the potential production rates at the LHC, as we shall discuss in section 4.2.

The Lightest Dark Higgsino

All three spectra presented in figure 4.1 exhibit a very light dark Higgsino $\lesssim .1 \text{ GeV}$. From the corresponding superpotential (2.88), we conclude that it is stable, being the lightest R - and H -odd state at the same time (see also section 2.2.1). The potential role of the lightest dark Higgsino as dark matter candidate was to some extent explored in [75], where it was shown that a very light ($\lesssim 1 \text{ GeV}$) dark neutralino would yield a too large dark matter relic density. Therefore the authors restricted their investigation to regions in parameter space ($\tan \beta \sim 1.5 - 2.25$) providing higher masses ($\sim 30 - 65 \text{ GeV}$) for the dark matter candidate. Unfortunately in our model $\tan \beta$ is generically fixed to a very large value ~ 40 by the requirement of top-bottom unification.

According to (2.97) the lightest dark Higgsino being significantly heavier than 1 GeV would require a hierarchy in the Yukawa couplings of the dark Higgs sector, where

$$\mathbf{Y}_{113}^{SH} \sim \mathbf{Y}_{131}^{SH} \gg \mathbf{Y}_{311}^{SH}. \quad (4.5)$$

This would also provide a stronger admixture in the lightest mass eigenstate of the dark Higgsinos coupling to the electroweak gauge bosons according to (2.98). At the stage of our investigation presented here, the Yukawa couplings of the dark Higgs sector are taken to be unified at the orbifold compactification scale (within the current setting of the MCMC, see table 3.3). The RG evolution does not distort this degeneracy so significantly as to yield a heavier lightest dark Higgsino. Rendering the H -parity an approximate symmetry would not solve the problem either as the lightest dark Higgsino would still be stable (then constituting the lightest R -parity odd state).

It remains a task for the future to investigate if (with an extended space of free parameters) one can find consistent scenarios in which the annihilation channels into standard model particles are not as strongly suppressed as to overshoot the relic density.

For the remainder of this thesis, we shall ignore this issue and dedicate our attention to collider phenomenology.

4.2 Z' Production at the LHC

The extra $U(1)$ in the gauge group below the intermediate symmetry scale results in an additional neutral current mediated by the heavy Z' boson. In this section we present our investigation of its effects on $pp \rightarrow \mu^+\mu^-$ scattering at the LHC. This process has been selected, as the corresponding observables are relatively easy to calculate and the di-muon final state can be detected at the LHC with very high efficiency.

As outlined in section 3.4, we have implemented the full model into the multi-purpose event generator WHIZARD using the FeynRules interface.

The coupling of the heavy Z' boson to matter is calculated by WHIZARD from EXSPECT's output (see section B.4.1-B.4.3) according to

$$g' = \frac{M_{Z'}}{\sqrt{(Q'_{H^d})^2 v_d^2 + (Q'_{H^u})^2 v_u^2 + (Q'_S)^2 v_s^2}}, \quad (4.6)$$

where the vevs have been obtained from $M_Z, \tan \beta, \mu_{\text{eff}}$ and \mathbf{Y}^{SH} .

Prior to the investigation of the Z' resonance, we calculated its total decay width in WHIZARD. All kinematically accessible (tree-level) decay channels into two- and three-particle final states (the latter originating from the mixing among the SM's Z and the Z' (2.103)) have been taken into account:

$$\begin{aligned} \text{Scenario A: } & \Gamma_{Z'} = 37.4 \text{ GeV}, \\ \text{Scenario B: } & \Gamma_{Z'} = 39.5 \text{ GeV}, \\ \text{Scenario C: } & \Gamma_{Z'} = 39.9 \text{ GeV}, \end{aligned} \quad (4.7)$$

For the calculation of the total cross section, we used the `cteq611.LHpdf` PDF-set at LO [76, 77] to account for the non-trivial substructure of the colliding proton beams and applied the following kinematic cuts

$$\begin{aligned} |\eta| &< 2.5 && \text{(detector acceptance)} \\ p_T &> 50 \text{ GeV} && \text{(for each muon)} \\ M_{\mu\mu} &> 1.5 \text{ TeV} && \text{(invar. mass of muon pair)} \end{aligned} \quad (4.8)$$

The total cross section for the process $pp \rightarrow \mu^+\mu^-$ at 14 TeV center-of-mass energy subject to the cuts listed above is then evaluated to

$$\text{Scenario A: } \sigma_{\text{tot}} = (1.689 \pm 0.004) \text{ fb},$$

$$\begin{aligned} \text{Scenario B: } \sigma_{\text{tot}} &= (1.660 \pm 0.004) \text{ fb}, \\ \text{Scenario C: } \sigma_{\text{tot}} &= (2.450 \pm 0.005) \text{ fb}. \end{aligned} \quad (4.9)$$

It should be noted, that the errors in the above equations contain only the statistical uncertainties on the numerical integration in WHIZARD. A suitable observable to study the implications of our model on LHC physics is the cross section of $pp \rightarrow \mu^+ \mu^-$ differentiated with respect to the invariant mass of the muon pair $M_{\mu\mu}$. We have calculated the differential cross section for each of our three scenarios, from a sample of $N_{\text{tot}} = 10^5$ weighted events (with weight $\langle w_i \rangle = \sigma_{\text{tot}}$ as in (4.9)) generated with WHIZARD. For each sample we produced a histogram counting the number of events N as a function of $M_{\mu\mu}$ (with $\Delta M = 5$ GeV binning). The differential cross section in the i^{th} bin is then given by

$$\frac{\partial \sigma}{\partial M_{\mu\mu}}(M_{\mu\mu}^i) = \frac{N(M_{\mu\mu}^i)}{\Delta M \langle \sum_i w_i \rangle} \sigma_{\text{tot}} = \frac{N(M_{\mu\mu}^i)}{\Delta M} \frac{1}{N_{\text{tot}}}. \quad (4.10)$$

For better readability and to reduce the impact of statistical fluctuations in the regime of low event counts, we have furthermore averaged over bins of 50 GeV away from the Z' resonance. The results for the three spectra from figure 4.1 are shown in figure 4.2. We note from (4.9) and figure 4.2 that the cross section for scenario A and B are significantly lower than the for scenario C, which reflects that the likelihood to find partons $q\bar{q}$ carrying large momentum fractions of the protons decreases with higher energies.

In order to estimate whether or not the scenarios presented here are within the reach of the LHC, we requested the generation of the number of events corresponding to an integrated luminosity of 100 fb^{-1} . The results for all three scenarios is displayed in figure 4.3. Away from the respective peaks, the plots in figure 4.3 are dominated by statistical fluctuations. Nonetheless, in the region of the resonances the peaks are very distinct, showing that the Z' boson in each of the three scenarios presented here could very well be detected at the (14 TeV) LHC.

4.2.1 Forward-Backward Asymmetry in the Di-Muon Channel

The forward-backward asymmetry A_{FB} (see e.g. [78, 79]) for Drell-Yan processes $q\bar{q} \rightarrow \mu^+ \mu^-$ is defined as

$$A_{FB} \equiv \frac{\sigma_F - \sigma_B}{\sigma_F + \sigma_B}, \quad (4.11)$$

with

$$\sigma_F \equiv \int_0^1 \frac{d\sigma(q\bar{q} \rightarrow \mu^+ \mu^-)}{d \cos \theta^*} d \cos \theta^*, \quad \sigma_B \equiv \int_{-1}^0 \frac{d\sigma(q\bar{q} \rightarrow \mu^+ \mu^-)}{d \cos \theta^*} d \cos \theta^*.$$

In the above equation, θ^* denotes the angle between the outgoing muon and the incoming quark in the rest frame of the muon pair. In terms of the four momenta

k of the μ^- and \bar{k} of the μ^+ in the lab frame the angle is given by

$$\cos \theta^* = 2 \frac{\bar{k}_0 - \bar{k}_3}{\bar{k}_0 - \bar{k}_3 + k_0 - k_3} - 1, \quad (4.12)$$

with the direction of the incoming quark and anti-quark being fixed. The latter point already indicates that the application of A_{FB} as a precisely measurable observable at the LHC is limited, as it is generally not known from which proton in the $pp \rightarrow \mu^+ \mu^-$ scattering the quark and anti-quark originated from.

Before going into further detail, we shall demonstrate at this point how we used the forward-backward asymmetry at the partonic level to cross-check the implementation of our model into WHIZARD:

In [78], the forward-backward asymmetry A_{FB} for $q\bar{q} \rightarrow \gamma, Z, Z' \rightarrow \mu^+ \mu^-$ was calculated:

$$A_{FB} = \frac{3}{4} \frac{|A_{LL}|^2 + |A_{RR}|^2 - |A_{LR}|^2 - |A_{RL}|^2}{|A_{LL}|^2 + |A_{RR}|^2 + |A_{LR}|^2 + |A_{RL}|^2} \quad (4.13)$$

where

$$\begin{aligned} A_{ij} &\equiv A(q_i \bar{q} \rightarrow \mu_j^+ \mu^-) \\ &= -Q_{q_i}^e e^2 + \frac{g_Z^2 Q_{q_i}^Z Q_{\mu_j}^Z s}{s - M_Z^2 + iM_Z \Gamma_Z} + \frac{(g')^2 Q_{q_i}' Q_{\mu_j}' s}{s - M_{Z'}^2 + iM_{Z'} \Gamma_{Z'}}. \end{aligned} \quad (4.14)$$

Here, the couplings of the Z boson to the fermions are given by

$$g_Z Q^Z = \frac{e}{s_w c_w} (c_w^2 T_3 - s_w^2 Y), \quad (4.15)$$

where s_w and c_w denote the sin and the cos of the weak mixing angle, respectively. As for the models studied in [80], we compared the theoretical prediction of A_{FB} according to (4.14) with the results obtained from the implementation of our model in WHIZARD. We have found perfect agreement between the analytical results and the numerical evaluation. The results for each of our three scenarios are displayed in figure 4.4. As mentioned earlier, the results for A_{FB} at the partonic level are not of great use when it comes to LHC phenomenology: Although it is in principle possible to unfold the $pp \rightarrow \mu^+ \mu^-$ events such that one can conclude (to some extent) from which proton the quark originated (see the detailed analysis from [80]), it is impossible to determine whether an up- or down-type quark pair annihilated into the vector bosons.

In order to provide a result that can be compared to data subjected to the analysis in [80], we calculated the forward-backward asymmetry A_{FB} for the process $pp \rightarrow \mu^+ \mu^-$ at Monte Carlo truth-level. That is, we decided a priori which proton would contain the quark and which the antiquark involved in the Drell-Yan process $q\bar{q} \rightarrow \mu^+ \mu^-$. This analysis has been carried out numerically at LO for all of the three spectra presented in this chapter. The results are shown in figure 4.5.

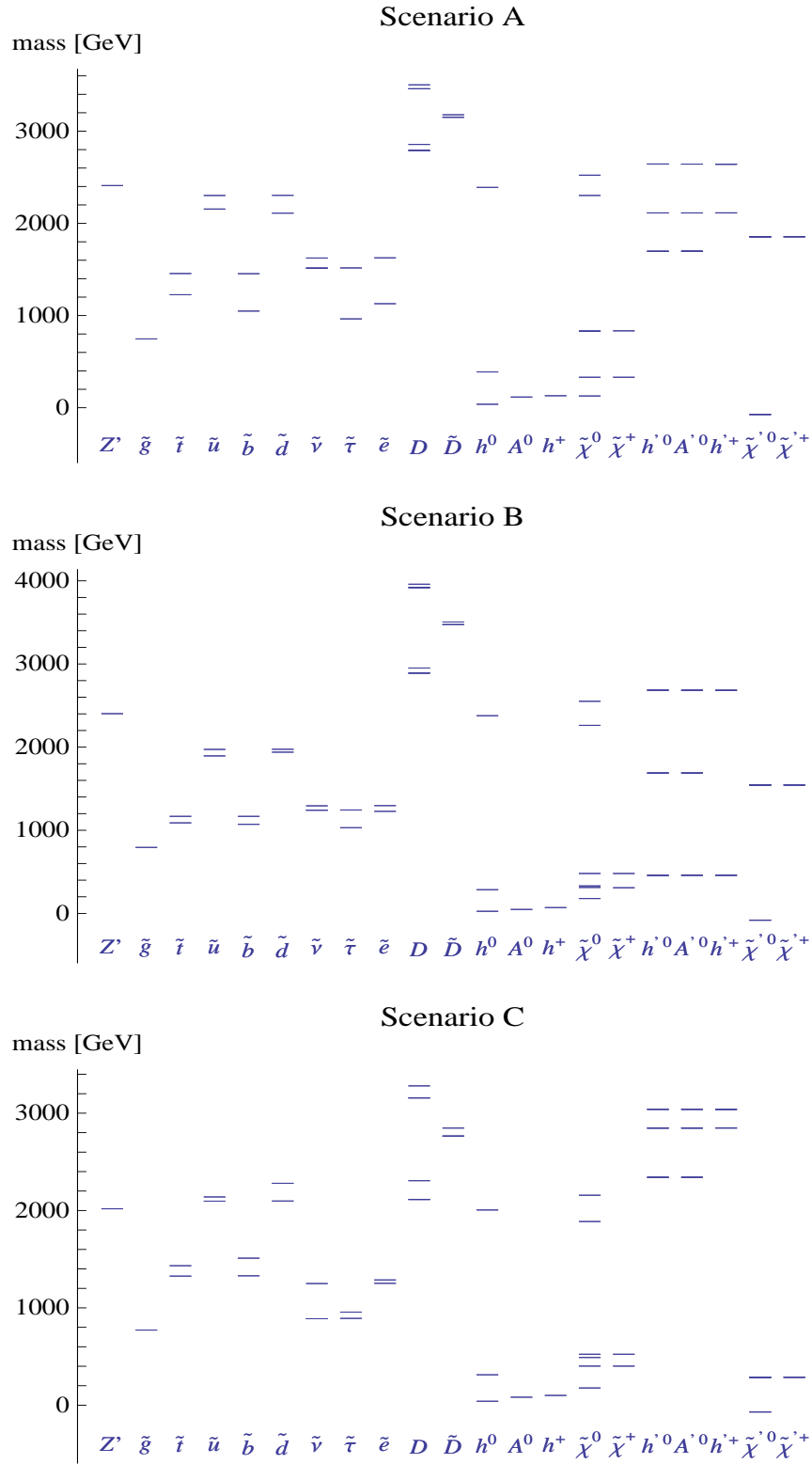


Figure 4.1: Three TeV-scale mass spectra of our model corresponding to the sets of input parameters presented in table 4.1.

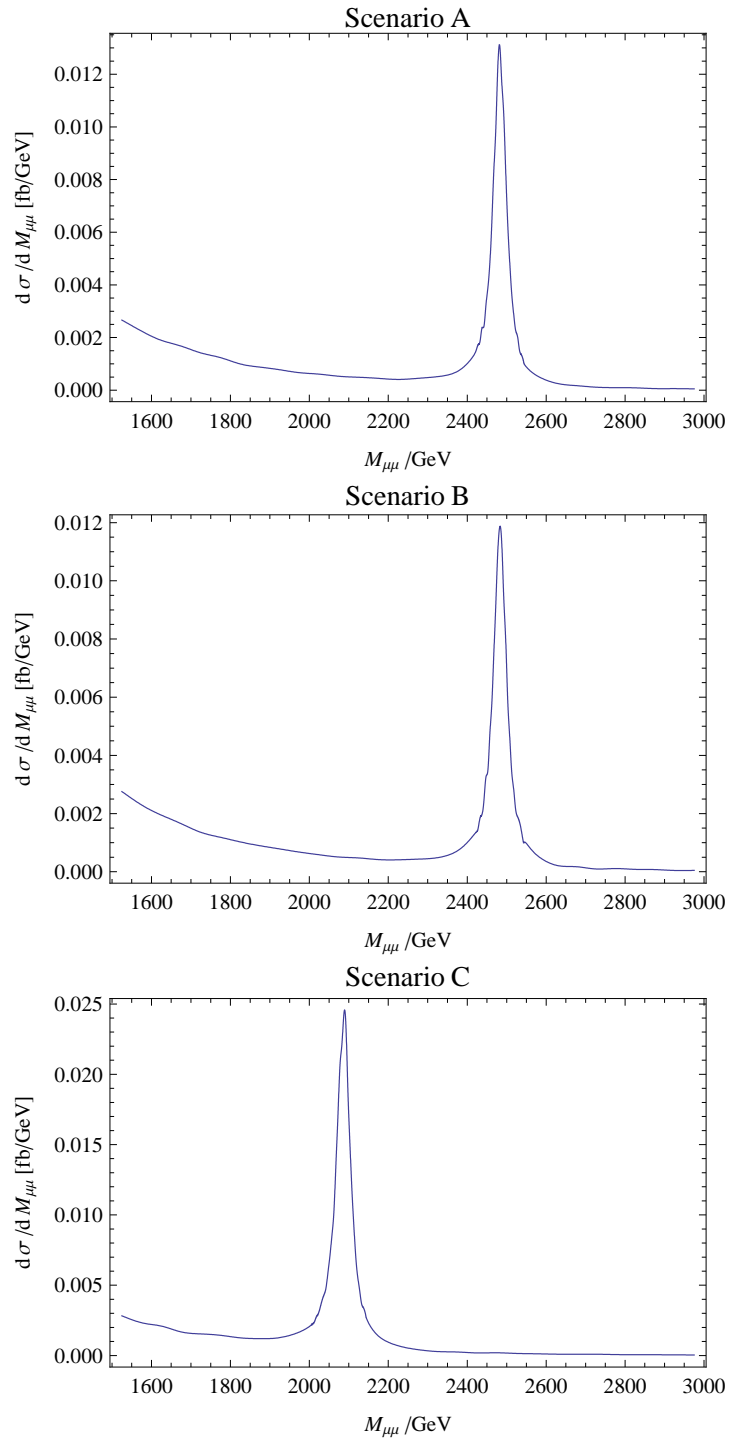


Figure 4.2: Differential cross sections of $pp \rightarrow \mu^+\mu^-$ as function of the invariant mass of the di-muon pair at $\sqrt{s} = 14$ each obtained from a sample of 10^5 events according to (4.10).

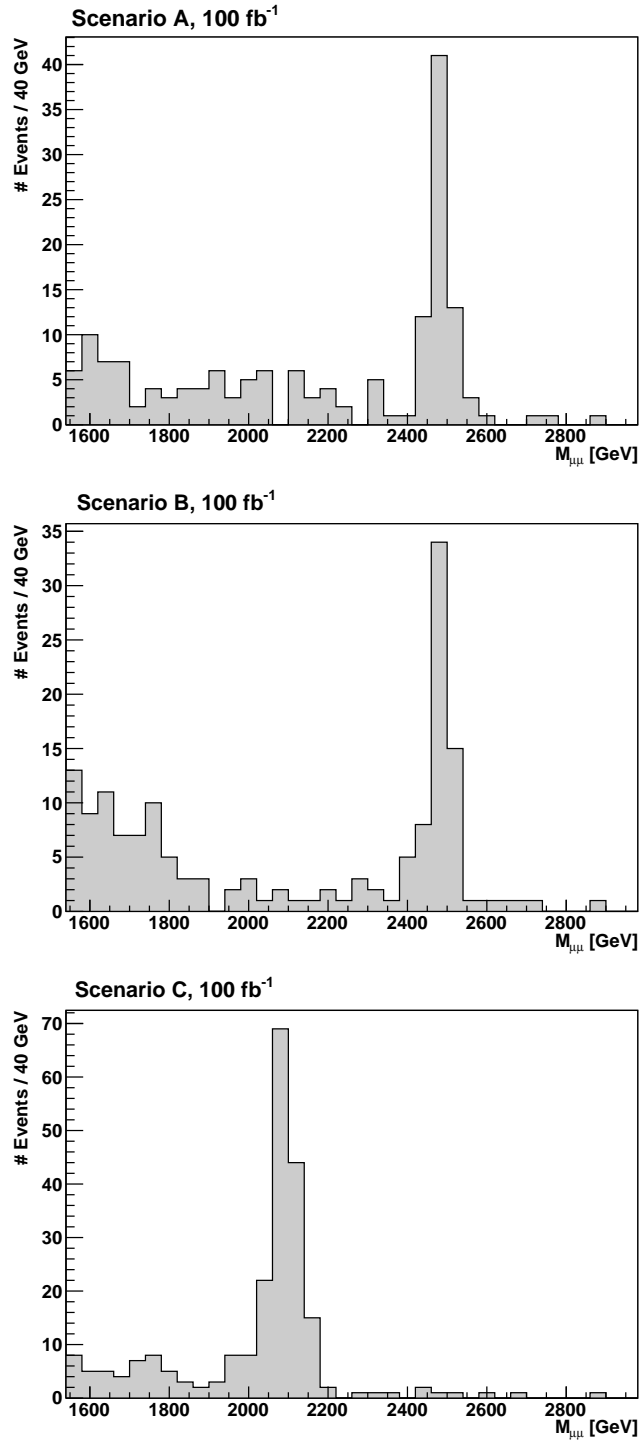


Figure 4.3: Expected event rates for $pp \rightarrow \mu^+\mu^-$ as function of the invariant mass of the di-muon pair.

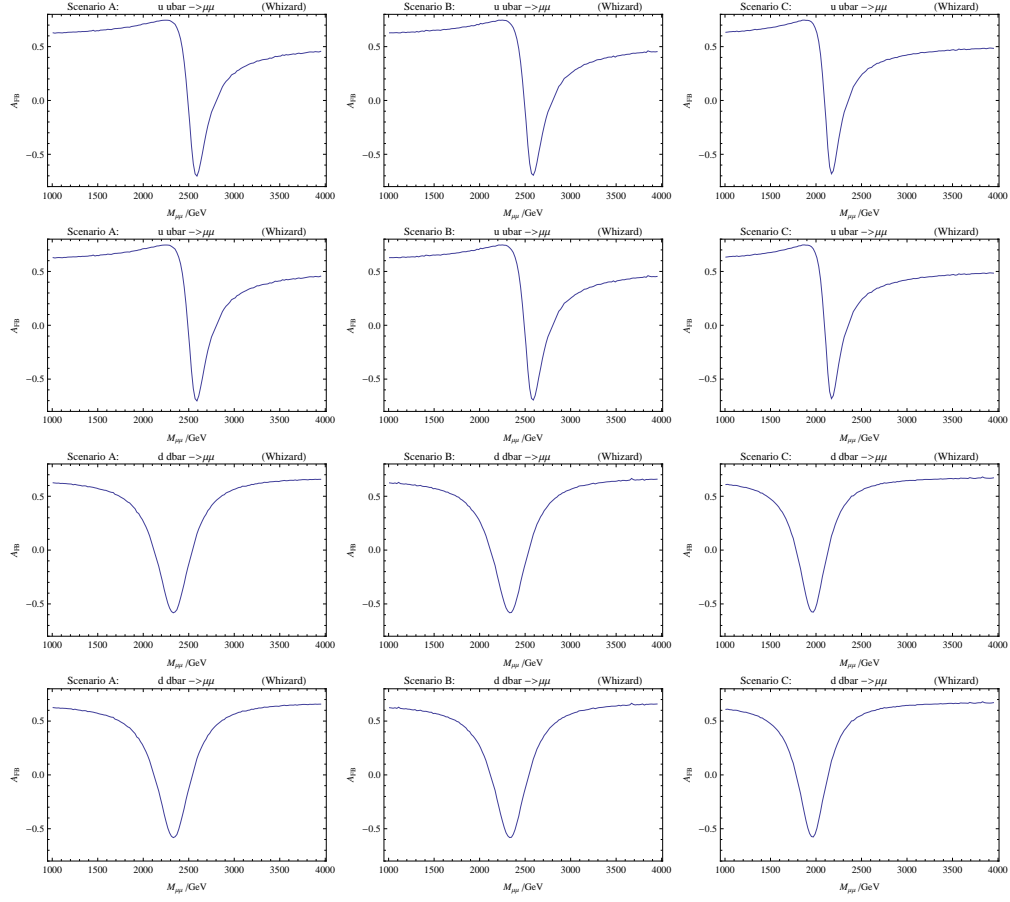


Figure 4.4: Comparison of the theoretical prediction according to (4.14) of the forward-backward asymmetry in quark-antiquark scattering as function of $M_{\mu\mu}$ with the results obtained from the implementation of our model in WHIZARD.

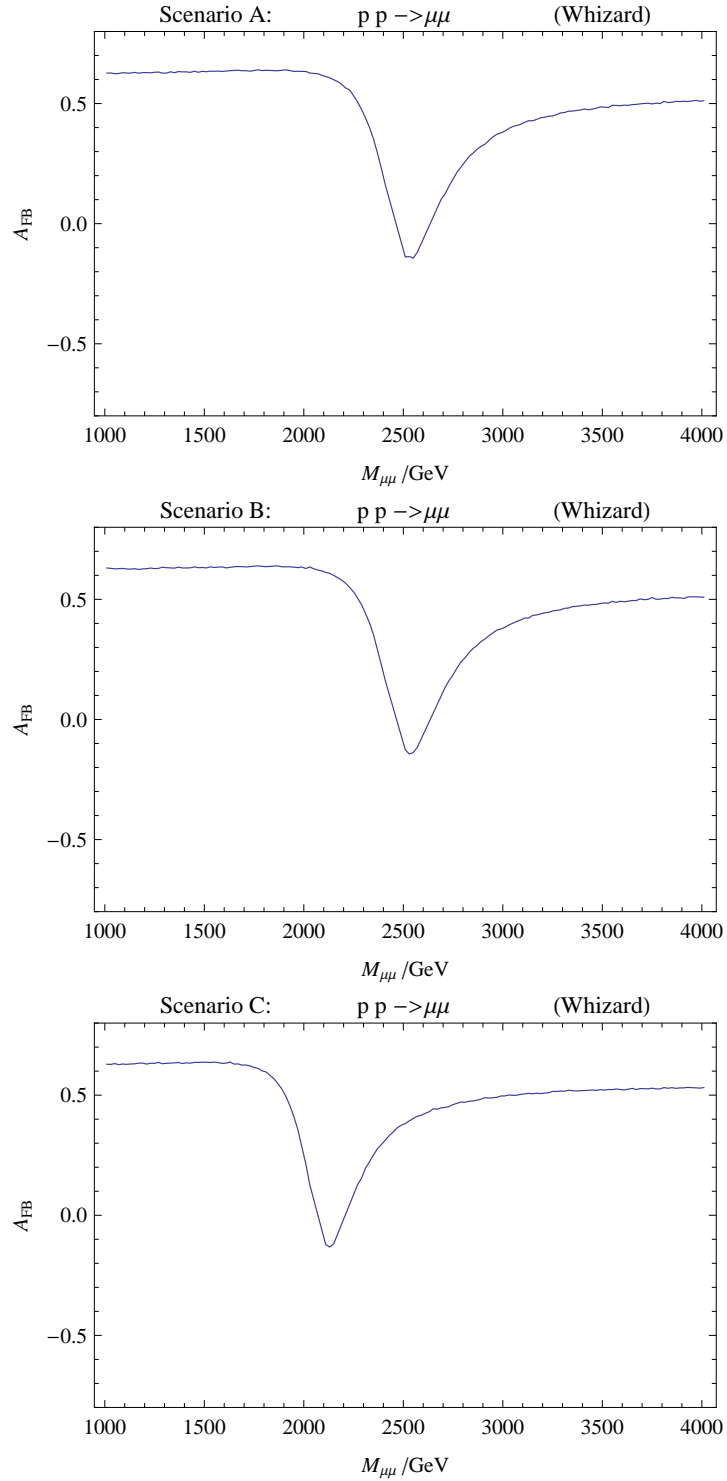


Figure 4.5: A_{FB} as function of $M_{\mu\mu}$ for $pp \rightarrow \mu^+ \mu^-$ (at truth level). The differential cross sections have been calculated using WHIZARD.

Chapter 5

Conclusions

In this thesis, we have demonstrated how a supersymmetric theory with $U(1)$ -extended gauge group can be placed in the context of grand unification. We found, that with the minimal particle content (dictated by anomaly-freedom) unification can only be realized with at least one intermediate symmetry breaking scale, which can be associated with the mass scale of the right-handed neutrino. We have briefly discussed the shortcomings of the Pati-Salam group serving as gauge group above this intermediate scale and the notion of E_6 being the unified gauge group.

The solution presented here is based on the left-right symmetric extension of the standard model's gauge group above the intermediate scale, leading to gauge coupling unification at around the Planck scale. Furthermore, we have found a six-dimensional orbifold construction with E_6 as gauge group in the extra-dimensional bulk, that allows for the identification of the gauge coupling unification scale with the compactification scale of the extra dimensions. In this context, various aspects regarding the consistency of our solution – the assignments of the orbifold action on group space, the realization of supersymmetry in six dimensions, the field content in the bulk ensuring anomaly freedom, as well as the localization of the matter appearing below the compactification scale at the orbifold's fixed points – have been addressed.

Although the construction of the model started from an extension of the NMSSM at the TeV scale, the implications from the underlying unification structure on the appearance of the model at low energies is highly non-trivial: The renormalization group equations used to derive the TeV-scale Lagrangian from the theory specified at the orbifold compactification scale form a large set of coupled differential equations with complex interdependencies. At the intermediate symmetry scale the Lagrangian parameters are subject to symmetry constraints, which most notably require the unification of the top and the bottom Yukawa coupling. This in turn has strong implications on the structure of the vacuum breaking the electroweak symmetry to electromagnetism.

In chapter 3 we have documented in detail the design of our automated spectrum generator `EXSPECT` where the above mentioned structures have been translated into algorithms that allow for a numerical evaluation. The search for sets of input parameters leading to physically viable spectra at the TeV scale involves the investigation of the high-dimensional space of free parameters at the orbifold compactification scale. For this reason, we used a Monte-Carlo Markov-Chain approach, providing a powerful framework for multi-dimensional optimization, which at this stage of investigation resulted in the discovery of the scenarios presented in chapter 4.

This discovery first of all shows that our model leads indeed to a realistic phenomenology¹, with the tension among the RG evolution and the Higgs potential

¹With the caveat that the impact of the lightest dark Higgsino on cosmological observables

minimization being resolved. Furthermore the corresponding TeV-scale spectra allowed us to derive first predictions regarding the current LHC-experiment at CERN using an implementation of our model in the event generator WHIZARD. We have found that, with the heavy neutral gauge boson Z' having masses in the ballpark of 2–2.5 TeV and a rather narrow width (roughly 40 GeV), it will be detectable at the LHC once upgraded to 14 TeV center-of-mass energy. In addition, we have calculate the forward-backward asymmetry in the $pp \rightarrow \mu^+ \mu^-$ channel, which may reveal the coupling structure of the Z' bosons to fermions, depending on the Z' mass and the performance of the LHC.

5.1 Outlook

The theoretical description of our model is almost complete, up to the specification of the potential leading to the breaking of the intermediate symmetry. It is clear, that in principle such a potential exists [53], but it involves dimension-six operators suppressed by the square of the orbifold compactification scale (in our model). The precise origin of this non-renormalizable contribution in the context of our orbifold construction will be one of the topics of our future research.

Regarding the TeV-scale phenomenology of our model, it is obvious that there is a variety of exciting new channels that call for further investigation [81]: Apart from the “generic” SUSY phenomenology, the exotic leptoquark fields and the dark Higgs sector may result in interesting signatures at the LHC. In this context, it should be noted that the spectra presented in this work should not be taken to be representative “benchmark”-scenarios of our model. With such a high-dimensional space of free parameters, it is a non-trivial task to make general statements about truly intrinsic features of the corresponding TeV-scale spectra. The setting of the Monte-Carlo Markov Chain presented in section 3.3 was aimed at the initial discovery of spectra. A larger coverage of the parameter space requires slight modifications of the parameters determining the behavior of the random walk, like e.g. the width of the sampling distribution. Clearly, this will be a (run-) time-consuming endeavor, but we hope to be able to provide new results in [81].

requires further investigation [81].

Appendix A

Orbifolds and Extended Supersymmetry

A.1 A toy model

As an introduction to symmetry breaking by orbifold boundary conditions, we present a non-supersymmetric Yang-Mills theory in five spacetime dimensions. In this example¹, we will see how a symmetry constraint on the extra dimension reduces the gauge invariance from $SO(4)$ in five spacetime dimensions, to $SO(3)$ in the resulting four-dimensional theory. Let at first the fifth dimension be compactified to a circle S^1 ($-R\pi, R\pi$). We denote the fifth component of the gauge field as $\Sigma \equiv A_5$. On the compact dimension, we can Fourier expand the gauge fields in this coordinate

$$\begin{aligned} A_\mu(x^\mu, x^5) &= A_\mu^{(0)}(x^\mu) + \sum_{n=1}^{\infty} (A_\mu^{(n)}(x^\mu) e^{inx_5/R} + \text{h.c.}), \\ \Sigma(x^\mu, x^5) &= \Sigma^{(0)}(x^\mu) + \sum_{n=1}^{\infty} (\Sigma^{(n)}(x^\mu) e^{inx_5/R} + \text{h.c.}). \end{aligned} \quad (\text{A.1})$$

By choosing a suitable gauge fixing term [42], one can render the fifth component of the gauge field independent of x_5 , leaving only the zero mode as physical degree of freedom in the spectrum, $\Sigma(x^\mu, x^5) \equiv \Sigma^{(0)}(x^\mu)$. With this at hand, the action describing the theory can be written as

$$\begin{aligned} S &= \text{tr} \int d^4x \int dx_5 \left[-\frac{1}{4} F_{mn} F^{mn} \right] \quad m, n = 0, \dots, 4 \\ &\stackrel{\text{i.p.}}{=} \text{tr} \int d^4x \int dx_5 \left[-\frac{1}{4} F_{\mu\nu} F^{\mu\nu} + \frac{1}{2} (D_\mu \Sigma_5^{(0)})^2 + \frac{1}{2} (\partial_5 A_\mu)^2 \right]. \end{aligned} \quad (\text{A.2})$$

Upon insertion of the mode decomposition from (A.1), the integration over x_5 can be performed, showing the equivalence of the five dimensional theory (A.2) to a 4D action with massless fields corresponding to the zero modes from (A.1) and a *tower* of massive fields with masses $\propto n/R$ corresponding to the higher modes in (A.1). This is commonly referred to as *Kaluza-Klein* decomposition [82]. At energy scales well below the compactification scale $\sim 1/R$, the massive fields can be integrated out, leading to a theory that contains only the massless modes from (A.1).

The transition from the smooth manifold C representing the extra dimensions like in the above example to a setup where the manifold contains singularities is called *orbifolding*. Generally speaking, one introduces a symmetry group G acting *non-freely* on C , i.e. there are fixed points on C under the action of G . The space C/G is then called orbifold.

¹We follow [42] closely, having adjusted the conventions to those used throughout this work

In the above 5D case, boundary conditions can be imposed by replacing the compact fifth dimension by the interval $(0, R\pi]$ which is related to the original circle by an orbifold action which identifies the two hemispheres via:

$$\theta : x_5 \longrightarrow -x_5. \quad (\text{A.3})$$

This is typically called the S^1/\mathbb{Z}_2 orbifold. From its Lorentz properties (assuming a trivial embedding of the orbifold action) it follows that Σ is odd as well under the orbifold action. In addition to the orbifold action, one can assign a *gauge twist* G_θ acting on the space of the gauge group, while respecting the orbifold symmetry (\mathbb{Z}_2 in this case). Representing the $SO(4)$ generators by real 4×4 matrices, the action is invariant under the gauge twist in group space

$$G_\theta T^{ij} = +T^{ij}, \quad G_\theta T^{i4} = -T^{i4} \quad \text{with } i, j = 1, 2, 3. \quad (\text{A.4})$$

Imposing the boundary conditions (A.3) and the gauge-twist (A.4) on the mode decomposition (A.1) one obtains, that the only massless modes left in the theory are

$$A_\mu^{ij}(x^\mu)^{(0)}, \quad \Sigma_5^{i4}(x^\mu)^{(0)}, \quad (\text{A.5})$$

where the $SO(4)$ matrices have been absorbed into the definition of the gauge fields. The action describing the low energy effective theory for $E \ll 1/R$ then reads:

$$S_{\text{eff}} \propto \int d^4x \left[-\frac{1}{4} F_{\mu\nu}^{ij(0)} F_{ji}^{\mu\nu(0)} + \frac{1}{2} (D_\mu \Sigma_5^{(0)})^2 \right]. \quad (\text{A.6})$$

We have obtained a $SO(3)$ invariant action with a gauge field coupled to a scalar field transforming as a triplet. In addition to fields living in the *bulk* of five-dimensional spacetime, four-dimensional Weyl fermions can be confined to one of the *fixed points* of the sphere. They can be coupled to the gauge field evaluated at the boundary, if they transform according to a non-trivial representation of the 4D gauge group. The corresponding action reads

$$S_\chi = \int d^4x \bar{\chi}^i(x) (i\partial_\mu \delta^{ij} + g A_\mu^{ij}(x, x_5 = R\pi)) \chi^j(x). \quad (\text{A.7})$$

A.2 $N = 2$ Supersymmetry in 4D

For completeness and a better understanding of the orbifold construction presented in chapter 2, in this and the next section we sketch the relation of $N = 2$ SUSY in 4D and $N = 1$ SUSY in 6D, following [44] closely.

In $N = 2$ supersymmetry the gauge multiplet has a spectrum which can be compared to the superposition of an $N = 1$ gauge multiplet with a chiral multiplet (see table A.1). To construct a $N = 2$ supersymmetric theory one can therefore start from a $N = 1$ supersymmetric non-Abelian gauge theory of a massless chiral

	helicity :	-1	$-\frac{1}{2}$	0	$\frac{1}{2}$	1
$\underline{N=2}$	gauge	1	2	1+1	2	1
$\underline{N=1}$	gauge	1	1	0	1	1
	chiral	0	1	1+1	1	0

Table A.1: On-shell degrees of freedom per helicity quantum numbers in massless $N = 1$ and $N = 2$ supermultiplets (both in 4D)

multiplet in the adjoint representation of the gauge group:

$$L = \text{tr} \left[-\frac{1}{4} F_{\mu\nu} F^{\mu\nu} + \frac{1}{2} \bar{\lambda} i \not{D} \lambda + \frac{1}{2} \bar{\psi} i \not{D} \psi + \frac{1}{2} (D_\mu M)^2 + \frac{1}{2} (D_\mu N)^2 - i \bar{\psi} [\lambda, M] - i \bar{\psi} \gamma_5 [\lambda, N] + \frac{1}{2} [M, N]^2 \right], \quad (\text{A.8})$$

where M, N denote the real scalars, and ψ (4-component Majorana spinor) the fermionic degrees of freedom belonging to the chiral multiplet. λ is the gaugino from the vector multiplet in Wess-Zumino gauge. Auxiliary fields have been integrated out for simplicity.

Renaming $\lambda = \lambda_1$ and $\psi = \lambda_2$, one can define a *symplectic Majorana spinor* from the corresponding two-component spinors $\lambda_{\alpha i}$ and $\bar{\lambda}_{\dot{\alpha}}^i \equiv (\lambda_{\alpha i})^\dagger$ via

$$\lambda^i \equiv \begin{pmatrix} -i\epsilon^{ij} \lambda_{\alpha j} \\ \bar{\lambda}^{\dot{\alpha} i} \end{pmatrix}; \quad \bar{\lambda}_i = (\lambda_i^\alpha, i\epsilon_{ij} \bar{\lambda}_{\dot{\alpha}}^j). \quad (\text{A.9})$$

This rather unintuitive notation has the nice feature of rendering (A.8) manifestly $SU(2)$ invariant under rotating the spinor doublet:

$$\mathcal{L} = \text{tr} \left[-\frac{1}{4} F_{\mu\nu} F^{\mu\nu} + \frac{1}{2} \bar{\lambda}_i i \not{D} \lambda_i + \frac{1}{2} (D_\mu M)^2 + \frac{1}{2} (D_\mu N)^2 - i \bar{\lambda}_i [\lambda^i, M] - i \bar{\lambda}_i \gamma_5 [\lambda^i, N] + \frac{1}{2} [M, N]^2 \right]. \quad (\text{A.10})$$

Evidently, supersymmetry does not commute with this $SU(2)$ as the gauge field is a singlet but the gaugino is not. Its generators have to be a doublet of the two symmetry transformations in terms of the original $N = 1$ fields:

$$\delta A_\mu = i \bar{\xi} \gamma_\mu \lambda \quad \text{and} \quad \delta' A_\mu = i \xi' \gamma_\mu \psi. \quad (\text{A.11})$$

There are additional chiral $U(1)_R$ transformations under which the action is invariant:

$$\begin{aligned} (M + iN) &\longrightarrow e^{i\theta} (M + iN), \\ \lambda^i &\longrightarrow e^{i\gamma^5 \theta/2} \lambda^i, \\ A^\mu &\longrightarrow A^\mu. \end{aligned} \quad (\text{A.12})$$

The component fields transform under this $N = 2$ SUSY in this notation as:

$$\begin{aligned}\delta A_\mu &= i\bar{\xi}_i \gamma_\mu \lambda^i \\ \delta M &= i\bar{\xi}_i \lambda^i \\ \delta N &= i\bar{\xi}_i \gamma_5 \lambda^i \\ \delta \lambda^i &= -\frac{i}{2} \sigma^{\mu\nu} \xi^i F_{\mu\nu} - \mathcal{D}(M + \gamma_5 N) \xi^i - i\gamma_5 \xi^i [M, N].\end{aligned}$$

A more detailed analysis [44] shows that indeed this leads to an algebra

$$[\delta^{(1)}, \delta^{(2)}] = 2i\bar{\xi}_i^{(1)} \gamma_\mu \xi^{i(2)} \partial^\mu + \delta_{\text{gauge}} + \text{field equations},$$

up to a gauge transformation (restoring the Wess-Zumino gauge), and the field equations (as we have omitted auxiliary fields), as it corresponds to the $N = 2$ superalgebra

$$\{Q^i, \bar{Q}^j\} = 2\delta^{ij} \mathcal{P}. \quad (\text{A.13})$$

A.3 Conventions

Using $\sigma^0 = \bar{\sigma}^0 = 1$, $\sigma^i = -\bar{\sigma}^i$ and the 5D Dirac algebra

$$\gamma^\mu = \begin{pmatrix} 0 & \sigma^\mu \\ \bar{\sigma}^\mu & 0 \end{pmatrix}, \quad \gamma^5 = \begin{pmatrix} -i & 0 \\ 0 & i \end{pmatrix} \quad (\text{A.14})$$

we define the 6D Dirac algebra as

$$\Gamma^\mu = \begin{pmatrix} 0 & \gamma^\mu \\ \gamma^\mu & 0 \end{pmatrix}, \quad \Gamma^5 = \begin{pmatrix} 0 & \gamma^5 \\ \gamma^5 & 0 \end{pmatrix}, \quad \Gamma^6 = \begin{pmatrix} 0 & -1 \\ 1 & 0 \end{pmatrix} \quad (\text{A.15})$$

and the 6D chirality operator as

$$i\Gamma^7 = \begin{pmatrix} -1 & 0 \\ 0 & 1 \end{pmatrix} \quad (\text{A.16})$$

In this basis,

$$\exp\left[\frac{\phi}{4} [\Gamma^5, \Gamma^6]\right] = \text{diag}\left(e^{-i\phi/2}, e^{i\phi/2}, e^{i\phi/2}, e^{-i\phi/2}\right) \sim U(1) \subset SO(1, 5) \quad (\text{A.17})$$

corresponds to a counter-clockwise rotation with angle ϕ about the origin in the extra dimensional space,

$$\bar{\Psi}(\Gamma^5 + i\Gamma^6)\Psi \longrightarrow e^{i\phi} \bar{\Psi}(\Gamma^5 + i\Gamma^6)\Psi.$$

A.4 $N = 1$ Supersymmetry in 6D

The supersymmetric Lagrangian in 6D for a gauge field A_M and the corresponding gaugino λ reads

$$L = \text{tr} \left[-\frac{1}{4} F^{MN} F_{MN} + \frac{i}{2} \bar{\lambda} \Gamma^M D_M \lambda \right], \quad (\text{A.18})$$

where the 6D representation of the Dirac matrices from appendix A.3 have been used.

The SUSY transformations under which (A.18) forms a density are given by

$$\begin{aligned} \delta A_M &= i \bar{\xi} \Gamma_M \lambda - i \bar{\lambda} \Gamma_M \xi \\ \delta \lambda &= \frac{1}{4} [\Gamma_M, \Gamma_N] \xi F^{MN}. \end{aligned} \quad (\text{A.19})$$

The $N = 1$ SUSY Lagrangian in 6D (A.18) is related the 4D $N = 2$ SUSY case from (A.10) via *trivial dimensional reduction*, i.e. the assumption that all fields do not depend on the two extra dimensions. First, the chiral 6D spinor λ is re-parametrized in terms of an unconstrained four-spinor χ

$$\lambda \equiv \begin{pmatrix} \chi \\ 0 \end{pmatrix}, \quad (\text{A.20})$$

yielding

$$\bar{\lambda} \Gamma^A D_A \lambda = \bar{\chi} \gamma^\mu D_\mu \chi - \bar{\chi} \gamma^5 D_5 \chi - \bar{\chi} \gamma^6 D_6 \chi. \quad (\text{A.21})$$

Removing explicitly all dependence on x_5, x_6 from (A.18), that is setting the respective partial derivatives to zero, one arrives at

$$\begin{aligned} L = \text{tr} \left[-\frac{1}{4} F_{\mu\nu} F^{\mu\nu} + \frac{1}{2} \bar{\chi} i \not{D} \chi + \frac{1}{2} (D_\mu A_5)^2 + \frac{1}{2} (D_\mu A_6)^2 \right. \\ \left. - \bar{\chi} [\chi, M] - \bar{\chi} \gamma_5 [\chi, N] + \frac{1}{2} [M, N]^2 \right], \end{aligned} \quad (\text{A.22})$$

which is – upon an identification of

$$\begin{aligned} \chi &= \frac{1}{\sqrt{2}} (\lambda - i\psi), \\ A_5 &= N, \quad A_6 = M \end{aligned} \quad (\text{A.23})$$

identical to the $N = 2$ Lagrangian in 4D (A.8).

Rotations in the 5–6 plane amount to $U(1)^R$ transformation in the $N = 2$ picture. This can be understood by tracing the action of the Lorentz transformations on the 6D gaugino via (A.20) back to the two fermionic fields from the 4D $N = 2$

gauge multiplet

$$\lambda_{6D} = \begin{pmatrix} \chi \\ 0 \end{pmatrix} \xrightarrow{(A.23)} \frac{1}{\sqrt{2}} \begin{pmatrix} e^{\gamma_5 \theta/2} (\lambda - i\psi) \\ 0 \end{pmatrix}. \quad (A.24)$$

Consequently, in two component spinor notation

$$\begin{aligned} (\lambda_\alpha, \psi_\alpha) &\longrightarrow e^{-i\theta/2} (\lambda_\alpha, \psi_\alpha) \\ (\bar{\lambda}^{\dot{\alpha}}, \bar{\psi}^{\dot{\alpha}}) &\longrightarrow e^{i\theta/2} (\bar{\lambda}^{\dot{\alpha}}, \bar{\psi}^{\dot{\alpha}}), \end{aligned} \quad (A.25)$$

which corresponds to the transformation behavior of the fermions in (A.12), when λ, ψ are embedded into symplectic Majorana spinors according to (A.9). The rotation among the fifth and sixth component of the 6D gauge field represented in the complex plane and the trivial transformation of the four components of the gauge field in the 4D subspace complete the analogy with (A.12).

This is a very important result for the construction of orbifolded GUT within the context of supersymmetry, as the spectrum of the massless zero modes of the fields, do not depend on the extra dimensions.

Finally, we note that the $N = 2$ supersymmetry algebra in four spacetime dimensions with two central charges

$$\begin{aligned} \{Q_i, \bar{Q}_j\} &= 2\delta_{ij}\gamma_\mu P^\mu + 2i\epsilon^{ij}Z_1 + 2i\epsilon^{ij}\gamma_5 Z_2 \\ [Q_i, P_\mu] &= [Q_i, Z_k] = 0 \\ [P_\nu, P_\mu] &= [P_\nu, Z_k] = [Z_1, Z_2] = 0 \end{aligned} \quad (A.26)$$

can be recast into a six dimensional $N = 1$ SUSY form

$$\begin{aligned} \{Q, \bar{Q}\} &= (\mathbf{1} + \Gamma_7)\Gamma^a P_a \\ \{Q, Q\} &= [Q, P^a] = [P^a, P^b] = 0 \end{aligned} \quad (A.27)$$

by identifying

$$Q = \frac{1}{\sqrt{2}} \begin{pmatrix} 0 \\ Q_1 - iQ_2 \end{pmatrix}; \quad P_5 = -Z_2; \quad P_6 = -Z_1 \quad (A.28)$$

Appendix B

Supplements

B.1 Two Loop Unification

The unification scheme of the gauge coupling constants at the two loop level is shown in figure B.1. In the intermediate symmetry regime the additional particle content is chosen according to (2.4a). The most striking difference of the

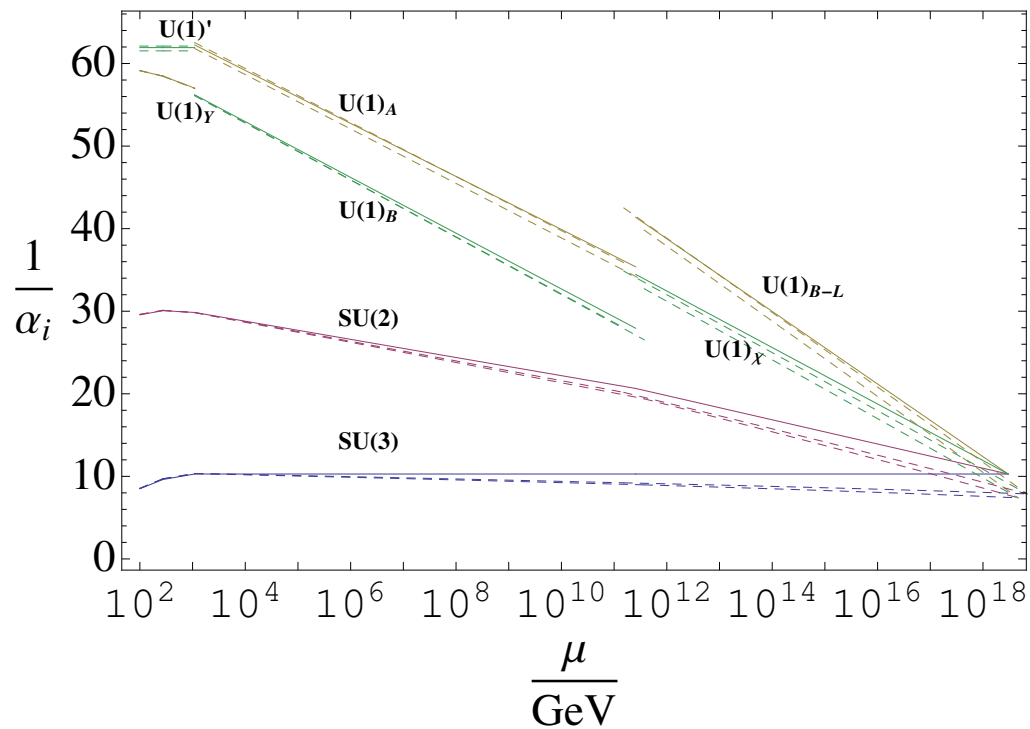
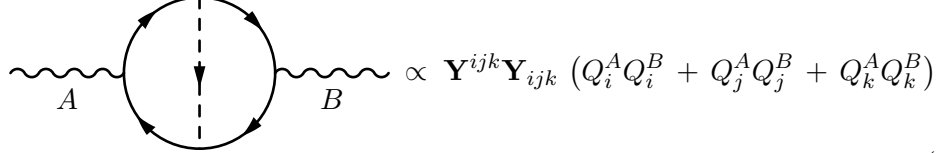


Figure B.1: Unification of the gauge couplings at the one (solid line) and two loop level (dashed lines). The lower dashed line shows the pure gauge RG flow, whereas the upper dashed lines includes the contribution of one generation of Yukawa couplings set to one.

one vs. two loop RG evolution is that the beta function of the strong coupling does not vanish anymore, as the matter contributions overcompensate the gauge bosons self interactions' tendency toward asymptotic freedom. This results in slightly higher intermediate and unification scales. In the presence of Yukawa couplings, the RG evolution approaches the one loop curves. Note that in this case, figure B.1 does not account for a small residual mixing among the two $U(1)$ groups below the intermediate scale: The condition (2.11d) ensures the absence of kinetic mixing terms originating from two-loop diagrams where in figure B.1

a gauge boson line is added. However, as the Yukawa couplings have generally non-degenerate values, there is a small contribution from diagrams like



$$\propto \mathbf{Y}^{ijk} \mathbf{Y}_{ijk} (Q_i^A Q_i^B + Q_j^A Q_j^B + Q_k^A Q_k^B). \quad (\text{B.1})$$

If all Yukawa couplings had identical values, this contribution would vanish according to (2.11d). As the right-handed neutrino is integrated out below the intermediate scale, its superpotential interactions do not contribute to the RG flow of the gauge couplings anymore, resulting in a two-loop induced gauge kinetic mixing, unless all Yukawa couplings vanish.

Throughout this work we have used the RG evolution at the one-loop level, which has advantages regarding the runtime of numerical evaluations. The comparison to the two-loop calculation as shown for the gauge couplings in figure B.1 demonstrates, that all qualitative features of our analysis remain unchanged at higher precision. The potential quantitative changes¹ amount to an uncertainty on the model's free parameters at the unification scale, which seems to be tolerable. The predictions for coupling of the Z' boson to matter hardly change when progressing from one- to two-loop order unification.

B.2 Dark Higgs Masses

The entries of the mass matrix of the scalar dark Higgs fields are given by

$$\begin{aligned} m_{h_{11}^{dd}}^2 &= (\mathbf{m}_{H^d}^2)_{11} + ((\mathbf{Y}_{113}^{SH})^2 + (\mathbf{Y}_{213}^{SH})^2) \frac{v_u^2}{2} + ((\mathbf{Y}_{311}^{SH})^2 + (\mathbf{Y}_{312}^{SH})^2) \frac{v_s^2}{2} \\ &\quad + \mathcal{D}_Y(H^d) + \mathcal{D}'(H^d) + \mathcal{D}_2(H^d) \\ m_{h_{12}^{dd}}^2 &= (\mathbf{m}_{H^d}^2)_{12} + (\mathbf{Y}_{113}^{SH} \mathbf{Y}_{123}^{SH} + \mathbf{Y}_{213}^{SH} \mathbf{Y}_{223}^{SH}) \frac{v_u^2}{2} + (\mathbf{Y}_{311}^{SH} \mathbf{Y}_{321}^{SH} + \mathbf{Y}_{312}^{SH} \mathbf{Y}_{322}^{SH}) \frac{v_s^2}{2} \\ m_{h_{22}^{dd}}^2 &= (\mathbf{m}_{H^d}^2)_{22} + ((\mathbf{Y}_{123}^{SH})^2 + (\mathbf{Y}_{223}^{SH})^2) \frac{v_u^2}{2} + ((\mathbf{Y}_{321}^{SH})^2 + (\mathbf{Y}_{322}^{SH})^2) \frac{v_s^2}{2} \\ &\quad + \mathcal{D}_Y(H^d) + \mathcal{D}'(H^d) + \mathcal{D}_2(H^d) \\ m_{h_{11}^{uu}}^2 &= (\mathbf{m}_{H^u}^2)_{11} + ((\mathbf{Y}_{131}^{SH})^2 + (\mathbf{Y}_{231}^{SH})^2) \frac{v_d^2}{2} + ((\mathbf{Y}_{311}^{SH})^2 + (\mathbf{Y}_{321}^{SH})^2) \frac{v_s^2}{2} \\ &\quad + \mathcal{D}_Y(H^u) + \mathcal{D}'(H^u) + \mathcal{D}_2(H^u) \\ m_{h_{12}^{uu}}^2 &= (\mathbf{m}_{H^u}^2)_{12} + (\mathbf{Y}_{131}^{SH} \mathbf{Y}_{132}^{SH} + \mathbf{Y}_{231}^{SH} \mathbf{Y}_{232}^{SH}) \frac{v_d^2}{2} + (\mathbf{Y}_{311}^{SH} \mathbf{Y}_{312}^{SH} + \mathbf{Y}_{321}^{SH} \mathbf{Y}_{322}^{SH}) \frac{v_s^2}{2} \\ m_{h_{22}^{uu}}^2 &= (\mathbf{m}_{H^u}^2)_{22} + ((\mathbf{Y}_{132}^{SH})^2 + (\mathbf{Y}_{232}^{SH})^2) \frac{v_d^2}{2} + ((\mathbf{Y}_{312}^{SH})^2 + (\mathbf{Y}_{322}^{SH})^2) \frac{v_s^2}{2} \end{aligned}$$

¹These may be sizable ($\sim 10\%$) for some quantities dependent on the strong coupling constant such as the gluino mass.

$$\begin{aligned}
& + \mathcal{D}_Y(H^u) + \mathcal{D}'(H^u) + \mathcal{D}_2(H^u) \\
m_{h_{11}^{ss}}^2 &= (\mathbf{m}_S^2)_{11} + ((\mathbf{Y}_{113}^{SH})^2 + (\mathbf{Y}_{123}^{SH})^2) \frac{v_u^2}{2} + ((\mathbf{Y}_{131}^{SH})^2 + (\mathbf{Y}_{132}^{SH})^2) \frac{v_d^2}{2} + \mathcal{D}'(S) \\
m_{h_{12}^{ss}}^2 &= (\mathbf{m}_S^2)_{12} + (\mathbf{Y}_{113}^{SH} \mathbf{Y}_{213}^{SH} + \mathbf{Y}_{123}^{SH} \mathbf{Y}_{223}^{SH}) \frac{v_u^2}{2} + (\mathbf{Y}_{131}^{SH} \mathbf{Y}_{231}^{SH} + \mathbf{Y}_{132}^{SH} \mathbf{Y}_{232}^{SH}) \frac{v_d^2}{2} \\
m_{h_{22}^{ss}}^2 &= (\mathbf{m}_S^2)_{22} + ((\mathbf{Y}_{213}^{SH})^2 + (\mathbf{Y}_{223}^{SH})^2) \frac{v_u^2}{2} + ((\mathbf{Y}_{231}^{SH})^2 + (\mathbf{Y}_{232}^{SH})^2) \frac{v_d^2}{2} + \mathcal{D}'(S) \\
m_{h_{11}^{du}}^2 &= -\mathbf{h}_{311}^{SH} \frac{v_s}{\sqrt{2}} + (\mathbf{Y}_{131}^{SH} \mathbf{Y}_{113}^{SH} + \mathbf{Y}_{231}^{SH} \mathbf{Y}_{213}^{SH} + \mathbf{Y}_{311}^{SH} \mathbf{Y}_{333}^{SH}) \frac{v_u v_d}{2} \\
m_{h_{12}^{du}}^2 &= -\mathbf{h}_{312}^{SH} \frac{v_s}{\sqrt{2}} + (\mathbf{Y}_{132}^{SH} \mathbf{Y}_{113}^{SH} + \mathbf{Y}_{232}^{SH} \mathbf{Y}_{213}^{SH} + \mathbf{Y}_{312}^{SH} \mathbf{Y}_{333}^{SH}) \frac{v_u v_d}{2} \\
m_{h_{11}^{ds}}^2 &= -\mathbf{h}_{113}^{SH} \frac{v_u}{\sqrt{2}} + (\mathbf{Y}_{131}^{SH} \mathbf{Y}_{311}^{SH} + \mathbf{Y}_{132}^{SH} \mathbf{Y}_{312}^{SH} + \mathbf{Y}_{113}^{SH} \mathbf{Y}_{333}^{SH}) \frac{v_s v_d}{2} \\
m_{h_{12}^{ds}}^2 &= -\mathbf{h}_{213}^{SH} \frac{v_u}{\sqrt{2}} + (\mathbf{Y}_{231}^{SH} \mathbf{Y}_{311}^{SH} + \mathbf{Y}_{232}^{SH} \mathbf{Y}_{312}^{SH} + \mathbf{Y}_{213}^{SH} \mathbf{Y}_{333}^{SH}) \frac{v_s v_d}{2} \\
m_{h_{21}^{du}}^2 &= -\mathbf{h}_{321}^{SH} \frac{v_s}{\sqrt{2}} + (\mathbf{Y}_{131}^{SH} \mathbf{Y}_{123}^{SH} + \mathbf{Y}_{231}^{SH} \mathbf{Y}_{223}^{SH} + \mathbf{Y}_{321}^{SH} \mathbf{Y}_{333}^{SH}) \frac{v_u v_d}{2} \\
m_{h_{22}^{du}}^2 &= -\mathbf{h}_{322}^{SH} \frac{v_s}{\sqrt{2}} + (\mathbf{Y}_{132}^{SH} \mathbf{Y}_{123}^{SH} + \mathbf{Y}_{232}^{SH} \mathbf{Y}_{223}^{SH} + \mathbf{Y}_{322}^{SH} \mathbf{Y}_{333}^{SH}) \frac{v_u v_d}{2} \\
m_{h_{21}^{ds}}^2 &= -\mathbf{h}_{123}^{SH} \frac{v_u}{\sqrt{2}} + (\mathbf{Y}_{131}^{SH} \mathbf{Y}_{321}^{SH} + \mathbf{Y}_{132}^{SH} \mathbf{Y}_{322}^{SH} + \mathbf{Y}_{123}^{SH} \mathbf{Y}_{333}^{SH}) \frac{v_s v_d}{2} \\
m_{h_{22}^{ds}}^2 &= -\mathbf{h}_{223}^{SH} \frac{v_u}{\sqrt{2}} + (\mathbf{Y}_{231}^{SH} \mathbf{Y}_{321}^{SH} + \mathbf{Y}_{232}^{SH} \mathbf{Y}_{322}^{SH} + \mathbf{Y}_{223}^{SH} \mathbf{Y}_{333}^{SH}) \frac{v_s v_d}{2} \\
m_{h_{11}^{us}}^2 &= -\mathbf{h}_{131}^{SH} \frac{v_d}{\sqrt{2}} + (\mathbf{Y}_{113}^{SH} \mathbf{Y}_{311}^{SH} + \mathbf{Y}_{123}^{SH} \mathbf{Y}_{321}^{SH} + \mathbf{Y}_{131}^{SH} \mathbf{Y}_{333}^{SH}) \frac{v_s v_u}{2} \\
m_{h_{12}^{us}}^2 &= -\mathbf{h}_{231}^{SH} \frac{v_d}{\sqrt{2}} + (\mathbf{Y}_{213}^{SH} \mathbf{Y}_{311}^{SH} + \mathbf{Y}_{223}^{SH} \mathbf{Y}_{321}^{SH} + \mathbf{Y}_{231}^{SH} \mathbf{Y}_{333}^{SH}) \frac{v_s v_u}{2} \\
m_{h_{21}^{us}}^2 &= -\mathbf{h}_{132}^{SH} \frac{v_d}{\sqrt{2}} + (\mathbf{Y}_{113}^{SH} \mathbf{Y}_{312}^{SH} + \mathbf{Y}_{123}^{SH} \mathbf{Y}_{322}^{SH} + \mathbf{Y}_{132}^{SH} \mathbf{Y}_{333}^{SH}) \frac{v_s v_u}{2} \\
m_{h_{22}^{us}}^2 &= -\mathbf{h}_{232}^{SH} \frac{v_d}{\sqrt{2}} + (\mathbf{Y}_{213}^{SH} \mathbf{Y}_{312}^{SH} + \mathbf{Y}_{223}^{SH} \mathbf{Y}_{322}^{SH} + \mathbf{Y}_{232}^{SH} \mathbf{Y}_{333}^{SH}) \frac{v_s v_u}{2}. \tag{B.2}
\end{aligned}$$

Correspondingly, the mass matrix for the CP-odd dark Higgs fields reads:

$$\begin{aligned}
m_{A_{11}^{dd}}^2 &= (\mathbf{m}_{H^d}^2)_{11} + ((\mathbf{Y}_{113}^{SH})^2 + (\mathbf{Y}_{213}^{SH})^2) \frac{v_u^2}{2} + ((\mathbf{Y}_{311}^{SH})^2 + (\mathbf{Y}_{312}^{SH})^2) \frac{v_s^2}{2} \\
& + \mathcal{D}_Y(H^d) + \mathcal{D}'(H^d) + \mathcal{D}_2(H^d) \\
m_{A_{12}^{dd}}^2 &= (\mathbf{m}_{H^d}^2)_{12} + (\mathbf{Y}_{113}^{SH} \mathbf{Y}_{123}^{SH} + \mathbf{Y}_{213}^{SH} \mathbf{Y}_{223}^{SH}) \frac{v_u^2}{2} + (\mathbf{Y}_{311}^{SH} \mathbf{Y}_{321}^{SH} + \mathbf{Y}_{312}^{SH} \mathbf{Y}_{322}^{SH}) \frac{v_s^2}{2} \\
m_{A_{22}^{dd}}^2 &= (\mathbf{m}_{H^d}^2)_{22} + ((\mathbf{Y}_{123}^{SH})^2 + (\mathbf{Y}_{223}^{SH})^2) \frac{v_u^2}{2} + ((\mathbf{Y}_{321}^{SH})^2 + (\mathbf{Y}_{322}^{SH})^2) \frac{v_s^2}{2} \\
& + \mathcal{D}_Y(H^d) + \mathcal{D}'(H^d) + \mathcal{D}_2(H^d) \\
m_{A_{11}^{uu}}^2 &= (\mathbf{m}_{H^u}^2)_{11} + ((\mathbf{Y}_{131}^{SH})^2 + (\mathbf{Y}_{231}^{SH})^2) \frac{v_d^2}{2} + ((\mathbf{Y}_{311}^{SH})^2 + (\mathbf{Y}_{321}^{SH})^2) \frac{v_s^2}{2} \\
& + \mathcal{D}_Y(H^u) + \mathcal{D}'(H^u) + \mathcal{D}_2(H^u)
\end{aligned}$$

$$\begin{aligned}
m_{A_{12}^{uu}}^2 &= (\mathbf{m}_{H^u}^2)_{12} + (\mathbf{Y}_{131}^{SH}\mathbf{Y}_{132}^{SH} + \mathbf{Y}_{231}^{SH}\mathbf{Y}_{232}^{SH}) \frac{v_d^2}{2} + (\mathbf{Y}_{311}^{SH}\mathbf{Y}_{312}^{SH} + \mathbf{Y}_{321}^{SH}\mathbf{Y}_{322}^{SH}) \frac{v_s^2}{2} \\
m_{A_{22}^{uu}}^2 &= (\mathbf{m}_{H^u}^2)_{22} + ((\mathbf{Y}_{132}^{SH})^2 + (\mathbf{Y}_{232}^{SH})^2) \frac{v_d^2}{2} + ((\mathbf{Y}_{312}^{SH})^2 + (\mathbf{Y}_{322}^{SH})^2) \frac{v_s^2}{2} \\
&\quad + \mathcal{D}_Y(H^u) + \mathcal{D}'(H^u) + \mathcal{D}_2(H^u) \\
m_{A_{11}^{ss}}^2 &= (\mathbf{m}_S^2)_{11} + ((\mathbf{Y}_{113}^{SH})^2 + (\mathbf{Y}_{123}^{SH})^2) \frac{v_u^2}{2} + ((\mathbf{Y}_{131}^{SH})^2 + (\mathbf{Y}_{132}^{SH})^2) \frac{v_d^2}{2} + \mathcal{D}'(S) \\
m_{h_{12}^{ss}}^2 &= (\mathbf{m}_S^2)_{12} + (\mathbf{Y}_{113}^{SH}\mathbf{Y}_{213}^{SH} + \mathbf{Y}_{123}^{SH}\mathbf{Y}_{223}^{SH}) \frac{v_u^2}{2} + (\mathbf{Y}_{131}^{SH}\mathbf{Y}_{231}^{SH} + \mathbf{Y}_{132}^{SH}\mathbf{Y}_{232}^{SH}) \frac{v_d^2}{2} \\
m_{A_{22}^{ss}}^2 &= (\mathbf{m}_S^2)_{22} + ((\mathbf{Y}_{213}^{SH})^2 + (\mathbf{Y}_{223}^{SH})^2) \frac{v_u^2}{2} + ((\mathbf{Y}_{231}^{SH})^2 + (\mathbf{Y}_{232}^{SH})^2) \frac{v_d^2}{2} + \mathcal{D}'(S) \\
m_{A_{11}^{du}}^2 &= \mathbf{h}_{311}^{SH} \frac{v_s}{\sqrt{2}} + (\mathbf{Y}_{131}^{SH}\mathbf{Y}_{113}^{SH} + \mathbf{Y}_{231}^{SH}\mathbf{Y}_{213}^{SH} - \mathbf{Y}_{311}^{SH}\mathbf{Y}_{333}^{SH}) \frac{v_u v_d}{2} \\
m_{A_{12}^{du}}^2 &= \mathbf{h}_{312}^{SH} \frac{v_s}{\sqrt{2}} + (\mathbf{Y}_{132}^{SH}\mathbf{Y}_{113}^{SH} + \mathbf{Y}_{232}^{SH}\mathbf{Y}_{213}^{SH} - \mathbf{Y}_{312}^{SH}\mathbf{Y}_{333}^{SH}) \frac{v_u v_d}{2} \\
m_{A_{11}^{ds}}^2 &= \mathbf{h}_{113}^{SH} \frac{v_u}{\sqrt{2}} + (\mathbf{Y}_{131}^{SH}\mathbf{Y}_{311}^{SH} + \mathbf{Y}_{132}^{SH}\mathbf{Y}_{312}^{SH} - \mathbf{Y}_{113}^{SH}\mathbf{Y}_{333}^{SH}) \frac{v_s v_d}{2} \\
m_{A_{12}^{ds}}^2 &= \mathbf{h}_{213}^{SH} \frac{v_u}{\sqrt{2}} + (\mathbf{Y}_{231}^{SH}\mathbf{Y}_{311}^{SH} + \mathbf{Y}_{232}^{SH}\mathbf{Y}_{312}^{SH} - \mathbf{Y}_{213}^{SH}\mathbf{Y}_{333}^{SH}) \frac{v_s v_d}{2} \\
m_{A_{21}^{du}}^2 &= \mathbf{h}_{321}^{SH} \frac{v_s}{\sqrt{2}} + (\mathbf{Y}_{131}^{SH}\mathbf{Y}_{123}^{SH} + \mathbf{Y}_{231}^{SH}\mathbf{Y}_{223}^{SH} - \mathbf{Y}_{321}^{SH}\mathbf{Y}_{333}^{SH}) \frac{v_u v_d}{2} \\
m_{A_{22}^{du}}^2 &= \mathbf{h}_{322}^{SH} \frac{v_s}{\sqrt{2}} + (\mathbf{Y}_{132}^{SH}\mathbf{Y}_{123}^{SH} + \mathbf{Y}_{232}^{SH}\mathbf{Y}_{223}^{SH} - \mathbf{Y}_{322}^{SH}\mathbf{Y}_{333}^{SH}) \frac{v_u v_d}{2} \\
m_{A_{21}^{ds}}^2 &= \mathbf{h}_{123}^{SH} \frac{v_u}{\sqrt{2}} + (\mathbf{Y}_{131}^{SH}\mathbf{Y}_{321}^{SH} + \mathbf{Y}_{132}^{SH}\mathbf{Y}_{322}^{SH} - \mathbf{Y}_{123}^{SH}\mathbf{Y}_{333}^{SH}) \frac{v_s v_d}{2} \\
m_{A_{22}^{ds}}^2 &= \mathbf{h}_{223}^{SH} \frac{v_u}{\sqrt{2}} + (\mathbf{Y}_{231}^{SH}\mathbf{Y}_{321}^{SH} + \mathbf{Y}_{232}^{SH}\mathbf{Y}_{322}^{SH} - \mathbf{Y}_{223}^{SH}\mathbf{Y}_{333}^{SH}) \frac{v_s v_d}{2} \\
m_{A_{11}^{us}}^2 &= \mathbf{h}_{131}^{SH} \frac{v_d}{\sqrt{2}} + (\mathbf{Y}_{113}^{SH}\mathbf{Y}_{311}^{SH} + \mathbf{Y}_{123}^{SH}\mathbf{Y}_{321}^{SH} - \mathbf{Y}_{131}^{SH}\mathbf{Y}_{333}^{SH}) \frac{v_s v_u}{2} \\
m_{A_{12}^{us}}^2 &= \mathbf{h}_{231}^{SH} \frac{v_d}{\sqrt{2}} + (\mathbf{Y}_{213}^{SH}\mathbf{Y}_{311}^{SH} + \mathbf{Y}_{223}^{SH}\mathbf{Y}_{321}^{SH} - \mathbf{Y}_{231}^{SH}\mathbf{Y}_{333}^{SH}) \frac{v_s v_u}{2} \\
m_{A_{21}^{us}}^2 &= \mathbf{h}_{132}^{SH} \frac{v_d}{\sqrt{2}} + (\mathbf{Y}_{113}^{SH}\mathbf{Y}_{312}^{SH} + \mathbf{Y}_{123}^{SH}\mathbf{Y}_{322}^{SH} - \mathbf{Y}_{132}^{SH}\mathbf{Y}_{333}^{SH}) \frac{v_s v_u}{2} \\
m_{A_{22}^{us}}^2 &= \mathbf{h}_{232}^{SH} \frac{v_d}{\sqrt{2}} + (\mathbf{Y}_{213}^{SH}\mathbf{Y}_{312}^{SH} + \mathbf{Y}_{223}^{SH}\mathbf{Y}_{322}^{SH} - \mathbf{Y}_{232}^{SH}\mathbf{Y}_{333}^{SH}) \frac{v_s v_u}{2} \tag{B.3}
\end{aligned}$$

The entries of the charged dark Higgs mass matrix read in the basis $(H_1^{d-}, H_2^{d-}, H_1^{u+\star}, H_2^{u+\star})$:

$$\begin{aligned}
m_{h_{11}^\pm}^2 &= (\mathbf{m}_{H^d}^2)_{11} + ((\mathbf{Y}_{311}^{SH})^2 + (\mathbf{Y}_{312}^{SH})^2) \frac{v_s^2}{2} \\
&\quad + \mathcal{D}_Y(H^d) + \mathcal{D}'(H^d) + \mathcal{D}_2(H^d) \\
m_{h_{12}^\pm}^2 &= (\mathbf{m}_{H^d}^2)_{12} + (\mathbf{Y}_{311}^{SH}\mathbf{Y}_{321}^{SH} + \mathbf{Y}_{312}^{SH}\mathbf{Y}_{322}^{SH}) \frac{v_s^2}{2} \\
m_{h_{22}^\pm}^2 &= (\mathbf{m}_{H^d}^2)_{22} + ((\mathbf{Y}_{321}^{SH})^2 + (\mathbf{Y}_{322}^{SH})^2) \frac{v_s^2}{2}
\end{aligned}$$

$$\begin{aligned}
& + \mathcal{D}_Y(H^d) + \mathcal{D}'(H^d) + \mathcal{D}_2(H^d) \\
m_{h_{33}}^2 &= (\mathbf{m}_{H^u}^2)_{11} + ((\mathbf{Y}_{311}^{SH})^2 + (\mathbf{Y}_{321}^{SH})^2) \frac{v_s^2}{2} \\
& + \mathcal{D}_Y(H^u) + \mathcal{D}'(H^u) + \mathcal{D}_2(H^u) \\
m_{h_{34}}^2 &= (\mathbf{m}_{H^u}^2)_{12} + (\mathbf{Y}_{311}^{SH} \mathbf{Y}_{312}^{SH} + \mathbf{Y}_{321}^{SH} \mathbf{Y}_{322}^{SH}) \frac{v_s^2}{2} \\
m_{h_{44}}^2 &= (\mathbf{m}_{H^u}^2)_{22} + ((\mathbf{Y}_{312}^{SH})^2 + (\mathbf{Y}_{322}^{SH})^2) \frac{v_s^2}{2} \\
& + \mathcal{D}_Y(H^u) + \mathcal{D}'(H^u) + \mathcal{D}_2(H^u) \\
m_{h_{13}}^2 &= \mathbf{h}_{311}^{SH} \frac{v_s}{\sqrt{2}} - \mathbf{Y}_{311}^{SH} \mathbf{Y}_{333}^{SH} \frac{v_u v_d}{2} \\
m_{h_{14}}^2 &= \mathbf{h}_{312}^{SH} \frac{v_s}{\sqrt{2}} - \mathbf{Y}_{312}^{SH} \mathbf{Y}_{333}^{SH} \frac{v_u v_d}{2} \\
m_{h_{23}}^2 &= \mathbf{h}_{321}^{SH} \frac{v_s}{\sqrt{2}} - \mathbf{Y}_{321}^{SH} \mathbf{Y}_{333}^{SH} \frac{v_u v_d}{2} \\
m_{h_{24}}^2 &= \mathbf{h}_{322}^{SH} \frac{v_s}{\sqrt{2}} - \mathbf{Y}_{322}^{SH} \mathbf{Y}_{333}^{SH} \frac{v_u v_d}{2}. \tag{B.4}
\end{aligned}$$

The dark Higgs mass matrices are due to their rank in general not analytically diagonalizable. However, if one assumes the Yukawa and SSB couplings to be diagonal in the generations of the dark Higgs fields, (B.2)-(B.4) become block-diagonal.

B.3 Performance of the Random Walk

We give the result of the random walk through the test-landscape (3.27) in form of the projections on each of the five dimensions in figure B.2. In this way the comparison to the results obtained with the Vegas algorithm [70] is straightforward. Their corresponding results can be found at <http://omnibus.uni-freiburg.de/~ob76/adScan/>. The plots shown in figure B.2 confirm, that our algorithm not only finds all the maxima, but – as a matter of fact – investigates them more thoroughly than the Vegas algorithm and discovers higher peaks.

B.4 Complete TeV-Scale Spectrum Information

The complete information on a TeV-scale spectrum is outputted by EXSPECT in terms of a SINDARIN file, ready to be used by the event generator WHIZARD. In the following we give the SINDARIN files corresponding to the three scenarios presented in chapter 4.

B.4.1 Scenario A: EXSPECT Output

```

## goodness = 1
alpha = 0.00787402
MZ = 91.182
WZ = 2.495
## alpha at MZ
## Mass of Z (pole mass)
## Width of Z

```

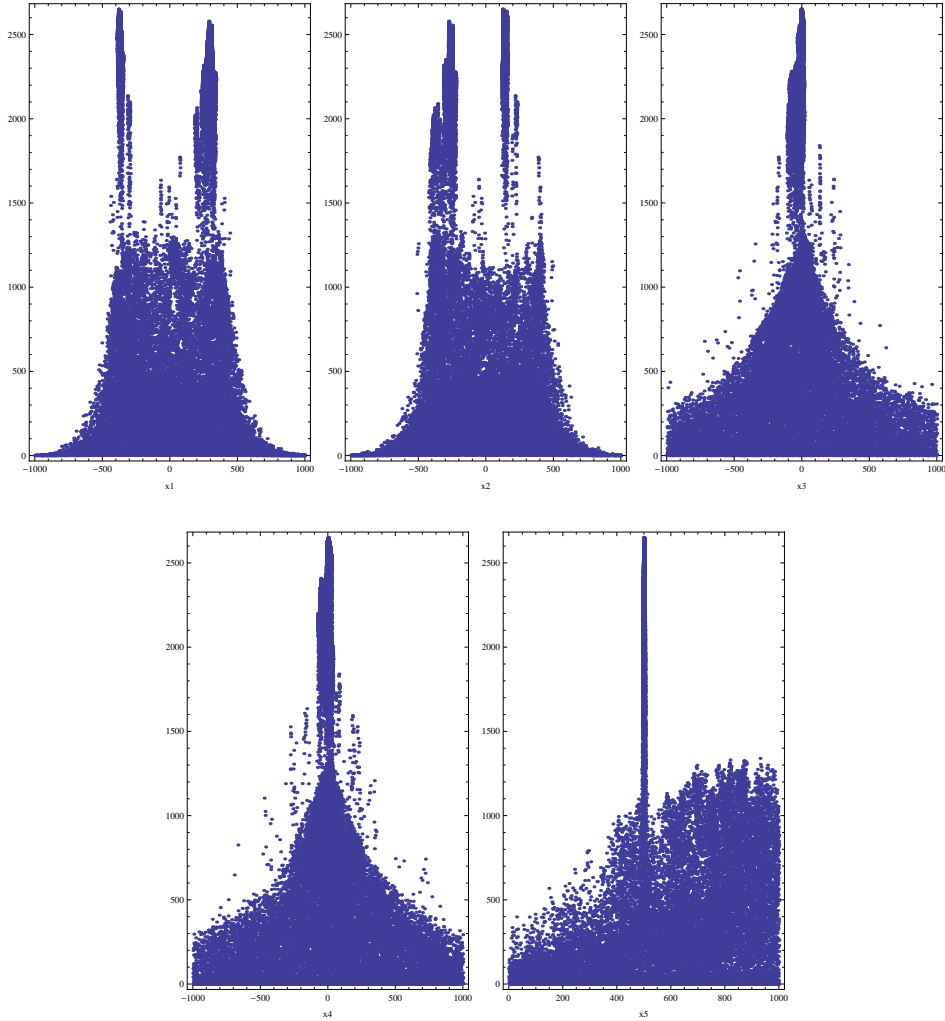


Figure B.2: The results from the test run of the random walk used by EXSPECT. The test function from (3.27) was evaluated at 40000 points. Here we show the projections on each coordinate.

```

MW = 80.4
WW = 2.085
alpha_s = 1.118
MZp = 2483.69
QXe = -0.191852
QXL = -0.29898
QXu = -0.13537
QXd = -0.327221
QXQ = -0.163611
QXHd = 0.490832
QXHd = 0.29898
QXlq = 0.462591
QXlqc = 0.327221
QXS = -0.789812
QYe = 0.774597
QYL = -0.387298

## Mass of W (pole mass)
## Width of W
## alpha_s at MZ
## Mass of Z' (pole mass)
## U(1)' charge of e^c (GUT norm)
## U(1)' charge of L (GUT norm)
## U(1)' charge of u^c (GUT norm)
## U(1)' charge of d^c (GUT norm)
## U(1)' charge of Q (GUT norm)
## U(1)' charge of H^d (GUT norm)
## U(1)' charge of H^u (GUT norm)
## U(1)' charge of D (GUT norm)
## U(1)' charge of D^c (GUT norm)
## U(1)' charge of S (GUT norm)
## U(1)_Y charge of e^c (GUT norm)
## U(1)_Y charge of L (GUT norm)

```



```

QYu = -0.516398      ## U(1)_Y charge of u^c (GUT norm)
QYd = 0.258199      ## U(1)_Y charge of d^c (GUT norm)
QYQ = 0.129099      ## U(1)_Y charge of Q (GUT norm)
QYHd = -0.387298    ## U(1)_Y charge of H^d (GUT norm)
QYHu = 0.387298     ## U(1)_Y charge of H^u (GUT norm)
QYlq = 0.258199     ## U(1)_Y charge of D (GUT norm)
QYlqc = -0.258199  ## U(1)_Y charge of D^c (GUT norm)
QYS = 0              ## U(1)_Y charge of S (GUT norm)
MUEff = 898.368     ## effective mu parameter
tanbe = 40.3326     ## tan beta = vu/vd
YSH = 0.181498     ## Y^SH_{333}
ASH = 6.71248      ## h^SH_{333}
YS11 = 0.389487    ## Y^SH_{311}
YS12 = 0           ## Y^SH_{312}
YS21 = 0           ## Y^SH_{321}
YS22 = 0.389487    ## Y^SH_{322}
YHd11 = 0.314827   ## Y^SH_{131}
YHd12 = 0          ## Y^SH_{132}
YHd21 = 0          ## Y^SH_{231}
YHd22 = 0.314827   ## Y^SH_{232}
YHu11 = 0.315669   ## Y^SH_{113}
YHu12 = 0          ## Y^SH_{123}
YHu21 = 0          ## Y^SH_{213}
YHu22 = 0.315669   ## Y^SH_{223}
YD11 = 0.501101    ## Lepto-Quark coupling: d^c Q L
YDc1 = 0.445648    ## Lepto-Quark coupling: e^c u^c d^c
YD12 = 0.501101    ## Lepto-Quark coupling: d^c Q L
YDc2 = 0.445648    ## Lepto-Quark coupling: e^c u^c d^c
YD13 = 0.42581     ## Lepto-Quark coupling: d^c Q L
YDc3 = 0.377555    ## Lepto-Quark coupling: e^c u^c d^c
AS11 = -40.2843    ## h^SH_{311}
AS12 = 0           ## h^SH_{312}
AS21 = 0           ## h^SH_{321}
AS22 = -40.2843    ## h^SH_{322}
AHd11 = 301.652    ## h^SH_{131}
AHd12 = 0          ## h^SH_{132}
AHd21 = 0          ## h^SH_{231}
AHd22 = 301.652    ## h^SH_{232}
AHu11 = 307.534    ## h^SH_{113}
AHu12 = 0          ## h^SH_{123}
AHu21 = 0          ## h^SH_{213}
AHu22 = 307.534    ## h^SH_{223}
Ad1 = 0            ## Trilinear SSB (MSSM-like)
Au1 = 0            ## Trilinear SSB (MSSM-like)
Ae1 = 0            ## Trilinear SSB (MSSM-like)
AD11 = 2105.95     ## Trilinear SSB slepton-squark
ADc1 = -461.271    ## Trilinear SSB slepton-squark
ASD1 = 431.325     ## Trilinear SSB Leptoquark-singlet
Ad2 = 0            ## Trilinear SSB (MSSM-like)
Au2 = 0            ## Trilinear SSB (MSSM-like)
Ae2 = 0            ## Trilinear SSB (MSSM-like)
AD12 = 2105.95     ## Trilinear SSB slepton-squark
ADc2 = -461.271    ## Trilinear SSB slepton-squark
ASD2 = 431.325     ## Trilinear SSB Leptoquark-singlet
Ad3 = -279.2       ## Trilinear SSB (MSSM-like)
Au3 = -363.186     ## Trilinear SSB (MSSM-like)
Ae3 = 0            ## Trilinear SSB (MSSM-like)
AD13 = 2060.13     ## Trilinear SSB slepton-squark
ADc3 = -216.309    ## Trilinear SSB slepton-squark
ASD3 = 424.603     ## Trilinear SSB Leptoquark-singlet
RZZpri1 = 1        ## ZZ' mixing
RZZpri12 = 0.000430095 ## ZZ' mixing
RZZpri21 = -0.000430095 ## ZZ' mixing
RZZpri22 = 1        ## ZZ' mixing

```

```
RNN11 = -0.00541558      ## neutralino mixing
RNN12 = 0.992319        ## neutralino mixing
RNN13 = 0.0422084       ## neutralino mixing
RNN14 = 0.116152        ## neutralino mixing
RNN15 = 0.000204327     ## neutralino mixing
RNN16 = 0.000257652     ## neutralino mixing
RNN21 = 0.998537        ## neutralino mixing
RNN22 = 0.0118703       ## neutralino mixing
RNN23 = -0.0275143      ## neutralino mixing
RNN24 = -0.0448571      ## neutralino mixing
RNN25 = -0.0025888      ## neutralino mixing
RNN26 = 0.00264803      ## neutralino mixing
RNN31 = -0.000347499    ## neutralino mixing
RNN32 = 0.00131971      ## neutralino mixing
RNN33 = -0.00668468     ## neutralino mixing
RNN34 = -0.0060429      ## neutralino mixing
RNN35 = -0.691286       ## neutralino mixing
RNN36 = -0.722524       ## neutralino mixing
RNN41 = 0.0521267       ## neutralino mixing
RNN42 = -0.111458       ## neutralino mixing
RNN43 = 0.704868        ## neutralino mixing
RNN44 = 0.698526        ## neutralino mixing
RNN45 = -0.00658434     ## neutralino mixing
RNN46 = -0.0062925      ## neutralino mixing
RNN51 = -0.0127433      ## neutralino mixing
RNN52 = 0.0523132      ## neutralino mixing
RNN53 = 0.707482        ## neutralino mixing
RNN54 = -0.704607       ## neutralino mixing
RNN55 = 0.00693536      ## neutralino mixing
RNN56 = -0.0071863      ## neutralino mixing
RNN61 = -0.00384422     ## neutralino mixing
RNN62 = 0.000493301     ## neutralino mixing
RNN63 = 0.00687382      ## neutralino mixing
RNN64 = -0.00715392     ## neutralino mixing
RNN65 = -0.722514       ## neutralino mixing
RNN66 = 0.691275        ## neutralino mixing
RUU11 = -0.98744        ## chargino mixing
RUU12 = -0.157996       ## chargino mixing
RUU21 = 0.157996        ## chargino mixing
RUU22 = -0.98744        ## chargino mixing
RVV11 = -0.997243       ## chargino mixing
RVV12 = -0.0742044     ## chargino mixing
RVV21 = 0.0742044       ## chargino mixing
RVV22 = -0.997243       ## chargino mixing
RdNN11 = -0.000702664   ## dark neutralino mixing
RdNN12 = 0               ## dark neutralino mixing
RdNN13 = 0               ## dark neutralino mixing
RdNN14 = -0.707114      ## dark neutralino mixing
RdNN15 = -0.7071        ## dark neutralino mixing
RdNN16 = 0               ## dark neutralino mixing
RdNN21 = -0.0284621     ## dark neutralino mixing
RdNN22 = 0               ## dark neutralino mixing
RdNN23 = 0               ## dark neutralino mixing
RdNN24 = 0.706827       ## dark neutralino mixing
RdNN25 = -0.706813      ## dark neutralino mixing
RdNN26 = 0               ## dark neutralino mixing
RdNN31 = 0.999595       ## dark neutralino mixing
RdNN32 = 0               ## dark neutralino mixing
RdNN33 = 0               ## dark neutralino mixing
RdNN34 = 0.0196289      ## dark neutralino mixing
RdNN35 = -0.0206226     ## dark neutralino mixing
RdNN36 = 0               ## dark neutralino mixing
RdNN41 = 0               ## dark neutralino mixing
RdNN42 = -0.000702664   ## dark neutralino mixing
```

```
RdNN43 = -0.707114      ## dark neutralino mixing
RdNN44 = 0              ## dark neutralino mixing
RdNN45 = 0              ## dark neutralino mixing
RdNN46 = -0.7071       ## dark neutralino mixing
RdNN51 = 0              ## dark neutralino mixing
RdNN52 = -0.0284621    ## dark neutralino mixing
RdNN53 = 0.706827     ## dark neutralino mixing
RdNN54 = 0              ## dark neutralino mixing
RdNN55 = 0              ## dark neutralino mixing
RdNN56 = -0.706813    ## dark neutralino mixing
RdNN61 = 0              ## dark neutralino mixing
RdNN62 = 0.999595     ## dark neutralino mixing
RdNN63 = 0.0196289    ## dark neutralino mixing
RdNN64 = 0              ## dark neutralino mixing
RdNN65 = 0              ## dark neutralino mixing
RdNN66 = -0.0206226   ## dark neutralino mixing
RdUU11 = 1             ## dark chargino mixing
RdUU12 = 0             ## dark chargino mixing
RdUU21 = 0             ## dark chargino mixing
RdUU22 = 1             ## dark chargino mixing
RdVV11 = 1             ## dark chargino mixing
RdVV12 = 0             ## dark chargino mixing
RdVV21 = 0             ## dark chargino mixing
RdVV22 = 1             ## dark chargino mixing
Rse11 = 0              ## slepton mixing
Rse12 = 1              ## slepton mixing
Rse21 = 1              ## slepton mixing
Rse22 = 0              ## slepton mixing
Rsmu11 = 0             ## slepton mixing
Rsmu12 = 1             ## slepton mixing
Rsmu21 = 1             ## slepton mixing
Rsmu22 = 0             ## slepton mixing
Rstau11 = 0            ## slepton mixing
Rstau12 = 1            ## slepton mixing
Rstau21 = 1            ## slepton mixing
Rstau22 = 0            ## slepton mixing
Rsu11 = 0              ## squark mixing
Rsu12 = 1              ## squark mixing
Rsu21 = 1              ## squark mixing
Rsu22 = 0              ## squark mixing
Rsc11 = 0              ## squark mixing
Rsc12 = 1              ## squark mixing
Rsc21 = 1              ## squark mixing
Rsc22 = 0              ## squark mixing
Rst11 = 0.103018      ## squark mixing
Rst12 = 0.994679     ## squark mixing
Rst21 = 0.994679     ## squark mixing
Rst22 = -0.103018    ## squark mixing
Rsd11 = 0              ## squark mixing
Rsd12 = 1              ## squark mixing
Rsd21 = 1              ## squark mixing
Rsd22 = 0              ## squark mixing
Rss11 = 0              ## squark mixing
Rss12 = 1              ## squark mixing
Rss21 = 1              ## squark mixing
Rss22 = 0              ## squark mixing
Rsb11 = 0.131646     ## squark mixing
Rsb12 = 0.991297     ## squark mixing
Rsb21 = 0.991297     ## squark mixing
Rsb22 = -0.131646    ## squark mixing
Rlq111 = -0.681964   ## leptoquark mixing
Rlq112 = 0.731386    ## leptoquark mixing
Rlq121 = 0.731386    ## leptoquark mixing
Rlq122 = 0.681964    ## leptoquark mixing
```

```
Rlq211 = -0.681964      ## leptoquark mixing
Rlq212 = 0.731386      ## leptoquark mixing
Rlq221 = 0.731386      ## leptoquark mixing
Rlq222 = 0.681964      ## leptoquark mixing
Rlq311 = -0.691364     ## leptoquark mixing
Rlq312 = 0.722507     ## leptoquark mixing
Rlq321 = 0.722507     ## leptoquark mixing
Rlq322 = 0.691364     ## leptoquark mixing
hOmix11 = -0.0265712   ## CP-even higgs mixing
hOmix12 = 0.999647     ## CP-even higgs mixing
hOmix13 = -0.000350561 ## CP-even higgs mixing
hOmix21 = -0.999639    ## CP-even higgs mixing
hOmix22 = -0.0265724   ## CP-even higgs mixing
hOmix23 = -0.00400719  ## CP-even higgs mixing
hOmix31 = -0.00401509  ## CP-even higgs mixing
hOmix32 = 0.000243958  ## CP-even higgs mixing
hOmix33 = 0.999992     ## CP-even higgs mixing
AOmix11 = 0            ## CP-odd higgs mixing
AOmix12 = 0.0248015    ## CP-odd higgs mixing
AOmix13 = 0.999692     ## CP-odd higgs mixing
AOmix21 = -0.0351105   ## CP-odd higgs mixing
AOmix22 = -0.999076    ## CP-odd higgs mixing
AOmix23 = 0.0247862    ## CP-odd higgs mixing
AOmix31 = 0.999383     ## CP-odd higgs mixing
AOmix32 = -0.0350997   ## CP-odd higgs mixing
AOmix33 = 0.000870793  ## CP-odd higgs mixing
dhOmix11 = 0.0344528   ## CP-even dark higgs mixing
dhOmix12 = -5.25236e-08 ## CP-even dark higgs mixing
dhOmix13 = 0.996501    ## CP-even dark higgs mixing
dhOmix14 = -1.22129e-16 ## CP-even dark higgs mixing
dhOmix15 = -1.26894e-17 ## CP-even dark higgs mixing
dhOmix16 = -0.0761502  ## CP-even dark higgs mixing
dhOmix21 = 5.25236e-08  ## CP-even dark higgs mixing
dhOmix22 = 0.0344528   ## CP-even dark higgs mixing
dhOmix23 = -2.11049e-16 ## CP-even dark higgs mixing
dhOmix24 = -0.996501    ## CP-even dark higgs mixing
dhOmix25 = -0.0761502  ## CP-even dark higgs mixing
dhOmix26 = -7.99891e-16 ## CP-even dark higgs mixing
dhOmix31 = -0.0379516  ## CP-even dark higgs mixing
dhOmix32 = 5.78576e-08  ## CP-even dark higgs mixing
dhOmix33 = -0.074836   ## CP-even dark higgs mixing
dhOmix34 = 5.63246e-16  ## CP-even dark higgs mixing
dhOmix35 = 6.91009e-17  ## CP-even dark higgs mixing
dhOmix36 = -0.996473   ## CP-even dark higgs mixing
dhOmix41 = -5.78576e-08 ## CP-even dark higgs mixing
dhOmix42 = -0.0379516  ## CP-even dark higgs mixing
dhOmix43 = -1.53383e-17 ## CP-even dark higgs mixing
dhOmix44 = 0.074836    ## CP-even dark higgs mixing
dhOmix45 = -0.996473   ## CP-even dark higgs mixing
dhOmix46 = -3.01335e-17 ## CP-even dark higgs mixing
dhOmix51 = 0.998685    ## CP-even dark higgs mixing
dhOmix52 = -1.5225e-06  ## CP-even dark higgs mixing
dhOmix53 = -0.0372213  ## CP-even dark higgs mixing
dhOmix54 = 8.55979e-16 ## CP-even dark higgs mixing
dhOmix55 = 2.18467e-16 ## CP-even dark higgs mixing
dhOmix56 = -0.0352405  ## CP-even dark higgs mixing
dhOmix61 = 1.5225e-06   ## CP-even dark higgs mixing
dhOmix62 = 0.998685    ## CP-even dark higgs mixing
dhOmix63 = 3.83457e-18 ## CP-even dark higgs mixing
dhOmix64 = 0.0372213  ## CP-even dark higgs mixing
dhOmix65 = -0.0352405  ## CP-even dark higgs mixing
dhOmix66 = 7.53338e-18 ## CP-even dark higgs mixing
dAOmix11 = -0.00044217 ## CP-odd dark higgs mixing
dAOmix12 = 0.0350028   ## CP-odd dark higgs mixing
```

```

dAOmix13 = 1.25137e-16      ## CP-odd dark higgs mixing
dAOmix14 = 0.996441        ## CP-odd dark higgs mixing
dAOmix15 = -0.076676       ## CP-odd dark higgs mixing
dAOmix16 = 1.76894e-17     ## CP-odd dark higgs mixing
dAOmix21 = -0.0350028      ## CP-odd dark higgs mixing
dAOmix22 = -0.00044217     ## CP-odd dark higgs mixing
dAOmix23 = -0.996441      ## CP-odd dark higgs mixing
dAOmix24 = 1.63588e-16     ## CP-odd dark higgs mixing
dAOmix25 = 5.55639e-16     ## CP-odd dark higgs mixing
dAOmix26 = -0.076676       ## CP-odd dark higgs mixing
dAOmix31 = -0.000194149    ## CP-odd dark higgs mixing
dAOmix32 = 0.0153691      ## CP-odd dark higgs mixing
dAOmix33 = 4.33497e-16     ## CP-odd dark higgs mixing
dAOmix34 = 0.0761772      ## CP-odd dark higgs mixing
dAOmix35 = 0.996976       ## CP-odd dark higgs mixing
dAOmix36 = 5.36076e-17     ## CP-odd dark higgs mixing
dAOmix41 = -0.0153691     ## CP-odd dark higgs mixing
dAOmix42 = -0.000194149    ## CP-odd dark higgs mixing
dAOmix43 = -0.0761772     ## CP-odd dark higgs mixing
dAOmix44 = -9.75627e-18   ## CP-odd dark higgs mixing
dAOmix45 = -1.90088e-17   ## CP-odd dark higgs mixing
dAOmix46 = 0.996976       ## CP-odd dark higgs mixing
dAOmix51 = 0.0126222      ## CP-odd dark higgs mixing
dAOmix52 = -0.999189      ## CP-odd dark higgs mixing
dAOmix53 = -1.57483e-16   ## CP-odd dark higgs mixing
dAOmix54 = 0.0360783      ## CP-odd dark higgs mixing
dAOmix55 = 0.012649       ## CP-odd dark higgs mixing
dAOmix56 = -3.61375e-18   ## CP-odd dark higgs mixing
dAOmix61 = 0.999189       ## CP-odd dark higgs mixing
dAOmix62 = 0.0126222      ## CP-odd dark higgs mixing
dAOmix63 = -0.0360783     ## CP-odd dark higgs mixing
dAOmix64 = 2.68297e-18    ## CP-odd dark higgs mixing
dAOmix65 = 5.22743e-18    ## CP-odd dark higgs mixing
dAOmix66 = 0.012649       ## CP-odd dark higgs mixing
dcHmix11 = 0.997009       ## charged dark higgs mixing
dcHmix12 = 0               ## charged dark higgs mixing
dcHmix13 = -0.0772884     ## charged dark higgs mixing
dcHmix14 = 0               ## charged dark higgs mixing
dcHmix21 = 0.0772884     ## charged dark higgs mixing
dcHmix22 = 0               ## charged dark higgs mixing
dcHmix23 = 0.997009       ## charged dark higgs mixing
dcHmix24 = 0               ## charged dark higgs mixing
dcHmix31 = 0               ## charged dark higgs mixing
dcHmix32 = 0.997009       ## charged dark higgs mixing
dcHmix33 = 0               ## charged dark higgs mixing
dcHmix34 = -0.0772884     ## charged dark higgs mixing
dcHmix41 = 0               ## charged dark higgs mixing
dcHmix42 = 0.0772884     ## charged dark higgs mixing
dcHmix43 = 0               ## charged dark higgs mixing
dcHmix44 = 0.997009       ## charged dark higgs mixing
Me1 = 0                    ## fermion masses
Mu1 = 0                    ## fermion masses
Md1 = 0                    ## fermion masses
Mnue = 0                   ## fermion masses
Mnum = 0                   ## fermion masses
Mnut = 0                   ## fermion masses
Mlqino1 = 3224.92         ## fermionic leptoquark masses
Me2 = 0                    ## fermion masses
Mu2 = 0                    ## fermion masses
Md2 = 0                    ## fermion masses
Mnue = 0                   ## fermion masses
Mnum = 0                   ## fermion masses
Mnut = 0                   ## fermion masses
Mlqino2 = 3224.92         ## fermionic leptoquark masses

```

```
Me3 = 1.777          ## fermion masses
Mu3 = 172.9         ## fermion masses
Md3 = 4.19          ## fermion masses
Mnue = 0            ## fermion masses
Mnum = 0            ## fermion masses
Mnut = 0            ## fermion masses
Mlqino3 = 3251.11   ## fermionic leptoquark masses
Mneu1 = 200.881     ## neutralino masses
Mneu2 = 404.198     ## neutralino masses
Mneu3 = -901.859    ## neutralino masses
Mneu4 = 906.9       ## neutralino masses
Mneu5 = -2376.41    ## neutralino masses
Mneu6 = 2596.03     ## neutralino masses
Mch1 = 404.185      ## chargino masses
Mch2 = 907.498      ## chargino masses
Mglu = -820.19      ## gluino mass
Mdneu1 = 0.0772367  ## dark neutralino masses
Mdneu2 = 0.0772367  ## dark neutralino masses
Mdneu3 = 1928.6     ## dark neutralino masses
Mdneu4 = 1928.6     ## dark neutralino masses
Mdneu5 = -1928.68   ## dark neutralino masses
Mdneu6 = -1928.68   ## dark neutralino masses
Mdchar1 = 1927.86   ## dark chargino masses
Mdchar2 = 1927.86   ## dark chargino masses
Msn1 = 1587.82      ## sparticle masses
Msn2 = 1587.82      ## sparticle masses
Msn3 = 1697.62      ## sparticle masses
Mse1 = 1037.3       ## sparticle masses
Mse2 = 1589.84      ## sparticle masses
Msmu1 = 1037.3      ## sparticle masses
Msmu2 = 1589.84     ## sparticle masses
Mstau1 = 1201.92    ## sparticle masses
Mstau2 = 1699.51    ## sparticle masses
Musq1 = 2228.87     ## sparticle masses
Musq2 = 2376.06     ## sparticle masses
Mcsq1 = 2228.87     ## sparticle masses
Mcsq2 = 2376.06     ## sparticle masses
Mtsq1 = 1299.54     ## sparticle masses
Mtsq2 = 1529.19     ## sparticle masses
Mdsq1 = 2184.03     ## sparticle masses
Mdsq2 = 2377.41     ## sparticle masses
Mssq1 = 2184.03     ## sparticle masses
Mssq2 = 2377.41     ## sparticle masses
Mbsq1 = 1121.65     ## sparticle masses
Mbsq2 = 1527.47     ## sparticle masses
Mlq11 = 2864.53     ## scalar leptoquark masses
Mlq12 = 3533.51     ## scalar leptoquark masses
Mlq21 = 2864.53     ## scalar leptoquark masses
Mlq22 = 3533.51     ## scalar leptoquark masses
Mlq31 = 2929.59     ## scalar leptoquark masses
Mlq32 = 3576.27     ## scalar leptoquark masses
Mh01 = 110.963      ## CP-even Higgs masses
Mh02 = 463.847      ## CP-even Higgs masses
Mh03 = 2463.65      ## CP-even Higgs masses
MA0 = 190.41        ## CP-odd Higgs mass
MH = 204.18         ## charged Higgs masses
Mdh01 = 1770.88     ## dark CP-even Higgs masses
Mdh02 = 1770.88     ## dark CP-even Higgs masses
Mdh03 = 2186.68     ## dark CP-even Higgs masses
Mdh04 = 2186.68     ## dark CP-even Higgs masses
Mdh05 = 2717.09     ## dark CP-even Higgs masses
Mdh06 = 2717.09     ## dark CP-even Higgs masses
MdA01 = 1772.21     ## dark CP-odd Higgs masses
MdA02 = 1772.21     ## dark CP-odd Higgs masses
```

```

MdA03 = 2186.65      ## dark CP-odd Higgs masses
MdA04 = 2186.65      ## dark CP-odd Higgs masses
MdA05 = 2716.25      ## dark CP-odd Higgs masses
MdA06 = 2716.25      ## dark CP-odd Higgs masses
MdcH1 = 2186.92      ## dark CP-odd Higgs masses
MdcH2 = 2186.92      ## dark charged Higgs masses
MdcH3 = 2714.95      ## dark charged Higgs masses
MdcH4 = 2714.95      ## dark charged Higgs masses

```

B.4.2 Scenario B: EXSPECT Output

```

## goodness = 1
alpha = 0.00787402   ## alpha at MZ
MZ = 91.182          ## Mass of Z (pole mass)
WZ = 2.495           ## Width of Z
MW = 80.4            ## Mass of W (pole mass)
WW = 2.085           ## Width of W
alphas = 1.118       ## alpha_s at MZ
MZp = 2482.6         ## Mass of Z' (pole mass)
QXe = -0.191852      ## U(1)' charge of e^c (GUT norm)
QXL = -0.29898       ## U(1)' charge of L (GUT norm)
QXu = -0.13537       ## U(1)' charge of u^c (GUT norm)
QXd = -0.327221      ## U(1)' charge of d^c (GUT norm)
QXQ = -0.163611      ## U(1)' charge of Q (GUT norm)
QXHd = 0.490832      ## U(1)' charge of H^d (GUT norm)
QXHu = 0.29898       ## U(1)' charge of H^u (GUT norm)
QXlq = 0.462591      ## U(1)' charge of D (GUT norm)
QXlqc = 0.327221     ## U(1)' charge of D^c (GUT norm)
QXS = -0.789812      ## U(1)' charge of S (GUT norm)
QYe = 0.774597       ## U(1)_Y charge of e^c (GUT norm)
QYL = -0.387298      ## U(1)_Y charge of L (GUT norm)
QYu = -0.516398      ## U(1)_Y charge of u^c (GUT norm)
QYd = 0.258199       ## U(1)_Y charge of d^c (GUT norm)
QYQ = 0.129099       ## U(1)_Y charge of Q (GUT norm)
QYHd = -0.387298     ## U(1)_Y charge of H^d (GUT norm)
QYHu = 0.387298      ## U(1)_Y charge of H^u (GUT norm)
QYlq = 0.258199      ## U(1)_Y charge of D (GUT norm)
QYlqc = -0.258199    ## U(1)_Y charge of D^c (GUT norm)
QYS = 0               ## U(1)_Y charge of S (GUT norm)
MUEff = 406.406      ## effective mu parameter
tanbe = 41.2594       ## tan beta = vu/vd
YSH = 0.0821425      ## Y^SH_{333}
ASH = 3.81959        ## h^SH_{333}
YS11 = 0.328312      ## Y^SH_{311}
YS12 = 0              ## Y^SH_{312}
YS21 = 0              ## Y^SH_{321}
YS22 = 0.328312      ## Y^SH_{322}
YHd11 = 0.40869      ## Y^SH_{131}
YHd12 = 0            ## Y^SH_{132}
YHd21 = 0            ## Y^SH_{231}
YHd22 = 0.40869      ## Y^SH_{232}
YHu11 = 0.410307     ## Y^SH_{113}
YHu12 = 0            ## Y^SH_{123}
YHu21 = 0            ## Y^SH_{213}
YHu22 = 0.410307     ## Y^SH_{223}
YD11 = 0.605781      ## Lepto-Quark coupling: d^c Q L
YDc1 = 0.391921      ## Lepto-Quark coupling: e^c u^c d^c
YD12 = 0.605781      ## Lepto-Quark coupling: d^c Q L
YDc2 = 0.391921      ## Lepto-Quark coupling: e^c u^c d^c
YD13 = 0.515959      ## Lepto-Quark coupling: d^c Q L
YDc3 = 0.328493      ## Lepto-Quark coupling: e^c u^c d^c
AS11 = -724.531      ## h^SH_{311}
AS12 = 0              ## h^SH_{312}
AS21 = 0              ## h^SH_{321}

```

```
AS22 = -724.531          ## h^SH_{322}
AHd11 = 89.9466         ## h^SH_{131}
AHd12 = 0               ## h^SH_{132}
AHd21 = 0               ## h^SH_{231}
AHd22 = 89.9466         ## h^SH_{232}
AHu11 = 88.7768         ## h^SH_{113}
AHu12 = 0               ## h^SH_{123}
AHu21 = 0               ## h^SH_{213}
AHu22 = 88.7768         ## h^SH_{223}
Ad1 = 0                 ## Trilinear SSB (MSSM-like)
Au1 = 0                 ## Trilinear SSB (MSSM-like)
Ae1 = 0                 ## Trilinear SSB (MSSM-like)
AD11 = -1.46876         ## Trilinear SSB slepton-squark
ADc1 = 1050.8           ## Trilinear SSB slepton-squark
ASD1 = 724.524          ## Trilinear SSB Leptoquark-singlet
Ad2 = 0                 ## Trilinear SSB (MSSM-like)
Au2 = 0                 ## Trilinear SSB (MSSM-like)
Ae2 = 0                 ## Trilinear SSB (MSSM-like)
AD12 = -1.46876         ## Trilinear SSB slepton-squark
ADc2 = 1050.8           ## Trilinear SSB slepton-squark
ASD2 = 724.524          ## Trilinear SSB Leptoquark-singlet
Ad3 = 133.439           ## Trilinear SSB (MSSM-like)
Au3 = 130.699           ## Trilinear SSB (MSSM-like)
Ae3 = 0                 ## Trilinear SSB (MSSM-like)
AD13 = 167.319         ## Trilinear SSB slepton-squark
ADc3 = 1030.06          ## Trilinear SSB slepton-squark
ASD3 = 720.473          ## Trilinear SSB Leptoquark-singlet
RZZpri11 = 1            ## ZZ' mixing
RZZpri12 = 0.000430463 ## ZZ' mixing
RZZpri21 = -0.000430463 ## ZZ' mixing
RZZpri22 = 1            ## ZZ' mixing
RNN11 = 0.0322015       ## neutralino mixing
RNN12 = -0.343306       ## neutralino mixing
RNN13 = -0.0613319      ## neutralino mixing
RNN14 = -0.936666       ## neutralino mixing
RNN15 = -0.000256694    ## neutralino mixing
RNN16 = -0.000334146    ## neutralino mixing
RNN21 = -0.975162       ## neutralino mixing
RNN22 = -0.212394       ## neutralino mixing
RNN23 = 0.0471629       ## neutralino mixing
RNN24 = 0.0412336       ## neutralino mixing
RNN25 = 0.00334078      ## neutralino mixing
RNN26 = -0.00355839     ## neutralino mixing
RNN31 = 0.000415244     ## neutralino mixing
RNN32 = -0.00266672     ## neutralino mixing
RNN33 = 0.00251015     ## neutralino mixing
RNN34 = 0.000379775    ## neutralino mixing
RNN35 = 0.686264        ## neutralino mixing
RNN36 = 0.727343        ## neutralino mixing
RNN41 = -0.185842       ## neutralino mixing
RNN42 = 0.658469        ## neutralino mixing
RNN43 = -0.700803       ## neutralino mixing
RNN44 = -0.201844       ## neutralino mixing
RNN45 = 0.00320489     ## neutralino mixing
RNN46 = 0.00202037     ## neutralino mixing
RNN51 = -0.115949       ## neutralino mixing
RNN52 = 0.635124        ## neutralino mixing
RNN53 = 0.70909         ## neutralino mixing
RNN54 = -0.283201       ## neutralino mixing
RNN55 = 0.00929911     ## neutralino mixing
RNN56 = -0.00867838     ## neutralino mixing
RNN61 = -0.00640048     ## neutralino mixing
RNN62 = 0.00765167     ## neutralino mixing
RNN63 = 0.00858521     ## neutralino mixing
```



```
RNN64 = -0.00363216      ## neutralino mixing
RNN65 = -0.727279       ## neutralino mixing
RNN66 = 0.686207        ## neutralino mixing
RUU11 = -0.285376       ## chargino mixing
RUU12 = -0.958416       ## chargino mixing
RUU21 = 0.958416        ## chargino mixing
RUU22 = -0.285376       ## chargino mixing
RVV11 = 0.400273        ## chargino mixing
RVV12 = 0.916396        ## chargino mixing
RVV21 = 0.916396        ## chargino mixing
RVV22 = -0.400273       ## chargino mixing
RdNN11 = -0.00105533    ## dark neutralino mixing
RdNN12 = 0               ## dark neutralino mixing
RdNN13 = 0               ## dark neutralino mixing
RdNN14 = -0.707123      ## dark neutralino mixing
RdNN15 = -0.70709       ## dark neutralino mixing
RdNN16 = 0               ## dark neutralino mixing
RdNN21 = -0.0438836     ## dark neutralino mixing
RdNN22 = 0               ## dark neutralino mixing
RdNN23 = 0               ## dark neutralino mixing
RdNN24 = 0.706442       ## dark neutralino mixing
RdNN25 = -0.706409      ## dark neutralino mixing
RdNN26 = 0               ## dark neutralino mixing
RdNN31 = 0.999036       ## dark neutralino mixing
RdNN32 = 0               ## dark neutralino mixing
RdNN33 = 0               ## dark neutralino mixing
RdNN34 = 0.0302841      ## dark neutralino mixing
RdNN35 = -0.0317766     ## dark neutralino mixing
RdNN36 = 0               ## dark neutralino mixing
RdNN41 = 0               ## dark neutralino mixing
RdNN42 = -0.00105533    ## dark neutralino mixing
RdNN43 = -0.707123      ## dark neutralino mixing
RdNN44 = 0               ## dark neutralino mixing
RdNN45 = 0               ## dark neutralino mixing
RdNN46 = -0.70709       ## dark neutralino mixing
RdNN51 = 0               ## dark neutralino mixing
RdNN52 = -0.0438836     ## dark neutralino mixing
RdNN53 = 0.706442       ## dark neutralino mixing
RdNN54 = 0               ## dark neutralino mixing
RdNN55 = 0               ## dark neutralino mixing
RdNN56 = -0.706409      ## dark neutralino mixing
RdNN61 = 0               ## dark neutralino mixing
RdNN62 = 0.999036       ## dark neutralino mixing
RdNN63 = 0.0302841      ## dark neutralino mixing
RdNN64 = 0               ## dark neutralino mixing
RdNN65 = 0               ## dark neutralino mixing
RdNN66 = -0.0317766     ## dark neutralino mixing
RdUU11 = 1               ## dark chargino mixing
RdUU12 = 0               ## dark chargino mixing
RdUU21 = 0               ## dark chargino mixing
RdUU22 = 1               ## dark chargino mixing
RdVV11 = 1               ## dark chargino mixing
RdVV12 = 0               ## dark chargino mixing
RdVV21 = 0               ## dark chargino mixing
RdVV22 = 1               ## dark chargino mixing
Rse11 = 0               ## slepton mixing
Rse12 = 1               ## slepton mixing
Rse21 = 1               ## slepton mixing
Rse22 = 0               ## slepton mixing
Rsmu11 = 0              ## slepton mixing
Rsmu12 = 1              ## slepton mixing
Rsmu21 = 1              ## slepton mixing
Rsmu22 = 0              ## slepton mixing
Rstau11 = 0             ## slepton mixing
```

```
Rstau12 = 1          ## slepton mixing
Rstau21 = 1          ## slepton mixing
Rstau22 = 0          ## slepton mixing
Rsu11 = 0            ## squark mixing
Rsu12 = 1            ## squark mixing
Rsu21 = 1            ## squark mixing
Rsu22 = 0            ## squark mixing
Rsc11 = 0            ## squark mixing
Rsc12 = 1            ## squark mixing
Rsc21 = 1            ## squark mixing
Rsc22 = 0            ## squark mixing
Rst11 = -0.112293    ## squark mixing
Rst12 = 0.993675     ## squark mixing
Rst21 = 0.993675     ## squark mixing
Rst22 = 0.112293    ## squark mixing
Rsd11 = 0            ## squark mixing
Rsd12 = 1            ## squark mixing
Rsd21 = 1            ## squark mixing
Rsd22 = 0            ## squark mixing
Rss11 = 0            ## squark mixing
Rss12 = 1            ## squark mixing
Rss21 = 1            ## squark mixing
Rss22 = 0            ## squark mixing
Rsb11 = 0.267839     ## squark mixing
Rsb12 = 0.963464     ## squark mixing
Rsb21 = 0.963464     ## squark mixing
Rsb22 = -0.267839    ## squark mixing
Rlq111 = -0.70237    ## leptoquark mixing
Rlq112 = 0.711812    ## leptoquark mixing
Rlq121 = 0.711812    ## leptoquark mixing
Rlq122 = 0.70237     ## leptoquark mixing
Rlq211 = -0.70237    ## leptoquark mixing
Rlq212 = 0.711812    ## leptoquark mixing
Rlq221 = 0.711812    ## leptoquark mixing
Rlq222 = 0.70237     ## leptoquark mixing
Rlq311 = -0.698289   ## leptoquark mixing
Rlq312 = 0.715816    ## leptoquark mixing
Rlq321 = 0.715816    ## leptoquark mixing
Rlq322 = 0.698289    ## leptoquark mixing
hOmix11 = -0.0280388 ## CP-even higgs mixing
hOmix12 = 0.999607   ## CP-even higgs mixing
hOmix13 = -0.000527577 ## CP-even higgs mixing
hOmix21 = -0.999541   ## CP-even higgs mixing
hOmix22 = -0.028043   ## CP-even higgs mixing
hOmix23 = -0.0115041  ## CP-even higgs mixing
hOmix31 = -0.0115144  ## CP-even higgs mixing
hOmix32 = 0.000204773 ## CP-even higgs mixing
hOmix33 = 0.999934    ## CP-even higgs mixing
AOmix11 = 0           ## CP-odd higgs mixing
AOmix12 = 0.0242447   ## CP-odd higgs mixing
AOmix13 = 0.999706    ## CP-odd higgs mixing
AOmix21 = -0.0351263   ## CP-odd higgs mixing
AOmix22 = -0.999089    ## CP-odd higgs mixing
AOmix23 = 0.0242298   ## CP-odd higgs mixing
AOmix31 = 0.999383    ## CP-odd higgs mixing
AOmix32 = -0.0351159   ## CP-odd higgs mixing
AOmix33 = 0.000851627 ## CP-odd higgs mixing
dhOmix11 = -0.781533   ## CP-even dark higgs mixing
dhOmix12 = -1.87755e-16 ## CP-even dark higgs mixing
dhOmix13 = 0.0418233   ## CP-even dark higgs mixing
dhOmix14 = -0.000314408 ## CP-even dark higgs mixing
dhOmix15 = -0.62246    ## CP-even dark higgs mixing
dhOmix16 = -4.69816e-17 ## CP-even dark higgs mixing
dhOmix21 = 1.36472e-16 ## CP-even dark higgs mixing
```

```

dh0mix22 = -0.781533          ## CP-even dark higgs mixing
dh0mix23 = -0.000314408      ## CP-even dark higgs mixing
dh0mix24 = -0.0418233        ## CP-even dark higgs mixing
dh0mix25 = 1.1397e-16        ## CP-even dark higgs mixing
dh0mix26 = -0.62246          ## CP-even dark higgs mixing
dh0mix31 = 0.62289           ## CP-even dark higgs mixing
dh0mix32 = 1.9607e-16        ## CP-even dark higgs mixing
dh0mix33 = -0.00341606       ## CP-even dark higgs mixing
dh0mix34 = 2.56803e-05       ## CP-even dark higgs mixing
dh0mix35 = -0.782302        ## CP-even dark higgs mixing
dh0mix36 = -7.27576e-17     ## CP-even dark higgs mixing
dh0mix41 = -1.76693e-16     ## CP-even dark higgs mixing
dh0mix42 = 0.62289           ## CP-even dark higgs mixing
dh0mix43 = 2.56803e-05       ## CP-even dark higgs mixing
dh0mix44 = 0.00341606       ## CP-even dark higgs mixing
dh0mix45 = 8.84965e-17      ## CP-even dark higgs mixing
dh0mix46 = -0.782302        ## CP-even dark higgs mixing
dh0mix51 = -0.0348458       ## CP-even dark higgs mixing
dh0mix52 = 2.38325e-17      ## CP-even dark higgs mixing
dh0mix53 = -0.999091        ## CP-even dark higgs mixing
dh0mix54 = 0.00751069       ## CP-even dark higgs mixing
dh0mix55 = -0.0233822       ## CP-even dark higgs mixing
dh0mix56 = 1.09213e-16      ## CP-even dark higgs mixing
dh0mix61 = 5.85631e-19      ## CP-even dark higgs mixing
dh0mix62 = -0.0348458       ## CP-even dark higgs mixing
dh0mix63 = 0.00751069       ## CP-even dark higgs mixing
dh0mix64 = 0.999091        ## CP-even dark higgs mixing
dh0mix65 = -2.93312e-19     ## CP-even dark higgs mixing
dh0mix66 = -0.0233822       ## CP-even dark higgs mixing
dA0mix11 = -0.781983        ## CP-odd dark higgs mixing
dA0mix12 = -1.30657e-16     ## CP-odd dark higgs mixing
dA0mix13 = -0.0266569       ## CP-odd dark higgs mixing
dA0mix14 = -0.000150085     ## CP-odd dark higgs mixing
dA0mix15 = -3.27099e-17     ## CP-odd dark higgs mixing
dA0mix16 = -0.622729       ## CP-odd dark higgs mixing
dA0mix21 = -9.50902e-17     ## CP-odd dark higgs mixing
dA0mix22 = 0.781983        ## CP-odd dark higgs mixing
dA0mix23 = -0.000150085     ## CP-odd dark higgs mixing
dA0mix24 = 0.0266569       ## CP-odd dark higgs mixing
dA0mix25 = 0.622729       ## CP-odd dark higgs mixing
dA0mix26 = -7.83098e-17     ## CP-odd dark higgs mixing
dA0mix31 = -0.622839       ## CP-odd dark higgs mixing
dA0mix32 = -7.83611e-17     ## CP-odd dark higgs mixing
dA0mix33 = -0.00494693      ## CP-odd dark higgs mixing
dA0mix34 = -2.78525e-05     ## CP-odd dark higgs mixing
dA0mix35 = 9.65757e-17     ## CP-odd dark higgs mixing
dA0mix36 = 0.782334        ## CP-odd dark higgs mixing
dA0mix41 = -1.22961e-16     ## CP-odd dark higgs mixing
dA0mix42 = 0.622839       ## CP-odd dark higgs mixing
dA0mix43 = -2.78525e-05     ## CP-odd dark higgs mixing
dA0mix44 = 0.00494693      ## CP-odd dark higgs mixing
dA0mix45 = -0.782334       ## CP-odd dark higgs mixing
dA0mix46 = 6.15495e-17     ## CP-odd dark higgs mixing
dA0mix51 = 0.0239356       ## CP-odd dark higgs mixing
dA0mix52 = -2.33134e-17    ## CP-odd dark higgs mixing
dA0mix53 = -0.999617       ## CP-odd dark higgs mixing
dA0mix54 = -0.00562811     ## CP-odd dark higgs mixing
dA0mix55 = -1.18126e-16    ## CP-odd dark higgs mixing
dA0mix56 = 0.0127348       ## CP-odd dark higgs mixing
dA0mix61 = 5.87051e-19     ## CP-odd dark higgs mixing
dA0mix62 = -0.0239356      ## CP-odd dark higgs mixing
dA0mix63 = -0.00562811     ## CP-odd dark higgs mixing
dA0mix64 = 0.999617       ## CP-odd dark higgs mixing
dA0mix65 = -0.0127348     ## CP-odd dark higgs mixing

```

```

dAOmix66 = -2.93856e-19      ## CP-odd dark higgs mixing
dcHmix11 = 0.782001         ## charged dark higgs mixing
dcHmix12 = 0                 ## charged dark higgs mixing
dcHmix13 = -0.623277        ## charged dark higgs mixing
dcHmix14 = 0                 ## charged dark higgs mixing
dcHmix21 = 0.623277         ## charged dark higgs mixing
dcHmix22 = 0                 ## charged dark higgs mixing
dcHmix23 = 0.782001         ## charged dark higgs mixing
dcHmix24 = 0                 ## charged dark higgs mixing
dcHmix31 = 0                 ## charged dark higgs mixing
dcHmix32 = 0.782001         ## charged dark higgs mixing
dcHmix33 = 0                 ## charged dark higgs mixing
dcHmix34 = -0.623277        ## charged dark higgs mixing
dcHmix41 = 0                 ## charged dark higgs mixing
dcHmix42 = 0.623277         ## charged dark higgs mixing
dcHmix43 = 0                 ## charged dark higgs mixing
dcHmix44 = 0.782001         ## charged dark higgs mixing
Me1 = 0                      ## fermion masses
Mu1 = 0                      ## fermion masses
Md1 = 0                      ## fermion masses
Mnue = 0                     ## fermion masses
Mnum = 0                     ## fermion masses
Mnut = 0                     ## fermion masses
Mlqino1 = 3552.99            ## fermionic leptoquark masses
Me2 = 0                      ## fermion masses
Mu2 = 0                      ## fermion masses
Md2 = 0                      ## fermion masses
Mnue = 0                     ## fermion masses
Mnum = 0                     ## fermion masses
Mnut = 0                     ## fermion masses
Mlqino2 = 3552.99            ## fermionic leptoquark masses
Me3 = 1.777                  ## fermion masses
Mu3 = 172.9                  ## fermion masses
Md3 = 4.19                   ## fermion masses
Mnue = 0                     ## fermion masses
Mnum = 0                     ## fermion masses
Mnut = 0                     ## fermion masses
Mlqino3 = 3584.78            ## fermionic leptoquark masses
Mneu1 = -259.977             ## neutralino masses
Mneu2 = -392.838             ## neutralino masses
Mneu3 = 411.624              ## neutralino masses
Mneu4 = -561.241             ## neutralino masses
Mneu5 = 2342.46              ## neutralino masses
Mneu6 = -2631.23            ## neutralino masses
Mch1 = 389.736               ## chargino masses
Mch2 = 561.208               ## chargino masses
Mglu = -875.446              ## gluino mass
Mdneu1 = 0.151035            ## dark neutralino masses
Mdneu2 = 0.151035            ## dark neutralino masses
Mdneu3 = 1625.84             ## dark neutralino masses
Mdneu4 = 1625.84             ## dark neutralino masses
Mdneu5 = -1625.99            ## dark neutralino masses
Mdneu6 = -1625.99            ## dark neutralino masses
Mdchar1 = 1624.35            ## dark chargino masses
Mdchar2 = 1624.35            ## dark chargino masses
Msn1 = 1322.54               ## sparticle masses
Msn2 = 1322.54               ## sparticle masses
Msn3 = 1374.36               ## sparticle masses
Mse1 = 1111.57               ## sparticle masses
Mse2 = 1324.96               ## sparticle masses
Msmu1 = 1111.57              ## sparticle masses
Msmu2 = 1324.96              ## sparticle masses
Mstau1 = 1308.74             ## sparticle masses
Mstau2 = 1376.69             ## sparticle masses

```

```

Musq1 = 1976.85      ## sparticle masses
Musq2 = 2055.42      ## sparticle masses
Mcsq1 = 1976.85      ## sparticle masses
Mcsq2 = 2055.42      ## sparticle masses
Mtsq1 = 1173.39      ## sparticle masses
Mtsq2 = 1251.81      ## sparticle masses
Mdsq1 = 2018.28      ## sparticle masses
Mdsq2 = 2056.98      ## sparticle masses
Mssq1 = 2018.28      ## sparticle masses
Mssq2 = 2056.98      ## sparticle masses
Mbsq1 = 1149.81      ## sparticle masses
Mbsq2 = 1251.03      ## sparticle masses
Mlq11 = 2970.2       ## scalar leptoquark masses
Mlq12 = 3998.99      ## scalar leptoquark masses
Mlq21 = 2970.2       ## scalar leptoquark masses
Mlq22 = 3998.99      ## scalar leptoquark masses
Mlq31 = 3031.4       ## scalar leptoquark masses
Mlq32 = 4039.89      ## scalar leptoquark masses
Mh01 = 107.156       ## CP-even Higgs masses
Mh02 = 367.495       ## CP-even Higgs masses
Mh03 = 2458.09       ## CP-even Higgs masses
MA0 = 129.53         ## CP-odd Higgs mass
MH = 151.671        ## charged Higgs masses
Mdh01 = 530.028      ## dark CP-even Higgs masses
Mdh02 = 530.028      ## dark CP-even Higgs masses
Mdh03 = 1769.45      ## dark CP-even Higgs masses
Mdh04 = 1769.45      ## dark CP-even Higgs masses
Mdh05 = 2764.69      ## dark CP-even Higgs masses
Mdh06 = 2764.69      ## dark CP-even Higgs masses
Mda01 = 531.976      ## dark CP-odd Higgs masses
Mda02 = 531.976      ## dark CP-odd Higgs masses
Mda03 = 1769.42      ## dark CP-odd Higgs masses
Mda04 = 1769.42      ## dark CP-odd Higgs masses
Mda05 = 2764.33      ## dark CP-odd Higgs masses
Mda06 = 2764.33      ## dark CP-odd Higgs masses
MdcH1 = 531.819      ## dark CP-odd Higgs masses
MdcH2 = 531.819      ## dark charged Higgs masses
MdcH3 = 2763.6       ## dark charged Higgs masses
MdcH4 = 2763.6       ## dark charged Higgs masses

```

B.4.3 Scenario C: EXSPECT Output

```

## goodness = 1
alpha = 0.00787402   ## alpha at MZ
MZ = 91.182          ## Mass of Z (pole mass)
WZ = 2.495           ## Width of Z
MW = 80.4            ## Mass of W (pole mass)
WW = 2.085           ## Width of W
alphas = 1.118       ## alpha_s at MZ
MZp = 2087.08        ## Mass of Z' (pole mass)
QXe = -0.191852      ## U(1)' charge of e^c (GUT norm)
QXL = -0.29898       ## U(1)' charge of L (GUT norm)
QXu = -0.13537       ## U(1)' charge of u^c (GUT norm)
QXd = -0.327221     ## U(1)' charge of d^c (GUT norm)
QQQ = -0.163611     ## U(1)' charge of Q (GUT norm)
QXHd = 0.490832     ## U(1)' charge of H^d (GUT norm)
QXHu = 0.29898       ## U(1)' charge of H^u (GUT norm)
QXlq = 0.462591     ## U(1)' charge of D (GUT norm)
QXlqc = 0.327221    ## U(1)' charge of D^c (GUT norm)
QXS = -0.789812     ## U(1)' charge of S (GUT norm)
QYe = 0.774597       ## U(1)_Y charge of e^c (GUT norm)
QYL = -0.387298     ## U(1)_Y charge of L (GUT norm)
QYu = -0.516398     ## U(1)_Y charge of u^c (GUT norm)
QYd = 0.258199      ## U(1)_Y charge of d^c (GUT norm)

```

```

QYQ = 0.129099          ## U(1)_Y charge of Q (GUT norm)
QYHd = -0.387298       ## U(1)_Y charge of H^d (GUT norm)
QYHu = 0.387298        ## U(1)_Y charge of H^u (GUT norm)
QY1q = 0.258199        ## U(1)_Y charge of D (GUT norm)
QY1qc = -0.258199      ## U(1)_Y charge of D^c (GUT norm)
QYS = 0                 ## U(1)_Y charge of S (GUT norm)
MUEff = 554.605        ## effective mu parameter
tanbe = 42.2568        ## tan beta = vu/vd
YSH = 0.133344         ## Y^SH_{333}
ASH = 1.28671          ## h^SH_{333}
YS11 = 0.0855699      ## Y^SH_{311}
YS12 = 0                ## Y^SH_{312}
YS21 = 0                ## Y^SH_{321}
YS22 = 0.0855699      ## Y^SH_{322}
YHd11 = 0.0898019     ## Y^SH_{131}
YHd12 = 0              ## Y^SH_{132}
YHd21 = 0              ## Y^SH_{231}
YHd22 = 0.0898019     ## Y^SH_{232}
YHu11 = 0.0904714     ## Y^SH_{113}
YHu12 = 0              ## Y^SH_{123}
YHu21 = 0              ## Y^SH_{213}
YHu22 = 0.0904714     ## Y^SH_{223}
YD11 = 0.774479       ## Lepto-Quark coupling: d^c Q L
YDc1 = 0.848333       ## Lepto-Quark coupling: e^c u^c d^c
YD12 = 0.774479       ## Lepto-Quark coupling: d^c Q L
YDc2 = 0.848333       ## Lepto-Quark coupling: e^c u^c d^c
YD13 = 0.667078       ## Lepto-Quark coupling: d^c Q L
YDc3 = 0.741481       ## Lepto-Quark coupling: e^c u^c d^c
AS11 = -9.61244        ## h^SH_{311}
AS12 = 0                ## h^SH_{312}
AS21 = 0                ## h^SH_{321}
AS22 = -9.61244        ## h^SH_{322}
AHd11 = 157.776        ## h^SH_{131}
AHd12 = 0              ## h^SH_{132}
AHd21 = 0              ## h^SH_{231}
AHd22 = 157.776        ## h^SH_{232}
AHu11 = 160.028        ## h^SH_{113}
AHu12 = 0              ## h^SH_{123}
AHu21 = 0              ## h^SH_{213}
AHu22 = 160.028        ## h^SH_{223}
Ad1 = 0                ## Trilinear SSB (MSSM-like)
Au1 = 0                ## Trilinear SSB (MSSM-like)
Ae1 = 0                ## Trilinear SSB (MSSM-like)
AD11 = 604.017         ## Trilinear SSB slepton-squark
ADc1 = -50.8026        ## Trilinear SSB slepton-squark
ASD1 = 669.426         ## Trilinear SSB Leptoquark-singlet
Ad2 = 0                ## Trilinear SSB (MSSM-like)
Au2 = 0                ## Trilinear SSB (MSSM-like)
Ae2 = 0                ## Trilinear SSB (MSSM-like)
AD12 = 604.017         ## Trilinear SSB slepton-squark
ADc2 = -50.8026        ## Trilinear SSB slepton-squark
ASD2 = 669.426         ## Trilinear SSB Leptoquark-singlet
Ad3 = 636.547          ## Trilinear SSB (MSSM-like)
Au3 = 598.486          ## Trilinear SSB (MSSM-like)
Ae3 = 0                ## Trilinear SSB (MSSM-like)
AD13 = 535.436         ## Trilinear SSB slepton-squark
ADc3 = -112.58         ## Trilinear SSB slepton-squark
ASD3 = 665.976        ## Trilinear SSB Leptoquark-singlet
RZZpri11 = 1           ## ZZ' mixing
RZZpri12 = 0.000609328 ## ZZ' mixing
RZZpri21 = -0.000609328 ## ZZ' mixing
RZZpri22 = 1           ## ZZ' mixing
RNN11 = 0.0123214     ## neutralino mixing
RNN12 = -0.842898     ## neutralino mixing

```

```
RNN13 = 0.0547051      ## neutralino mixing
RNN14 = 0.535143      ## neutralino mixing
RNN15 = -0.00032373   ## neutralino mixing
RNN16 = -0.00044718   ## neutralino mixing
RNN21 = -0.994114     ## neutralino mixing
RNN22 = -0.0656187    ## neutralino mixing
RNN23 = -0.0394967    ## neutralino mixing
RNN24 = -0.0764298    ## neutralino mixing
RNN25 = 0.00371055    ## neutralino mixing
RNN26 = -0.00396156   ## neutralino mixing
RNN31 = 0.000389077   ## neutralino mixing
RNN32 = -0.00350089   ## neutralino mixing
RNN33 = -0.00523533   ## neutralino mixing
RNN34 = -0.00396465   ## neutralino mixing
RNN35 = 0.683864      ## neutralino mixing
RNN36 = 0.729571      ## neutralino mixing
RNN41 = -0.0990029    ## neutralino mixing
RNN42 = 0.408514      ## neutralino mixing
RNN43 = 0.702785      ## neutralino mixing
RNN44 = 0.573891      ## neutralino mixing
RNN45 = 0.00623552    ## neutralino mixing
RNN46 = 0.00432997    ## neutralino mixing
RNN51 = -0.0417824    ## neutralino mixing
RNN52 = 0.343942      ## neutralino mixing
RNN53 = -0.70812      ## neutralino mixing
RNN54 = 0.615087      ## neutralino mixing
RNN55 = 0.0100784     ## neutralino mixing
RNN56 = -0.0095132    ## neutralino mixing
RNN61 = -0.00612068   ## neutralino mixing
RNN62 = 0.00500196    ## neutralino mixing
RNN63 = -0.00890884   ## neutralino mixing
RNN64 = 0.00906028    ## neutralino mixing
RNN65 = -0.729504     ## neutralino mixing
RNN66 = 0.683813      ## neutralino mixing
RUU11 = -0.813239     ## chargino mixing
RUU12 = -0.581931     ## chargino mixing
RUU21 = 0.581931      ## chargino mixing
RUU22 = -0.813239     ## chargino mixing
RVV11 = 0.871874      ## chargino mixing
RVV12 = 0.48973       ## chargino mixing
RVV21 = 0.48973       ## chargino mixing
RVV22 = -0.871874    ## chargino mixing
RdNN11 = -0.00103332  ## dark neutralino mixing
RdNN12 = 0             ## dark neutralino mixing
RdNN13 = 0             ## dark neutralino mixing
RdNN14 = -0.707123    ## dark neutralino mixing
RdNN15 = -0.70709     ## dark neutralino mixing
RdNN16 = 0             ## dark neutralino mixing
RdNN21 = -0.0441626   ## dark neutralino mixing
RdNN22 = 0             ## dark neutralino mixing
RdNN23 = 0             ## dark neutralino mixing
RdNN24 = 0.706433     ## dark neutralino mixing
RdNN25 = -0.706401    ## dark neutralino mixing
RdNN26 = 0             ## dark neutralino mixing
RdNN31 = 0.999024     ## dark neutralino mixing
RdNN32 = 0             ## dark neutralino mixing
RdNN33 = 0             ## dark neutralino mixing
RdNN34 = 0.030497     ## dark neutralino mixing
RdNN35 = -0.0319584   ## dark neutralino mixing
RdNN36 = 0             ## dark neutralino mixing
RdNN41 = 0             ## dark neutralino mixing
RdNN42 = -0.00103332  ## dark neutralino mixing
RdNN43 = -0.707123    ## dark neutralino mixing
RdNN44 = 0             ## dark neutralino mixing
```

```
RdNN45 = 0 ## dark neutralino mixing
RdNN46 = -0.70709 ## dark neutralino mixing
RdNN51 = 0 ## dark neutralino mixing
RdNN52 = -0.0441626 ## dark neutralino mixing
RdNN53 = 0.706433 ## dark neutralino mixing
RdNN54 = 0 ## dark neutralino mixing
RdNN55 = 0 ## dark neutralino mixing
RdNN56 = -0.706401 ## dark neutralino mixing
RdNN61 = 0 ## dark neutralino mixing
RdNN62 = 0.999024 ## dark neutralino mixing
RdNN63 = 0.030497 ## dark neutralino mixing
RdNN64 = 0 ## dark neutralino mixing
RdNN65 = 0 ## dark neutralino mixing
RdNN66 = -0.0319584 ## dark neutralino mixing
RdUU11 = 1 ## dark chargino mixing
RdUU12 = 0 ## dark chargino mixing
RdUU21 = 0 ## dark chargino mixing
RdUU22 = 1 ## dark chargino mixing
RdVV11 = 1 ## dark chargino mixing
RdVV12 = 0 ## dark chargino mixing
RdVV21 = 0 ## dark chargino mixing
RdVV22 = 1 ## dark chargino mixing
Rse11 = 1 ## slepton mixing
Rse12 = 0 ## slepton mixing
Rse21 = 0 ## slepton mixing
Rse22 = 1 ## slepton mixing
Rsmu11 = 1 ## slepton mixing
Rsmu12 = 0 ## slepton mixing
Rsmu21 = 0 ## slepton mixing
Rsmu22 = 1 ## slepton mixing
Rstau11 = 1 ## slepton mixing
Rstau12 = 0 ## slepton mixing
Rstau21 = 0 ## slepton mixing
Rstau22 = 1 ## slepton mixing
Rsu11 = 1 ## squark mixing
Rsu12 = 0 ## squark mixing
Rsu21 = 0 ## squark mixing
Rsu22 = 1 ## squark mixing
Rsc11 = 1 ## squark mixing
Rsc12 = 0 ## squark mixing
Rsc21 = 0 ## squark mixing
Rsc22 = 1 ## squark mixing
Rst11 = 0.935652 ## squark mixing
Rst12 = 0.352924 ## squark mixing
Rst21 = -0.352924 ## squark mixing
Rst22 = 0.935652 ## squark mixing
Rsd11 = 1 ## squark mixing
Rsd12 = 0 ## squark mixing
Rsd21 = 0 ## squark mixing
Rsd22 = 1 ## squark mixing
Rss11 = 1 ## squark mixing
Rss12 = 0 ## squark mixing
Rss21 = 0 ## squark mixing
Rss22 = 1 ## squark mixing
Rsb11 = 0.9873 ## squark mixing
Rsb12 = -0.158869 ## squark mixing
Rsb21 = 0.158869 ## squark mixing
Rsb22 = 0.9873 ## squark mixing
Rlq111 = -0.647104 ## leptoquark mixing
Rlq112 = 0.762401 ## leptoquark mixing
Rlq121 = 0.762401 ## leptoquark mixing
Rlq122 = 0.647104 ## leptoquark mixing
Rlq211 = -0.647104 ## leptoquark mixing
Rlq212 = 0.762401 ## leptoquark mixing
```

```

Rlq221 = 0.762401      ## leptoquark mixing
Rlq222 = 0.647104      ## leptoquark mixing
Rlq311 = -0.664651     ## leptoquark mixing
Rlq312 = 0.747154     ## leptoquark mixing
Rlq321 = 0.747154     ## leptoquark mixing
Rlq322 = 0.664651     ## leptoquark mixing
h0mix11 = -0.0272795   ## CP-even higgs mixing
h0mix12 = 0.999628     ## CP-even higgs mixing
h0mix13 = -0.000587871 ## CP-even higgs mixing
h0mix21 = -0.999579    ## CP-even higgs mixing
h0mix22 = -0.027284    ## CP-even higgs mixing
h0mix23 = -0.00991883  ## CP-even higgs mixing
h0mix31 = -0.00993118  ## CP-even higgs mixing
h0mix32 = 0.000317042  ## CP-even higgs mixing
h0mix33 = 0.999951     ## CP-even higgs mixing
A0mix11 = 0.0236788    ## CP-odd higgs mixing
A0mix12 = 0            ## CP-odd higgs mixing
A0mix13 = 0.99972     ## CP-odd higgs mixing
A0mix21 = -0.998847    ## CP-odd higgs mixing
A0mix22 = -0.0417744   ## CP-odd higgs mixing
A0mix23 = 0.0236582    ## CP-odd higgs mixing
A0mix31 = -0.0417627   ## CP-odd higgs mixing
A0mix32 = 0.999127     ## CP-odd higgs mixing
A0mix33 = 0.000989169  ## CP-odd higgs mixing
dh0mix11 = -0.0102587  ## CP-even dark higgs mixing
dh0mix12 = 0           ## CP-even dark higgs mixing
dh0mix13 = 0.999357    ## CP-even dark higgs mixing
dh0mix14 = 0           ## CP-even dark higgs mixing
dh0mix15 = -0.0343624  ## CP-even dark higgs mixing
dh0mix16 = 0           ## CP-even dark higgs mixing
dh0mix21 = -2.77317e-16 ## CP-even dark higgs mixing
dh0mix22 = 0.0102587   ## CP-even dark higgs mixing
dh0mix23 = -9.44543e-18 ## CP-even dark higgs mixing
dh0mix24 = -0.999357   ## CP-even dark higgs mixing
dh0mix25 = -1.91909e-16 ## CP-even dark higgs mixing
dh0mix26 = 0.0343624   ## CP-even dark higgs mixing
dh0mix31 = 0.00363893  ## CP-even dark higgs mixing
dh0mix32 = -1.95629e-18 ## CP-even dark higgs mixing
dh0mix33 = -0.0343266  ## CP-even dark higgs mixing
dh0mix34 = 2.27148e-16 ## CP-even dark higgs mixing
dh0mix35 = -0.999404   ## CP-even dark higgs mixing
dh0mix36 = -8.00552e-18 ## CP-even dark higgs mixing
dh0mix41 = 0           ## CP-even dark higgs mixing
dh0mix42 = -0.00363893 ## CP-even dark higgs mixing
dh0mix43 = 0           ## CP-even dark higgs mixing
dh0mix44 = 0.0343266   ## CP-even dark higgs mixing
dh0mix45 = 0           ## CP-even dark higgs mixing
dh0mix46 = 0.999404    ## CP-even dark higgs mixing
dh0mix51 = -0.999941   ## CP-even dark higgs mixing
dh0mix52 = -1.41551e-18 ## CP-even dark higgs mixing
dh0mix53 = -0.0103776  ## CP-even dark higgs mixing
dh0mix54 = 1.9127e-16  ## CP-even dark higgs mixing
dh0mix55 = -0.00328444  ## CP-even dark higgs mixing
dh0mix56 = -6.85863e-18 ## CP-even dark higgs mixing
dh0mix61 = 0           ## CP-even dark higgs mixing
dh0mix62 = 0.999941    ## CP-even dark higgs mixing
dh0mix63 = 0           ## CP-even dark higgs mixing
dh0mix64 = 0.0103776   ## CP-even dark higgs mixing
dh0mix65 = 0           ## CP-even dark higgs mixing
dh0mix66 = 0.00328444  ## CP-even dark higgs mixing
dA0mix11 = 0.0102948   ## CP-odd dark higgs mixing
dA0mix12 = 0           ## CP-odd dark higgs mixing
dA0mix13 = 0.999353    ## CP-odd dark higgs mixing
dA0mix14 = 0           ## CP-odd dark higgs mixing

```

```

dAOmix15 = 0 ## CP-odd dark higgs mixing
dAOmix16 = -0.0344523 ## CP-odd dark higgs mixing
dAOmix21 = 4.55865e-16 ## CP-odd dark higgs mixing
dAOmix22 = -0.0102948 ## CP-odd dark higgs mixing
dAOmix23 = -1.55817e-17 ## CP-odd dark higgs mixing
dAOmix24 = 0.999353 ## CP-odd dark higgs mixing
dAOmix25 = -0.0344523 ## CP-odd dark higgs mixing
dAOmix26 = -3.15757e-16 ## CP-odd dark higgs mixing
dAOmix31 = -0.000519242 ## CP-odd dark higgs mixing
dAOmix32 = -3.47524e-18 ## CP-odd dark higgs mixing
dAOmix33 = 0.0344594 ## CP-odd dark higgs mixing
dAOmix34 = 3.52595e-16 ## CP-odd dark higgs mixing
dAOmix35 = -1.22569e-17 ## CP-odd dark higgs mixing
dAOmix36 = 0.999406 ## CP-odd dark higgs mixing
dAOmix41 = 0 ## CP-odd dark higgs mixing
dAOmix42 = 0.000519242 ## CP-odd dark higgs mixing
dAOmix43 = 0 ## CP-odd dark higgs mixing
dAOmix44 = 0.0344594 ## CP-odd dark higgs mixing
dAOmix45 = 0.999406 ## CP-odd dark higgs mixing
dAOmix46 = 0 ## CP-odd dark higgs mixing
dAOmix51 = -0.999947 ## CP-odd dark higgs mixing
dAOmix52 = -3.80377e-18 ## CP-odd dark higgs mixing
dAOmix53 = 0.0102708 ## CP-odd dark higgs mixing
dAOmix54 = 3.91223e-16 ## CP-odd dark higgs mixing
dAOmix55 = -1.36321e-17 ## CP-odd dark higgs mixing
dAOmix56 = -0.00087366 ## CP-odd dark higgs mixing
dAOmix61 = 0 ## CP-odd dark higgs mixing
dAOmix62 = 0.999947 ## CP-odd dark higgs mixing
dAOmix63 = 0 ## CP-odd dark higgs mixing
dAOmix64 = 0.0102708 ## CP-odd dark higgs mixing
dAOmix65 = -0.00087366 ## CP-odd dark higgs mixing
dAOmix66 = 0 ## CP-odd dark higgs mixing
dcHmix11 = 0.999394 ## charged dark higgs mixing
dcHmix12 = 0 ## charged dark higgs mixing
dcHmix13 = -0.0348135 ## charged dark higgs mixing
dcHmix14 = 0 ## charged dark higgs mixing
dcHmix21 = 0.0348135 ## charged dark higgs mixing
dcHmix22 = 0 ## charged dark higgs mixing
dcHmix23 = 0.999394 ## charged dark higgs mixing
dcHmix24 = 0 ## charged dark higgs mixing
dcHmix31 = 0 ## charged dark higgs mixing
dcHmix32 = 0.999394 ## charged dark higgs mixing
dcHmix33 = 0 ## charged dark higgs mixing
dcHmix34 = -0.0348135 ## charged dark higgs mixing
dcHmix41 = 0 ## charged dark higgs mixing
dcHmix42 = 0.0348135 ## charged dark higgs mixing
dcHmix43 = 0 ## charged dark higgs mixing
dcHmix44 = 0.999394 ## charged dark higgs mixing
Me1 = 0 ## fermion masses
Mu1 = 0 ## fermion masses
Md1 = 0 ## fermion masses
Mnue = 0 ## fermion masses
Mnum = 0 ## fermion masses
Mnut = 0 ## fermion masses
Mlqino1 = 2834.21 ## fermionic leptoquark masses
Me2 = 0 ## fermion masses
Mu2 = 0 ## fermion masses
Md2 = 0 ## fermion masses
Mnue = 0 ## fermion masses
Mnum = 0 ## fermion masses
Mnut = 0 ## fermion masses
Mlqino2 = 2834.21 ## fermionic leptoquark masses
Me3 = 1.777 ## fermion masses
Mu3 = 172.9 ## fermion masses

```

```

Md3 = 4.19                ## fermion masses
Mnue = 0                  ## fermion masses
Mnum = 0                  ## fermion masses
Mnut = 0                  ## fermion masses
Mlqino3 = 2916.24         ## fermionic leptoquark masses
Mneu1 = -246.17           ## neutralino masses
Mneu2 = -470.983         ## neutralino masses
Mneu3 = 559.306          ## neutralino masses
Mneu4 = -592.885         ## neutralino masses
Mneu5 = 1956.47          ## neutralino masses
Mneu6 = -2226.6          ## neutralino masses
Mch1 = 470.753           ## chargino masses
Mch2 = 592.978           ## chargino masses
Mglu = -840.923          ## gluino mass
Mdneu1 = 0.0326099       ## dark neutralino masses
Mdneu2 = 0.0326099       ## dark neutralino masses
Mdneu3 = 356.233         ## dark neutralino masses
Mdneu4 = 356.233         ## dark neutralino masses
Mdneu5 = -356.266        ## dark neutralino masses
Mdneu6 = -356.266        ## dark neutralino masses
Mdchar1 = 355.902        ## dark chargino masses
Mdchar2 = 355.902        ## dark chargino masses
Msn1 = 957.762           ## sparticle masses
Msn2 = 957.762           ## sparticle masses
Msn3 = 1319.07           ## sparticle masses
Mse1 = 961.109           ## sparticle masses
Mse2 = 1025.77           ## sparticle masses
Msmu1 = 961.109          ## sparticle masses
Msmu2 = 1025.77          ## sparticle masses
Mstau1 = 1321.5           ## sparticle masses
Mstau2 = 1356.3           ## sparticle masses
Musq1 = 2165.64           ## sparticle masses
Musq2 = 2209.02           ## sparticle masses
Mcsq1 = 2165.64           ## sparticle masses
Mcsq2 = 2209.02           ## sparticle masses
Mtsq1 = 1395.68           ## sparticle masses
Mtsq2 = 1502.33           ## sparticle masses
Mdsq1 = 2167.12           ## sparticle masses
Mdsq2 = 2349.34           ## sparticle masses
Mssq1 = 2167.12           ## sparticle masses
Mssq2 = 2349.34           ## sparticle masses
Mbsq1 = 1398.49           ## sparticle masses
Mbsq2 = 1579.97           ## sparticle masses
Mlq11 = 2183.12           ## scalar leptoquark masses
Mlq12 = 3226.37           ## scalar leptoquark masses
Mlq21 = 2183.12           ## scalar leptoquark masses
Mlq22 = 3226.37           ## scalar leptoquark masses
Mlq31 = 2375.68           ## scalar leptoquark masses
Mlq32 = 3349.86           ## scalar leptoquark masses
Mh01 = 110.278           ## CP-even Higgs masses
Mh02 = 386.104           ## CP-even Higgs masses
Mh03 = 2074.95           ## CP-even Higgs masses
MA0 = 153.131            ## CP-odd Higgs mass
MH = 171.293             ## charged Higgs masses
Mdh01 = 2410.82          ## dark CP-even Higgs masses
Mdh02 = 2410.82          ## dark CP-even Higgs masses
Mdh03 = 2916.29          ## dark CP-even Higgs masses
Mdh04 = 2916.29          ## dark CP-even Higgs masses
Mdh05 = 3109.08          ## dark CP-even Higgs masses
Mdh06 = 3109.08          ## dark CP-even Higgs masses
MdA01 = 2410.83          ## dark CP-odd Higgs masses
MdA02 = 2410.83          ## dark CP-odd Higgs masses
MdA03 = 2916.29          ## dark CP-odd Higgs masses
MdA04 = 2916.29          ## dark CP-odd Higgs masses

```

MdA05 = 3109.08	## dark CP-odd Higgs masses
MdA06 = 3109.08	## dark CP-odd Higgs masses
MdcH1 = 2917.3	## dark CP-odd Higgs masses
MdcH2 = 2917.3	## dark charged Higgs masses
MdcH3 = 3108.05	## dark charged Higgs masses
MdcH4 = 3108.05	## dark charged Higgs masses

B.5 RGEs above the intermediate scale

B.5.1 Running of the Gauge Couplings

$$\begin{aligned}
\frac{dg_3}{dt} &= \frac{1}{16\pi^2}(0)g_3^3 \\
\frac{dg_{2L}}{dt} &= \frac{1}{16\pi^2}(4)g_{2L}^3 \\
\frac{dg_{2R}}{dt} &= \frac{1}{16\pi^2}(4)g_{2R}^3 \\
\frac{dg_{B-L}}{dt} &= \frac{1}{16\pi^2}(\beta^{Q_{B-L}})g_{B-L}^3 \\
\frac{dg_\chi}{dt} &= \frac{1}{16\pi^2}(\beta^{Q_\chi})g_\chi^3
\end{aligned}$$

B.5.2 Running of the Gaugino Masses

$$\begin{aligned}
\frac{dM_3}{dt} &= \frac{1}{16\pi^2}0g_3^2M_3 \\
\frac{dM_{2L}}{dt} &= \frac{1}{16\pi^2}8g_{2L}^2M_{2L} \\
\frac{dM_{2R}}{dt} &= \frac{1}{16\pi^2}8g_{2R}^2M_{2R} \\
\frac{dM_{B-L}}{dt} &= \frac{1}{16\pi^2}2\beta^{Q_{B-L}}g_{B-L}^2M_{B-L} \\
\frac{dM_\chi}{dt} &= \frac{1}{16\pi^2}2\beta^{Q_\chi}g_\chi^2M_\chi
\end{aligned}$$

B.5.3 Running of the Yukawa Couplings

$$\begin{aligned}
\frac{d\mathbf{Y}_{333}^Q}{dt} &= \frac{1}{16\pi^2} \left[-\mathbf{Y}_{333}^Q \left(\sum_{i=Q_L, Q_R, H} (\mathcal{C}_3(i)g_3^2 + \mathcal{C}_{2L}(i)g_{2L}^2 + \mathcal{C}_{2R}(i)g_{2R}^2 + \mathcal{C}_{B-L}(i)g_{B-L}^2 + \mathcal{C}_\chi(i)g_\chi^2) \right) \right. \\
&\quad \left. + 7\mathbf{Y}_{333}^Q \mathbf{Y}_{333}^Q \mathbf{Y}_{333}^Q + \mathbf{Y}_{333}^Q \mathbf{Y}_{333}^{Dc} \mathbf{Y}_{333}^{Dc} + \mathbf{Y}_{333}^Q \mathbf{Y}_{333}^D \mathbf{Y}_{333}^D + \mathbf{Y}_{333}^Q \mathbf{Y}_{131}^{SH} \mathbf{Y}_{131}^{SH} \right. \\
&\quad \left. + \mathbf{Y}_{333}^Q \mathbf{Y}_{232}^{SH} \mathbf{Y}_{232}^{SH} + \mathbf{Y}_{333}^Q \mathbf{Y}_{333}^{SH} \mathbf{Y}_{333}^{SH} \right] \\
\frac{d\mathbf{Y}_{111}^D}{dt} &= \frac{1}{16\pi^2} \left[-\mathbf{Y}_{111}^D \left(\sum_{i=L_R, Q_R, D} (\mathcal{C}_3(i)g_3^2 + \mathcal{C}_{2R}(i)g_{2R}^2 + \mathcal{C}_{B-L}(i)g_{B-L}^2 + \mathcal{C}_\chi(i)g_\chi^2) \right) \right. \\
&\quad \left. + 6\mathbf{Y}_{111}^D \mathbf{Y}_{111}^D \mathbf{Y}_{111}^D + \mathbf{Y}_{111}^D \mathbf{Y}_{113}^{SD} \mathbf{Y}_{113}^{SD} \right]
\end{aligned}$$

$$\begin{aligned}
\frac{d\mathbf{Y}_{222}^D}{dt} &= \frac{1}{16\pi^2} \left[-\mathbf{Y}_{222}^D \left(\sum_{i=L_R, Q_R, D} (\mathcal{C}_3(i) g_3^2 + \mathcal{C}_{2R}(i) g_{2R}^2 + \mathcal{C}_{B-L}(i) g_{B-L}^2 + \mathcal{C}_\chi(i) g_\chi^2) \right) \right. \\
&\quad \left. + 6\mathbf{Y}_{222}^D \mathbf{Y}_{222}^D \mathbf{Y}_{222}^D + \mathbf{Y}_{222}^D \mathbf{Y}_{223}^{SD} \mathbf{Y}_{223}^{SD} \right] \\
\frac{d\mathbf{Y}_{333}^D}{dt} &= \frac{1}{16\pi^2} \left[-\mathbf{Y}_{333}^D \left(\sum_{i=L_R, Q_R, D} (\mathcal{C}_3(i) g_3^2 + \mathcal{C}_{2R}(i) g_{2R}^2 + \mathcal{C}_{B-L}(i) g_{B-L}^2 + \mathcal{C}_\chi(i) g_\chi^2) \right) \right. \\
&\quad \left. + 6\mathbf{Y}_{333}^D \mathbf{Y}_{333}^D \mathbf{Y}_{333}^D + 2\mathbf{Y}_{333}^D \mathbf{Y}_{333}^Q \mathbf{Y}_{333}^Q + \mathbf{Y}_{333}^D \mathbf{Y}_{333}^{SD} \mathbf{Y}_{333}^{SD} \right] \\
\frac{d\mathbf{Y}_{111}^{Dc}}{dt} &= \frac{1}{16\pi^2} \left[-\mathbf{Y}_{111}^{Dc} \left(\sum_{i=L_L, Q_L, D^c} (\mathcal{C}_3(i) g_3^2 + \mathcal{C}_{2L}(i) g_{2L}^2 + \mathcal{C}_{B-L}(i) g_{B-L}^2 + \mathcal{C}_\chi(i) g_\chi^2) \right) \right. \\
&\quad \left. + 6\mathbf{Y}_{111}^{Dc} \mathbf{Y}_{111}^{Dc} \mathbf{Y}_{111}^{Dc} + \mathbf{Y}_{111}^{Dc} \mathbf{Y}_{113}^{SD} \mathbf{Y}_{113}^{SD} \right] \\
\frac{d\mathbf{Y}_{222}^{Dc}}{dt} &= \frac{1}{16\pi^2} \left[-\mathbf{Y}_{222}^{Dc} \left(\sum_{i=L_L, Q_L, D^c} (\mathcal{C}_3(i) g_3^2 + \mathcal{C}_{2L}(i) g_{2L}^2 + \mathcal{C}_{B-L}(i) g_{B-L}^2 + \mathcal{C}_\chi(i) g_\chi^2) \right) \right. \\
&\quad \left. + 6\mathbf{Y}_{222}^{Dc} \mathbf{Y}_{222}^{Dc} \mathbf{Y}_{222}^{Dc} + \mathbf{Y}_{222}^{Dc} \mathbf{Y}_{223}^{SD} \mathbf{Y}_{223}^{SD} \right] \\
\frac{d\mathbf{Y}_{333}^{Dc}}{dt} &= \frac{1}{16\pi^2} \left[-\mathbf{Y}_{333}^{Dc} \left(\sum_{i=L_L, Q_L, D^c} (\mathcal{C}_3(i) g_3^2 + \mathcal{C}_{2L}(i) g_{2L}^2 + \mathcal{C}_{B-L}(i) g_{B-L}^2 + \mathcal{C}_\chi(i) g_\chi^2) \right) \right. \\
&\quad \left. + 6\mathbf{Y}_{333}^{Dc} \mathbf{Y}_{333}^{Dc} \mathbf{Y}_{333}^{Dc} + 2\mathbf{Y}_{333}^{Dc} \mathbf{Y}_{333}^Q \mathbf{Y}_{333}^Q + \mathbf{Y}_{333}^{Dc} \mathbf{Y}_{333}^{SD} \mathbf{Y}_{333}^{SD} \right] \\
\frac{d\mathbf{Y}_{113}^{SD}}{dt} &= \frac{1}{16\pi^2} \left[-\mathbf{Y}_{113}^{SD} \left(\sum_{i=D, D^c, S} (\mathcal{C}_3(i) g_3^2 + \mathcal{C}_{B-L}(i) g_{B-L}^2 + \mathcal{C}_\chi(i) g_\chi^2) \right) \right. \\
&\quad + 2\mathbf{Y}_{113}^{SD} \mathbf{Y}_{111}^D \mathbf{Y}_{111}^D + 5\mathbf{Y}_{113}^{SD} \mathbf{Y}_{113}^{SD} \mathbf{Y}_{113}^{SD} + 2\mathbf{Y}_{113}^{SD} \mathbf{Y}_{111}^{Dc} \mathbf{Y}_{111}^{Dc} + 3\mathbf{Y}_{113}^{SD} \mathbf{Y}_{223}^{SD} \mathbf{Y}_{223}^{SD} \\
&\quad \left. + 3\mathbf{Y}_{113}^{SD} \mathbf{Y}_{333}^{SD} \mathbf{Y}_{333}^{SD} + 2\mathbf{Y}_{113}^{SD} \mathbf{Y}_{311}^{SH} \mathbf{Y}_{311}^{SH} + 2\mathbf{Y}_{113}^{SD} \mathbf{Y}_{322}^{SH} \mathbf{Y}_{322}^{SH} + 2\mathbf{Y}_{113}^{SD} \mathbf{Y}_{333}^{SH} \mathbf{Y}_{333}^{SH} \right] \\
\frac{d\mathbf{Y}_{223}^{SD}}{dt} &= \frac{1}{16\pi^2} \left[-\mathbf{Y}_{223}^{SD} \left(\sum_{i=D, D^c, S} (\mathcal{C}_3(i) g_3^2 + \mathcal{C}_{B-L}(i) g_{B-L}^2 + \mathcal{C}_\chi(i) g_\chi^2) \right) \right. \\
&\quad + 2\mathbf{Y}_{223}^{SD} \mathbf{Y}_{222}^D \mathbf{Y}_{222}^D + 5\mathbf{Y}_{223}^{SD} \mathbf{Y}_{223}^{SD} \mathbf{Y}_{223}^{SD} + 2\mathbf{Y}_{223}^{SD} \mathbf{Y}_{222}^{Dc} \mathbf{Y}_{222}^{Dc} + 3\mathbf{Y}_{223}^{SD} \mathbf{Y}_{113}^{SD} \mathbf{Y}_{113}^{SD} \\
&\quad \left. + 3\mathbf{Y}_{223}^{SD} \mathbf{Y}_{333}^{SD} \mathbf{Y}_{333}^{SD} + 2\mathbf{Y}_{223}^{SD} \mathbf{Y}_{311}^{SH} \mathbf{Y}_{311}^{SH} + 2\mathbf{Y}_{223}^{SD} \mathbf{Y}_{322}^{SH} \mathbf{Y}_{322}^{SH} + 2\mathbf{Y}_{223}^{SD} \mathbf{Y}_{333}^{SH} \mathbf{Y}_{333}^{SH} \right] \\
\frac{d\mathbf{Y}_{333}^{SD}}{dt} &= \frac{1}{16\pi^2} \left[-\mathbf{Y}_{333}^{SD} \left(\sum_{i=D, D^c, S} (\mathcal{C}_3(i) g_3^2 + \mathcal{C}_{B-L}(i) g_{B-L}^2 + \mathcal{C}_\chi(i) g_\chi^2) \right) \right. \\
&\quad + 2\mathbf{Y}_{333}^{SD} \mathbf{Y}_{333}^D \mathbf{Y}_{333}^D + 5\mathbf{Y}_{333}^{SD} \mathbf{Y}_{333}^{SD} \mathbf{Y}_{333}^{SD} + 2\mathbf{Y}_{333}^{SD} \mathbf{Y}_{333}^{Dc} \mathbf{Y}_{333}^{Dc} + 3\mathbf{Y}_{333}^{SD} \mathbf{Y}_{113}^{SD} \mathbf{Y}_{113}^{SD} \\
&\quad \left. + 3\mathbf{Y}_{333}^{SD} \mathbf{Y}_{223}^{SD} \mathbf{Y}_{223}^{SD} + 2\mathbf{Y}_{333}^{SD} \mathbf{Y}_{311}^{SH} \mathbf{Y}_{311}^{SH} + 2\mathbf{Y}_{333}^{SD} \mathbf{Y}_{322}^{SH} \mathbf{Y}_{322}^{SH} + 2\mathbf{Y}_{333}^{SD} \mathbf{Y}_{333}^{SH} \mathbf{Y}_{333}^{SH} \right] \\
\frac{d\mathbf{Y}_{311}^{SH}}{dt} &= \frac{1}{16\pi^2} \left[-\mathbf{Y}_{311}^{SH} \left(\sum_{i=S, H, H} (\mathcal{C}_{2L}(i) g_{2L}^2 + \mathcal{C}_{2R}(i) g_{2R}^2 + \mathcal{C}_\chi(i) g_\chi^2) \right) \right. \\
&\quad + 3\mathbf{Y}_{311}^{SH} \mathbf{Y}_{113}^{SD} \mathbf{Y}_{113}^{SD} + 3\mathbf{Y}_{311}^{SH} \mathbf{Y}_{223}^{SD} \mathbf{Y}_{223}^{SD} + 3\mathbf{Y}_{311}^{SH} \mathbf{Y}_{333}^{SD} \mathbf{Y}_{333}^{SD} + 4\mathbf{Y}_{311}^{SH} \mathbf{Y}_{311}^{SH} \mathbf{Y}_{311}^{SH} \\
&\quad \left. + 2\mathbf{Y}_{311}^{SH} \mathbf{Y}_{322}^{SH} \mathbf{Y}_{322}^{SH} + 2\mathbf{Y}_{311}^{SH} \mathbf{Y}_{333}^{SH} \mathbf{Y}_{333}^{SH} + 2\mathbf{Y}_{311}^{SH} \mathbf{Y}_{131}^{SH} \mathbf{Y}_{131}^{SH} \right] \\
\frac{d\mathbf{Y}_{322}^{SH}}{dt} &= \frac{1}{16\pi^2} \left[-\mathbf{Y}_{322}^{SH} \left(\sum_{i=S, H, H} (\mathcal{C}_{2L}(i) g_{2L}^2 + \mathcal{C}_{2R}(i) g_{2R}^2 + \mathcal{C}_\chi(i) g_\chi^2) \right) \right. \\
&\quad + 3\mathbf{Y}_{322}^{SH} \mathbf{Y}_{113}^{SD} \mathbf{Y}_{113}^{SD} + 3\mathbf{Y}_{322}^{SH} \mathbf{Y}_{223}^{SD} \mathbf{Y}_{223}^{SD} + 3\mathbf{Y}_{322}^{SH} \mathbf{Y}_{333}^{SD} \mathbf{Y}_{333}^{SD} + 2\mathbf{Y}_{322}^{SH} \mathbf{Y}_{311}^{SH} \mathbf{Y}_{311}^{SH} \\
&\quad \left. + 4\mathbf{Y}_{322}^{SH} \mathbf{Y}_{322}^{SH} \mathbf{Y}_{322}^{SH} + 2\mathbf{Y}_{322}^{SH} \mathbf{Y}_{333}^{SH} \mathbf{Y}_{333}^{SH} + 2\mathbf{Y}_{322}^{SH} \mathbf{Y}_{232}^{SH} \mathbf{Y}_{232}^{SH} \right] \\
\frac{d\mathbf{Y}_{131}^{SH}}{dt} &= \frac{1}{16\pi^2} \left[-\mathbf{Y}_{131}^{SH} \left(\sum_{i=S, H, H} (\mathcal{C}_{2L}(i) g_{2L}^2 + \mathcal{C}_{2R}(i) g_{2R}^2 + \mathcal{C}_\chi(i) g_\chi^2) \right) \right.
\end{aligned}$$

$$\begin{aligned}
& +6\mathbf{Y}_{131}^{SH}\mathbf{Y}_{131}^{SH}\mathbf{Y}_{131}^{SH} + 3\mathbf{Y}_{131}^{SH}\mathbf{Y}_{333}^Q\mathbf{Y}_{333}^Q + \mathbf{Y}_{131}^{SH}\mathbf{Y}_{232}^{SH}\mathbf{Y}_{232}^{SH} + \mathbf{Y}_{131}^{SH}\mathbf{Y}_{333}^{SH}\mathbf{Y}_{333}^{SH} \\
& + \mathbf{Y}_{131}^{SH}\mathbf{Y}_{311}^{SH}\mathbf{Y}_{311}^{SH} \Big] \\
\frac{d\mathbf{Y}_{232}^{SH}}{dt} &= \frac{1}{16\pi^2} \left[-\mathbf{Y}_{232}^{SH} \left(\sum_{i=S,H,H} (\mathcal{C}_{2L}(i)g_{2L}^2 + \mathcal{C}_{2R}(i)g_{2R}^2 + \mathcal{C}_\chi(i)g_\chi^2) \right) \right. \\
& + 6\mathbf{Y}_{232}^{SH}\mathbf{Y}_{232}^{SH}\mathbf{Y}_{232}^{SH} + 3\mathbf{Y}_{232}^{SH}\mathbf{Y}_{333}^Q\mathbf{Y}_{333}^Q + \mathbf{Y}_{232}^{SH}\mathbf{Y}_{131}^{SH}\mathbf{Y}_{131}^{SH} + \mathbf{Y}_{232}^{SH}\mathbf{Y}_{333}^{SH}\mathbf{Y}_{333}^{SH} \\
& \left. + \mathbf{Y}_{232}^{SH}\mathbf{Y}_{322}^{SH}\mathbf{Y}_{322}^{SH} \right] \\
\frac{d\mathbf{Y}_{333}^{SH}}{dt} &= \frac{1}{16\pi^2} \left[-\mathbf{Y}_{333}^{SH} \left(\sum_{i=S,H,H} (\mathcal{C}_{2L}(i)g_{2L}^2 + \mathcal{C}_{2R}(i)g_{2R}^2 + \mathcal{C}_\chi(i)g_\chi^2) \right) \right. \\
& + 3\mathbf{Y}_{333}^{SH}\mathbf{Y}_{113}^{SD}\mathbf{Y}_{113}^{SD} + 3\mathbf{Y}_{333}^{SH}\mathbf{Y}_{223}^{SD}\mathbf{Y}_{223}^{SD} + 3\mathbf{Y}_{333}^{SH}\mathbf{Y}_{333}^{SD}\mathbf{Y}_{333}^{SD} + 2\mathbf{Y}_{333}^{SH}\mathbf{Y}_{311}^{SH}\mathbf{Y}_{311}^{SH} \\
& + 2\mathbf{Y}_{333}^{SH}\mathbf{Y}_{322}^{SH}\mathbf{Y}_{322}^{SH} + 4\mathbf{Y}_{333}^{SH}\mathbf{Y}_{333}^{SH}\mathbf{Y}_{333}^{SH} + 6\mathbf{Y}_{333}^{SH}\mathbf{Y}_{333}^Q\mathbf{Y}_{333}^Q + 2\mathbf{Y}_{333}^{SH}\mathbf{Y}_{131}^{SH}\mathbf{Y}_{131}^{SH} \\
& \left. + 2\mathbf{Y}_{333}^{SH}\mathbf{Y}_{232}^{SH}\mathbf{Y}_{232}^{SH} \right]
\end{aligned} \tag{B.5}$$

B.5.4 Running of the Trilinear SSB-Terms

$$\begin{aligned}
\frac{d\mathbf{h}_{333}^Q}{dt} &= \frac{1}{16\pi^2} \left[-\mathbf{h}_{333}^Q \left(\sum_{i=Q_L, Q_R, H} (\mathcal{C}_3(i)g_3^2 + \mathcal{C}_{2L}(i)g_{2L}^2 + \mathcal{C}_{2R}(i)g_{2R}^2 + \mathcal{C}_{B-L}(i)g_{B-L}^2 \right. \right. \\
& \left. \left. + \mathcal{C}_\chi(i)g_\chi^2) \right) \right. \\
& + 2\mathbf{Y}_{333}^Q \left(\sum_{i=Q_L, Q_R, H} (\mathcal{C}_3(i)g_3^2 M_3 + \mathcal{C}_{2L}(i)g_{2L}^2 M_{2L} + \mathcal{C}_{2R}(i)g_{2R}^2 M_{2R} \right. \\
& \left. \left. + \mathcal{C}_{B-L}(i)g_{B-L}^2 M_{B-L} + \mathcal{C}_\chi(i)g_\chi^2 M_\chi) \right) \right. \\
& + 21\mathbf{h}_{333}^Q\mathbf{Y}_{333}^Q\mathbf{Y}_{333}^Q + \mathbf{h}_{333}^Q\mathbf{Y}_{333}^{Dc}\mathbf{Y}_{333}^{Dc} + \mathbf{h}_{333}^Q\mathbf{Y}_{333}^D\mathbf{Y}_{333}^D + \mathbf{h}_{333}^Q\mathbf{Y}_{131}^{SH}\mathbf{Y}_{131}^{SH} \\
& + \mathbf{h}_{333}^Q\mathbf{Y}_{232}^{SH}\mathbf{Y}_{232}^{SH} + \mathbf{h}_{333}^Q\mathbf{Y}_{333}^{SH}\mathbf{Y}_{333}^{SH} + 2\mathbf{Y}_{333}^Q\mathbf{Y}_{333}^{Dc}\mathbf{h}_{333}^{Dc} + 2\mathbf{Y}_{333}^Q\mathbf{Y}_{333}^D\mathbf{h}_{333}^D \\
& \left. + 2\mathbf{Y}_{333}^Q\mathbf{Y}_{131}^{SH}\mathbf{h}_{131}^{SH} + 2\mathbf{Y}_{333}^Q\mathbf{Y}_{232}^{SH}\mathbf{h}_{232}^{SH} + 2\mathbf{Y}_{333}^Q\mathbf{Y}_{333}^{SH}\mathbf{h}_{333}^{SH} \right] \\
\frac{d\mathbf{h}_{111}^D}{dt} &= \frac{1}{16\pi^2} \left[-\mathbf{h}_{111}^D \left(\sum_{i=L_R, Q_R, D} (\mathcal{C}_3(i)g_3^2 + \mathcal{C}_{2R}(i)g_{2R}^2 + \mathcal{C}_{B-L}(i)g_{B-L}^2 + \mathcal{C}_\chi(i)g_\chi^2) \right) \right. \\
& + 2\mathbf{Y}_{111}^D \left(\sum_{i=L_R, Q_R, D} (\mathcal{C}_3(i)g_3^2 M_3 + \mathcal{C}_{2R}(i)g_{2R}^2 M_{2R} + \mathcal{C}_{B-L}(i)g_{B-L}^2 M_{B-L} \right. \\
& \left. \left. + \mathcal{C}_\chi(i)g_\chi^2 M_\chi) \right) \right. \\
& \left. + 18\mathbf{h}_{111}^D\mathbf{Y}_{111}^D\mathbf{Y}_{111}^D + \mathbf{h}_{111}^D\mathbf{Y}_{113}^{SD}\mathbf{Y}_{113}^{SD} + 2\mathbf{Y}_{111}^D\mathbf{Y}_{113}^{SD}\mathbf{h}_{113}^{SD} \right] \\
\frac{d\mathbf{h}_{222}^D}{dt} &= \frac{1}{16\pi^2} \left[-\mathbf{h}_{222}^D \left(\sum_{i=L_R, Q_R, D} (\mathcal{C}_3(i)g_3^2 + \mathcal{C}_{2R}(i)g_{2R}^2 + \mathcal{C}_{B-L}(i)g_{B-L}^2 + \mathcal{C}_\chi(i)g_\chi^2) \right) \right. \\
& + 2\mathbf{Y}_{222}^D \left(\sum_{i=L_R, Q_R, D} (\mathcal{C}_3(i)g_3^2 M_3 + \mathcal{C}_{2R}(i)g_{2R}^2 M_{2R} + \mathcal{C}_{B-L}(i)g_{B-L}^2 M_{B-L} \right. \\
& \left. \left. + \mathcal{C}_\chi(i)g_\chi^2 M_\chi) \right) \right. \\
& \left. + 18\mathbf{h}_{222}^D\mathbf{Y}_{222}^D\mathbf{Y}_{222}^D + \mathbf{h}_{222}^D\mathbf{Y}_{223}^{SD}\mathbf{Y}_{223}^{SD} + 2\mathbf{Y}_{222}^D\mathbf{Y}_{223}^{SD}\mathbf{h}_{223}^{SD} \right] \\
\frac{d\mathbf{h}_{333}^D}{dt} &= \frac{1}{16\pi^2} \left[-\mathbf{h}_{333}^D \left(\sum_{i=L_R, Q_R, D} (\mathcal{C}_3(i)g_3^2 + \mathcal{C}_{2R}(i)g_{2R}^2 + \mathcal{C}_{B-L}(i)g_{B-L}^2 + \mathcal{C}_\chi(i)g_\chi^2) \right) \right.
\end{aligned}$$

$$\begin{aligned}
& +2\mathbf{Y}_{333}^D \left(\sum_{i=L_R, Q_R, D} (\mathcal{C}_3(i) g_3^2 M_3 + \mathcal{C}_{2R}(i) g_{2R}^2 M_{2R} + \mathcal{C}_{B-L}(i) g_{B-L}^2 M_{B-L} \right. \\
& \left. + \mathcal{C}_\chi(i) g_\chi^2 M_\chi) \right) \\
& +18\mathbf{h}_{333}^D \mathbf{Y}_{333}^D \mathbf{Y}_{333}^D + 2\mathbf{h}_{333}^D \mathbf{Y}_{333}^Q \mathbf{Y}_{333}^Q + \mathbf{h}_{333}^D \mathbf{Y}_{333}^{SD} \mathbf{Y}_{333}^{SD} + 4\mathbf{Y}_{333}^D \mathbf{Y}_{333}^Q \mathbf{h}_{333}^Q \\
& +2\mathbf{Y}_{333}^D \mathbf{Y}_{333}^{SD} \mathbf{h}_{333}^{SD} \Big] \\
\frac{d\mathbf{h}_{111}^{Dc}}{dt} &= \frac{1}{16\pi^2} \left[-\mathbf{h}_{111}^{Dc} \left(\sum_{i=L_L, Q_L, D^c} (\mathcal{C}_3(i) g_3^2 + \mathcal{C}_{2L}(i) g_{2L}^2 + \mathcal{C}_{B-L}(i) g_{B-L}^2 + \mathcal{C}_\chi(i) g_\chi^2) \right) \right. \\
& +2\mathbf{Y}_{111}^{Dc} \left(\sum_{i=L_L, Q_L, D^c} (\mathcal{C}_3(i) g_3^2 M_3 + \mathcal{C}_{2L}(i) g_{2L}^2 M_{2L} + \mathcal{C}_{B-L}(i) g_{B-L}^2 M_{B-L} \right. \\
& \left. + \mathcal{C}_\chi(i) g_\chi^2 M_\chi) \right) \\
& \left. +18\mathbf{h}_{111}^{Dc} \mathbf{Y}_{111}^{Dc} \mathbf{Y}_{111}^{Dc} + \mathbf{h}_{111}^{Dc} \mathbf{Y}_{113}^{SD} \mathbf{Y}_{113}^{SD} + 2\mathbf{Y}_{111}^{Dc} \mathbf{Y}_{113}^{SD} \mathbf{h}_{113}^{SD} \right] \\
\frac{d\mathbf{h}_{222}^{Dc}}{dt} &= \frac{1}{16\pi^2} \left[-\mathbf{h}_{222}^{Dc} \left(\sum_{i=L_L, Q_L, D^c} (\mathcal{C}_3(i) g_3^2 + \mathcal{C}_{2L}(i) g_{2L}^2 + \mathcal{C}_{B-L}(i) g_{B-L}^2 + \mathcal{C}_\chi(i) g_\chi^2) \right) \right. \\
& +2\mathbf{Y}_{222}^{Dc} \left(\sum_{i=L_L, Q_L, D^c} (\mathcal{C}_3(i) g_3^2 M_3 + \mathcal{C}_{2L}(i) g_{2L}^2 M_{2L} + \mathcal{C}_{B-L}(i) g_{B-L}^2 M_{B-L} \right. \\
& \left. + \mathcal{C}_\chi(i) g_\chi^2 M_\chi) \right) \\
& \left. +18\mathbf{h}_{222}^{Dc} \mathbf{Y}_{222}^{Dc} \mathbf{Y}_{222}^{Dc} + \mathbf{h}_{222}^{Dc} \mathbf{Y}_{223}^{SD} \mathbf{Y}_{223}^{SD} + 2\mathbf{Y}_{222}^{Dc} \mathbf{Y}_{223}^{SD} \mathbf{h}_{223}^{SD} \right] \\
\frac{d\mathbf{h}_{333}^{Dc}}{dt} &= \frac{1}{16\pi^2} \left[-\mathbf{h}_{333}^{Dc} \left(\sum_{i=L_L, Q_L, D^c} (\mathcal{C}_3(i) g_3^2 + \mathcal{C}_{2L}(i) g_{2L}^2 + \mathcal{C}_{B-L}(i) g_{B-L}^2 + \mathcal{C}_\chi(i) g_\chi^2) \right) \right. \\
& +2\mathbf{Y}_{333}^{Dc} \left(\sum_{i=L_L, Q_L, D^c} (\mathcal{C}_3(i) g_3^2 M_3 + \mathcal{C}_{2L}(i) g_{2L}^2 M_{2L} + \mathcal{C}_{B-L}(i) g_{B-L}^2 M_{B-L} \right. \\
& \left. + \mathcal{C}_\chi(i) g_\chi^2 M_\chi) \right) \\
& +18\mathbf{h}_{333}^{Dc} \mathbf{Y}_{333}^{Dc} \mathbf{Y}_{333}^{Dc} + 2\mathbf{h}_{333}^{Dc} \mathbf{Y}_{333}^Q \mathbf{Y}_{333}^Q + \mathbf{h}_{333}^{Dc} \mathbf{Y}_{333}^{SD} \mathbf{Y}_{333}^{SD} + 4\mathbf{Y}_{333}^{Dc} \mathbf{Y}_{333}^Q \mathbf{h}_{333}^Q \\
& \left. +2\mathbf{Y}_{333}^{Dc} \mathbf{Y}_{333}^{SD} \mathbf{h}_{333}^{SD} \right] \\
\frac{d\mathbf{h}_{113}^{SD}}{dt} &= \frac{1}{16\pi^2} \left[-\mathbf{h}_{113}^{SD} \left(\sum_{i=D, D^c, S} (\mathcal{C}_3(i) g_3^2 + \mathcal{C}_{B-L}(i) g_{B-L}^2 + \mathcal{C}_\chi(i) g_\chi^2) \right) \right. \\
& +2\mathbf{Y}_{113}^{SD} \left(\sum_{i=D, D^c, S} (\mathcal{C}_3(i) g_3^2 M_3 + \mathcal{C}_{B-L}(i) g_{B-L}^2 M_{B-L} + \mathcal{C}_\chi(i) g_\chi^2 M_\chi) \right) \\
& +2\mathbf{h}_{113}^{SD} \mathbf{Y}_{111}^D \mathbf{Y}_{111}^D + 15\mathbf{h}_{113}^{SD} \mathbf{Y}_{113}^{SD} \mathbf{Y}_{113}^{SD} + 2\mathbf{h}_{113}^{SD} \mathbf{Y}_{111}^{Dc} \mathbf{Y}_{111}^{Dc} + 3\mathbf{h}_{113}^{SD} \mathbf{Y}_{223}^{SD} \mathbf{Y}_{223}^{SD} \\
& +3\mathbf{h}_{113}^{SD} \mathbf{Y}_{333}^{SD} \mathbf{Y}_{333}^{SD} + 2\mathbf{h}_{113}^{SD} \mathbf{Y}_{311}^{SH} \mathbf{Y}_{311}^{SH} + 2\mathbf{h}_{113}^{SD} \mathbf{Y}_{322}^{SH} \mathbf{Y}_{322}^{SH} + 2\mathbf{h}_{113}^{SD} \mathbf{Y}_{333}^{SH} \mathbf{Y}_{333}^{SH} \\
& +4\mathbf{Y}_{113}^{SD} \mathbf{Y}_{111}^D \mathbf{h}_{111}^D + 4\mathbf{Y}_{113}^{SD} \mathbf{Y}_{111}^{Dc} \mathbf{h}_{111}^{Dc} + 6\mathbf{Y}_{113}^{SD} \mathbf{Y}_{223}^{SD} \mathbf{h}_{223}^{SD} + 6\mathbf{Y}_{113}^{SD} \mathbf{Y}_{333}^{SD} \mathbf{h}_{333}^{SD} \\
& \left. +4\mathbf{Y}_{113}^{SD} \mathbf{Y}_{311}^{SH} \mathbf{h}_{311}^{SH} + 4\mathbf{Y}_{113}^{SD} \mathbf{Y}_{322}^{SH} \mathbf{h}_{322}^{SH} + 4\mathbf{Y}_{113}^{SD} \mathbf{Y}_{333}^{SH} \mathbf{h}_{333}^{SH} \right] \\
\frac{d\mathbf{h}_{223}^{SD}}{dt} &= \frac{1}{16\pi^2} \left[-\mathbf{h}_{223}^{SD} \left(\sum_{i=D, D^c, S} (\mathcal{C}_3(i) g_3^2 + \mathcal{C}_{B-L}(i) g_{B-L}^2 + \mathcal{C}_\chi(i) g_\chi^2) \right) \right. \\
& +2\mathbf{Y}_{223}^{SD} \left(\sum_{i=D, D^c, S} (\mathcal{C}_3(i) g_3^2 M_3 + \mathcal{C}_{B-L}(i) g_{B-L}^2 M_{B-L} + \mathcal{C}_\chi(i) g_\chi^2 M_\chi) \right) \\
& +2\mathbf{h}_{223}^{SD} \mathbf{Y}_{222}^D \mathbf{Y}_{222}^D + 15\mathbf{h}_{223}^{SD} \mathbf{Y}_{223}^{SD} \mathbf{Y}_{223}^{SD} + 2\mathbf{h}_{223}^{SD} \mathbf{Y}_{222}^{Dc} \mathbf{Y}_{222}^{Dc} + 3\mathbf{h}_{223}^{SD} \mathbf{Y}_{113}^{SD} \mathbf{Y}_{113}^{SD} \\
& \left. +3\mathbf{h}_{223}^{SD} \mathbf{Y}_{333}^{SD} \mathbf{Y}_{333}^{SD} + 2\mathbf{h}_{223}^{SD} \mathbf{Y}_{311}^{SH} \mathbf{Y}_{311}^{SH} + 2\mathbf{h}_{223}^{SD} \mathbf{Y}_{322}^{SH} \mathbf{Y}_{322}^{SH} + 2\mathbf{h}_{223}^{SD} \mathbf{Y}_{333}^{SH} \mathbf{Y}_{333}^{SH} \right]
\end{aligned}$$

$$\begin{aligned}
& +4\mathbf{Y}_{223}^{SD}\mathbf{Y}_{222}^D\mathbf{h}_{222}^D + 4\mathbf{Y}_{223}^{SD}\mathbf{Y}_{222}^{Dc}\mathbf{h}_{222}^{Dc} + 6\mathbf{Y}_{223}^{SD}\mathbf{Y}_{113}^{SD}\mathbf{h}_{113}^{SD} + 6\mathbf{Y}_{223}^{SD}\mathbf{Y}_{333}^{SD}\mathbf{h}_{333}^{SD} \\
& +4\mathbf{Y}_{223}^{SD}\mathbf{Y}_{311}^{SH}\mathbf{h}_{311}^{SH} + 4\mathbf{Y}_{223}^{SD}\mathbf{Y}_{322}^{SH}\mathbf{h}_{322}^{SH} + 4\mathbf{Y}_{223}^{SD}\mathbf{Y}_{333}^{SH}\mathbf{h}_{333}^{SH} \Big] \\
\frac{d\mathbf{h}_{333}^{SD}}{dt} &= \frac{1}{16\pi^2} \left[-\mathbf{h}_{333}^{SD} \left(\sum_{i=D,D^c,S} (\mathcal{C}_3(i)g_3^2 + \mathcal{C}_{B-L}(i)g_{B-L}^2 + \mathcal{C}_\chi(i)g_\chi^2) \right) \right. \\
& +2\mathbf{Y}_{333}^{SD} \left(\sum_{i=D,D^c,S} (\mathcal{C}_3(i)g_3^2M_3 + \mathcal{C}_{B-L}(i)g_{B-L}^2M_{B-L} + \mathcal{C}_\chi(i)g_\chi^2M_\chi) \right) \\
& +2\mathbf{h}_{333}^{SD}\mathbf{Y}_{333}^D\mathbf{Y}_{333}^D + 15\mathbf{h}_{333}^{SD}\mathbf{Y}_{333}^{SD}\mathbf{Y}_{333}^{SD} + 2\mathbf{h}_{333}^{SD}\mathbf{Y}_{333}^{Dc}\mathbf{Y}_{333}^{Dc} + 3\mathbf{h}_{333}^{SD}\mathbf{Y}_{113}^{SD}\mathbf{Y}_{113}^{SD} \\
& +3\mathbf{h}_{333}^{SD}\mathbf{Y}_{223}^{SD}\mathbf{Y}_{223}^{SD} + 2\mathbf{h}_{333}^{SD}\mathbf{Y}_{311}^{SH}\mathbf{Y}_{311}^{SH} + 2\mathbf{h}_{333}^{SD}\mathbf{Y}_{322}^{SH}\mathbf{Y}_{322}^{SH} + 2\mathbf{h}_{333}^{SD}\mathbf{Y}_{333}^{SH}\mathbf{Y}_{333}^{SH} \\
& +4\mathbf{Y}_{333}^{SD}\mathbf{Y}_{333}^D\mathbf{h}_{333}^D + 4\mathbf{Y}_{333}^{SD}\mathbf{Y}_{333}^{Dc}\mathbf{h}_{333}^{Dc} + 6\mathbf{Y}_{333}^{SD}\mathbf{Y}_{113}^{SD}\mathbf{h}_{113}^{SD} + 6\mathbf{Y}_{333}^{SD}\mathbf{Y}_{223}^{SD}\mathbf{h}_{223}^{SD} \\
& \left. +4\mathbf{Y}_{333}^{SD}\mathbf{Y}_{311}^{SH}\mathbf{h}_{311}^{SH} + 4\mathbf{Y}_{333}^{SD}\mathbf{Y}_{322}^{SH}\mathbf{h}_{322}^{SH} + 4\mathbf{Y}_{333}^{SD}\mathbf{Y}_{333}^{SH}\mathbf{h}_{333}^{SH} \right] \\
\frac{d\mathbf{h}_{311}^{SH}}{dt} &= \frac{1}{16\pi^2} \left[-\mathbf{h}_{311}^{SH} \left(\sum_{i=S,H,H} (\mathcal{C}_{2L}(i)g_{2L}^2 + \mathcal{C}_{2R}(i)g_{2R}^2 + \mathcal{C}_\chi(i)g_\chi^2) \right) \right. \\
& +2\mathbf{Y}_{311}^{SH} \left(\sum_{i=S,H,H} (\mathcal{C}_{2L}(i)g_{2L}^2M_{2L} + \mathcal{C}_{2R}(i)g_{2R}^2M_{2R} + \mathcal{C}_\chi(i)g_\chi^2M_\chi) \right) \\
& +3\mathbf{h}_{311}^{SH}\mathbf{Y}_{113}^{SD}\mathbf{Y}_{113}^{SD} + 3\mathbf{h}_{311}^{SH}\mathbf{Y}_{223}^{SD}\mathbf{Y}_{223}^{SD} + 3\mathbf{h}_{311}^{SH}\mathbf{Y}_{333}^{SD}\mathbf{Y}_{333}^{SD} + 12\mathbf{h}_{311}^{SH}\mathbf{Y}_{311}^{SH}\mathbf{Y}_{311}^{SH} \\
& +2\mathbf{h}_{311}^{SH}\mathbf{Y}_{322}^{SH}\mathbf{Y}_{322}^{SH} + 2\mathbf{h}_{311}^{SH}\mathbf{Y}_{333}^{SH}\mathbf{Y}_{333}^{SH} + 2\mathbf{h}_{311}^{SH}\mathbf{Y}_{131}^{SH}\mathbf{Y}_{131}^{SH} + 6\mathbf{Y}_{311}^{SH}\mathbf{Y}_{113}^{SD}\mathbf{h}_{113}^{SD} \\
& +6\mathbf{Y}_{311}^{SH}\mathbf{Y}_{223}^{SD}\mathbf{h}_{223}^{SD} + 6\mathbf{Y}_{311}^{SH}\mathbf{Y}_{333}^{SD}\mathbf{h}_{333}^{SD} + 4\mathbf{Y}_{311}^{SH}\mathbf{Y}_{322}^{SH}\mathbf{h}_{322}^{SH} + 4\mathbf{Y}_{311}^{SH}\mathbf{Y}_{333}^{SH}\mathbf{h}_{333}^{SH} \\
& \left. +4\mathbf{Y}_{311}^{SH}\mathbf{Y}_{131}^{SH}\mathbf{h}_{131}^{SH} \right] \\
\frac{d\mathbf{h}_{322}^{SH}}{dt} &= \frac{1}{16\pi^2} \left[-\mathbf{h}_{322}^{SH} \left(\sum_{i=S,H,H} (\mathcal{C}_{2L}(i)g_{2L}^2 + \mathcal{C}_{2R}(i)g_{2R}^2 + \mathcal{C}_\chi(i)g_\chi^2) \right) \right. \\
& +2\mathbf{Y}_{322}^{SH} \left(\sum_{i=S,H,H} (\mathcal{C}_{2L}(i)g_{2L}^2M_{2L} + \mathcal{C}_{2R}(i)g_{2R}^2M_{2R} + \mathcal{C}_\chi(i)g_\chi^2M_\chi) \right) \\
& +3\mathbf{h}_{322}^{SH}\mathbf{Y}_{113}^{SD}\mathbf{Y}_{113}^{SD} + 3\mathbf{h}_{322}^{SH}\mathbf{Y}_{223}^{SD}\mathbf{Y}_{223}^{SD} + 3\mathbf{h}_{322}^{SH}\mathbf{Y}_{333}^{SD}\mathbf{Y}_{333}^{SD} + 2\mathbf{h}_{322}^{SH}\mathbf{Y}_{311}^{SH}\mathbf{Y}_{311}^{SH} \\
& +12\mathbf{h}_{322}^{SH}\mathbf{Y}_{322}^{SH}\mathbf{Y}_{322}^{SH} + 2\mathbf{h}_{322}^{SH}\mathbf{Y}_{333}^{SH}\mathbf{Y}_{333}^{SH} + 2\mathbf{h}_{322}^{SH}\mathbf{Y}_{232}^{SH}\mathbf{Y}_{232}^{SH} + 6\mathbf{Y}_{322}^{SH}\mathbf{Y}_{113}^{SD}\mathbf{h}_{113}^{SD} \\
& +6\mathbf{Y}_{322}^{SH}\mathbf{Y}_{223}^{SD}\mathbf{h}_{223}^{SD} + 6\mathbf{Y}_{322}^{SH}\mathbf{Y}_{333}^{SD}\mathbf{h}_{333}^{SD} + 4\mathbf{Y}_{322}^{SH}\mathbf{Y}_{311}^{SH}\mathbf{h}_{311}^{SH} + 4\mathbf{Y}_{322}^{SH}\mathbf{Y}_{333}^{SH}\mathbf{h}_{333}^{SH} \\
& \left. +4\mathbf{Y}_{322}^{SH}\mathbf{Y}_{232}^{SH}\mathbf{h}_{232}^{SH} \right] \\
\frac{d\mathbf{h}_{131}^{SH}}{dt} &= \frac{1}{16\pi^2} \left[-\mathbf{h}_{131}^{SH} \left(\sum_{i=S,H,H} (\mathcal{C}_{2L}(i)g_{2L}^2 + \mathcal{C}_{2R}(i)g_{2R}^2 + \mathcal{C}_\chi(i)g_\chi^2) \right) \right. \\
& +2\mathbf{Y}_{131}^{SH} \left(\sum_{i=S,H,H} (\mathcal{C}_{2L}(i)g_{2L}^2M_{2L} + \mathcal{C}_{2R}(i)g_{2R}^2M_{2R} + \mathcal{C}_\chi(i)g_\chi^2M_\chi) \right) \\
& +18\mathbf{h}_{131}^{SH}\mathbf{Y}_{131}^{SH}\mathbf{Y}_{131}^{SH} + 3\mathbf{h}_{131}^{SH}\mathbf{Y}_{333}^Q\mathbf{Y}_{333}^Q + \mathbf{h}_{131}^{SH}\mathbf{Y}_{232}^{SH}\mathbf{Y}_{232}^{SH} + \mathbf{h}_{131}^{SH}\mathbf{Y}_{333}^{SH}\mathbf{Y}_{333}^{SH} \\
& +\mathbf{h}_{131}^{SH}\mathbf{Y}_{311}^{SH}\mathbf{Y}_{311}^{SH} + 6\mathbf{Y}_{131}^{SH}\mathbf{Y}_{333}^Q\mathbf{h}_{333}^Q + 2\mathbf{Y}_{131}^{SH}\mathbf{Y}_{232}^{SH}\mathbf{h}_{232}^{SH} + 2\mathbf{Y}_{131}^{SH}\mathbf{Y}_{333}^{SH}\mathbf{h}_{333}^{SH} \\
& \left. +2\mathbf{Y}_{131}^{SH}\mathbf{Y}_{311}^{SH}\mathbf{h}_{311}^{SH} \right] \\
\frac{d\mathbf{h}_{232}^{SH}}{dt} &= \frac{1}{16\pi^2} \left[-\mathbf{h}_{232}^{SH} \left(\sum_{i=S,H,H} (\mathcal{C}_{2L}(i)g_{2L}^2 + \mathcal{C}_{2R}(i)g_{2R}^2 + \mathcal{C}_\chi(i)g_\chi^2) \right) \right. \\
& +2\mathbf{Y}_{232}^{SH} \left(\sum_{i=S,H,H} (\mathcal{C}_{2L}(i)g_{2L}^2M_{2L} + \mathcal{C}_{2R}(i)g_{2R}^2M_{2R} + \mathcal{C}_\chi(i)g_\chi^2M_\chi) \right) \\
& +18\mathbf{h}_{232}^{SH}\mathbf{Y}_{232}^{SH}\mathbf{Y}_{232}^{SH} + 3\mathbf{h}_{232}^{SH}\mathbf{Y}_{333}^Q\mathbf{Y}_{333}^Q + \mathbf{h}_{232}^{SH}\mathbf{Y}_{131}^{SH}\mathbf{Y}_{131}^{SH} + \mathbf{h}_{232}^{SH}\mathbf{Y}_{333}^{SH}\mathbf{Y}_{333}^{SH} \\
& +\mathbf{h}_{232}^{SH}\mathbf{Y}_{322}^{SH}\mathbf{Y}_{322}^{SH} + 6\mathbf{Y}_{232}^{SH}\mathbf{Y}_{333}^Q\mathbf{h}_{333}^Q + 2\mathbf{Y}_{232}^{SH}\mathbf{Y}_{131}^{SH}\mathbf{h}_{131}^{SH} + 2\mathbf{Y}_{232}^{SH}\mathbf{Y}_{333}^{SH}\mathbf{h}_{333}^{SH} \\
& \left. +2\mathbf{Y}_{232}^{SH}\mathbf{Y}_{322}^{SH}\mathbf{h}_{322}^{SH} \right]
\end{aligned}$$

$$\begin{aligned}
& +2\mathbf{Y}_{232}^{SH}\mathbf{Y}_{322}^{SH}\mathbf{h}_{322}^{SH}] \\
\frac{d\mathbf{h}_{333}^{SH}}{dt} = & \frac{1}{16\pi^2} \left[-\mathbf{h}_{333}^{SH} \left(\sum_{i=S,H,H} (\mathcal{C}_{2L}(i)g_{2L}^2 + \mathcal{C}_{2R}(i)g_{2R}^2 + \mathcal{C}_\chi(i)g_\chi^2) \right) \right. \\
& +2\mathbf{Y}_{333}^{SH} \left(\sum_{i=S,H,H} (\mathcal{C}_{2L}(i)g_{2L}^2M_{2L} + \mathcal{C}_{2R}(i)g_{2R}^2M_{2R} + \mathcal{C}_\chi(i)g_\chi^2M_\chi) \right) \\
& +3\mathbf{h}_{333}^{SH}\mathbf{Y}_{113}^{SD}\mathbf{Y}_{113}^{SD} + 3\mathbf{h}_{333}^{SH}\mathbf{Y}_{223}^{SD}\mathbf{Y}_{223}^{SD} + 3\mathbf{h}_{333}^{SH}\mathbf{Y}_{333}^{SD}\mathbf{Y}_{333}^{SD} + 2\mathbf{h}_{333}^{SH}\mathbf{Y}_{311}^{SH}\mathbf{Y}_{311}^{SH} \\
& +2\mathbf{h}_{333}^{SH}\mathbf{Y}_{322}^{SH}\mathbf{Y}_{322}^{SH} + 12\mathbf{h}_{333}^{SH}\mathbf{Y}_{333}^{SH}\mathbf{Y}_{333}^{SH} + 6\mathbf{h}_{333}^{SH}\mathbf{Y}_{333}^Q\mathbf{Y}_{333}^Q + 2\mathbf{h}_{333}^{SH}\mathbf{Y}_{131}^{SH}\mathbf{Y}_{131}^{SH} \\
& +2\mathbf{h}_{333}^{SH}\mathbf{Y}_{232}^{SH}\mathbf{Y}_{232}^{SH} + 6\mathbf{Y}_{333}^{SH}\mathbf{Y}_{113}^{SD}\mathbf{h}_{113}^{SD} + 6\mathbf{Y}_{333}^{SH}\mathbf{Y}_{223}^{SD}\mathbf{h}_{223}^{SD} + 6\mathbf{Y}_{333}^{SH}\mathbf{Y}_{333}^{SD}\mathbf{h}_{333}^{SD} \\
& +4\mathbf{Y}_{333}^{SH}\mathbf{Y}_{311}^{SH}\mathbf{h}_{311}^{SH} + 4\mathbf{Y}_{333}^{SH}\mathbf{Y}_{322}^{SH}\mathbf{h}_{322}^{SH} + 12\mathbf{Y}_{333}^{SH}\mathbf{Y}_{333}^Q\mathbf{h}_{333}^Q + 4\mathbf{Y}_{333}^{SH}\mathbf{Y}_{131}^{SH}\mathbf{h}_{131}^{SH} \\
& \left. +4\mathbf{Y}_{333}^{SH}\mathbf{Y}_{232}^{SH}\mathbf{h}_{232}^{SH} \right]
\end{aligned}$$

B.5.5 Running of the Scalar SSB-Masses

$$\begin{aligned}
\frac{d(\mathbf{m}_{LL}^2)_{11}}{dt} = & \frac{1}{16\pi^2} \left[6\mathbf{h}_{111}^{Dc}\mathbf{h}_{111}^{Dc} \right. \\
& +6(\mathbf{m}_{LL}^2)_{11}\mathbf{Y}_{111}^{Dc}\mathbf{Y}_{111}^{Dc} + 6(\mathbf{m}_{D^c}^2)_{11}\mathbf{Y}_{111}^{Dc}\mathbf{Y}_{111}^{Dc} + 6(\mathbf{m}_{Q_L}^2)_{11}\mathbf{Y}_{111}^{Dc}\mathbf{Y}_{111}^{Dc} \\
& -8(\mathcal{C}_{2L}(L_L)M_{2L}^2g_{2L}^2 + \mathcal{C}_{B-L}(L_L)M_{B-L}^2g_{B-L}^2 + \mathcal{C}_\chi(L_L)M_\chi^2g_\chi^2) \\
& \left. +2Q_{B-L}^{LL}g_{B-L}^2\mathcal{S}_{B-L} + 2Q_\chi^{LL}g_\chi^2\mathcal{S}_\chi \right]
\end{aligned}$$

$$\begin{aligned}
\frac{d(\mathbf{m}_{LL}^2)_{22}}{dt} = & \frac{1}{16\pi^2} \left[6\mathbf{h}_{222}^{Dc}\mathbf{h}_{222}^{Dc} \right. \\
& +6(\mathbf{m}_{LL}^2)_{22}\mathbf{Y}_{222}^{Dc}\mathbf{Y}_{222}^{Dc} + 6(\mathbf{m}_{D^c}^2)_{22}\mathbf{Y}_{222}^{Dc}\mathbf{Y}_{222}^{Dc} + 6(\mathbf{m}_{Q_L}^2)_{22}\mathbf{Y}_{222}^{Dc}\mathbf{Y}_{222}^{Dc} \\
& -8(\mathcal{C}_{2L}(L_L)M_{2L}^2g_{2L}^2 + \mathcal{C}_{B-L}(L_L)M_{B-L}^2g_{B-L}^2 + \mathcal{C}_\chi(L_L)M_\chi^2g_\chi^2) \\
& \left. +2Q_{B-L}^{LL}g_{B-L}^2\mathcal{S}_{B-L} + 2Q_\chi^{LL}g_\chi^2\mathcal{S}_\chi \right]
\end{aligned}$$

$$\begin{aligned}
\frac{d(\mathbf{m}_{LL}^2)_{33}}{dt} = & \frac{1}{16\pi^2} \left[6\mathbf{h}_{333}^{Dc}\mathbf{h}_{333}^{Dc} \right. \\
& +6(\mathbf{m}_{LL}^2)_{33}\mathbf{Y}_{333}^{Dc}\mathbf{Y}_{333}^{Dc} + 6(\mathbf{m}_{D^c}^2)_{33}\mathbf{Y}_{333}^{Dc}\mathbf{Y}_{333}^{Dc} + 6(\mathbf{m}_{Q_L}^2)_{33}\mathbf{Y}_{333}^{Dc}\mathbf{Y}_{333}^{Dc} \\
& -8(\mathcal{C}_{2L}(L_L)M_{2L}^2g_{2L}^2 + \mathcal{C}_{B-L}(L_L)M_{B-L}^2g_{B-L}^2 + \mathcal{C}_\chi(L_L)M_\chi^2g_\chi^2) \\
& \left. +2Q_{B-L}^{LL}g_{B-L}^2\mathcal{S}_{B-L} + 2Q_\chi^{LL}g_\chi^2\mathcal{S}_\chi \right]
\end{aligned}$$

$$\begin{aligned}
\frac{d(\mathbf{m}_{LR}^2)_{11}}{dt} = & \frac{1}{16\pi^2} \left[6\mathbf{h}_{111}^D\mathbf{h}_{111}^D \right. \\
& +6(\mathbf{m}_{LR}^2)_{11}\mathbf{Y}_{111}^D\mathbf{Y}_{111}^D + 6(\mathbf{m}_D^2)_{11}\mathbf{Y}_{111}^D\mathbf{Y}_{111}^D + 6(\mathbf{m}_{Q_R}^2)_{11}\mathbf{Y}_{111}^D\mathbf{Y}_{111}^D \\
& -8(\mathcal{C}_{2R}(L_R)M_{2R}^2g_{2R}^2 + \mathcal{C}_{B-L}(L_R)M_{B-L}^2g_{B-L}^2 + \mathcal{C}_\chi(L_R)M_\chi^2g_\chi^2) \\
& \left. +2Q_{B-L}^{LR}g_{B-L}^2\mathcal{S}_{B-L} + 2Q_\chi^{LR}g_\chi^2\mathcal{S}_\chi \right]
\end{aligned}$$

$$\begin{aligned}
\frac{d(\mathbf{m}_{LR}^2)_{22}}{dt} = & \frac{1}{16\pi^2} \left[6\mathbf{h}_{222}^D\mathbf{h}_{222}^D \right. \\
& +6(\mathbf{m}_{LR}^2)_{22}\mathbf{Y}_{222}^D\mathbf{Y}_{222}^D + 6(\mathbf{m}_D^2)_{22}\mathbf{Y}_{222}^D\mathbf{Y}_{222}^D + 6(\mathbf{m}_{Q_R}^2)_{22}\mathbf{Y}_{222}^D\mathbf{Y}_{222}^D \\
& -8(\mathcal{C}_{2R}(L_R)M_{2R}^2g_{2R}^2 + \mathcal{C}_{B-L}(L_R)M_{B-L}^2g_{B-L}^2 + \mathcal{C}_\chi(L_R)M_\chi^2g_\chi^2) \\
& \left. +2Q_{B-L}^{LR}g_{B-L}^2\mathcal{S}_{B-L} + 2Q_\chi^{LR}g_\chi^2\mathcal{S}_\chi \right]
\end{aligned}$$

$$\frac{d(\mathbf{m}_{LR}^2)_{33}}{dt} = \frac{1}{16\pi^2} \left[6\mathbf{h}_{333}^D\mathbf{h}_{333}^D \right]$$

$$\begin{aligned}
& +6(\mathbf{m}_{L_R}^2)_{33} \mathbf{Y}_{333}^D \mathbf{Y}_{333}^D + 6(\mathbf{m}_D^2)_{33} \mathbf{Y}_{333}^D \mathbf{Y}_{333}^D + 6(\mathbf{m}_{Q_R}^2)_{33} \mathbf{Y}_{333}^D \mathbf{Y}_{333}^D \\
& -8(\mathcal{C}_{2R}(L_R)M_{2R}^2g_{2R}^2 + \mathcal{C}_{B-L}(L_R)M_{B-L}^2g_{B-L}^2 + \mathcal{C}_\chi(L_R)M_\chi^2g_\chi^2) \\
& +2Q_{B-L}^{LR}g_{B-L}^2\mathcal{S}_{B-L} + 2Q_\chi^{LR}g_\chi^2\mathcal{S}_\chi \Big] \\
\frac{d(\mathbf{m}_{Q_L}^2)_{11}}{dt} &= \frac{1}{16\pi^2} \Big[2\mathbf{h}_{111}^{Dc} \mathbf{h}_{111}^{Dc} \\
& +2(\mathbf{m}_{Q_L}^2)_{11} \mathbf{Y}_{111}^{Dc} \mathbf{Y}_{111}^{Dc} + 2(\mathbf{m}_{D^c}^2)_{11} \mathbf{Y}_{111}^{Dc} \mathbf{Y}_{111}^{Dc} + 2(\mathbf{m}_{L_L}^2)_{11} \mathbf{Y}_{111}^{Dc} \mathbf{Y}_{111}^{Dc} \\
& -8(\mathcal{C}_3(Q_L)M_3^2g_3^2 + \mathcal{C}_{2L}(Q_L)M_{2L}^2g_{2L}^2 + \mathcal{C}_{B-L}(Q_L)M_{B-L}^2g_{B-L}^2 + \mathcal{C}_\chi(Q_L)M_\chi^2g_\chi^2) \\
& +2Q_{B-L}^{QL}g_{B-L}^2\mathcal{S}_{B-L} + 2Q_\chi^{QL}g_\chi^2\mathcal{S}_\chi \Big] \\
\frac{d(\mathbf{m}_{Q_L}^2)_{22}}{dt} &= \frac{1}{16\pi^2} \Big[2\mathbf{h}_{222}^{Dc} \mathbf{h}_{222}^{Dc} \\
& +2(\mathbf{m}_{Q_L}^2)_{22} \mathbf{Y}_{222}^{Dc} \mathbf{Y}_{222}^{Dc} + 2(\mathbf{m}_{D^c}^2)_{22} \mathbf{Y}_{222}^{Dc} \mathbf{Y}_{222}^{Dc} + 2(\mathbf{m}_{L_L}^2)_{22} \mathbf{Y}_{222}^{Dc} \mathbf{Y}_{222}^{Dc} \\
& -8(\mathcal{C}_3(Q_L)M_3^2g_3^2 + \mathcal{C}_{2L}(Q_L)M_{2L}^2g_{2L}^2 + \mathcal{C}_{B-L}(Q_L)M_{B-L}^2g_{B-L}^2 + \mathcal{C}_\chi(Q_L)M_\chi^2g_\chi^2) \\
& +2Q_{B-L}^{QL}g_{B-L}^2\mathcal{S}_{B-L} + 2Q_\chi^{QL}g_\chi^2\mathcal{S}_\chi \Big] \\
\frac{d(\mathbf{m}_{Q_L}^2)_{33}}{dt} &= \frac{1}{16\pi^2} \Big[4\mathbf{h}_{333}^Q \mathbf{h}_{333}^Q + 2\mathbf{h}_{333}^{Dc} \mathbf{h}_{333}^{Dc} \\
& +4(\mathbf{m}_{Q_L}^2)_{33} \mathbf{Y}_{333}^Q \mathbf{Y}_{333}^Q + 2(\mathbf{m}_{Q_L}^2)_{33} \mathbf{Y}_{333}^{Dc} \mathbf{Y}_{333}^{Dc} + 4(\mathbf{m}_H^2)_{33} \mathbf{Y}_{333}^Q \mathbf{Y}_{333}^Q \\
& +4(\mathbf{m}_{Q_R}^2)_{33} \mathbf{Y}_{333}^Q \mathbf{Y}_{333}^Q + 2(\mathbf{m}_{D^c}^2)_{33} \mathbf{Y}_{333}^{Dc} \mathbf{Y}_{333}^{Dc} + 2(\mathbf{m}_{L_L}^2)_{33} \mathbf{Y}_{333}^{Dc} \mathbf{Y}_{333}^{Dc} \\
& -8(\mathcal{C}_3(Q_L)M_3^2g_3^2 + \mathcal{C}_{2L}(Q_L)M_{2L}^2g_{2L}^2 + \mathcal{C}_{B-L}(Q_L)M_{B-L}^2g_{B-L}^2 + \mathcal{C}_\chi(Q_L)M_\chi^2g_\chi^2) \\
& +2Q_{B-L}^{QL}g_{B-L}^2\mathcal{S}_{B-L} + 2Q_\chi^{QL}g_\chi^2\mathcal{S}_\chi \Big] \\
\frac{d(\mathbf{m}_{Q_R}^2)_{11}}{dt} &= \frac{1}{16\pi^2} \Big[2\mathbf{h}_{111}^D \mathbf{h}_{111}^D \\
& +2(\mathbf{m}_{Q_R}^2)_{11} \mathbf{Y}_{111}^D \mathbf{Y}_{111}^D + 2(\mathbf{m}_D^2)_{11} \mathbf{Y}_{111}^D \mathbf{Y}_{111}^D + 2(\mathbf{m}_{L_R}^2)_{11} \mathbf{Y}_{111}^D \mathbf{Y}_{111}^D \\
& -8(\mathcal{C}_3(Q_R)M_3^2g_3^2 + \mathcal{C}_{2R}(Q_R)M_{2R}^2g_{2R}^2 + \mathcal{C}_{B-L}(Q_R)M_{B-L}^2g_{B-L}^2 + \mathcal{C}_\chi(Q_R)M_\chi^2g_\chi^2) \\
& +2Q_{B-L}^{QR}g_{B-L}^2\mathcal{S}_{B-L} + 2Q_\chi^{QR}g_\chi^2\mathcal{S}_\chi \Big] \\
\frac{d(\mathbf{m}_{Q_R}^2)_{22}}{dt} &= \frac{1}{16\pi^2} \Big[2\mathbf{h}_{222}^D \mathbf{h}_{222}^D \\
& +2(\mathbf{m}_{Q_R}^2)_{22} \mathbf{Y}_{222}^D \mathbf{Y}_{222}^D + 2(\mathbf{m}_D^2)_{22} \mathbf{Y}_{222}^D \mathbf{Y}_{222}^D + 2(\mathbf{m}_{L_R}^2)_{22} \mathbf{Y}_{222}^D \mathbf{Y}_{222}^D \\
& -8(\mathcal{C}_3(Q_R)M_3^2g_3^2 + \mathcal{C}_{2R}(Q_R)M_{2R}^2g_{2R}^2 + \mathcal{C}_{B-L}(Q_R)M_{B-L}^2g_{B-L}^2 + \mathcal{C}_\chi(Q_R)M_\chi^2g_\chi^2) \\
& +2Q_{B-L}^{QR}g_{B-L}^2\mathcal{S}_{B-L} + 2Q_\chi^{QR}g_\chi^2\mathcal{S}_\chi \Big] \\
\frac{d(\mathbf{m}_{Q_R}^2)_{33}}{dt} &= \frac{1}{16\pi^2} \Big[4\mathbf{h}_{333}^Q \mathbf{h}_{333}^Q + 2\mathbf{h}_{333}^D \mathbf{h}_{333}^D \\
& +4(\mathbf{m}_{Q_R}^2)_{33} \mathbf{Y}_{333}^Q \mathbf{Y}_{333}^Q + 2(\mathbf{m}_{Q_R}^2)_{33} \mathbf{Y}_{333}^D \mathbf{Y}_{333}^D + 4(\mathbf{m}_H^2)_{33} \mathbf{Y}_{333}^Q \mathbf{Y}_{333}^Q \\
& +4(\mathbf{m}_{Q_L}^2)_{33} \mathbf{Y}_{333}^Q \mathbf{Y}_{333}^Q + 2(\mathbf{m}_D^2)_{33} \mathbf{Y}_{333}^D \mathbf{Y}_{333}^D + 2(\mathbf{m}_{L_R}^2)_{33} \mathbf{Y}_{333}^D \mathbf{Y}_{333}^D \\
& -8(\mathcal{C}_3(Q_R)M_3^2g_3^2 + \mathcal{C}_{2R}(Q_R)M_{2R}^2g_{2R}^2 + \mathcal{C}_{B-L}(Q_R)M_{B-L}^2g_{B-L}^2 + \mathcal{C}_\chi(Q_R)M_\chi^2g_\chi^2) \\
& +2Q_{B-L}^{QR}g_{B-L}^2\mathcal{S}_{B-L} + 2Q_\chi^{QR}g_\chi^2\mathcal{S}_\chi \Big] \\
\frac{d(\mathbf{m}_H^2)_{11}}{dt} &= \frac{1}{16\pi^2} \Big[2\mathbf{h}_{311}^{SH} \mathbf{h}_{311}^{SH} + 2\mathbf{h}_{131}^{SH} \mathbf{h}_{131}^{SH} \\
& +10(\mathbf{m}_H^2)_{11} \mathbf{Y}_{311}^{SH} \mathbf{Y}_{311}^{SH} + 2(\mathbf{m}_H^2)_{11} \mathbf{Y}_{131}^{SH} \mathbf{Y}_{131}^{SH} + 8(\mathbf{m}_S^2)_{33} \mathbf{Y}_{311}^{SH} \mathbf{Y}_{311}^{SH} \\
& +2(\mathbf{m}_H^2)_{33} \mathbf{Y}_{131}^{SH} \mathbf{Y}_{131}^{SH} + 2(\mathbf{m}_S^2)_{11} \mathbf{Y}_{131}^{SH} \mathbf{Y}_{131}^{SH} \\
& -8(\mathcal{C}_{2L}(H)M_{2L}^2g_{2L}^2 + \mathcal{C}_{2R}(H)M_{2R}^2g_{2R}^2 + \mathcal{C}_\chi(H)M_\chi^2g_\chi^2) \Big]
\end{aligned}$$

$$\begin{aligned}
& +2Q_\chi^H g_\chi^2 \mathcal{S}_\chi \Big] \\
\frac{d(\mathbf{m}_H^2)_{22}}{dt} &= \frac{1}{16\pi^2} \Big[2\mathbf{h}_{322}^{SH} \mathbf{h}_{322}^{SH} + 2\mathbf{h}_{232}^{SH} \mathbf{h}_{232}^{SH} \\
& +10(\mathbf{m}_H^2)_{22} \mathbf{Y}_{322}^{SH} \mathbf{Y}_{322}^{SH} + 2(\mathbf{m}_H^2)_{22} \mathbf{Y}_{232}^{SH} \mathbf{Y}_{232}^{SH} + 8(\mathbf{m}_S^2)_{33} \mathbf{Y}_{322}^{SH} \mathbf{Y}_{322}^{SH} \\
& +2(\mathbf{m}_H^2)_{33} \mathbf{Y}_{232}^{SH} \mathbf{Y}_{232}^{SH} + 2(\mathbf{m}_S^2)_{22} \mathbf{Y}_{232}^{SH} \mathbf{Y}_{232}^{SH} \\
& -8(\mathcal{C}_{2L}(H)M_{2L}^2 g_{2L}^2 + \mathcal{C}_{2R}(H)M_{2R}^2 g_{2R}^2 + \mathcal{C}_\chi(H)M_\chi^2 g_\chi^2) \\
& +2Q_\chi^H g_\chi^2 \mathcal{S}_\chi \Big] \\
\frac{d(\mathbf{m}_H^2)_{33}}{dt} &= \frac{1}{16\pi^2} \Big[6\mathbf{h}_{333}^Q \mathbf{h}_{333}^Q + 2\mathbf{h}_{131}^{SH} \mathbf{h}_{131}^{SH} + 2\mathbf{h}_{232}^{SH} \mathbf{h}_{232}^{SH} + 2\mathbf{h}_{333}^{SH} \mathbf{h}_{333}^{SH} \\
& +6(\mathbf{m}_H^2)_{33} \mathbf{Y}_{333}^Q \mathbf{Y}_{333}^Q + 2(\mathbf{m}_H^2)_{33} \mathbf{Y}_{131}^{SH} \mathbf{Y}_{131}^{SH} + 2(\mathbf{m}_H^2)_{33} \mathbf{Y}_{232}^{SH} \mathbf{Y}_{232}^{SH} \\
& +10(\mathbf{m}_H^2)_{33} \mathbf{Y}_{333}^{SH} \mathbf{Y}_{333}^{SH} + 6(\mathbf{m}_{Q_R}^2)_{33} \mathbf{Y}_{333}^Q \mathbf{Y}_{333}^Q + 6(\mathbf{m}_{Q_L}^2)_{33} \mathbf{Y}_{333}^Q \mathbf{Y}_{333}^Q \\
& +2(\mathbf{m}_H^2)_{11} \mathbf{Y}_{131}^{SH} \mathbf{Y}_{131}^{SH} + 2(\mathbf{m}_S^2)_{11} \mathbf{Y}_{131}^{SH} \mathbf{Y}_{131}^{SH} + 2(\mathbf{m}_H^2)_{22} \mathbf{Y}_{232}^{SH} \mathbf{Y}_{232}^{SH} \\
& +2(\mathbf{m}_S^2)_{22} \mathbf{Y}_{232}^{SH} \mathbf{Y}_{232}^{SH} + 8(\mathbf{m}_S^2)_{33} \mathbf{Y}_{333}^{SH} \mathbf{Y}_{333}^{SH} \\
& -8(\mathcal{C}_{2L}(H)M_{2L}^2 g_{2L}^2 + \mathcal{C}_{2R}(H)M_{2R}^2 g_{2R}^2 + \mathcal{C}_\chi(H)M_\chi^2 g_\chi^2) \\
& +2Q_\chi^H g_\chi^2 \mathcal{S}_\chi \Big] \\
\frac{d(\mathbf{m}_D^2)_{11}}{dt} &= \frac{1}{16\pi^2} \Big[4\mathbf{h}_{111}^D \mathbf{h}_{111}^D + 2\mathbf{h}_{113}^{SD} \mathbf{h}_{113}^{SD} \\
& +4(\mathbf{m}_D^2)_{11} \mathbf{Y}_{111}^D \mathbf{Y}_{111}^D + 2(\mathbf{m}_D^2)_{11} \mathbf{Y}_{113}^{SD} \mathbf{Y}_{113}^{SD} + 4(\mathbf{m}_{Q_R}^2)_{11} \mathbf{Y}_{111}^D \mathbf{Y}_{111}^D \\
& +4(\mathbf{m}_{L_R}^2)_{11} \mathbf{Y}_{111}^D \mathbf{Y}_{111}^D + 2(\mathbf{m}_S^2)_{33} \mathbf{Y}_{113}^{SD} \mathbf{Y}_{113}^{SD} + 2(\mathbf{m}_{D^c}^2)_{11} \mathbf{Y}_{113}^{SD} \mathbf{Y}_{113}^{SD} \\
& -8(\mathcal{C}_3(D)M_3^2 g_3^2 + \mathcal{C}_{B-L}(D)M_{B-L}^2 g_{B-L}^2 + \mathcal{C}_\chi(D)M_\chi^2 g_\chi^2) \\
& +2Q_{B-L}^D g_{B-L}^2 \mathcal{S}_{B-L} + 2Q_\chi^D g_\chi^2 \mathcal{S}_\chi \Big] \\
\frac{d(\mathbf{m}_D^2)_{22}}{dt} &= \frac{1}{16\pi^2} \Big[4\mathbf{h}_{222}^D \mathbf{h}_{222}^D + 2\mathbf{h}_{223}^{SD} \mathbf{h}_{223}^{SD} \\
& +4(\mathbf{m}_D^2)_{22} \mathbf{Y}_{222}^D \mathbf{Y}_{222}^D + 2(\mathbf{m}_D^2)_{22} \mathbf{Y}_{223}^{SD} \mathbf{Y}_{223}^{SD} + 4(\mathbf{m}_{Q_R}^2)_{22} \mathbf{Y}_{222}^D \mathbf{Y}_{222}^D \\
& +4(\mathbf{m}_{L_R}^2)_{22} \mathbf{Y}_{222}^D \mathbf{Y}_{222}^D + 2(\mathbf{m}_S^2)_{33} \mathbf{Y}_{223}^{SD} \mathbf{Y}_{223}^{SD} + 2(\mathbf{m}_{D^c}^2)_{22} \mathbf{Y}_{223}^{SD} \mathbf{Y}_{223}^{SD} \\
& -8(\mathcal{C}_3(D)M_3^2 g_3^2 + \mathcal{C}_{B-L}(D)M_{B-L}^2 g_{B-L}^2 + \mathcal{C}_\chi(D)M_\chi^2 g_\chi^2) \\
& +2Q_{B-L}^D g_{B-L}^2 \mathcal{S}_{B-L} + 2Q_\chi^D g_\chi^2 \mathcal{S}_\chi \Big] \\
\frac{d(\mathbf{m}_D^2)_{33}}{dt} &= \frac{1}{16\pi^2} \Big[4\mathbf{h}_{333}^D \mathbf{h}_{333}^D + 2\mathbf{h}_{333}^{SD} \mathbf{h}_{333}^{SD} \\
& +4(\mathbf{m}_D^2)_{33} \mathbf{Y}_{333}^D \mathbf{Y}_{333}^D + 2(\mathbf{m}_D^2)_{33} \mathbf{Y}_{333}^{SD} \mathbf{Y}_{333}^{SD} + 4(\mathbf{m}_{Q_R}^2)_{33} \mathbf{Y}_{333}^D \mathbf{Y}_{333}^D \\
& +4(\mathbf{m}_{L_R}^2)_{33} \mathbf{Y}_{333}^D \mathbf{Y}_{333}^D + 2(\mathbf{m}_S^2)_{33} \mathbf{Y}_{333}^{SD} \mathbf{Y}_{333}^{SD} + 2(\mathbf{m}_{D^c}^2)_{33} \mathbf{Y}_{333}^{SD} \mathbf{Y}_{333}^{SD} \\
& -8(\mathcal{C}_3(D)M_3^2 g_3^2 + \mathcal{C}_{B-L}(D)M_{B-L}^2 g_{B-L}^2 + \mathcal{C}_\chi(D)M_\chi^2 g_\chi^2) \\
& +2Q_{B-L}^D g_{B-L}^2 \mathcal{S}_{B-L} + 2Q_\chi^D g_\chi^2 \mathcal{S}_\chi \Big] \\
\frac{d(\mathbf{m}_{D^c}^2)_{11}}{dt} &= \frac{1}{16\pi^2} \Big[4\mathbf{h}_{111}^{Dc} \mathbf{h}_{111}^{Dc} + 2\mathbf{h}_{113}^{SD} \mathbf{h}_{113}^{SD} \\
& +4(\mathbf{m}_{D^c}^2)_{11} \mathbf{Y}_{111}^{Dc} \mathbf{Y}_{111}^{Dc} + 2(\mathbf{m}_{D^c}^2)_{11} \mathbf{Y}_{113}^{SD} \mathbf{Y}_{113}^{SD} + 4(\mathbf{m}_{Q_L}^2)_{11} \mathbf{Y}_{111}^{Dc} \mathbf{Y}_{111}^{Dc} \\
& +4(\mathbf{m}_{L_L}^2)_{11} \mathbf{Y}_{111}^{Dc} \mathbf{Y}_{111}^{Dc} + 2(\mathbf{m}_S^2)_{33} \mathbf{Y}_{113}^{SD} \mathbf{Y}_{113}^{SD} + 2(\mathbf{m}_D^2)_{11} \mathbf{Y}_{113}^{SD} \mathbf{Y}_{113}^{SD} \\
& -8(\mathcal{C}_3(D^c)M_3^2 g_3^2 + \mathcal{C}_{B-L}(D^c)M_{B-L}^2 g_{B-L}^2 + \mathcal{C}_\chi(D^c)M_\chi^2 g_\chi^2) \\
& +2Q_{B-L}^{D^c} g_{B-L}^2 \mathcal{S}_{B-L} + 2Q_\chi^{D^c} g_\chi^2 \mathcal{S}_\chi \Big]
\end{aligned}$$

$$\begin{aligned}
\frac{d(\mathbf{m}_{D^c}^2)_{22}}{dt} &= \frac{1}{16\pi^2} \left[4\mathbf{h}_{222}^{D^c} \mathbf{h}_{222}^{D^c} + 2\mathbf{h}_{223}^{SD} \mathbf{h}_{223}^{SD} \right. \\
&\quad + 4(\mathbf{m}_{D^c}^2)_{22} \mathbf{Y}_{222}^{D^c} \mathbf{Y}_{222}^{D^c} + 2(\mathbf{m}_{D^c}^2)_{22} \mathbf{Y}_{223}^{SD} \mathbf{Y}_{223}^{SD} + 4(\mathbf{m}_{Q_L}^2)_{22} \mathbf{Y}_{222}^{D^c} \mathbf{Y}_{222}^{D^c} \\
&\quad + 4(\mathbf{m}_{L_L}^2)_{22} \mathbf{Y}_{222}^{D^c} \mathbf{Y}_{222}^{D^c} + 2(\mathbf{m}_S^2)_{33} \mathbf{Y}_{223}^{SD} \mathbf{Y}_{223}^{SD} + 2(\mathbf{m}_D^2)_{22} \mathbf{Y}_{223}^{SD} \mathbf{Y}_{223}^{SD} \\
&\quad - 8(\mathcal{C}_3(D^c)M_3^2 g_3^2 + \mathcal{C}_{B-L}(D^c)M_{B-L}^2 g_{B-L}^2 + \mathcal{C}_\chi(D^c)M_\chi^2 g_\chi^2) \\
&\quad \left. + 2Q_{B-L}^{D^c} g_{B-L}^2 \mathcal{S}_{B-L} + 2Q_\chi^{D^c} g_\chi^2 \mathcal{S}_\chi \right] \\
\frac{d(\mathbf{m}_{D^c}^2)_{33}}{dt} &= \frac{1}{16\pi^2} \left[4\mathbf{h}_{333}^{D^c} \mathbf{h}_{333}^{D^c} + 2\mathbf{h}_{333}^{SD} \mathbf{h}_{333}^{SD} \right. \\
&\quad + 4(\mathbf{m}_{D^c}^2)_{33} \mathbf{Y}_{333}^{D^c} \mathbf{Y}_{333}^{D^c} + 2(\mathbf{m}_{D^c}^2)_{33} \mathbf{Y}_{333}^{SD} \mathbf{Y}_{333}^{SD} + 4(\mathbf{m}_{Q_L}^2)_{33} \mathbf{Y}_{333}^{D^c} \mathbf{Y}_{333}^{D^c} \\
&\quad + 4(\mathbf{m}_{L_L}^2)_{33} \mathbf{Y}_{333}^{D^c} \mathbf{Y}_{333}^{D^c} + 2(\mathbf{m}_S^2)_{33} \mathbf{Y}_{333}^{SD} \mathbf{Y}_{333}^{SD} + 2(\mathbf{m}_D^2)_{33} \mathbf{Y}_{333}^{SD} \mathbf{Y}_{333}^{SD} \\
&\quad - 8(\mathcal{C}_3(D^c)M_3^2 g_3^2 + \mathcal{C}_{B-L}(D^c)M_{B-L}^2 g_{B-L}^2 + \mathcal{C}_\chi(D^c)M_\chi^2 g_\chi^2) \\
&\quad \left. + 2Q_{B-L}^{D^c} g_{B-L}^2 \mathcal{S}_{B-L} + 2Q_\chi^{D^c} g_\chi^2 \mathcal{S}_\chi \right] \\
\frac{d(\mathbf{m}_S^2)_{11}}{dt} &= \frac{1}{16\pi^2} \left[8\mathbf{h}_{131}^{SH} \mathbf{h}_{131}^{SH} \right. \\
&\quad + 8(\mathbf{m}_S^2)_{11} \mathbf{Y}_{131}^{SH} \mathbf{Y}_{131}^{SH} + 8(\mathbf{m}_H^2)_{11} \mathbf{Y}_{131}^{SH} \mathbf{Y}_{131}^{SH} + 8(\mathbf{m}_H^2)_{33} \mathbf{Y}_{131}^{SH} \mathbf{Y}_{131}^{SH} \\
&\quad - 8(\mathcal{C}_\chi(S)M_\chi^2 g_\chi^2) \\
&\quad \left. + 2Q_\chi^S g_\chi^2 \mathcal{S}_\chi \right] \\
\frac{d(\mathbf{m}_S^2)_{22}}{dt} &= \frac{1}{16\pi^2} \left[8\mathbf{h}_{232}^{SH} \mathbf{h}_{232}^{SH} \right. \\
&\quad + 8(\mathbf{m}_S^2)_{22} \mathbf{Y}_{232}^{SH} \mathbf{Y}_{232}^{SH} + 8(\mathbf{m}_H^2)_{22} \mathbf{Y}_{232}^{SH} \mathbf{Y}_{232}^{SH} + 8(\mathbf{m}_H^2)_{33} \mathbf{Y}_{232}^{SH} \mathbf{Y}_{232}^{SH} \\
&\quad - 8(\mathcal{C}_\chi(S)M_\chi^2 g_\chi^2) \\
&\quad \left. + 2Q_\chi^S g_\chi^2 \mathcal{S}_\chi \right] \\
\frac{d(\mathbf{m}_S^2)_{33}}{dt} &= \frac{1}{16\pi^2} \left[6\mathbf{h}_{113}^{SD} \mathbf{h}_{113}^{SD} + 6\mathbf{h}_{223}^{SD} \mathbf{h}_{223}^{SD} + 6\mathbf{h}_{333}^{SD} \mathbf{h}_{333}^{SD} + 4\mathbf{h}_{311}^{SH} \mathbf{h}_{311}^{SH} \right. \\
&\quad + 4\mathbf{h}_{322}^{SH} \mathbf{h}_{322}^{SH} + 4\mathbf{h}_{333}^{SH} \mathbf{h}_{333}^{SH} \\
&\quad + 6(\mathbf{m}_S^2)_{33} \mathbf{Y}_{113}^{SD} \mathbf{Y}_{113}^{SD} + 6(\mathbf{m}_S^2)_{33} \mathbf{Y}_{223}^{SD} \mathbf{Y}_{223}^{SD} + 6(\mathbf{m}_S^2)_{33} \mathbf{Y}_{333}^{SD} \mathbf{Y}_{333}^{SD} \\
&\quad + 4(\mathbf{m}_S^2)_{33} \mathbf{Y}_{311}^{SH} \mathbf{Y}_{311}^{SH} + 4(\mathbf{m}_S^2)_{33} \mathbf{Y}_{322}^{SH} \mathbf{Y}_{322}^{SH} + 4(\mathbf{m}_S^2)_{33} \mathbf{Y}_{333}^{SH} \mathbf{Y}_{333}^{SH} \\
&\quad + 6(\mathbf{m}_{D^c}^2)_{11} \mathbf{Y}_{113}^{SD} \mathbf{Y}_{113}^{SD} + 6(\mathbf{m}_D^2)_{11} \mathbf{Y}_{113}^{SD} \mathbf{Y}_{113}^{SD} + 6(\mathbf{m}_{D^c}^2)_{22} \mathbf{Y}_{223}^{SD} \mathbf{Y}_{223}^{SD} \\
&\quad + 6(\mathbf{m}_D^2)_{22} \mathbf{Y}_{223}^{SD} \mathbf{Y}_{223}^{SD} + 6(\mathbf{m}_{D^c}^2)_{33} \mathbf{Y}_{333}^{SD} \mathbf{Y}_{333}^{SD} + 6(\mathbf{m}_D^2)_{33} \mathbf{Y}_{333}^{SD} \mathbf{Y}_{333}^{SD} \\
&\quad + 16(\mathbf{m}_H^2)_{11} \mathbf{Y}_{311}^{SH} \mathbf{Y}_{311}^{SH} + 16(\mathbf{m}_H^2)_{22} \mathbf{Y}_{322}^{SH} \mathbf{Y}_{322}^{SH} + 16(\mathbf{m}_H^2)_{33} \mathbf{Y}_{333}^{SH} \mathbf{Y}_{333}^{SH} \\
&\quad - 8(\mathcal{C}_\chi(S)M_\chi^2 g_\chi^2) \\
&\quad \left. + 2Q_\chi^S g_\chi^2 \mathcal{S}_\chi \right] \\
\frac{d(\mathbf{m}_{V_{LL}}^2)_{11}}{dt} &= \frac{1}{16\pi^2} \left[\right. \\
&\quad - 8(\mathcal{C}_{2L}(V_{LL})M_{2L}^2 g_{2L}^2 + \mathcal{C}_{B-L}(V_{LL})M_{B-L}^2 g_{B-L}^2 + \mathcal{C}_\chi(V_{LL})M_\chi^2 g_\chi^2) \\
&\quad \left. + 2Q_{B-L}^{V_{LL}} g_{B-L}^2 \mathcal{S}_{B-L} + 2Q_\chi^{V_{LL}} g_\chi^2 \mathcal{S}_\chi \right] \\
\frac{d(\mathbf{m}_{V_{LL}}^2)_{22}}{dt} &= \frac{1}{16\pi^2} \left[\right. \\
&\quad - 8(\mathcal{C}_{2L}(V_{LL})M_{2L}^2 g_{2L}^2 + \mathcal{C}_{B-L}(V_{LL})M_{B-L}^2 g_{B-L}^2 + \mathcal{C}_\chi(V_{LL})M_\chi^2 g_\chi^2) \\
&\quad \left. + 2Q_{B-L}^{V_{LL}} g_{B-L}^2 \mathcal{S}_{B-L} + 2Q_\chi^{V_{LL}} g_\chi^2 \mathcal{S}_\chi \right]
\end{aligned}$$

$$\begin{aligned}
& +2Q_{B-L}^{V_{LL}} g_{B-L}^2 \mathcal{S}_{B-L} + 2Q_{\chi}^{V_{LL}} g_{\chi}^2 \mathcal{S}_{\chi} \Big] \\
\frac{d(\mathbf{m}_{V_{LR}}^2)_{11}}{dt} &= \frac{1}{16\pi^2} \Big[\\
& -8(C_{2R}(V_{LR})M_{2R}^2 g_{2R}^2 + C_{B-L}(V_{LR})M_{B-L}^2 g_{B-L}^2 + C_{\chi}(V_{LR})M_{\chi}^2 g_{\chi}^2) \\
& +2Q_{B-L}^{V_{LR}} g_{B-L}^2 \mathcal{S}_{B-L} + 2Q_{\chi}^{V_{LR}} g_{\chi}^2 \mathcal{S}_{\chi} \Big] \\
\frac{d(\mathbf{m}_{V_{LR}}^2)_{22}}{dt} &= \frac{1}{16\pi^2} \Big[\\
& -8(C_{2R}(V_{LR})M_{2R}^2 g_{2R}^2 + C_{B-L}(V_{LR})M_{B-L}^2 g_{B-L}^2 + C_{\chi}(V_{LR})M_{\chi}^2 g_{\chi}^2) \\
& +2Q_{B-L}^{V_{LR}} g_{B-L}^2 \mathcal{S}_{B-L} + 2Q_{\chi}^{V_{LR}} g_{\chi}^2 \mathcal{S}_{\chi} \Big]
\end{aligned}$$

where the following abbreviations have been employed:

$$\begin{aligned}
\mathcal{S}_{B-L} &= 2Q_{B-L}(\mathbf{m}_{LL}^2)_{11}^{LL} + 2Q_{B-L}(\mathbf{m}_{LL}^2)_{22}^{LL} + 2Q_{B-L}(\mathbf{m}_{LL}^2)_{33}^{LL} + 2Q_{B-L}(\mathbf{m}_{LR}^2)_{11}^{LR} \\
& + 2Q_{B-L}(\mathbf{m}_{LR}^2)_{22}^{LR} + 2Q_{B-L}(\mathbf{m}_{LR}^2)_{33}^{LR} + 6Q_{B-L}(\mathbf{m}_{QL}^2)_{11}^{QL} + 6Q_{B-L}(\mathbf{m}_{QL}^2)_{22}^{QL} \\
& + 6Q_{B-L}(\mathbf{m}_{QL}^2)_{33}^{QL} + 6Q_{B-L}(\mathbf{m}_{QR}^2)_{11}^{QR} + 6Q_{B-L}(\mathbf{m}_{QR}^2)_{22}^{QR} + 6Q_{B-L}(\mathbf{m}_{QR}^2)_{33}^{QR} \\
& + 3Q_{B-L}(\mathbf{m}_D^2)_{11}^D + 3Q_{B-L}(\mathbf{m}_D^2)_{22}^D + 3Q_{B-L}(\mathbf{m}_D^2)_{33}^D + 3Q_{B-L}(\mathbf{m}_{D^c}^2)_{11}^{D^c} \\
& + 3Q_{B-L}(\mathbf{m}_{D^c}^2)_{22}^{D^c} + 3Q_{B-L}(\mathbf{m}_{D^c}^2)_{33}^{D^c} + 2Q_{B-L}(\mathbf{m}_{V_{LL}}^2)_{11}^{V_{LL}} + 2Q_{B-L}(\mathbf{m}_{V_{LL}}^2)_{22}^{V_{LL}} \\
& + 2Q_{B-L}(\mathbf{m}_{V_{LR}}^2)_{11}^{V_{LR}} + 2Q_{B-L}(\mathbf{m}_{V_{LR}}^2)_{22}^{V_{LR}} \\
\mathcal{S}_{\chi} &= 2Q_{\chi}(\mathbf{m}_{LL}^2)_{11}^{LL} + 2Q_{\chi}(\mathbf{m}_{LL}^2)_{22}^{LL} + 2Q_{\chi}(\mathbf{m}_{LL}^2)_{33}^{LL} + 2Q_{\chi}(\mathbf{m}_{LR}^2)_{11}^{LR} \\
& + 2Q_{\chi}(\mathbf{m}_{LR}^2)_{22}^{LR} + 2Q_{\chi}(\mathbf{m}_{LR}^2)_{33}^{LR} + 6Q_{\chi}(\mathbf{m}_{QL}^2)_{11}^{QL} + 6Q_{\chi}(\mathbf{m}_{QL}^2)_{22}^{QL} \\
& + 6Q_{\chi}(\mathbf{m}_{QL}^2)_{33}^{QL} + 6Q_{\chi}(\mathbf{m}_{QR}^2)_{11}^{QR} + 6Q_{\chi}(\mathbf{m}_{QR}^2)_{22}^{QR} + 6Q_{\chi}(\mathbf{m}_{QR}^2)_{33}^{QR} \\
& + 4Q_{\chi}(\mathbf{m}_H^2)_{11}^H + 4Q_{\chi}(\mathbf{m}_H^2)_{22}^H + 4Q_{\chi}(\mathbf{m}_H^2)_{33}^H + 3Q_{\chi}(\mathbf{m}_D^2)_{11}^D \\
& + 3Q_{\chi}(\mathbf{m}_D^2)_{22}^D + 3Q_{\chi}(\mathbf{m}_D^2)_{33}^D + 3Q_{\chi}(\mathbf{m}_{D^c}^2)_{11}^{D^c} + 3Q_{\chi}(\mathbf{m}_{D^c}^2)_{22}^{D^c} \\
& + 3Q_{\chi}(\mathbf{m}_{D^c}^2)_{33}^{D^c} + 1Q_{\chi}(\mathbf{m}_S^2)_{11}^S + 1Q_{\chi}(\mathbf{m}_S^2)_{22}^S + 1Q_{\chi}(\mathbf{m}_S^2)_{33}^S \\
& + 2Q_{\chi}(\mathbf{m}_{V_{LL}}^2)_{11}^{V_{LL}} + 2Q_{\chi}(\mathbf{m}_{V_{LL}}^2)_{22}^{V_{LL}} + 2Q_{\chi}(\mathbf{m}_{V_{LR}}^2)_{11}^{V_{LR}} + 2Q_{\chi}(\mathbf{m}_{V_{LR}}^2)_{22}^{V_{LR}}
\end{aligned}$$

B.6 RGEs below Λ_{int}

B.6.1 Running of the Gauge Couplings

$$\begin{aligned}
\frac{dg_3}{dt} &= \frac{1}{16\pi^2}(0)g_3^3 \\
\frac{dg_{2L}}{dt} &= \frac{1}{16\pi^2}(3)g_{2L}^3
\end{aligned}$$

$$\begin{aligned}\frac{dg_A}{dt} &= \frac{1}{16\pi^2} (9)g_A^3 \\ \frac{dg_B}{dt} &= \frac{1}{16\pi^2} (\beta^{Q_B})g_B^3\end{aligned}$$

B.6.2 Running of the Gaugino Masses

$$\begin{aligned}\frac{dM_3}{dt} &= \frac{1}{16\pi^2} 0g_3^2 M_3 \\ \frac{dM_{2L}}{dt} &= \frac{1}{16\pi^2} 6g_{2L}^2 M_{2L} \\ \frac{dM_A}{dt} &= \frac{1}{16\pi^2} 18g_A^2 M_A \\ \frac{dM_B}{dt} &= \frac{1}{16\pi^2} 2\beta^{Q_B} g_B^2 M_B \\ \frac{dM_{AB}}{dt} &= \frac{1}{16\pi^2} (\beta^A g_A^2 + \beta^B g_B^2) M_{AB}\end{aligned}$$

B.6.3 Running of the Yukawa Couplings

$$\begin{aligned}\frac{d\mathbf{Y}_{333}^d}{dt} &= \frac{1}{16\pi^2} \left[-\mathbf{Y}_{333}^d \left(\sum_{i=Q_L, d^c, H^d} (\mathcal{C}_3(i) g_3^2 + \mathcal{C}_{2L}(i) g_{2L}^2 + \mathcal{C}_A(i) g_A^2 + \mathcal{C}_B(i) g_B^2) \right) \right. \\ &\quad + 6\mathbf{Y}_{333}^d \mathbf{Y}_{333}^d \mathbf{Y}_{333}^d + \mathbf{Y}_{333}^d \mathbf{Y}_{333}^u \mathbf{Y}_{333}^u + \mathbf{Y}_{333}^d \mathbf{Y}_{333}^{Dc} \mathbf{Y}_{333}^{Dc} + \mathbf{Y}_{333}^d \mathbf{Y}_{131}^{SH} \mathbf{Y}_{131}^{SH} \\ &\quad \left. + \mathbf{Y}_{333}^d \mathbf{Y}_{232}^{SH} \mathbf{Y}_{232}^{SH} + \mathbf{Y}_{333}^d \mathbf{Y}_{333}^{SH} \mathbf{Y}_{333}^{SH} \right] \\ \frac{d\mathbf{Y}_{333}^u}{dt} &= \frac{1}{16\pi^2} \left[-\mathbf{Y}_{333}^u \left(\sum_{i=Q_L, u^c, H^u} (\mathcal{C}_3(i) g_3^2 + \mathcal{C}_{2L}(i) g_{2L}^2 + \mathcal{C}_A(i) g_A^2 + \mathcal{C}_B(i) g_B^2) \right) \right. \\ &\quad + \mathbf{Y}_{333}^u \mathbf{Y}_{333}^d \mathbf{Y}_{333}^d + 6\mathbf{Y}_{333}^u \mathbf{Y}_{333}^u \mathbf{Y}_{333}^u + \mathbf{Y}_{333}^u \mathbf{Y}_{333}^{Dc} \mathbf{Y}_{333}^{Dc} + \mathbf{Y}_{333}^u \mathbf{Y}_{333}^D \mathbf{Y}_{333}^D \\ &\quad \left. + \mathbf{Y}_{333}^u \mathbf{Y}_{113}^{SH} \mathbf{Y}_{113}^{SH} + \mathbf{Y}_{333}^u \mathbf{Y}_{223}^{SH} \mathbf{Y}_{223}^{SH} + \mathbf{Y}_{333}^u \mathbf{Y}_{333}^{SH} \mathbf{Y}_{333}^{SH} \right] \\ \frac{d\mathbf{Y}_{111}^D}{dt} &= \frac{1}{16\pi^2} \left[-\mathbf{Y}_{111}^D \left(\sum_{i=e^c, u^c, D} (\mathcal{C}_3(i) g_3^2 + \mathcal{C}_A(i) g_A^2 + \mathcal{C}_B(i) g_B^2) \right) \right. \\ &\quad \left. + 5\mathbf{Y}_{111}^D \mathbf{Y}_{111}^D \mathbf{Y}_{111}^D + \mathbf{Y}_{111}^D \mathbf{Y}_{113}^{SD} \mathbf{Y}_{113}^{SD} \right] \\ \frac{d\mathbf{Y}_{222}^D}{dt} &= \frac{1}{16\pi^2} \left[-\mathbf{Y}_{222}^D \left(\sum_{i=e^c, u^c, D} (\mathcal{C}_3(i) g_3^2 + \mathcal{C}_A(i) g_A^2 + \mathcal{C}_B(i) g_B^2) \right) \right. \\ &\quad \left. + 5\mathbf{Y}_{222}^D \mathbf{Y}_{222}^D \mathbf{Y}_{222}^D + \mathbf{Y}_{222}^D \mathbf{Y}_{223}^{SD} \mathbf{Y}_{223}^{SD} \right] \\ \frac{d\mathbf{Y}_{333}^D}{dt} &= \frac{1}{16\pi^2} \left[-\mathbf{Y}_{333}^D \left(\sum_{i=e^c, u^c, D} (\mathcal{C}_3(i) g_3^2 + \mathcal{C}_A(i) g_A^2 + \mathcal{C}_B(i) g_B^2) \right) \right. \\ &\quad \left. + 5\mathbf{Y}_{333}^D \mathbf{Y}_{333}^D \mathbf{Y}_{333}^D + 2\mathbf{Y}_{333}^D \mathbf{Y}_{333}^u \mathbf{Y}_{333}^u + \mathbf{Y}_{333}^D \mathbf{Y}_{333}^{SD} \mathbf{Y}_{333}^{SD} \right] \\ \frac{d\mathbf{Y}_{111}^{Dc}}{dt} &= \frac{1}{16\pi^2} \left[-\mathbf{Y}_{111}^{Dc} \left(\sum_{i=L_L, Q_L, D^c} (\mathcal{C}_3(i) g_3^2 + \mathcal{C}_{2L}(i) g_{2L}^2 + \mathcal{C}_A(i) g_A^2 + \mathcal{C}_B(i) g_B^2) \right) \right. \\ &\quad \left. + 6\mathbf{Y}_{111}^{Dc} \mathbf{Y}_{111}^{Dc} \mathbf{Y}_{111}^{Dc} + \mathbf{Y}_{111}^{Dc} \mathbf{Y}_{113}^{SD} \mathbf{Y}_{113}^{SD} \right]\end{aligned}$$

$$\begin{aligned}
\frac{d\mathbf{Y}_{222}^{Dc}}{dt} &= \frac{1}{16\pi^2} \left[-\mathbf{Y}_{222}^{Dc} \left(\sum_{i=L_L, Q_L, D^c} (\mathcal{C}_3(i) g_3^2 + \mathcal{C}_{2L}(i) g_{2L}^2 + \mathcal{C}_A(i) g_A^2 + \mathcal{C}_B(i) g_B^2) \right) \right. \\
&\quad \left. + 6\mathbf{Y}_{222}^{Dc} \mathbf{Y}_{222}^{Dc} \mathbf{Y}_{222}^{Dc} + \mathbf{Y}_{222}^{Dc} \mathbf{Y}_{223}^{SD} \mathbf{Y}_{223}^{SD} \right] \\
\frac{d\mathbf{Y}_{333}^{Dc}}{dt} &= \frac{1}{16\pi^2} \left[-\mathbf{Y}_{333}^{Dc} \left(\sum_{i=L_L, Q_L, D^c} (\mathcal{C}_3(i) g_3^2 + \mathcal{C}_{2L}(i) g_{2L}^2 + \mathcal{C}_A(i) g_A^2 + \mathcal{C}_B(i) g_B^2) \right) \right. \\
&\quad \left. + 6\mathbf{Y}_{333}^{Dc} \mathbf{Y}_{333}^{Dc} \mathbf{Y}_{333}^{Dc} + \mathbf{Y}_{333}^{Dc} \mathbf{Y}_{333}^d \mathbf{Y}_{333}^d + \mathbf{Y}_{333}^{Dc} \mathbf{Y}_{333}^u \mathbf{Y}_{333}^u + \mathbf{Y}_{333}^{Dc} \mathbf{Y}_{333}^{SD} \mathbf{Y}_{333}^{SD} \right] \\
\frac{d\mathbf{Y}_{113}^{SD}}{dt} &= \frac{1}{16\pi^2} \left[-\mathbf{Y}_{113}^{SD} \left(\sum_{i=D, D^c, S} (\mathcal{C}_3(i) g_3^2 + \mathcal{C}_A(i) g_A^2 + \mathcal{C}_B(i) g_B^2) \right) \right. \\
&\quad + \mathbf{Y}_{113}^{SD} \mathbf{Y}_{111}^D \mathbf{Y}_{111}^D + 5\mathbf{Y}_{113}^{SD} \mathbf{Y}_{113}^{SD} \mathbf{Y}_{113}^{SD} + 2\mathbf{Y}_{113}^{SD} \mathbf{Y}_{111}^{Dc} \mathbf{Y}_{111}^{Dc} + 3\mathbf{Y}_{113}^{SD} \mathbf{Y}_{223}^{SD} \mathbf{Y}_{223}^{SD} \\
&\quad \left. + 3\mathbf{Y}_{113}^{SD} \mathbf{Y}_{333}^{SD} \mathbf{Y}_{333}^{SD} + 2\mathbf{Y}_{113}^{SD} \mathbf{Y}_{311}^{SH} \mathbf{Y}_{311}^{SH} + 2\mathbf{Y}_{113}^{SD} \mathbf{Y}_{322}^{SH} \mathbf{Y}_{322}^{SH} + 2\mathbf{Y}_{113}^{SD} \mathbf{Y}_{333}^{SH} \mathbf{Y}_{333}^{SH} \right] \\
\frac{d\mathbf{Y}_{223}^{SD}}{dt} &= \frac{1}{16\pi^2} \left[-\mathbf{Y}_{223}^{SD} \left(\sum_{i=D, D^c, S} (\mathcal{C}_3(i) g_3^2 + \mathcal{C}_A(i) g_A^2 + \mathcal{C}_B(i) g_B^2) \right) \right. \\
&\quad + \mathbf{Y}_{223}^{SD} \mathbf{Y}_{222}^D \mathbf{Y}_{222}^D + 5\mathbf{Y}_{223}^{SD} \mathbf{Y}_{223}^{SD} \mathbf{Y}_{223}^{SD} + 2\mathbf{Y}_{223}^{SD} \mathbf{Y}_{222}^{Dc} \mathbf{Y}_{222}^{Dc} + 3\mathbf{Y}_{223}^{SD} \mathbf{Y}_{113}^{SD} \mathbf{Y}_{113}^{SD} \\
&\quad \left. + 3\mathbf{Y}_{223}^{SD} \mathbf{Y}_{333}^{SD} \mathbf{Y}_{333}^{SD} + 2\mathbf{Y}_{223}^{SD} \mathbf{Y}_{311}^{SH} \mathbf{Y}_{311}^{SH} + 2\mathbf{Y}_{223}^{SD} \mathbf{Y}_{322}^{SH} \mathbf{Y}_{322}^{SH} + 2\mathbf{Y}_{223}^{SD} \mathbf{Y}_{333}^{SH} \mathbf{Y}_{333}^{SH} \right] \\
\frac{d\mathbf{Y}_{333}^{SD}}{dt} &= \frac{1}{16\pi^2} \left[-\mathbf{Y}_{333}^{SD} \left(\sum_{i=D, D^c, S} (\mathcal{C}_3(i) g_3^2 + \mathcal{C}_A(i) g_A^2 + \mathcal{C}_B(i) g_B^2) \right) \right. \\
&\quad + \mathbf{Y}_{333}^{SD} \mathbf{Y}_{333}^D \mathbf{Y}_{333}^D + 5\mathbf{Y}_{333}^{SD} \mathbf{Y}_{333}^{SD} \mathbf{Y}_{333}^{SD} + 2\mathbf{Y}_{333}^{SD} \mathbf{Y}_{333}^{Dc} \mathbf{Y}_{333}^{Dc} + 3\mathbf{Y}_{333}^{SD} \mathbf{Y}_{113}^{SD} \mathbf{Y}_{113}^{SD} \\
&\quad \left. + 3\mathbf{Y}_{333}^{SD} \mathbf{Y}_{223}^{SD} \mathbf{Y}_{223}^{SD} + 2\mathbf{Y}_{333}^{SD} \mathbf{Y}_{311}^{SH} \mathbf{Y}_{311}^{SH} + 2\mathbf{Y}_{333}^{SD} \mathbf{Y}_{322}^{SH} \mathbf{Y}_{322}^{SH} + 2\mathbf{Y}_{333}^{SD} \mathbf{Y}_{333}^{SH} \mathbf{Y}_{333}^{SH} \right] \\
\frac{d\mathbf{Y}_{311}^{SH}}{dt} &= \frac{1}{16\pi^2} \left[-\mathbf{Y}_{311}^{SH} \left(\sum_{i=S, H^d, H^u} (\mathcal{C}_{2L}(i) g_{2L}^2 + \mathcal{C}_A(i) g_A^2 + \mathcal{C}_B(i) g_B^2) \right) \right. \\
&\quad + 3\mathbf{Y}_{311}^{SH} \mathbf{Y}_{113}^{SD} \mathbf{Y}_{113}^{SD} + 3\mathbf{Y}_{311}^{SH} \mathbf{Y}_{223}^{SD} \mathbf{Y}_{223}^{SD} + 3\mathbf{Y}_{311}^{SH} \mathbf{Y}_{333}^{SD} \mathbf{Y}_{333}^{SD} + 4\mathbf{Y}_{311}^{SH} \mathbf{Y}_{311}^{SH} \mathbf{Y}_{311}^{SH} \\
&\quad \left. + 2\mathbf{Y}_{311}^{SH} \mathbf{Y}_{322}^{SH} \mathbf{Y}_{322}^{SH} + 2\mathbf{Y}_{311}^{SH} \mathbf{Y}_{333}^{SH} \mathbf{Y}_{333}^{SH} + \mathbf{Y}_{311}^{SH} \mathbf{Y}_{113}^{SH} \mathbf{Y}_{113}^{SH} + \mathbf{Y}_{311}^{SH} \mathbf{Y}_{131}^{SH} \mathbf{Y}_{131}^{SH} \right] \\
\frac{d\mathbf{Y}_{322}^{SH}}{dt} &= \frac{1}{16\pi^2} \left[-\mathbf{Y}_{322}^{SH} \left(\sum_{i=S, H^d, H^u} (\mathcal{C}_{2L}(i) g_{2L}^2 + \mathcal{C}_A(i) g_A^2 + \mathcal{C}_B(i) g_B^2) \right) \right. \\
&\quad + 3\mathbf{Y}_{322}^{SH} \mathbf{Y}_{113}^{SD} \mathbf{Y}_{113}^{SD} + 3\mathbf{Y}_{322}^{SH} \mathbf{Y}_{223}^{SD} \mathbf{Y}_{223}^{SD} + 3\mathbf{Y}_{322}^{SH} \mathbf{Y}_{333}^{SD} \mathbf{Y}_{333}^{SD} + 2\mathbf{Y}_{322}^{SH} \mathbf{Y}_{311}^{SH} \mathbf{Y}_{311}^{SH} \\
&\quad \left. + 4\mathbf{Y}_{322}^{SH} \mathbf{Y}_{322}^{SH} \mathbf{Y}_{322}^{SH} + 2\mathbf{Y}_{322}^{SH} \mathbf{Y}_{333}^{SH} \mathbf{Y}_{333}^{SH} + \mathbf{Y}_{322}^{SH} \mathbf{Y}_{223}^{SH} \mathbf{Y}_{223}^{SH} + \mathbf{Y}_{322}^{SH} \mathbf{Y}_{232}^{SH} \mathbf{Y}_{232}^{SH} \right] \\
\frac{d\mathbf{Y}_{131}^{SH}}{dt} &= \frac{1}{16\pi^2} \left[-\mathbf{Y}_{131}^{SH} \left(\sum_{i=S, H^d, H^u} (\mathcal{C}_{2L}(i) g_{2L}^2 + \mathcal{C}_A(i) g_A^2 + \mathcal{C}_B(i) g_B^2) \right) \right. \\
&\quad + 4\mathbf{Y}_{131}^{SH} \mathbf{Y}_{131}^{SH} \mathbf{Y}_{131}^{SH} + 2\mathbf{Y}_{131}^{SH} \mathbf{Y}_{113}^{SH} \mathbf{Y}_{113}^{SH} + 3\mathbf{Y}_{131}^{SH} \mathbf{Y}_{333}^d \mathbf{Y}_{333}^d + \mathbf{Y}_{131}^{SH} \mathbf{Y}_{232}^{SH} \mathbf{Y}_{232}^{SH} \\
&\quad \left. + \mathbf{Y}_{131}^{SH} \mathbf{Y}_{333}^{SH} \mathbf{Y}_{333}^{SH} + \mathbf{Y}_{131}^{SH} \mathbf{Y}_{311}^{SH} \mathbf{Y}_{311}^{SH} \right] \\
\frac{d\mathbf{Y}_{232}^{SH}}{dt} &= \frac{1}{16\pi^2} \left[-\mathbf{Y}_{232}^{SH} \left(\sum_{i=S, H^d, H^u} (\mathcal{C}_{2L}(i) g_{2L}^2 + \mathcal{C}_A(i) g_A^2 + \mathcal{C}_B(i) g_B^2) \right) \right. \\
&\quad + 4\mathbf{Y}_{232}^{SH} \mathbf{Y}_{232}^{SH} \mathbf{Y}_{232}^{SH} + 2\mathbf{Y}_{232}^{SH} \mathbf{Y}_{223}^{SH} \mathbf{Y}_{223}^{SH} + 3\mathbf{Y}_{232}^{SH} \mathbf{Y}_{333}^d \mathbf{Y}_{333}^d + \mathbf{Y}_{232}^{SH} \mathbf{Y}_{131}^{SH} \mathbf{Y}_{131}^{SH} \\
&\quad \left. + \mathbf{Y}_{232}^{SH} \mathbf{Y}_{333}^{SH} \mathbf{Y}_{333}^{SH} + \mathbf{Y}_{232}^{SH} \mathbf{Y}_{322}^{SH} \mathbf{Y}_{322}^{SH} \right] \\
\frac{d\mathbf{Y}_{113}^{SH}}{dt} &= \frac{1}{16\pi^2} \left[-\mathbf{Y}_{113}^{SH} \left(\sum_{i=S, H^d, H^u} (\mathcal{C}_{2L}(i) g_{2L}^2 + \mathcal{C}_A(i) g_A^2 + \mathcal{C}_B(i) g_B^2) \right) \right. \\
&\quad \left. + 2\mathbf{Y}_{113}^{SH} \mathbf{Y}_{131}^{SH} \mathbf{Y}_{131}^{SH} + 4\mathbf{Y}_{113}^{SH} \mathbf{Y}_{113}^{SH} \mathbf{Y}_{113}^{SH} + \mathbf{Y}_{113}^{SH} \mathbf{Y}_{311}^{SH} \mathbf{Y}_{311}^{SH} + 3\mathbf{Y}_{113}^{SH} \mathbf{Y}_{333}^u \mathbf{Y}_{333}^u \right]
\end{aligned}$$

$$\begin{aligned}
& + \mathbf{Y}_{113}^{SH} \mathbf{Y}_{223}^{SH} \mathbf{Y}_{223}^{SH} + \mathbf{Y}_{113}^{SH} \mathbf{Y}_{333}^{SH} \mathbf{Y}_{333}^{SH} \Big] \\
\frac{d\mathbf{Y}_{223}^{SH}}{dt} &= \frac{1}{16\pi^2} \left[-\mathbf{Y}_{223}^{SH} \left(\sum_{i=S,H^d,H^u} (C_{2L}(i) g_{2L}^2 + C_A(i) g_A^2 + C_B(i) g_B^2) \right) \right. \\
& + 2\mathbf{Y}_{223}^{SH} \mathbf{Y}_{232}^{SH} \mathbf{Y}_{232}^{SH} + 4\mathbf{Y}_{223}^{SH} \mathbf{Y}_{223}^{SH} \mathbf{Y}_{223}^{SH} + \mathbf{Y}_{223}^{SH} \mathbf{Y}_{322}^{SH} \mathbf{Y}_{322}^{SH} + 3\mathbf{Y}_{223}^{SH} \mathbf{Y}_{333}^u \mathbf{Y}_{333}^u \\
& \left. + \mathbf{Y}_{223}^{SH} \mathbf{Y}_{113}^{SH} \mathbf{Y}_{113}^{SH} + \mathbf{Y}_{223}^{SH} \mathbf{Y}_{333}^{SH} \mathbf{Y}_{333}^{SH} \right] \\
\frac{d\mathbf{Y}_{333}^{SH}}{dt} &= \frac{1}{16\pi^2} \left[-\mathbf{Y}_{333}^{SH} \left(\sum_{i=S,H^d,H^u} (C_{2L}(i) g_{2L}^2 + C_A(i) g_A^2 + C_B(i) g_B^2) \right) \right. \\
& + 3\mathbf{Y}_{333}^{SH} \mathbf{Y}_{113}^{SD} \mathbf{Y}_{113}^{SD} + 3\mathbf{Y}_{333}^{SH} \mathbf{Y}_{223}^{SD} \mathbf{Y}_{223}^{SD} + 3\mathbf{Y}_{333}^{SH} \mathbf{Y}_{333}^{SD} \mathbf{Y}_{333}^{SD} + 2\mathbf{Y}_{333}^{SH} \mathbf{Y}_{311}^{SH} \mathbf{Y}_{311}^{SH} \\
& + 2\mathbf{Y}_{333}^{SH} \mathbf{Y}_{322}^{SH} \mathbf{Y}_{322}^{SH} + 4\mathbf{Y}_{333}^{SH} \mathbf{Y}_{333}^{SH} \mathbf{Y}_{333}^{SH} + 3\mathbf{Y}_{333}^{SH} \mathbf{Y}_{333}^d \mathbf{Y}_{333}^d + \mathbf{Y}_{333}^{SH} \mathbf{Y}_{131}^{SH} \mathbf{Y}_{131}^{SH} \\
& \left. + \mathbf{Y}_{333}^{SH} \mathbf{Y}_{232}^{SH} \mathbf{Y}_{232}^{SH} + 3\mathbf{Y}_{333}^{SH} \mathbf{Y}_{333}^u \mathbf{Y}_{333}^u + \mathbf{Y}_{333}^{SH} \mathbf{Y}_{113}^{SH} \mathbf{Y}_{113}^{SH} + \mathbf{Y}_{333}^{SH} \mathbf{Y}_{223}^{SH} \mathbf{Y}_{223}^{SH} \right]
\end{aligned} \tag{B.6}$$

Running of the Yukawa couplings from $M_{Z'}$ to M_{SSM} with an MSSM-like particle content.

$$\begin{aligned}
\frac{d\mathbf{Y}_{333}^d}{dt} &= \frac{1}{16\pi^2} \left[-\mathbf{Y}_{333}^d \left(\sum_{i=Q_L,d^c,H^d} (C_3(i) g_3^2 + C_{2L}(i) g_{2L}^2 + C_Y(i) g_Y^2) \right) \right. \\
& \left. + 6\mathbf{Y}_{333}^d \mathbf{Y}_{333}^d \mathbf{Y}_{333}^d + \mathbf{Y}_{333}^d \mathbf{Y}_{333}^u \mathbf{Y}_{333}^u \right] \\
\frac{d\mathbf{Y}_{333}^u}{dt} &= \frac{1}{16\pi^2} \left[-\mathbf{Y}_{333}^u \left(\sum_{i=Q_L,u^c,H^u} (C_3(i) g_3^2 + C_{2L}(i) g_{2L}^2 + C_Y(i) g_Y^2) \right) \right. \\
& \left. + \mathbf{Y}_{333}^u \mathbf{Y}_{333}^d \mathbf{Y}_{333}^d + 6\mathbf{Y}_{333}^u \mathbf{Y}_{333}^u \mathbf{Y}_{333}^u \right]
\end{aligned} \tag{B.7}$$

Running of the Yukawa couplings from M_{SSM} to M_Z to with standard model particle content and two Higgs doublets.

$$\begin{aligned}
\frac{d\mathbf{Y}_{333}^d}{dt} &= \frac{1}{16\pi^2} \left[-\mathbf{Y}_{333}^d \left(\sum_{i=Q_L,d^c,H^d} (C_3(i) g_3^2 + C_{2L}(i) g_{2L}^2 + C_Y(i) g_Y^2) \right) \right. \\
& \left. + \frac{9}{2} \mathbf{Y}_{333}^d \mathbf{Y}_{333}^d \mathbf{Y}_{333}^d + \frac{1}{2} \mathbf{Y}_{333}^d \mathbf{Y}_{333}^u \mathbf{Y}_{333}^u \right] \\
\frac{d\mathbf{Y}_{333}^u}{dt} &= \frac{1}{16\pi^2} \left[-\mathbf{Y}_{333}^u \left(\sum_{i=Q_L,u^c,H^u} (C_3(i) g_3^2 + C_{2L}(i) g_{2L}^2 + C_Y(i) g_Y^2) \right) \right. \\
& \left. + \frac{1}{2} \mathbf{Y}_{333}^u \mathbf{Y}_{333}^d \mathbf{Y}_{333}^d + \frac{9}{2} \mathbf{Y}_{333}^u \mathbf{Y}_{333}^u \mathbf{Y}_{333}^u \right]
\end{aligned} \tag{B.8}$$

B.6.4 Running of the Trilinear SSB-Terms

$$\begin{aligned}
\frac{d\mathbf{h}_{333}^d}{dt} &= \frac{1}{16\pi^2} \left[-\mathbf{h}_{333}^d \left(\sum_{i=Q_L,d^c,H^d} (C_3(i) g_3^2 + C_{2L}(i) g_{2L}^2 + C_A(i) g_A^2 + C_B(i) g_B^2) \right) \right. \\
& + 2\mathbf{Y}_{333}^d \left(\sum_{i=Q_L,d^c,H^d} (C_3(i) g_3^2 M_3 + C_{2L}(i) g_{2L}^2 M_{2L} + C_A(i) g_A^2 M_A + \right. \\
& \left. \left. 2C_{AB}(i) g_A g_B M_{AB} + C_B(i) g_B^2 M_B) \right) \right. \\
& \left. + 18\mathbf{h}_{333}^d \mathbf{Y}_{333}^d \mathbf{Y}_{333}^d + \mathbf{h}_{333}^d \mathbf{Y}_{333}^u \mathbf{Y}_{333}^u + \mathbf{h}_{333}^d \mathbf{Y}_{333}^{Dc} \mathbf{Y}_{333}^{Dc} + \mathbf{h}_{333}^d \mathbf{Y}_{131}^{SH} \mathbf{Y}_{131}^{SH} \right]
\end{aligned}$$

$$\begin{aligned}
& +\mathbf{h}_{333}^d \mathbf{Y}_{232}^{SH} \mathbf{Y}_{232}^{SH} + \mathbf{h}_{333}^d \mathbf{Y}_{333}^{SH} \mathbf{Y}_{333}^{SH} + 2\mathbf{Y}_{333}^d \mathbf{Y}_{333}^u \mathbf{h}_{333}^u + 2\mathbf{Y}_{333}^d \mathbf{Y}_{333}^{Dc} \mathbf{h}_{333}^{Dc} \\
& + 2\mathbf{Y}_{333}^d \mathbf{Y}_{131}^{SH} \mathbf{h}_{131}^{SH} + 2\mathbf{Y}_{333}^d \mathbf{Y}_{232}^{SH} \mathbf{h}_{232}^{SH} + 2\mathbf{Y}_{333}^d \mathbf{Y}_{333}^{SH} \mathbf{h}_{333}^{SH} \Big] \\
\frac{d\mathbf{h}_{333}^u}{dt} &= \frac{1}{16\pi^2} \left[-\mathbf{h}_{333}^u \left(\sum_{i=Q_L, u^c, H^u} (\mathcal{C}_3(i) g_3^2 + \mathcal{C}_{2L}(i) g_{2L}^2 + \mathcal{C}_A(i) g_A^2 + \mathcal{C}_B(i) g_B^2) \right) \right. \\
& + 2\mathbf{Y}_{333}^u \left(\sum_{i=Q_L, u^c, H^u} (\mathcal{C}_3(i) g_3^2 M_3 + \mathcal{C}_{2L}(i) g_{2L}^2 M_{2L} + \mathcal{C}_A(i) g_A^2 M_A + \right. \\
& \quad \left. \left. 2\mathcal{C}_{AB}(i) g_A g_B M_{AB} + \mathcal{C}_B(i) g_B^2 M_B) \right) \right. \\
& + \mathbf{h}_{333}^u \mathbf{Y}_{333}^d \mathbf{Y}_{333}^d + 18\mathbf{h}_{333}^u \mathbf{Y}_{333}^u \mathbf{Y}_{333}^u + \mathbf{h}_{333}^u \mathbf{Y}_{333}^{Dc} \mathbf{Y}_{333}^{Dc} + \mathbf{h}_{333}^u \mathbf{Y}_{333}^D \mathbf{Y}_{333}^D \\
& + \mathbf{h}_{333}^u \mathbf{Y}_{113}^{SH} \mathbf{Y}_{113}^{SH} + \mathbf{h}_{333}^u \mathbf{Y}_{223}^{SH} \mathbf{Y}_{223}^{SH} + \mathbf{h}_{333}^u \mathbf{Y}_{333}^{SH} \mathbf{Y}_{333}^{SH} + 2\mathbf{Y}_{333}^u \mathbf{Y}_{333}^d \mathbf{h}_{333}^d \\
& + 2\mathbf{Y}_{333}^u \mathbf{Y}_{333}^{Dc} \mathbf{h}_{333}^{Dc} + 2\mathbf{Y}_{333}^u \mathbf{Y}_{333}^D \mathbf{h}_{333}^D + 2\mathbf{Y}_{333}^u \mathbf{Y}_{113}^{SH} \mathbf{h}_{113}^{SH} + 2\mathbf{Y}_{333}^u \mathbf{Y}_{223}^{SH} \mathbf{h}_{223}^{SH} \\
& \left. + 2\mathbf{Y}_{333}^u \mathbf{Y}_{333}^{SH} \mathbf{h}_{333}^{SH} \right] \\
\frac{d\mathbf{h}_{111}^D}{dt} &= \frac{1}{16\pi^2} \left[-\mathbf{h}_{111}^D \left(\sum_{i=e^c, u^c, D} (\mathcal{C}_3(i) g_3^2 + \mathcal{C}_A(i) g_A^2 + \mathcal{C}_B(i) g_B^2) \right) \right. \\
& + 2\mathbf{Y}_{111}^D \left(\sum_{i=e^c, u^c, D} (\mathcal{C}_3(i) g_3^2 M_3 + \mathcal{C}_A(i) g_A^2 M_A + \right. \\
& \quad \left. \left. 2\mathcal{C}_{AB}(i) g_A g_B M_{AB} + \mathcal{C}_B(i) g_B^2 M_B) \right) \right. \\
& + 15\mathbf{h}_{111}^D \mathbf{Y}_{111}^D \mathbf{Y}_{111}^D + \mathbf{h}_{111}^D \mathbf{Y}_{113}^{SD} \mathbf{Y}_{113}^{SD} + 2\mathbf{Y}_{111}^D \mathbf{Y}_{113}^{SD} \mathbf{h}_{113}^{SD} \Big] \\
\frac{d\mathbf{h}_{222}^D}{dt} &= \frac{1}{16\pi^2} \left[-\mathbf{h}_{222}^D \left(\sum_{i=e^c, u^c, D} (\mathcal{C}_3(i) g_3^2 + \mathcal{C}_A(i) g_A^2 + \mathcal{C}_B(i) g_B^2) \right) \right. \\
& + 2\mathbf{Y}_{222}^D \left(\sum_{i=e^c, u^c, D} (\mathcal{C}_3(i) g_3^2 M_3 + \mathcal{C}_A(i) g_A^2 M_A + \right. \\
& \quad \left. \left. 2\mathcal{C}_{AB}(i) g_A g_B M_{AB} + \mathcal{C}_B(i) g_B^2 M_B) \right) \right. \\
& + 15\mathbf{h}_{222}^D \mathbf{Y}_{222}^D \mathbf{Y}_{222}^D + \mathbf{h}_{222}^D \mathbf{Y}_{223}^{SD} \mathbf{Y}_{223}^{SD} + 2\mathbf{Y}_{222}^D \mathbf{Y}_{223}^{SD} \mathbf{h}_{223}^{SD} \Big] \\
\frac{d\mathbf{h}_{333}^D}{dt} &= \frac{1}{16\pi^2} \left[-\mathbf{h}_{333}^D \left(\sum_{i=e^c, u^c, D} (\mathcal{C}_3(i) g_3^2 + \mathcal{C}_A(i) g_A^2 + \mathcal{C}_B(i) g_B^2) \right) \right. \\
& + 2\mathbf{Y}_{333}^D \left(\sum_{i=e^c, u^c, D} (\mathcal{C}_3(i) g_3^2 M_3 + \mathcal{C}_A(i) g_A^2 M_A + \right. \\
& \quad \left. \left. 2\mathcal{C}_{AB}(i) g_A g_B M_{AB} + \mathcal{C}_B(i) g_B^2 M_B) \right) \right. \\
& + 15\mathbf{h}_{333}^D \mathbf{Y}_{333}^D \mathbf{Y}_{333}^D + 2\mathbf{h}_{333}^D \mathbf{Y}_{333}^u \mathbf{Y}_{333}^u + \mathbf{h}_{333}^D \mathbf{Y}_{333}^{SD} \mathbf{Y}_{333}^{SD} + 4\mathbf{Y}_{333}^D \mathbf{Y}_{333}^u \mathbf{h}_{333}^u \\
& \left. + 2\mathbf{Y}_{333}^D \mathbf{Y}_{333}^{SD} \mathbf{h}_{333}^{SD} \right] \\
\frac{d\mathbf{h}_{111}^{Dc}}{dt} &= \frac{1}{16\pi^2} \left[-\mathbf{h}_{111}^{Dc} \left(\sum_{i=L_L, Q_L, D^c} (\mathcal{C}_3(i) g_3^2 + \mathcal{C}_{2L}(i) g_{2L}^2 + \mathcal{C}_A(i) g_A^2 + \mathcal{C}_B(i) g_B^2) \right) \right. \\
& + 2\mathbf{Y}_{111}^{Dc} \left(\sum_{i=L_L, Q_L, D^c} (\mathcal{C}_3(i) g_3^2 M_3 + \mathcal{C}_{2L}(i) g_{2L}^2 M_{2L} + \mathcal{C}_A(i) g_A^2 M_A + \right. \\
& \quad \left. \left. 2\mathcal{C}_{AB}(i) g_A g_B M_{AB} + \mathcal{C}_B(i) g_B^2 M_B) \right) \right. \\
& + 18\mathbf{h}_{111}^{Dc} \mathbf{Y}_{111}^{Dc} \mathbf{Y}_{111}^{Dc} + \mathbf{h}_{111}^{Dc} \mathbf{Y}_{113}^{SD} \mathbf{Y}_{113}^{SD} + 2\mathbf{Y}_{111}^{Dc} \mathbf{Y}_{113}^{SD} \mathbf{h}_{113}^{SD} \Big] \\
\frac{d\mathbf{h}_{222}^{Dc}}{dt} &= \frac{1}{16\pi^2} \left[-\mathbf{h}_{222}^{Dc} \left(\sum_{i=L_L, Q_L, D^c} (\mathcal{C}_3(i) g_3^2 + \mathcal{C}_{2L}(i) g_{2L}^2 + \mathcal{C}_A(i) g_A^2 + \mathcal{C}_B(i) g_B^2) \right) \right.
\end{aligned}$$

$$\begin{aligned}
& +2\mathbf{Y}_{222}^{Dc} \left(\sum_{i=L_L, Q_L, D^c} (C_3(i) g_3^2 M_3 + C_{2L}(i) g_{2L}^2 M_{2L} + C_A(i) g_A^2 M_A + \right. \\
& \quad \left. 2C_{AB}(i) g_A g_B M_{AB} + C_B(i) g_B^2 M_B) \right) \\
& +18\mathbf{h}_{222}^{Dc} \mathbf{Y}_{222}^{Dc} \mathbf{Y}_{222}^{Dc} + \mathbf{h}_{222}^{Dc} \mathbf{Y}_{223}^{SD} \mathbf{Y}_{223}^{SD} + 2\mathbf{Y}_{222}^{Dc} \mathbf{Y}_{223}^{SD} \mathbf{h}_{223}^{SD} \\
\frac{d\mathbf{h}_{333}^{Dc}}{dt} = & \frac{1}{16\pi^2} \left[-\mathbf{h}_{333}^{Dc} \left(\sum_{i=L_L, Q_L, D^c} (C_3(i) g_3^2 + C_{2L}(i) g_{2L}^2 + C_A(i) g_A^2 + C_B(i) g_B^2) \right) \right. \\
& +2\mathbf{Y}_{333}^{Dc} \left(\sum_{i=L_L, Q_L, D^c} (C_3(i) g_3^2 M_3 + C_{2L}(i) g_{2L}^2 M_{2L} + C_A(i) g_A^2 M_A + \right. \\
& \quad \left. 2C_{AB}(i) g_A g_B M_{AB} + C_B(i) g_B^2 M_B) \right) \\
& +18\mathbf{h}_{333}^{Dc} \mathbf{Y}_{333}^{Dc} \mathbf{Y}_{333}^{Dc} + \mathbf{h}_{333}^{Dc} \mathbf{Y}_{333}^d \mathbf{Y}_{333}^d + \mathbf{h}_{333}^{Dc} \mathbf{Y}_{333}^u \mathbf{Y}_{333}^u + \mathbf{h}_{333}^{Dc} \mathbf{Y}_{333}^{SD} \mathbf{Y}_{333}^{SD} \\
& \left. +2\mathbf{Y}_{333}^{Dc} \mathbf{Y}_{333}^d \mathbf{h}_{333}^d + 2\mathbf{Y}_{333}^{Dc} \mathbf{Y}_{333}^u \mathbf{h}_{333}^u + 2\mathbf{Y}_{333}^{Dc} \mathbf{Y}_{333}^{SD} \mathbf{h}_{333}^{SD} \right] \\
\frac{d\mathbf{h}_{113}^{SD}}{dt} = & \frac{1}{16\pi^2} \left[-\mathbf{h}_{113}^{SD} \left(\sum_{i=D, D^c, S} (C_3(i) g_3^2 + C_A(i) g_A^2 + C_B(i) g_B^2) \right) \right. \\
& +2\mathbf{Y}_{113}^{SD} \left(\sum_{i=D, D^c, S} (C_3(i) g_3^2 M_3 + C_A(i) g_A^2 M_A + \right. \\
& \quad \left. 2C_{AB}(i) g_A g_B M_{AB} + C_B(i) g_B^2 M_B) \right) \\
& +\mathbf{h}_{113}^{SD} \mathbf{Y}_{111}^D \mathbf{Y}_{111}^D + 15\mathbf{h}_{113}^{SD} \mathbf{Y}_{113}^{SD} \mathbf{Y}_{113}^{SD} + 2\mathbf{h}_{113}^{SD} \mathbf{Y}_{111}^{Dc} \mathbf{Y}_{111}^{Dc} + 3\mathbf{h}_{113}^{SD} \mathbf{Y}_{223}^{SD} \mathbf{Y}_{223}^{SD} \\
& +3\mathbf{h}_{113}^{SD} \mathbf{Y}_{333}^{SD} \mathbf{Y}_{333}^{SD} + 2\mathbf{h}_{113}^{SD} \mathbf{Y}_{311}^{SH} \mathbf{Y}_{311}^{SH} + 2\mathbf{h}_{113}^{SD} \mathbf{Y}_{322}^{SH} \mathbf{Y}_{322}^{SH} + 2\mathbf{h}_{113}^{SD} \mathbf{Y}_{333}^{SH} \mathbf{Y}_{333}^{SH} \\
& +2\mathbf{Y}_{113}^{SD} \mathbf{Y}_{111}^D \mathbf{h}_{111}^D + 4\mathbf{Y}_{113}^{SD} \mathbf{Y}_{111}^{Dc} \mathbf{h}_{111}^{Dc} + 6\mathbf{Y}_{113}^{SD} \mathbf{Y}_{223}^{SD} \mathbf{h}_{223}^{SD} + 6\mathbf{Y}_{113}^{SD} \mathbf{Y}_{333}^{SD} \mathbf{h}_{333}^{SD} \\
& +4\mathbf{Y}_{113}^{SD} \mathbf{Y}_{311}^{SH} \mathbf{h}_{311}^{SH} + 4\mathbf{Y}_{113}^{SD} \mathbf{Y}_{322}^{SH} \mathbf{h}_{322}^{SH} + 4\mathbf{Y}_{113}^{SD} \mathbf{Y}_{333}^{SH} \mathbf{h}_{333}^{SH} \\
\frac{d\mathbf{h}_{223}^{SD}}{dt} = & \frac{1}{16\pi^2} \left[-\mathbf{h}_{223}^{SD} \left(\sum_{i=D, D^c, S} (C_3(i) g_3^2 + C_A(i) g_A^2 + C_B(i) g_B^2) \right) \right. \\
& +2\mathbf{Y}_{223}^{SD} \left(\sum_{i=D, D^c, S} (C_3(i) g_3^2 M_3 + C_A(i) g_A^2 M_A + \right. \\
& \quad \left. 2C_{AB}(i) g_A g_B M_{AB} + C_B(i) g_B^2 M_B) \right) \\
& +\mathbf{h}_{223}^{SD} \mathbf{Y}_{222}^D \mathbf{Y}_{222}^D + 15\mathbf{h}_{223}^{SD} \mathbf{Y}_{223}^{SD} \mathbf{Y}_{223}^{SD} + 2\mathbf{h}_{223}^{SD} \mathbf{Y}_{222}^{Dc} \mathbf{Y}_{222}^{Dc} + 3\mathbf{h}_{223}^{SD} \mathbf{Y}_{113}^{SD} \mathbf{Y}_{113}^{SD} \\
& +3\mathbf{h}_{223}^{SD} \mathbf{Y}_{333}^{SD} \mathbf{Y}_{333}^{SD} + 2\mathbf{h}_{223}^{SD} \mathbf{Y}_{311}^{SH} \mathbf{Y}_{311}^{SH} + 2\mathbf{h}_{223}^{SD} \mathbf{Y}_{322}^{SH} \mathbf{Y}_{322}^{SH} + 2\mathbf{h}_{223}^{SD} \mathbf{Y}_{333}^{SH} \mathbf{Y}_{333}^{SH} \\
& +2\mathbf{Y}_{223}^{SD} \mathbf{Y}_{222}^D \mathbf{h}_{222}^D + 4\mathbf{Y}_{223}^{SD} \mathbf{Y}_{222}^{Dc} \mathbf{h}_{222}^{Dc} + 6\mathbf{Y}_{223}^{SD} \mathbf{Y}_{113}^{SD} \mathbf{h}_{113}^{SD} + 6\mathbf{Y}_{223}^{SD} \mathbf{Y}_{333}^{SD} \mathbf{h}_{333}^{SD} \\
& +4\mathbf{Y}_{223}^{SD} \mathbf{Y}_{311}^{SH} \mathbf{h}_{311}^{SH} + 4\mathbf{Y}_{223}^{SD} \mathbf{Y}_{322}^{SH} \mathbf{h}_{322}^{SH} + 4\mathbf{Y}_{223}^{SD} \mathbf{Y}_{333}^{SH} \mathbf{h}_{333}^{SH} \\
\frac{d\mathbf{h}_{333}^{SD}}{dt} = & \frac{1}{16\pi^2} \left[-\mathbf{h}_{333}^{SD} \left(\sum_{i=D, D^c, S} (C_3(i) g_3^2 + C_A(i) g_A^2 + C_B(i) g_B^2) \right) \right. \\
& +2\mathbf{Y}_{333}^{SD} \left(\sum_{i=D, D^c, S} (C_3(i) g_3^2 M_3 + C_A(i) g_A^2 M_A + \right. \\
& \quad \left. 2C_{AB}(i) g_A g_B M_{AB} + C_B(i) g_B^2 M_B) \right) \\
& +\mathbf{h}_{333}^{SD} \mathbf{Y}_{333}^D \mathbf{Y}_{333}^D + 15\mathbf{h}_{333}^{SD} \mathbf{Y}_{333}^{SD} \mathbf{Y}_{333}^{SD} + 2\mathbf{h}_{333}^{SD} \mathbf{Y}_{333}^{Dc} \mathbf{Y}_{333}^{Dc} + 3\mathbf{h}_{333}^{SD} \mathbf{Y}_{113}^{SD} \mathbf{Y}_{113}^{SD} \\
& +3\mathbf{h}_{333}^{SD} \mathbf{Y}_{223}^{SD} \mathbf{Y}_{223}^{SD} + 2\mathbf{h}_{333}^{SD} \mathbf{Y}_{311}^{SH} \mathbf{Y}_{311}^{SH} + 2\mathbf{h}_{333}^{SD} \mathbf{Y}_{322}^{SH} \mathbf{Y}_{322}^{SH} + 2\mathbf{h}_{333}^{SD} \mathbf{Y}_{333}^{SH} \mathbf{Y}_{333}^{SH} \\
& +2\mathbf{Y}_{333}^{SD} \mathbf{Y}_{333}^D \mathbf{h}_{333}^D + 4\mathbf{Y}_{333}^{SD} \mathbf{Y}_{333}^{Dc} \mathbf{h}_{333}^{Dc} + 6\mathbf{Y}_{333}^{SD} \mathbf{Y}_{113}^{SD} \mathbf{h}_{113}^{SD} + 6\mathbf{Y}_{333}^{SD} \mathbf{Y}_{223}^{SD} \mathbf{h}_{223}^{SD} \\
& +4\mathbf{Y}_{333}^{SD} \mathbf{Y}_{311}^{SH} \mathbf{h}_{311}^{SH} + 4\mathbf{Y}_{333}^{SD} \mathbf{Y}_{322}^{SH} \mathbf{h}_{322}^{SH} + 4\mathbf{Y}_{333}^{SD} \mathbf{Y}_{333}^{SH} \mathbf{h}_{333}^{SH} \\
\end{aligned}$$

$$\begin{aligned}
\frac{d\mathbf{h}_{311}^{SH}}{dt} &= \frac{1}{16\pi^2} \left[-\mathbf{h}_{311}^{SH} \left(\sum_{i=S,H^d,H^u} (C_{2L}(i) g_{2L}^2 + C_A(i) g_A^2 + C_B(i) g_B^2) \right) \right. \\
&\quad + 2\mathbf{Y}_{311}^{SH} \left(\sum_{i=S,H^d,H^u} (C_{2L}(i) g_{2L}^2 M_{2L} + C_A(i) g_A^2 M_A + \right. \\
&\quad \quad \quad \left. \left. 2C_{AB}(i) g_{AGB} M_{AB} + C_B(i) g_B^2 M_B) \right) \right. \\
&\quad + 3\mathbf{h}_{311}^{SH} \mathbf{Y}_{113}^{SD} \mathbf{Y}_{113}^{SD} + 3\mathbf{h}_{311}^{SH} \mathbf{Y}_{223}^{SD} \mathbf{Y}_{223}^{SD} + 3\mathbf{h}_{311}^{SH} \mathbf{Y}_{333}^{SD} \mathbf{Y}_{333}^{SD} + 12\mathbf{h}_{311}^{SH} \mathbf{Y}_{311}^{SH} \mathbf{Y}_{311}^{SH} \\
&\quad + 2\mathbf{h}_{311}^{SH} \mathbf{Y}_{322}^{SH} \mathbf{Y}_{322}^{SH} + 2\mathbf{h}_{311}^{SH} \mathbf{Y}_{333}^{SH} \mathbf{Y}_{333}^{SH} + \mathbf{h}_{311}^{SH} \mathbf{Y}_{113}^{SH} \mathbf{Y}_{113}^{SH} + \mathbf{h}_{311}^{SH} \mathbf{Y}_{131}^{SH} \mathbf{Y}_{131}^{SH} \\
&\quad + 6\mathbf{Y}_{311}^{SH} \mathbf{Y}_{113}^{SD} \mathbf{h}_{113}^{SD} + 6\mathbf{Y}_{311}^{SH} \mathbf{Y}_{223}^{SD} \mathbf{h}_{223}^{SD} + 6\mathbf{Y}_{311}^{SH} \mathbf{Y}_{333}^{SD} \mathbf{h}_{333}^{SD} + 4\mathbf{Y}_{311}^{SH} \mathbf{Y}_{322}^{SH} \mathbf{h}_{322}^{SH} \\
&\quad \left. \left. + 4\mathbf{Y}_{311}^{SH} \mathbf{Y}_{333}^{SH} \mathbf{h}_{333}^{SH} + 2\mathbf{Y}_{311}^{SH} \mathbf{Y}_{113}^{SH} \mathbf{h}_{113}^{SH} + 2\mathbf{Y}_{311}^{SH} \mathbf{Y}_{131}^{SH} \mathbf{h}_{131}^{SH} \right] \right. \\
\frac{d\mathbf{h}_{322}^{SH}}{dt} &= \frac{1}{16\pi^2} \left[-\mathbf{h}_{322}^{SH} \left(\sum_{i=S,H^d,H^u} (C_{2L}(i) g_{2L}^2 + C_A(i) g_A^2 + C_B(i) g_B^2) \right) \right. \\
&\quad + 2\mathbf{Y}_{322}^{SH} \left(\sum_{i=S,H^d,H^u} (C_{2L}(i) g_{2L}^2 M_{2L} + C_A(i) g_A^2 M_A + \right. \\
&\quad \quad \quad \left. \left. 2C_{AB}(i) g_{AGB} M_{AB} + C_B(i) g_B^2 M_B) \right) \right. \\
&\quad + 3\mathbf{h}_{322}^{SH} \mathbf{Y}_{113}^{SD} \mathbf{Y}_{113}^{SD} + 3\mathbf{h}_{322}^{SH} \mathbf{Y}_{223}^{SD} \mathbf{Y}_{223}^{SD} + 3\mathbf{h}_{322}^{SH} \mathbf{Y}_{333}^{SD} \mathbf{Y}_{333}^{SD} + 2\mathbf{h}_{322}^{SH} \mathbf{Y}_{311}^{SH} \mathbf{Y}_{311}^{SH} \\
&\quad + 12\mathbf{h}_{322}^{SH} \mathbf{Y}_{322}^{SH} \mathbf{Y}_{322}^{SH} + 2\mathbf{h}_{322}^{SH} \mathbf{Y}_{333}^{SH} \mathbf{Y}_{333}^{SH} + \mathbf{h}_{322}^{SH} \mathbf{Y}_{223}^{SH} \mathbf{Y}_{223}^{SH} + \mathbf{h}_{322}^{SH} \mathbf{Y}_{232}^{SH} \mathbf{Y}_{232}^{SH} \\
&\quad + 6\mathbf{Y}_{322}^{SH} \mathbf{Y}_{113}^{SD} \mathbf{h}_{113}^{SD} + 6\mathbf{Y}_{322}^{SH} \mathbf{Y}_{223}^{SD} \mathbf{h}_{223}^{SD} + 6\mathbf{Y}_{322}^{SH} \mathbf{Y}_{333}^{SD} \mathbf{h}_{333}^{SD} + 4\mathbf{Y}_{322}^{SH} \mathbf{Y}_{311}^{SH} \mathbf{h}_{311}^{SH} \\
&\quad \left. \left. + 4\mathbf{Y}_{322}^{SH} \mathbf{Y}_{333}^{SH} \mathbf{h}_{333}^{SH} + 2\mathbf{Y}_{322}^{SH} \mathbf{Y}_{223}^{SH} \mathbf{h}_{223}^{SH} + 2\mathbf{Y}_{322}^{SH} \mathbf{Y}_{232}^{SH} \mathbf{h}_{232}^{SH} \right] \right. \\
\frac{d\mathbf{h}_{131}^{SH}}{dt} &= \frac{1}{16\pi^2} \left[-\mathbf{h}_{131}^{SH} \left(\sum_{i=S,H^d,H^u} (C_{2L}(i) g_{2L}^2 + C_A(i) g_A^2 + C_B(i) g_B^2) \right) \right. \\
&\quad + 2\mathbf{Y}_{131}^{SH} \left(\sum_{i=S,H^d,H^u} (C_{2L}(i) g_{2L}^2 M_{2L} + C_A(i) g_A^2 M_A + \right. \\
&\quad \quad \quad \left. \left. 2C_{AB}(i) g_{AGB} M_{AB} + C_B(i) g_B^2 M_B) \right) \right. \\
&\quad + 12\mathbf{h}_{131}^{SH} \mathbf{Y}_{131}^{SH} \mathbf{Y}_{131}^{SH} + 2\mathbf{h}_{131}^{SH} \mathbf{Y}_{113}^{SH} \mathbf{Y}_{113}^{SH} + 3\mathbf{h}_{131}^{SH} \mathbf{Y}_{333}^d \mathbf{Y}_{333}^d + \mathbf{h}_{131}^{SH} \mathbf{Y}_{232}^d \mathbf{Y}_{232}^d \\
&\quad + \mathbf{h}_{131}^{SH} \mathbf{Y}_{333}^{SH} \mathbf{Y}_{333}^{SH} + \mathbf{h}_{131}^{SH} \mathbf{Y}_{311}^{SH} \mathbf{Y}_{311}^{SH} + 4\mathbf{Y}_{131}^{SH} \mathbf{Y}_{113}^{SH} \mathbf{h}_{113}^{SH} + 6\mathbf{Y}_{131}^{SH} \mathbf{Y}_{333}^d \mathbf{h}_{333}^d \\
&\quad \left. \left. + 2\mathbf{Y}_{131}^{SH} \mathbf{Y}_{232}^{SH} \mathbf{h}_{232}^{SH} + 2\mathbf{Y}_{131}^{SH} \mathbf{Y}_{333}^{SH} \mathbf{h}_{333}^{SH} + 2\mathbf{Y}_{131}^{SH} \mathbf{Y}_{311}^{SH} \mathbf{h}_{311}^{SH} \right] \right. \\
\frac{d\mathbf{h}_{232}^{SH}}{dt} &= \frac{1}{16\pi^2} \left[-\mathbf{h}_{232}^{SH} \left(\sum_{i=S,H^d,H^u} (C_{2L}(i) g_{2L}^2 + C_A(i) g_A^2 + C_B(i) g_B^2) \right) \right. \\
&\quad + 2\mathbf{Y}_{232}^{SH} \left(\sum_{i=S,H^d,H^u} (C_{2L}(i) g_{2L}^2 M_{2L} + C_A(i) g_A^2 M_A + \right. \\
&\quad \quad \quad \left. \left. 2C_{AB}(i) g_{AGB} M_{AB} + C_B(i) g_B^2 M_B) \right) \right. \\
&\quad + 12\mathbf{h}_{232}^{SH} \mathbf{Y}_{232}^{SH} \mathbf{Y}_{232}^{SH} + 2\mathbf{h}_{232}^{SH} \mathbf{Y}_{223}^{SH} \mathbf{Y}_{223}^{SH} + 3\mathbf{h}_{232}^{SH} \mathbf{Y}_{333}^d \mathbf{Y}_{333}^d + \mathbf{h}_{232}^{SH} \mathbf{Y}_{131}^{SH} \mathbf{Y}_{131}^{SH} \\
&\quad + \mathbf{h}_{232}^{SH} \mathbf{Y}_{333}^{SH} \mathbf{Y}_{333}^{SH} + \mathbf{h}_{232}^{SH} \mathbf{Y}_{322}^{SH} \mathbf{Y}_{322}^{SH} + 4\mathbf{Y}_{232}^{SH} \mathbf{Y}_{223}^{SH} \mathbf{h}_{223}^{SH} + 6\mathbf{Y}_{232}^{SH} \mathbf{Y}_{333}^d \mathbf{h}_{333}^d \\
&\quad \left. \left. + 2\mathbf{Y}_{232}^{SH} \mathbf{Y}_{131}^{SH} \mathbf{h}_{131}^{SH} + 2\mathbf{Y}_{232}^{SH} \mathbf{Y}_{333}^{SH} \mathbf{h}_{333}^{SH} + 2\mathbf{Y}_{232}^{SH} \mathbf{Y}_{322}^{SH} \mathbf{h}_{322}^{SH} \right] \right. \\
\frac{d\mathbf{h}_{113}^{SH}}{dt} &= \frac{1}{16\pi^2} \left[-\mathbf{h}_{113}^{SH} \left(\sum_{i=S,H^d,H^u} (C_{2L}(i) g_{2L}^2 + C_A(i) g_A^2 + C_B(i) g_B^2) \right) \right. \\
&\quad + 2\mathbf{Y}_{113}^{SH} \left(\sum_{i=S,H^d,H^u} (C_{2L}(i) g_{2L}^2 M_{2L} + C_A(i) g_A^2 M_A + \right.
\end{aligned}$$

$$\begin{aligned}
& 2\mathcal{C}_{AB}(i)g_A g_B M_{AB} + \mathcal{C}_B(i)g_B^2 M_B) \\
& + 2\mathbf{h}_{113}^{SH} \mathbf{Y}_{131}^{SH} \mathbf{Y}_{131}^{SH} + 12\mathbf{h}_{113}^{SH} \mathbf{Y}_{113}^{SH} \mathbf{Y}_{113}^{SH} + \mathbf{h}_{113}^{SH} \mathbf{Y}_{311}^{SH} \mathbf{Y}_{311}^{SH} + 3\mathbf{h}_{113}^{SH} \mathbf{Y}_{333}^u \mathbf{Y}_{333}^u \\
& + \mathbf{h}_{113}^{SH} \mathbf{Y}_{223}^{SH} \mathbf{Y}_{223}^{SH} + \mathbf{h}_{113}^{SH} \mathbf{Y}_{333}^{SH} \mathbf{Y}_{333}^{SH} + 4\mathbf{Y}_{113}^{SH} \mathbf{Y}_{131}^{SH} \mathbf{h}_{131}^{SH} + 2\mathbf{Y}_{113}^{SH} \mathbf{Y}_{311}^{SH} \mathbf{h}_{311}^{SH} \\
& + 6\mathbf{Y}_{113}^{SH} \mathbf{Y}_{333}^u \mathbf{h}_{333}^u + 2\mathbf{Y}_{113}^{SH} \mathbf{Y}_{223}^{SH} \mathbf{h}_{223}^{SH} + 2\mathbf{Y}_{113}^{SH} \mathbf{Y}_{333}^{SH} \mathbf{h}_{333}^{SH}] \\
\frac{d\mathbf{h}_{223}^{SH}}{dt} = & \frac{1}{16\pi^2} \left[-\mathbf{h}_{223}^{SH} \left(\sum_{i=S, H^d, H^u} (\mathcal{C}_{2L}(i)g_{2L}^2 + \mathcal{C}_A(i)g_A^2 + \mathcal{C}_B(i)g_B^2) \right) \right. \\
& + 2\mathbf{Y}_{223}^{SH} \left(\sum_{i=S, H^d, H^u} (\mathcal{C}_{2L}(i)g_{2L}^2 M_{2L} + \mathcal{C}_A(i)g_A^2 M_A + \right. \\
& \left. \left. 2\mathcal{C}_{AB}(i)g_A g_B M_{AB} + \mathcal{C}_B(i)g_B^2 M_B) \right) \right. \\
& + 2\mathbf{h}_{223}^{SH} \mathbf{Y}_{232}^{SH} \mathbf{Y}_{232}^{SH} + 12\mathbf{h}_{223}^{SH} \mathbf{Y}_{223}^{SH} \mathbf{Y}_{223}^{SH} + \mathbf{h}_{223}^{SH} \mathbf{Y}_{322}^{SH} \mathbf{Y}_{322}^{SH} + 3\mathbf{h}_{223}^{SH} \mathbf{Y}_{333}^u \mathbf{Y}_{333}^u \\
& + \mathbf{h}_{223}^{SH} \mathbf{Y}_{113}^{SH} \mathbf{Y}_{113}^{SH} + \mathbf{h}_{223}^{SH} \mathbf{Y}_{333}^{SH} \mathbf{Y}_{333}^{SH} + 4\mathbf{Y}_{223}^{SH} \mathbf{Y}_{232}^{SH} \mathbf{h}_{232}^{SH} + 2\mathbf{Y}_{223}^{SH} \mathbf{Y}_{322}^{SH} \mathbf{h}_{322}^{SH} \\
& \left. + 6\mathbf{Y}_{223}^{SH} \mathbf{Y}_{333}^u \mathbf{h}_{333}^u + 2\mathbf{Y}_{223}^{SH} \mathbf{Y}_{113}^{SH} \mathbf{h}_{113}^{SH} + 2\mathbf{Y}_{223}^{SH} \mathbf{Y}_{333}^{SH} \mathbf{h}_{333}^{SH} \right] \\
\frac{d\mathbf{h}_{333}^{SH}}{dt} = & \frac{1}{16\pi^2} \left[-\mathbf{h}_{333}^{SH} \left(\sum_{i=S, H^d, H^u} (\mathcal{C}_{2L}(i)g_{2L}^2 + \mathcal{C}_A(i)g_A^2 + \mathcal{C}_B(i)g_B^2) \right) \right. \\
& + 2\mathbf{Y}_{333}^{SH} \left(\sum_{i=S, H^d, H^u} (\mathcal{C}_{2L}(i)g_{2L}^2 M_{2L} + \mathcal{C}_A(i)g_A^2 M_A + \right. \\
& \left. \left. 2\mathcal{C}_{AB}(i)g_A g_B M_{AB} + \mathcal{C}_B(i)g_B^2 M_B) \right) \right. \\
& + 3\mathbf{h}_{333}^{SH} \mathbf{Y}_{113}^{SD} \mathbf{Y}_{113}^{SD} + 3\mathbf{h}_{333}^{SH} \mathbf{Y}_{223}^{SD} \mathbf{Y}_{223}^{SD} + 3\mathbf{h}_{333}^{SH} \mathbf{Y}_{333}^{SD} \mathbf{Y}_{333}^{SD} + 2\mathbf{h}_{333}^{SH} \mathbf{Y}_{311}^{SH} \mathbf{Y}_{311}^{SH} \\
& + 2\mathbf{h}_{333}^{SH} \mathbf{Y}_{322}^{SH} \mathbf{Y}_{322}^{SH} + 12\mathbf{h}_{333}^{SH} \mathbf{Y}_{333}^{SH} \mathbf{Y}_{333}^{SH} + 3\mathbf{h}_{333}^{SH} \mathbf{Y}_{333}^d \mathbf{Y}_{333}^d + \mathbf{h}_{333}^{SH} \mathbf{Y}_{131}^{SH} \mathbf{Y}_{131}^{SH} \\
& + \mathbf{h}_{333}^{SH} \mathbf{Y}_{232}^{SH} \mathbf{Y}_{232}^{SH} + 3\mathbf{h}_{333}^{SH} \mathbf{Y}_{333}^u \mathbf{Y}_{333}^u + \mathbf{h}_{333}^{SH} \mathbf{Y}_{113}^{SH} \mathbf{Y}_{113}^{SH} + \mathbf{h}_{333}^{SH} \mathbf{Y}_{223}^{SH} \mathbf{Y}_{223}^{SH} \\
& + 6\mathbf{Y}_{333}^{SH} \mathbf{Y}_{113}^{SD} \mathbf{h}_{113}^{SD} + 6\mathbf{Y}_{333}^{SH} \mathbf{Y}_{223}^{SD} \mathbf{h}_{223}^{SD} + 6\mathbf{Y}_{333}^{SH} \mathbf{Y}_{333}^{SD} \mathbf{h}_{333}^{SD} + 4\mathbf{Y}_{333}^{SH} \mathbf{Y}_{311}^{SH} \mathbf{h}_{311}^{SH} \\
& + 4\mathbf{Y}_{333}^{SH} \mathbf{Y}_{322}^{SH} \mathbf{h}_{322}^{SH} + 6\mathbf{Y}_{333}^{SH} \mathbf{Y}_{333}^d \mathbf{h}_{333}^d + 2\mathbf{Y}_{333}^{SH} \mathbf{Y}_{131}^{SH} \mathbf{h}_{131}^{SH} + 2\mathbf{Y}_{333}^{SH} \mathbf{Y}_{232}^{SH} \mathbf{h}_{232}^{SH} \\
& \left. + 6\mathbf{Y}_{333}^{SH} \mathbf{Y}_{333}^u \mathbf{h}_{333}^u + 2\mathbf{Y}_{333}^{SH} \mathbf{Y}_{113}^{SH} \mathbf{h}_{113}^{SH} + 2\mathbf{Y}_{333}^{SH} \mathbf{Y}_{223}^{SH} \mathbf{h}_{223}^{SH} \right]
\end{aligned}$$

B.6.5 Running of the Scalar SSB-Masses

$$\begin{aligned}
\frac{d(\mathbf{m}_{L_L}^2)_{11}}{dt} = & \frac{1}{16\pi^2} \left[6\mathbf{h}_{111}^{Dc} \mathbf{h}_{111}^{Dc} \right. \\
& + 6(\mathbf{m}_{L_L}^2)_{11} \mathbf{Y}_{111}^{Dc} \mathbf{Y}_{111}^{Dc} + 6(\mathbf{m}_{Dc}^2)_{11} \mathbf{Y}_{111}^{Dc} \mathbf{Y}_{111}^{Dc} + 6(\mathbf{m}_{Q_L}^2)_{11} \mathbf{Y}_{111}^{Dc} \mathbf{Y}_{111}^{Dc} \\
& - 8(\mathcal{C}_{2L}(L_L)M_{2L}^2 g_{2L}^2 + \mathcal{C}_A(L_L)M_A^2 g_A^2 + \mathcal{C}_B(L_L)M_B^2 g_B^2 + 2\mathcal{C}_{AB}(L_L)g_A g_B M_{AB}^2) \\
& \left. + 2Q_A^{L_L} g_A^2 \mathcal{S}_A + 2Q_B^{L_L} g_B^2 \mathcal{S}_B \right] \\
\frac{d(\mathbf{m}_{L_L}^2)_{22}}{dt} = & \frac{1}{16\pi^2} \left[6\mathbf{h}_{222}^{Dc} \mathbf{h}_{222}^{Dc} \right. \\
& + 6(\mathbf{m}_{L_L}^2)_{22} \mathbf{Y}_{222}^{Dc} \mathbf{Y}_{222}^{Dc} + 6(\mathbf{m}_{Dc}^2)_{22} \mathbf{Y}_{222}^{Dc} \mathbf{Y}_{222}^{Dc} + 6(\mathbf{m}_{Q_L}^2)_{22} \mathbf{Y}_{222}^{Dc} \mathbf{Y}_{222}^{Dc} \\
& - 8(\mathcal{C}_{2L}(L_L)M_{2L}^2 g_{2L}^2 + \mathcal{C}_A(L_L)M_A^2 g_A^2 + \mathcal{C}_B(L_L)M_B^2 g_B^2 + 2\mathcal{C}_{AB}(L_L)g_A g_B M_{AB}^2) \\
& \left. + 2Q_A^{L_L} g_A^2 \mathcal{S}_A + 2Q_B^{L_L} g_B^2 \mathcal{S}_B \right] \\
\frac{d(\mathbf{m}_{L_L}^2)_{33}}{dt} = & \frac{1}{16\pi^2} \left[6\mathbf{h}_{333}^{Dc} \mathbf{h}_{333}^{Dc} \right.
\end{aligned}$$

$$\begin{aligned}
& +6 (\mathbf{m}_{LL}^2)_{33} \mathbf{Y}_{333}^{Dc} \mathbf{Y}_{333}^{Dc} + 6 (\mathbf{m}_{D^c}^2)_{33} \mathbf{Y}_{333}^{Dc} \mathbf{Y}_{333}^{Dc} + 6 (\mathbf{m}_{QL}^2)_{33} \mathbf{Y}_{333}^{Dc} \mathbf{Y}_{333}^{Dc} \\
& -8 (\mathcal{C}_{2L}(LL)M_{2L}^2g_{2L}^2 + \mathcal{C}_A(LL)M_A^2g_A^2 + \mathcal{C}_B(LL)M_B^2g_B^2 + 2\mathcal{C}_{AB}(LL)g_{AGB}M_{AB}^2) \\
& + 2Q_A^{LL}g_A^2\mathcal{S}_A + 2Q_B^{LL}g_B^2\mathcal{S}_B \Big] \\
\frac{d(\mathbf{m}_{e^c}^2)_{11}}{dt} &= \frac{1}{16\pi^2} \Big[6\mathbf{h}_{111}^D \mathbf{h}_{111}^D \\
& + 6 (\mathbf{m}_{e^c}^2)_{11} \mathbf{Y}_{111}^D \mathbf{Y}_{111}^D + 6 (\mathbf{m}_D^2)_{11} \mathbf{Y}_{111}^D \mathbf{Y}_{111}^D + 6 (\mathbf{m}_{u^c}^2)_{11} \mathbf{Y}_{111}^D \mathbf{Y}_{111}^D \\
& - 8 (\mathcal{C}_A(e^c)M_A^2g_A^2 + \mathcal{C}_B(e^c)M_B^2g_B^2 + 2\mathcal{C}_{AB}(e^c)g_{AGB}M_{AB}^2) \\
& + 2Q_A^{e^c}g_A^2\mathcal{S}_A + 2Q_B^{e^c}g_B^2\mathcal{S}_B \Big] \\
\frac{d(\mathbf{m}_{e^c}^2)_{22}}{dt} &= \frac{1}{16\pi^2} \Big[6\mathbf{h}_{222}^D \mathbf{h}_{222}^D \\
& + 6 (\mathbf{m}_{e^c}^2)_{22} \mathbf{Y}_{222}^D \mathbf{Y}_{222}^D + 6 (\mathbf{m}_D^2)_{22} \mathbf{Y}_{222}^D \mathbf{Y}_{222}^D + 6 (\mathbf{m}_{u^c}^2)_{22} \mathbf{Y}_{222}^D \mathbf{Y}_{222}^D \\
& - 8 (\mathcal{C}_A(e^c)M_A^2g_A^2 + \mathcal{C}_B(e^c)M_B^2g_B^2 + 2\mathcal{C}_{AB}(e^c)g_{AGB}M_{AB}^2) \\
& + 2Q_A^{e^c}g_A^2\mathcal{S}_A + 2Q_B^{e^c}g_B^2\mathcal{S}_B \Big] \\
\frac{d(\mathbf{m}_{e^c}^2)_{33}}{dt} &= \frac{1}{16\pi^2} \Big[6\mathbf{h}_{333}^D \mathbf{h}_{333}^D \\
& + 6 (\mathbf{m}_{e^c}^2)_{33} \mathbf{Y}_{333}^D \mathbf{Y}_{333}^D + 6 (\mathbf{m}_D^2)_{33} \mathbf{Y}_{333}^D \mathbf{Y}_{333}^D + 6 (\mathbf{m}_{u^c}^2)_{33} \mathbf{Y}_{333}^D \mathbf{Y}_{333}^D \\
& - 8 (\mathcal{C}_A(e^c)M_A^2g_A^2 + \mathcal{C}_B(e^c)M_B^2g_B^2 + 2\mathcal{C}_{AB}(e^c)g_{AGB}M_{AB}^2) \\
& + 2Q_A^{e^c}g_A^2\mathcal{S}_A + 2Q_B^{e^c}g_B^2\mathcal{S}_B \Big] \\
\frac{d(\mathbf{m}_{QL}^2)_{11}}{dt} &= \frac{1}{16\pi^2} \Big[2\mathbf{h}_{111}^{Dc} \mathbf{h}_{111}^{Dc} \\
& + 2 (\mathbf{m}_{QL}^2)_{11} \mathbf{Y}_{111}^{Dc} \mathbf{Y}_{111}^{Dc} + 2 (\mathbf{m}_{D^c}^2)_{11} \mathbf{Y}_{111}^{Dc} \mathbf{Y}_{111}^{Dc} + 2 (\mathbf{m}_{LL}^2)_{11} \mathbf{Y}_{111}^{Dc} \mathbf{Y}_{111}^{Dc} \\
& - 8 (\mathcal{C}_3(QL)M_3^2g_3^2 + \mathcal{C}_{2L}(QL)M_{2L}^2g_{2L}^2 + \mathcal{C}_A(QL)M_A^2g_A^2 + \mathcal{C}_B(QL)M_B^2g_B^2 \\
& + 2\mathcal{C}_{AB}(QL)g_{AGB}M_{AB}^2) + 2Q_A^{QL}g_A^2\mathcal{S}_A + 2Q_B^{QL}g_B^2\mathcal{S}_B \Big] \\
\frac{d(\mathbf{m}_{QL}^2)_{22}}{dt} &= \frac{1}{16\pi^2} \Big[2\mathbf{h}_{222}^{Dc} \mathbf{h}_{222}^{Dc} \\
& + 2 (\mathbf{m}_{QL}^2)_{22} \mathbf{Y}_{222}^{Dc} \mathbf{Y}_{222}^{Dc} + 2 (\mathbf{m}_{D^c}^2)_{22} \mathbf{Y}_{222}^{Dc} \mathbf{Y}_{222}^{Dc} + 2 (\mathbf{m}_{LL}^2)_{22} \mathbf{Y}_{222}^{Dc} \mathbf{Y}_{222}^{Dc} \\
& - 8 (\mathcal{C}_3(QL)M_3^2g_3^2 + \mathcal{C}_{2L}(QL)M_{2L}^2g_{2L}^2 + \mathcal{C}_A(QL)M_A^2g_A^2 + \mathcal{C}_B(QL)M_B^2g_B^2 \\
& + 2\mathcal{C}_{AB}(QL)g_{AGB}M_{AB}^2) + 2Q_A^{QL}g_A^2\mathcal{S}_A + 2Q_B^{QL}g_B^2\mathcal{S}_B \Big] \\
\frac{d(\mathbf{m}_{QL}^2)_{33}}{dt} &= \frac{1}{16\pi^2} \Big[2\mathbf{h}_{333}^d \mathbf{h}_{333}^d + 2\mathbf{h}_{333}^u \mathbf{h}_{333}^u + 2\mathbf{h}_{333}^{Dc} \mathbf{h}_{333}^{Dc} \\
& + 2 (\mathbf{m}_{QL}^2)_{33} \mathbf{Y}_{333}^d \mathbf{Y}_{333}^d + 2 (\mathbf{m}_{QL}^2)_{33} \mathbf{Y}_{333}^u \mathbf{Y}_{333}^u + 2 (\mathbf{m}_{QL}^2)_{33} \mathbf{Y}_{333}^{Dc} \mathbf{Y}_{333}^{Dc} \\
& + 2 (\mathbf{m}_{H^d}^2)_{33} \mathbf{Y}_{333}^d \mathbf{Y}_{333}^d + 2 (\mathbf{m}_{g^c}^2)_{33} \mathbf{Y}_{333}^d \mathbf{Y}_{333}^d + 2 (\mathbf{m}_{H^u}^2)_{33} \mathbf{Y}_{333}^u \mathbf{Y}_{333}^u \\
& + 2 (\mathbf{m}_{u^c}^2)_{33} \mathbf{Y}_{333}^u \mathbf{Y}_{333}^u + 2 (\mathbf{m}_{D^c}^2)_{33} \mathbf{Y}_{333}^{Dc} \mathbf{Y}_{333}^{Dc} + 2 (\mathbf{m}_{LL}^2)_{33} \mathbf{Y}_{333}^{Dc} \mathbf{Y}_{333}^{Dc} \\
& - 8 (\mathcal{C}_3(QL)M_3^2g_3^2 + \mathcal{C}_{2L}(QL)M_{2L}^2g_{2L}^2 + \mathcal{C}_A(QL)M_A^2g_A^2 + \mathcal{C}_B(QL)M_B^2g_B^2 \\
& + 2\mathcal{C}_{AB}(QL)g_{AGB}M_{AB}^2) + 2Q_A^{QL}g_A^2\mathcal{S}_A + 2Q_B^{QL}g_B^2\mathcal{S}_B \Big] \\
\frac{d(\mathbf{m}_{u^c}^2)_{11}}{dt} &= \frac{1}{16\pi^2} \Big[2\mathbf{h}_{111}^D \mathbf{h}_{111}^D \\
& + 2 (\mathbf{m}_{u^c}^2)_{11} \mathbf{Y}_{111}^D \mathbf{Y}_{111}^D + 2 (\mathbf{m}_D^2)_{11} \mathbf{Y}_{111}^D \mathbf{Y}_{111}^D + 2 (\mathbf{m}_{e^c}^2)_{11} \mathbf{Y}_{111}^D \mathbf{Y}_{111}^D \\
& - 8 (\mathcal{C}_3(u^c)M_3^2g_3^2 + \mathcal{C}_A(u^c)M_A^2g_A^2 + \mathcal{C}_B(u^c)M_B^2g_B^2 + 2\mathcal{C}_{AB}(u^c)g_{AGB}M_{AB}^2) \\
& + 2Q_A^{u^c}g_A^2\mathcal{S}_A + 2Q_B^{u^c}g_B^2\mathcal{S}_B \Big]
\end{aligned}$$

$$\begin{aligned}
\frac{d(\mathbf{m}_{u^c}^2)_{22}}{dt} &= \frac{1}{16\pi^2} \left[2\mathbf{h}_{222}^D \mathbf{h}_{222}^D \right. \\
&\quad + 2(\mathbf{m}_{u^c}^2)_{22} \mathbf{Y}_{222}^D \mathbf{Y}_{222}^D + 2(\mathbf{m}_D^2)_{22} \mathbf{Y}_{222}^D \mathbf{Y}_{222}^D + 2(\mathbf{m}_{e^c}^2)_{22} \mathbf{Y}_{222}^D \mathbf{Y}_{222}^D \\
&\quad - 8(\mathcal{C}_3(u^c)M_3^2 g_3^2 + \mathcal{C}_A(u^c)M_A^2 g_A^2 + \mathcal{C}_B(u^c)M_B^2 g_B^2 + 2\mathcal{C}_{AB}(u^c)g_A g_B M_{AB}^2) \\
&\quad \left. + 2Q_A^{u^c} g_A^2 \mathcal{S}_A + 2Q_B^{u^c} g_B^2 \mathcal{S}_B \right] \\
\frac{d(\mathbf{m}_{u^c}^2)_{33}}{dt} &= \frac{1}{16\pi^2} \left[4\mathbf{h}_{333}^u \mathbf{h}_{333}^u + 2\mathbf{h}_{333}^D \mathbf{h}_{333}^D \right. \\
&\quad + 4(\mathbf{m}_{u^c}^2)_{33} \mathbf{Y}_{333}^u \mathbf{Y}_{333}^u + 2(\mathbf{m}_{u^c}^2)_{33} \mathbf{Y}_{333}^D \mathbf{Y}_{333}^D + 4(\mathbf{m}_{H^u}^2)_{33} \mathbf{Y}_{333}^u \mathbf{Y}_{333}^u \\
&\quad + 4(\mathbf{m}_{Q_L}^2)_{33} \mathbf{Y}_{333}^u \mathbf{Y}_{333}^u + 2(\mathbf{m}_D^2)_{33} \mathbf{Y}_{333}^D \mathbf{Y}_{333}^D + 2(\mathbf{m}_{e^c}^2)_{33} \mathbf{Y}_{333}^D \mathbf{Y}_{333}^D \\
&\quad - 8(\mathcal{C}_3(u^c)M_3^2 g_3^2 + \mathcal{C}_A(u^c)M_A^2 g_A^2 + \mathcal{C}_B(u^c)M_B^2 g_B^2 + 2\mathcal{C}_{AB}(u^c)g_A g_B M_{AB}^2) \\
&\quad \left. + 2Q_A^{u^c} g_A^2 \mathcal{S}_A + 2Q_B^{u^c} g_B^2 \mathcal{S}_B \right] \\
\frac{d(\mathbf{m}_{d^c}^2)_{11}}{dt} &= \frac{1}{16\pi^2} \left[\right. \\
&\quad - 8(\mathcal{C}_3(d^c)M_3^2 g_3^2 + \mathcal{C}_A(d^c)M_A^2 g_A^2 + \mathcal{C}_B(d^c)M_B^2 g_B^2 + 2\mathcal{C}_{AB}(d^c)g_A g_B M_{AB}^2) \\
&\quad \left. + 2Q_A^{d^c} g_A^2 \mathcal{S}_A + 2Q_B^{d^c} g_B^2 \mathcal{S}_B \right] \\
\frac{d(\mathbf{m}_{d^c}^2)_{22}}{dt} &= \frac{1}{16\pi^2} \left[\right. \\
&\quad - 8(\mathcal{C}_3(d^c)M_3^2 g_3^2 + \mathcal{C}_A(d^c)M_A^2 g_A^2 + \mathcal{C}_B(d^c)M_B^2 g_B^2 + 2\mathcal{C}_{AB}(d^c)g_A g_B M_{AB}^2) \\
&\quad \left. + 2Q_A^{d^c} g_A^2 \mathcal{S}_A + 2Q_B^{d^c} g_B^2 \mathcal{S}_B \right] \\
\frac{d(\mathbf{m}_{d^c}^2)_{33}}{dt} &= \frac{1}{16\pi^2} \left[4\mathbf{h}_{333}^d \mathbf{h}_{333}^d \right. \\
&\quad + 4(\mathbf{m}_{d^c}^2)_{33} \mathbf{Y}_{333}^d \mathbf{Y}_{333}^d + 4(\mathbf{m}_{H^d}^2)_{33} \mathbf{Y}_{333}^d \mathbf{Y}_{333}^d + 4(\mathbf{m}_{Q_L}^2)_{33} \mathbf{Y}_{333}^d \mathbf{Y}_{333}^d \\
&\quad - 8(\mathcal{C}_3(d^c)M_3^2 g_3^2 + \mathcal{C}_A(d^c)M_A^2 g_A^2 + \mathcal{C}_B(d^c)M_B^2 g_B^2 + 2\mathcal{C}_{AB}(d^c)g_A g_B M_{AB}^2) \\
&\quad \left. + 2Q_A^{d^c} g_A^2 \mathcal{S}_A + 2Q_B^{d^c} g_B^2 \mathcal{S}_B \right] \\
\frac{d(\mathbf{m}_{H^d}^2)_{11}}{dt} &= \frac{1}{16\pi^2} \left[2\mathbf{h}_{311}^{SH} \mathbf{h}_{311}^{SH} + 2\mathbf{h}_{113}^{SH} \mathbf{h}_{113}^{SH} \right. \\
&\quad + 2(\mathbf{m}_{H^d}^2)_{11} \mathbf{Y}_{311}^{SH} \mathbf{Y}_{311}^{SH} + 2(\mathbf{m}_{H^d}^2)_{11} \mathbf{Y}_{113}^{SH} \mathbf{Y}_{113}^{SH} + 2(\mathbf{m}_{H^u}^2)_{11} \mathbf{Y}_{311}^{SH} \mathbf{Y}_{311}^{SH} \\
&\quad + 2(\mathbf{m}_S^2)_{33} \mathbf{Y}_{311}^{SH} \mathbf{Y}_{311}^{SH} + 2(\mathbf{m}_{H^u}^2)_{33} \mathbf{Y}_{113}^{SH} \mathbf{Y}_{113}^{SH} + 2(\mathbf{m}_S^2)_{11} \mathbf{Y}_{113}^{SH} \mathbf{Y}_{113}^{SH} \\
&\quad - 8(\mathcal{C}_{2L}(H^d)M_{2L}^2 g_{2L}^2 + \mathcal{C}_A(H^d)M_A^2 g_A^2 + \mathcal{C}_B(H^d)M_B^2 g_B^2 + 2\mathcal{C}_{AB}(H^d)g_A g_B M_{AB}^2) \\
&\quad \left. + 2Q_A^{H^d} g_A^2 \mathcal{S}_A + 2Q_B^{H^d} g_B^2 \mathcal{S}_B \right] \\
\frac{d(\mathbf{m}_{H^d}^2)_{22}}{dt} &= \frac{1}{16\pi^2} \left[2\mathbf{h}_{322}^{SH} \mathbf{h}_{322}^{SH} + 2\mathbf{h}_{223}^{SH} \mathbf{h}_{223}^{SH} \right. \\
&\quad + 2(\mathbf{m}_{H^d}^2)_{22} \mathbf{Y}_{322}^{SH} \mathbf{Y}_{322}^{SH} + 2(\mathbf{m}_{H^d}^2)_{22} \mathbf{Y}_{223}^{SH} \mathbf{Y}_{223}^{SH} + 2(\mathbf{m}_{H^u}^2)_{22} \mathbf{Y}_{322}^{SH} \mathbf{Y}_{322}^{SH} \\
&\quad + 2(\mathbf{m}_S^2)_{33} \mathbf{Y}_{322}^{SH} \mathbf{Y}_{322}^{SH} + 2(\mathbf{m}_{H^u}^2)_{33} \mathbf{Y}_{223}^{SH} \mathbf{Y}_{223}^{SH} + 2(\mathbf{m}_S^2)_{22} \mathbf{Y}_{223}^{SH} \mathbf{Y}_{223}^{SH} \\
&\quad - 8(\mathcal{C}_{2L}(H^d)M_{2L}^2 g_{2L}^2 + \mathcal{C}_A(H^d)M_A^2 g_A^2 + \mathcal{C}_B(H^d)M_B^2 g_B^2 + 2\mathcal{C}_{AB}(H^d)g_A g_B M_{AB}^2) \\
&\quad \left. + 2Q_A^{H^d} g_A^2 \mathcal{S}_A + 2Q_B^{H^d} g_B^2 \mathcal{S}_B \right] \\
\frac{d(\mathbf{m}_{H^d}^2)_{33}}{dt} &= \frac{1}{16\pi^2} \left[6\mathbf{h}_{333}^d \mathbf{h}_{333}^d + 2\mathbf{h}_{131}^{SH} \mathbf{h}_{131}^{SH} + 2\mathbf{h}_{232}^{SH} \mathbf{h}_{232}^{SH} + 2\mathbf{h}_{333}^{SH} \mathbf{h}_{333}^{SH} \right. \\
&\quad + 6(\mathbf{m}_{H^d}^2)_{33} \mathbf{Y}_{333}^d \mathbf{Y}_{333}^d + 2(\mathbf{m}_{H^d}^2)_{33} \mathbf{Y}_{131}^{SH} \mathbf{Y}_{131}^{SH} + 2(\mathbf{m}_{H^d}^2)_{33} \mathbf{Y}_{232}^{SH} \mathbf{Y}_{232}^{SH} \\
&\quad \left. + 2(\mathbf{m}_{H^d}^2)_{33} \mathbf{Y}_{333}^{SH} \mathbf{Y}_{333}^{SH} + 6(\mathbf{m}_{d^c}^2)_{33} \mathbf{Y}_{333}^d \mathbf{Y}_{333}^d + 6(\mathbf{m}_{Q_L}^2)_{33} \mathbf{Y}_{333}^d \mathbf{Y}_{333}^d \right]
\end{aligned}$$

$$\begin{aligned}
& +2(\mathbf{m}_{H^u}^2)_{11} \mathbf{Y}_{131}^{SH} \mathbf{Y}_{131}^{SH} + 2(\mathbf{m}_S^2)_{11} \mathbf{Y}_{131}^{SH} \mathbf{Y}_{131}^{SH} + 2(\mathbf{m}_{H^u}^2)_{22} \mathbf{Y}_{232}^{SH} \mathbf{Y}_{232}^{SH} \\
& +2(\mathbf{m}_S^2)_{22} \mathbf{Y}_{232}^{SH} \mathbf{Y}_{232}^{SH} + 2(\mathbf{m}_{H^u}^2)_{33} \mathbf{Y}_{333}^{SH} \mathbf{Y}_{333}^{SH} + 2(\mathbf{m}_S^2)_{33} \mathbf{Y}_{333}^{SH} \mathbf{Y}_{333}^{SH} \\
& -8 \left(\mathcal{C}_{2L}(H^d) M_{2L}^2 g_{2L}^2 + \mathcal{C}_A(H^d) M_{AgA}^2 + \mathcal{C}_B(H^d) M_B^2 g_B^2 + 2\mathcal{C}_{AB}(H^d) g_{AgB} M_{AB}^2 \right) \\
& +2Q_A^{H^d} g_A^2 \mathcal{S}_A + 2Q_B^{H^d} g_B^2 \mathcal{S}_B \Big] \\
\frac{d(\mathbf{m}_{H^u}^2)_{11}}{dt} &= \frac{1}{16\pi^2} \left[2\mathbf{h}_{311}^{SH} \mathbf{h}_{311}^{SH} + 2\mathbf{h}_{131}^{SH} \mathbf{h}_{131}^{SH} \right. \\
& +2(\mathbf{m}_{H^u}^2)_{11} \mathbf{Y}_{311}^{SH} \mathbf{Y}_{311}^{SH} + 2(\mathbf{m}_{H^u}^2)_{11} \mathbf{Y}_{131}^{SH} \mathbf{Y}_{131}^{SH} + 2(\mathbf{m}_{H^d}^2)_{11} \mathbf{Y}_{311}^{SH} \mathbf{Y}_{311}^{SH} \\
& +2(\mathbf{m}_S^2)_{33} \mathbf{Y}_{311}^{SH} \mathbf{Y}_{311}^{SH} + 2(\mathbf{m}_{H^d}^2)_{33} \mathbf{Y}_{131}^{SH} \mathbf{Y}_{131}^{SH} + 2(\mathbf{m}_S^2)_{11} \mathbf{Y}_{131}^{SH} \mathbf{Y}_{131}^{SH} \\
& -8 \left(\mathcal{C}_{2L}(H^u) M_{2L}^2 g_{2L}^2 + \mathcal{C}_A(H^u) M_{AgA}^2 + \mathcal{C}_B(H^u) M_B^2 g_B^2 + 2\mathcal{C}_{AB}(H^u) g_{AgB} M_{AB}^2 \right) \\
& \left. +2Q_A^{H^u} g_A^2 \mathcal{S}_A + 2Q_B^{H^u} g_B^2 \mathcal{S}_B \right] \\
\frac{d(\mathbf{m}_{H^u}^2)_{22}}{dt} &= \frac{1}{16\pi^2} \left[2\mathbf{h}_{322}^{SH} \mathbf{h}_{322}^{SH} + 2\mathbf{h}_{232}^{SH} \mathbf{h}_{232}^{SH} \right. \\
& +2(\mathbf{m}_{H^u}^2)_{22} \mathbf{Y}_{322}^{SH} \mathbf{Y}_{322}^{SH} + 2(\mathbf{m}_{H^u}^2)_{22} \mathbf{Y}_{232}^{SH} \mathbf{Y}_{232}^{SH} + 2(\mathbf{m}_{H^d}^2)_{22} \mathbf{Y}_{322}^{SH} \mathbf{Y}_{322}^{SH} \\
& +2(\mathbf{m}_S^2)_{33} \mathbf{Y}_{322}^{SH} \mathbf{Y}_{322}^{SH} + 2(\mathbf{m}_{H^d}^2)_{33} \mathbf{Y}_{232}^{SH} \mathbf{Y}_{232}^{SH} + 2(\mathbf{m}_S^2)_{22} \mathbf{Y}_{232}^{SH} \mathbf{Y}_{232}^{SH} \\
& -8 \left(\mathcal{C}_{2L}(H^u) M_{2L}^2 g_{2L}^2 + \mathcal{C}_A(H^u) M_{AgA}^2 + \mathcal{C}_B(H^u) M_B^2 g_B^2 + 2\mathcal{C}_{AB}(H^u) g_{AgB} M_{AB}^2 \right) \\
& \left. +2Q_A^{H^u} g_A^2 \mathcal{S}_A + 2Q_B^{H^u} g_B^2 \mathcal{S}_B \right] \\
\frac{d(\mathbf{m}_{H^u}^2)_{33}}{dt} &= \frac{1}{16\pi^2} \left[6\mathbf{h}_{333}^u \mathbf{h}_{333}^u + 2\mathbf{h}_{113}^{SH} \mathbf{h}_{113}^{SH} + 2\mathbf{h}_{223}^{SH} \mathbf{h}_{223}^{SH} + 2\mathbf{h}_{333}^{SH} \mathbf{h}_{333}^{SH} \right. \\
& +6(\mathbf{m}_{H^u}^2)_{33} \mathbf{Y}_{333}^u \mathbf{Y}_{333}^u + 2(\mathbf{m}_{H^u}^2)_{33} \mathbf{Y}_{113}^{SH} \mathbf{Y}_{113}^{SH} + 2(\mathbf{m}_{H^u}^2)_{33} \mathbf{Y}_{223}^{SH} \mathbf{Y}_{223}^{SH} \\
& +2(\mathbf{m}_{H^u}^2)_{33} \mathbf{Y}_{333}^{SH} \mathbf{Y}_{333}^{SH} + 6(\mathbf{m}_{u^c}^2)_{33} \mathbf{Y}_{333}^u \mathbf{Y}_{333}^u + 6(\mathbf{m}_{Q_L}^2)_{33} \mathbf{Y}_{333}^u \mathbf{Y}_{333}^u \\
& +2(\mathbf{m}_{H^d}^2)_{11} \mathbf{Y}_{113}^{SH} \mathbf{Y}_{113}^{SH} + 2(\mathbf{m}_S^2)_{11} \mathbf{Y}_{113}^{SH} \mathbf{Y}_{113}^{SH} + 2(\mathbf{m}_{H^d}^2)_{22} \mathbf{Y}_{223}^{SH} \mathbf{Y}_{223}^{SH} \\
& +2(\mathbf{m}_S^2)_{22} \mathbf{Y}_{223}^{SH} \mathbf{Y}_{223}^{SH} + 2(\mathbf{m}_{H^d}^2)_{33} \mathbf{Y}_{333}^{SH} \mathbf{Y}_{333}^{SH} + 2(\mathbf{m}_S^2)_{33} \mathbf{Y}_{333}^{SH} \mathbf{Y}_{333}^{SH} \\
& -8 \left(\mathcal{C}_{2L}(H^u) M_{2L}^2 g_{2L}^2 + \mathcal{C}_A(H^u) M_{AgA}^2 + \mathcal{C}_B(H^u) M_B^2 g_B^2 + 2\mathcal{C}_{AB}(H^u) g_{AgB} M_{AB}^2 \right) \\
& \left. +2Q_A^{H^u} g_A^2 \mathcal{S}_A + 2Q_B^{H^u} g_B^2 \mathcal{S}_B \right] \\
\frac{d(\mathbf{m}_D^2)_{11}}{dt} &= \frac{1}{16\pi^2} \left[2\mathbf{h}_{111}^D \mathbf{h}_{111}^D + 2\mathbf{h}_{113}^{SD} \mathbf{h}_{113}^{SD} \right. \\
& +2(\mathbf{m}_D^2)_{11} \mathbf{Y}_{111}^D \mathbf{Y}_{111}^D + 2(\mathbf{m}_D^2)_{11} \mathbf{Y}_{113}^{SD} \mathbf{Y}_{113}^{SD} + 2(\mathbf{m}_{u^c}^2)_{11} \mathbf{Y}_{111}^D \mathbf{Y}_{111}^D \\
& +2(\mathbf{m}_{e^c}^2)_{11} \mathbf{Y}_{111}^D \mathbf{Y}_{111}^D + 2(\mathbf{m}_S^2)_{33} \mathbf{Y}_{113}^{SD} \mathbf{Y}_{113}^{SD} + 2(\mathbf{m}_{D^c}^2)_{11} \mathbf{Y}_{113}^{SD} \mathbf{Y}_{113}^{SD} \\
& -8 \left(\mathcal{C}_3(D) M_3^2 g_3^2 + \mathcal{C}_A(D) M_{AgA}^2 + \mathcal{C}_B(D) M_B^2 g_B^2 + 2\mathcal{C}_{AB}(D) g_{AgB} M_{AB}^2 \right) \\
& \left. +2Q_A^D g_A^2 \mathcal{S}_A + 2Q_B^D g_B^2 \mathcal{S}_B \right] \\
\frac{d(\mathbf{m}_D^2)_{22}}{dt} &= \frac{1}{16\pi^2} \left[2\mathbf{h}_{222}^D \mathbf{h}_{222}^D + 2\mathbf{h}_{223}^{SD} \mathbf{h}_{223}^{SD} \right. \\
& +2(\mathbf{m}_D^2)_{22} \mathbf{Y}_{222}^D \mathbf{Y}_{222}^D + 2(\mathbf{m}_D^2)_{22} \mathbf{Y}_{223}^{SD} \mathbf{Y}_{223}^{SD} + 2(\mathbf{m}_{u^c}^2)_{22} \mathbf{Y}_{222}^D \mathbf{Y}_{222}^D \\
& +2(\mathbf{m}_{e^c}^2)_{22} \mathbf{Y}_{222}^D \mathbf{Y}_{222}^D + 2(\mathbf{m}_S^2)_{33} \mathbf{Y}_{223}^{SD} \mathbf{Y}_{223}^{SD} + 2(\mathbf{m}_{D^c}^2)_{22} \mathbf{Y}_{223}^{SD} \mathbf{Y}_{223}^{SD} \\
& -8 \left(\mathcal{C}_3(D) M_3^2 g_3^2 + \mathcal{C}_A(D) M_{AgA}^2 + \mathcal{C}_B(D) M_B^2 g_B^2 + 2\mathcal{C}_{AB}(D) g_{AgB} M_{AB}^2 \right) \\
& \left. +2Q_A^D g_A^2 \mathcal{S}_A + 2Q_B^D g_B^2 \mathcal{S}_B \right] \\
\frac{d(\mathbf{m}_D^2)_{33}}{dt} &= \frac{1}{16\pi^2} \left[2\mathbf{h}_{333}^D \mathbf{h}_{333}^D + 2\mathbf{h}_{333}^{SD} \mathbf{h}_{333}^{SD} \right. \\
& \left. +2(\mathbf{m}_D^2)_{33} \mathbf{Y}_{333}^D \mathbf{Y}_{333}^D + 2(\mathbf{m}_D^2)_{33} \mathbf{Y}_{333}^{SD} \mathbf{Y}_{333}^{SD} + 2(\mathbf{m}_{u^c}^2)_{33} \mathbf{Y}_{333}^D \mathbf{Y}_{333}^D \right]
\end{aligned}$$

$$\begin{aligned}
& +2(\mathbf{m}_{e^c}^2)_{33} \mathbf{Y}_{333}^D \mathbf{Y}_{333}^D + 2(\mathbf{m}_S^2)_{33} \mathbf{Y}_{333}^{SD} \mathbf{Y}_{333}^{SD} + 2(\mathbf{m}_{D^c}^2)_{33} \mathbf{Y}_{333}^{SD} \mathbf{Y}_{333}^{SD} \\
& -8(\mathcal{C}_3(D)M_3^2 g_3^2 + \mathcal{C}_A(D)M_A^2 g_A^2 + \mathcal{C}_B(D)M_B^2 g_B^2 + 2\mathcal{C}_{AB}(D)g_A g_B M_{AB}^2) \\
& +2Q_A^D g_A^2 \mathcal{S}_A + 2Q_B^D g_B^2 \mathcal{S}_B \Big] \\
\frac{d(\mathbf{m}_{D^c}^2)_{11}}{dt} &= \frac{1}{16\pi^2} \Big[4\mathbf{h}_{111}^{Dc} \mathbf{h}_{111}^{Dc} + 2\mathbf{h}_{113}^{SD} \mathbf{h}_{113}^{SD} \\
& +4(\mathbf{m}_{D^c}^2)_{11} \mathbf{Y}_{111}^{Dc} \mathbf{Y}_{111}^{Dc} + 2(\mathbf{m}_{D^c}^2)_{11} \mathbf{Y}_{113}^{SD} \mathbf{Y}_{113}^{SD} + 4(\mathbf{m}_{Q_L}^2)_{11} \mathbf{Y}_{111}^{Dc} \mathbf{Y}_{111}^{Dc} \\
& +4(\mathbf{m}_{L_L}^2)_{11} \mathbf{Y}_{111}^{Dc} \mathbf{Y}_{111}^{Dc} + 2(\mathbf{m}_S^2)_{33} \mathbf{Y}_{113}^{SD} \mathbf{Y}_{113}^{SD} + 2(\mathbf{m}_D^2)_{11} \mathbf{Y}_{113}^{SD} \mathbf{Y}_{113}^{SD} \\
& -8(\mathcal{C}_3(D^c)M_3^2 g_3^2 + \mathcal{C}_A(D^c)M_A^2 g_A^2 + \mathcal{C}_B(D^c)M_B^2 g_B^2 + 2\mathcal{C}_{AB}(D^c)g_A g_B M_{AB}^2) \\
& +2Q_A^{Dc} g_A^2 \mathcal{S}_A + 2Q_B^{Dc} g_B^2 \mathcal{S}_B \Big] \\
\frac{d(\mathbf{m}_{D^c}^2)_{22}}{dt} &= \frac{1}{16\pi^2} \Big[4\mathbf{h}_{222}^{Dc} \mathbf{h}_{222}^{Dc} + 2\mathbf{h}_{223}^{SD} \mathbf{h}_{223}^{SD} \\
& +4(\mathbf{m}_{D^c}^2)_{22} \mathbf{Y}_{222}^{Dc} \mathbf{Y}_{222}^{Dc} + 2(\mathbf{m}_{D^c}^2)_{22} \mathbf{Y}_{223}^{SD} \mathbf{Y}_{223}^{SD} + 4(\mathbf{m}_{Q_L}^2)_{22} \mathbf{Y}_{222}^{Dc} \mathbf{Y}_{222}^{Dc} \\
& +4(\mathbf{m}_{L_L}^2)_{22} \mathbf{Y}_{222}^{Dc} \mathbf{Y}_{222}^{Dc} + 2(\mathbf{m}_S^2)_{33} \mathbf{Y}_{223}^{SD} \mathbf{Y}_{223}^{SD} + 2(\mathbf{m}_D^2)_{22} \mathbf{Y}_{223}^{SD} \mathbf{Y}_{223}^{SD} \\
& -8(\mathcal{C}_3(D^c)M_3^2 g_3^2 + \mathcal{C}_A(D^c)M_A^2 g_A^2 + \mathcal{C}_B(D^c)M_B^2 g_B^2 + 2\mathcal{C}_{AB}(D^c)g_A g_B M_{AB}^2) \\
& +2Q_A^{Dc} g_A^2 \mathcal{S}_A + 2Q_B^{Dc} g_B^2 \mathcal{S}_B \Big] \\
\frac{d(\mathbf{m}_{D^c}^2)_{33}}{dt} &= \frac{1}{16\pi^2} \Big[4\mathbf{h}_{333}^{Dc} \mathbf{h}_{333}^{Dc} + 2\mathbf{h}_{333}^{SD} \mathbf{h}_{333}^{SD} \\
& +4(\mathbf{m}_{D^c}^2)_{33} \mathbf{Y}_{333}^{Dc} \mathbf{Y}_{333}^{Dc} + 2(\mathbf{m}_{D^c}^2)_{33} \mathbf{Y}_{333}^{SD} \mathbf{Y}_{333}^{SD} + 4(\mathbf{m}_{Q_L}^2)_{33} \mathbf{Y}_{333}^{Dc} \mathbf{Y}_{333}^{Dc} \\
& +4(\mathbf{m}_{L_L}^2)_{33} \mathbf{Y}_{333}^{Dc} \mathbf{Y}_{333}^{Dc} + 2(\mathbf{m}_S^2)_{33} \mathbf{Y}_{333}^{SD} \mathbf{Y}_{333}^{SD} + 2(\mathbf{m}_D^2)_{33} \mathbf{Y}_{333}^{SD} \mathbf{Y}_{333}^{SD} \\
& -8(\mathcal{C}_3(D^c)M_3^2 g_3^2 + \mathcal{C}_A(D^c)M_A^2 g_A^2 + \mathcal{C}_B(D^c)M_B^2 g_B^2 + 2\mathcal{C}_{AB}(D^c)g_A g_B M_{AB}^2) \\
& +2Q_A^{Dc} g_A^2 \mathcal{S}_A + 2Q_B^{Dc} g_B^2 \mathcal{S}_B \Big] \\
\frac{d(\mathbf{m}_S^2)_{11}}{dt} &= \frac{1}{16\pi^2} \Big[4\mathbf{h}_{131}^{SH} \mathbf{h}_{131}^{SH} + 4\mathbf{h}_{113}^{SH} \mathbf{h}_{113}^{SH} \\
& +4(\mathbf{m}_S^2)_{11} \mathbf{Y}_{131}^{SH} \mathbf{Y}_{131}^{SH} + 4(\mathbf{m}_S^2)_{11} \mathbf{Y}_{113}^{SH} \mathbf{Y}_{113}^{SH} + 4(\mathbf{m}_{H^u}^2)_{11} \mathbf{Y}_{131}^{SH} \mathbf{Y}_{131}^{SH} \\
& +4(\mathbf{m}_{H^d}^2)_{33} \mathbf{Y}_{131}^{SH} \mathbf{Y}_{131}^{SH} + 4(\mathbf{m}_{H^u}^2)_{33} \mathbf{Y}_{113}^{SH} \mathbf{Y}_{113}^{SH} + 4(\mathbf{m}_{H^d}^2)_{11} \mathbf{Y}_{113}^{SH} \mathbf{Y}_{113}^{SH} \\
& -8(\mathcal{C}_A(S)M_A^2 g_A^2 + \mathcal{C}_B(S)M_B^2 g_B^2 + 2\mathcal{C}_{AB}(S)g_A g_B M_{AB}^2) \\
& +2Q_A^S g_A^2 \mathcal{S}_A + 2Q_B^S g_B^2 \mathcal{S}_B \Big] \\
\frac{d(\mathbf{m}_S^2)_{22}}{dt} &= \frac{1}{16\pi^2} \Big[4\mathbf{h}_{232}^{SH} \mathbf{h}_{232}^{SH} + 4\mathbf{h}_{223}^{SH} \mathbf{h}_{223}^{SH} \\
& +4(\mathbf{m}_S^2)_{22} \mathbf{Y}_{232}^{SH} \mathbf{Y}_{232}^{SH} + 4(\mathbf{m}_S^2)_{22} \mathbf{Y}_{223}^{SH} \mathbf{Y}_{223}^{SH} + 4(\mathbf{m}_{H^u}^2)_{22} \mathbf{Y}_{232}^{SH} \mathbf{Y}_{232}^{SH} \\
& +4(\mathbf{m}_{H^d}^2)_{33} \mathbf{Y}_{232}^{SH} \mathbf{Y}_{232}^{SH} + 4(\mathbf{m}_{H^u}^2)_{33} \mathbf{Y}_{223}^{SH} \mathbf{Y}_{223}^{SH} + 4(\mathbf{m}_{H^d}^2)_{22} \mathbf{Y}_{223}^{SH} \mathbf{Y}_{223}^{SH} \\
& -8(\mathcal{C}_A(S)M_A^2 g_A^2 + \mathcal{C}_B(S)M_B^2 g_B^2 + 2\mathcal{C}_{AB}(S)g_A g_B M_{AB}^2) \\
& +2Q_A^S g_A^2 \mathcal{S}_A + 2Q_B^S g_B^2 \mathcal{S}_B \Big] \\
\frac{d(\mathbf{m}_S^2)_{33}}{dt} &= \frac{1}{16\pi^2} \Big[6\mathbf{h}_{113}^{SD} \mathbf{h}_{113}^{SD} + 6\mathbf{h}_{223}^{SD} \mathbf{h}_{223}^{SD} + 6\mathbf{h}_{333}^{SD} \mathbf{h}_{333}^{SD} + 4\mathbf{h}_{311}^{SH} \mathbf{h}_{311}^{SH} \\
& +4\mathbf{h}_{322}^{SH} \mathbf{h}_{322}^{SH} + 4\mathbf{h}_{333}^{SH} \mathbf{h}_{333}^{SH} \\
& +6(\mathbf{m}_S^2)_{33} \mathbf{Y}_{113}^{SD} \mathbf{Y}_{113}^{SD} + 6(\mathbf{m}_S^2)_{33} \mathbf{Y}_{223}^{SD} \mathbf{Y}_{223}^{SD} + 6(\mathbf{m}_S^2)_{33} \mathbf{Y}_{333}^{SD} \mathbf{Y}_{333}^{SD} \\
& +4(\mathbf{m}_S^2)_{33} \mathbf{Y}_{311}^{SH} \mathbf{Y}_{311}^{SH} + 4(\mathbf{m}_S^2)_{33} \mathbf{Y}_{322}^{SH} \mathbf{Y}_{322}^{SH} + 4(\mathbf{m}_S^2)_{33} \mathbf{Y}_{333}^{SH} \mathbf{Y}_{333}^{SH} \\
& +6(\mathbf{m}_{D^c}^2)_{11} \mathbf{Y}_{113}^{SD} \mathbf{Y}_{113}^{SD} + 6(\mathbf{m}_D^2)_{11} \mathbf{Y}_{113}^{SD} \mathbf{Y}_{113}^{SD} + 6(\mathbf{m}_{D^c}^2)_{22} \mathbf{Y}_{223}^{SD} \mathbf{Y}_{223}^{SD} \\
& +6(\mathbf{m}_D^2)_{22} \mathbf{Y}_{223}^{SD} \mathbf{Y}_{223}^{SD} + 6(\mathbf{m}_{D^c}^2)_{33} \mathbf{Y}_{333}^{SD} \mathbf{Y}_{333}^{SD} + 6(\mathbf{m}_D^2)_{33} \mathbf{Y}_{333}^{SD} \mathbf{Y}_{333}^{SD} \Big]
\end{aligned}$$

$$\begin{aligned}
& +4 \left(\mathbf{m}_{H^u}^2 \right)_{11} \mathbf{Y}_{311}^{SH} \mathbf{Y}_{311}^{SH} + 4 \left(\mathbf{m}_{H^d}^2 \right)_{11} \mathbf{Y}_{311}^{SH} \mathbf{Y}_{311}^{SH} + 4 \left(\mathbf{m}_{H^u}^2 \right)_{22} \mathbf{Y}_{322}^{SH} \mathbf{Y}_{322}^{SH} \\
& +4 \left(\mathbf{m}_{H^d}^2 \right)_{22} \mathbf{Y}_{322}^{SH} \mathbf{Y}_{322}^{SH} + 4 \left(\mathbf{m}_{H^u}^2 \right)_{33} \mathbf{Y}_{333}^{SH} \mathbf{Y}_{333}^{SH} + 4 \left(\mathbf{m}_{H^d}^2 \right)_{33} \mathbf{Y}_{333}^{SH} \mathbf{Y}_{333}^{SH} \\
& -8 \left(\mathcal{C}_A(S) M_{A^2}^2 g_A^2 + \mathcal{C}_B(S) M_{B^2}^2 g_B^2 + 2\mathcal{C}_{AB}(S) g_A g_B M_{AB}^2 \right) \\
& +2Q_A^S g_A^2 \mathcal{S}_A + 2Q_B^S g_B^2 \mathcal{S}_B \Big]
\end{aligned}$$

where the following abbreviations have been employed:

$$\begin{aligned}
\mathcal{S}_A & = 2Q_A \left(\mathbf{m}_{L^L}^2 \right)_{11}^{L^L} + 2Q_A \left(\mathbf{m}_{L^L}^2 \right)_{22}^{L^L} + 2Q_A \left(\mathbf{m}_{L^L}^2 \right)_{33}^{L^L} + 1Q_A \left(\mathbf{m}_{e^c}^2 \right)_{11}^{e^c} \\
& + 1Q_A \left(\mathbf{m}_{e^c}^2 \right)_{22}^{e^c} + 1Q_A \left(\mathbf{m}_{e^c}^2 \right)_{33}^{e^c} + 6Q_A \left(\mathbf{m}_{Q^L}^2 \right)_{11}^{Q^L} + 6Q_A \left(\mathbf{m}_{Q^L}^2 \right)_{22}^{Q^L} \\
& + 6Q_A \left(\mathbf{m}_{Q^L}^2 \right)_{33}^{Q^L} + 3Q_A \left(\mathbf{m}_{u^c}^2 \right)_{11}^{u^c} + 3Q_A \left(\mathbf{m}_{u^c}^2 \right)_{22}^{u^c} + 3Q_A \left(\mathbf{m}_{u^c}^2 \right)_{33}^{u^c} \\
& + 3Q_A \left(\mathbf{m}_{d^c}^2 \right)_{11}^{d^c} + 3Q_A \left(\mathbf{m}_{d^c}^2 \right)_{22}^{d^c} + 3Q_A \left(\mathbf{m}_{d^c}^2 \right)_{33}^{d^c} + 2Q_A \left(\mathbf{m}_{H^d}^2 \right)_{11}^{H^d} \\
& + 2Q_A \left(\mathbf{m}_{H^d}^2 \right)_{22}^{H^d} + 2Q_A \left(\mathbf{m}_{H^d}^2 \right)_{33}^{H^d} + 2Q_A \left(\mathbf{m}_{H^u}^2 \right)_{11}^{H^u} + 2Q_A \left(\mathbf{m}_{H^u}^2 \right)_{22}^{H^u} \\
& + 2Q_A \left(\mathbf{m}_{H^u}^2 \right)_{33}^{H^u} + 3Q_A \left(\mathbf{m}_D^2 \right)_{11}^D + 3Q_A \left(\mathbf{m}_D^2 \right)_{22}^D + 3Q_A \left(\mathbf{m}_D^2 \right)_{33}^D \\
& + 3Q_A \left(\mathbf{m}_{D^c}^2 \right)_{11}^{D^c} + 3Q_A \left(\mathbf{m}_{D^c}^2 \right)_{22}^{D^c} + 3Q_A \left(\mathbf{m}_{D^c}^2 \right)_{33}^{D^c} + 1Q_A \left(\mathbf{m}_S^2 \right)_{11}^S \\
& + 1Q_A \left(\mathbf{m}_S^2 \right)_{22}^S + 1Q_A \left(\mathbf{m}_S^2 \right)_{33}^S \\
\mathcal{S}_B & = 2Q_B \left(\mathbf{m}_{L^L}^2 \right)_{11}^{L^L} + 2Q_B \left(\mathbf{m}_{L^L}^2 \right)_{22}^{L^L} + 2Q_B \left(\mathbf{m}_{L^L}^2 \right)_{33}^{L^L} + 1Q_B \left(\mathbf{m}_{e^c}^2 \right)_{11}^{e^c} \\
& + 1Q_B \left(\mathbf{m}_{e^c}^2 \right)_{22}^{e^c} + 1Q_B \left(\mathbf{m}_{e^c}^2 \right)_{33}^{e^c} + 6Q_B \left(\mathbf{m}_{Q^L}^2 \right)_{11}^{Q^L} + 6Q_B \left(\mathbf{m}_{Q^L}^2 \right)_{22}^{Q^L} \\
& + 6Q_B \left(\mathbf{m}_{Q^L}^2 \right)_{33}^{Q^L} + 3Q_B \left(\mathbf{m}_{u^c}^2 \right)_{11}^{u^c} + 3Q_B \left(\mathbf{m}_{u^c}^2 \right)_{22}^{u^c} + 3Q_B \left(\mathbf{m}_{u^c}^2 \right)_{33}^{u^c} \\
& + 3Q_B \left(\mathbf{m}_{d^c}^2 \right)_{11}^{d^c} + 3Q_B \left(\mathbf{m}_{d^c}^2 \right)_{22}^{d^c} + 3Q_B \left(\mathbf{m}_{d^c}^2 \right)_{33}^{d^c} + 2Q_B \left(\mathbf{m}_{H^d}^2 \right)_{11}^{H^d} \\
& + 2Q_B \left(\mathbf{m}_{H^d}^2 \right)_{22}^{H^d} + 2Q_B \left(\mathbf{m}_{H^d}^2 \right)_{33}^{H^d} + 2Q_B \left(\mathbf{m}_{H^u}^2 \right)_{11}^{H^u} + 2Q_B \left(\mathbf{m}_{H^u}^2 \right)_{22}^{H^u} \\
& + 2Q_B \left(\mathbf{m}_{H^u}^2 \right)_{33}^{H^u} + 3Q_B \left(\mathbf{m}_D^2 \right)_{11}^D + 3Q_B \left(\mathbf{m}_D^2 \right)_{22}^D + 3Q_B \left(\mathbf{m}_D^2 \right)_{33}^D \\
& + 3Q_B \left(\mathbf{m}_{D^c}^2 \right)_{11}^{D^c} + 3Q_B \left(\mathbf{m}_{D^c}^2 \right)_{22}^{D^c} + 3Q_B \left(\mathbf{m}_{D^c}^2 \right)_{33}^{D^c} + 1Q_B \left(\mathbf{m}_S^2 \right)_{11}^S \\
& + 1Q_B \left(\mathbf{m}_S^2 \right)_{22}^S + 1Q_B \left(\mathbf{m}_S^2 \right)_{33}^S
\end{aligned}$$

Bibliography

- [1] S. L. Glashow, S. Weinberg, Phys. Rev. Lett. **20** (1968) 224-227. A. Salam, Conf. Proc. **C680519** (1968) 367-377.
- [2] M. Gell-Mann, Phys. Rev. **125** (1962) 1067-1084. H. Fritzsch, M. Gell-Mann, H. Leutwyler, Phys. Lett. **B47** (1973) 365-368.
- [3] P. W. Higgs, Phys. Rev. Lett. **13** (1964) 508-509. F. Englert, R. Brout, Phys. Rev. Lett. **13** (1964) 321-322.
- [4] E. Eichten and F. Feinberg, Phys. Rev. D **10** (1974) 3254. S. Dimopoulos and L. Susskind, Nucl. Phys. B **155** (1979) 237.
- [5] J. Wess and B. Zumino, Phys. Lett. B **49** (1974) 52. P. Fayet and J. Iliopoulos, Phys. Lett. B **51** (1974) 461.
- [6] N. Arkani-Hamed, S. Dimopoulos and G. Dvali, Phys. Today **55N2** (2002) 35.
- [7] C. T. Hill and E. H. Simmons, Phys. Rept. **381** (2003) 235 [Erratum-ibid. **390** (2004) 553] [arXiv:hep-ph/0203079]. F. Braam, M. Flossdorf, R. S. Chivukula, S. Di Chiara and E. H. Simmons, Phys. Rev. D **77** (2008) 055005 [arXiv:0711.1127 [hep-ph]].
- [8] J. Iliopoulos and B. Zumino, Nucl. Phys. B **76** (1974) 310.
- [9] Y. Shirman, arXiv:0907.0039 [hep-ph].
- [10] T. N. Sherry, IC/79/105.
- [11] M. Gell-Mann, P. Ramond and R. Slansky, Rev. Mod. Phys. **50** (1978) 721.
- [12] S. Heinemeyer, W. Hollik, G. Weiglein, Phys. Rept. **425** (2006) 265-368. [hep-ph/0412214].
- [13] H. Georgi, S. L. Glashow, Phys. Rev. Lett. **32** (1974) 438-441. H. Fritzsch, P. Minkowski, Annals Phys. **93** (1975) 193-266. H. Georgi, D. V. Nanopoulos, Nucl. Phys. **B159** (1979) 16. F. Gursev, P. Ramond, P. Sikivie, Phys. Lett. **B60** (1976) 177. F. Gursev, P. Sikivie, Phys. Rev. Lett. **36** (1976) 775. P. Ramond, Nucl. Phys. **B110** (1976) 214.
- [14] J. Terning, *Oxford, UK: Clarendon (2006) 324 p*
- [15] J. Wess, J. Bagger, *Princeton University Press (1992) 295 p*
- [16] M. Drees, R. Godbole and P. Roy, *Hackensack, USA: World Scientific (2004) 555 p*
- [17] S. Weinberg, Cambridge, UK: Univ. Pr. (2000) 419 p.
- [18] H. E. Haber, R. Hempfling, Phys. Rev. Lett. **66** (1991) 1815-1818. J. L. Lopez, D. V. Nanopoulos, Phys. Lett. **B266** (1991) 397-402.

- [19] J. C. Collins, “Renormalization,” *Cambridge University Press (1984)* 380 p.
- [20] R. Barbieri, G. R. Dvali and M. Moretti, *Phys. Lett. B* **312** (1993) 137.
- [21] P. Fayet, *Nucl. Phys.* **B90** (1975) 104-124.
- [22] S. A. Abel, *Nucl. Phys.* **B480** (1996) 55-72. [hep-ph/9609323].
- [23] M. E. Peskin and D. V. Schroeder, Reading, USA: Addison-Wesley (1995) 842 p
- [24] S. Y. Choi, H. E. Haber, J. Kalinowski and P. M. Zerwas, *Nucl. Phys. B* **778** (2007) 85 [hep-ph/0612218].
- [25] R. Slansky, *Phys. Rept.* **79** (1981) 1.
- [26] H. Georgi, *Front. Phys.* **54** (1982) 1.
- [27] W. Kilian and J. Reuter, “Unification without doublet-triplet splitting,” *Phys. Lett. B* **642**, 81 (2006) [arXiv:hep-ph/0606277].
- [28] R. Howl, S. F. King, *Phys. Lett.* **B652** (2007) 331-337. [arXiv:0705.0301 [hep-ph]].
- [29] F. Braam, J. Reuter and D. Wiesler, arXiv:0909.3081 [hep-ph].
- [30] J. C. Pati and A. Salam, *Phys. Rev. D* **10** (1974) 275 [Erratum-ibid. *D* **11** (1975) 703].
- [31] R. N. Mohapatra, G. Senjanovic, *Phys. Rev. Lett.* **44** (1980) 912.
- [32] M. D. Messier, eConfC **060409** (2006) 018 [hep-ex/0606013].
- [33] C. B. Dover, T. K. Gaisser, G. Steigman, *Phys. Rev. Lett.* **42** (1979) 1117. J. Kang, M. A. Luty, S. Nasri, *JHEP* **0809** (2008) 086. [hep-ph/0611322].
- [34] K. Griest and M. Sher, *Phys. Rev. D* **42** (1990) 3834.
- [35] F. Braam, A. Knochel and J. Reuter, *JHEP* **1006** (2010) 013 [arXiv:1001.4074 [hep-ph]].
- [36] P. Athron, S. F. King, R. Luo, D. J. Miller, S. Moretti and R. Nevzorov, arXiv:0909.4530 [hep-ph].
- [37] F. del Aguila, G. D. Coughlan and M. Quiros, *Nucl. Phys. B* **307** (1988) 633 [Erratum-ibid. *B* **312** (1989) 751].
- [38] F. Braam and J. Reuter, arXiv:1107.2806 [hep-ph], *to appear in EPJ C (in print)*.
- [39] K. Nakamura et al. (Particle Data Group), *J. Phys. G* **37**, 075021 (2010) and 2011 partial update for the 2012 edition.

- [40] S. Chatrchyan *et al.* [CMS Collaboration], *JHEP* **1105** (2011) 093 [arXiv:1103.0981 [hep-ex]].
- [41] J. R. Ellis, K. Enqvist, D. V. Nanopoulos, F. Zwirner, *Nucl. Phys.* **B276**, 14 (1986)
- [42] R. Sundrum, “Tasi 2004 lectures: To the fifth dimension and back,” [hep-th/0508134].
- [43] M. Quiros, [hep-ph/0606153]. T. Gherghetta, [arXiv:1008.2570 [hep-ph]]. T. Gherghetta, [hep-ph/0601213].
- [44] M. F. Sohnius, *Phys. Rept.* **128** (1985) 39-204. P. Fayet, *Nucl. Phys. B* **113** (1976) 135.
- [45] N. Marcus, A. Sagnotti and W. Siegel, *Nucl. Phys. B* **224**, 159 (1983); N. Arkani-Hamed, T. Gregoire, and J. G. Wacker, *JHEP* **03**, 055 (2002), [arXiv:hep-th/0101233]; A. Hebecker, *Nucl. Phys. B* **632**, 101 (2002) [arXiv:hep-ph/0112230];
- [46] G. Pólya, “Über die Analogie der Kristallsymmetrie in der Ebene”, *Zeitschrift für Kristallographie*, **60** (1924) 278.
- [47] A. Hebecker and M. Ratz, “Group-theoretical aspects of orbifold and conifold GUTs,” *Nucl. Phys. B* **670**, 3 (2003) [arXiv:hep-ph/0306049].
- [48] J. H. Conway, Cambridge Univ. Press, 1992
- [49] A. Love, W. A. Sabra and S. Thomas, *Nucl. Phys. B* **427** (1994) 181 [hep-th/9405198].
- [50] N. Arkani-Hamed, A. G. Cohen, H. Georgi, *Phys. Lett.* **B516** (2001) 395-402. [hep-th/0103135].
- [51] G. von Gersdorff and M. Quiros, *Phys. Rev. D* **68**, 105002 (2003) [arXiv:hep-th/0305024].
- [52] S. P. Martin and M. T. Vaughn, *Phys. Rev. D* **50**, 2282 (1994) [Erratum-ibid. *D* **78**, 039903 (2008)] [arXiv:hep-ph/9311340].
- [53] M. Drees, *Phys. Lett. B* **181** (1986) 279.
- [54] M. Dine, V. Kaplunovsky, M. L. Mangano, C. Nappi and N. Seiberg, *Nucl. Phys. B* **259** (1985) 549.
- [55] C. F. Kolda and S. P. Martin, *Phys. Rev. D* **53** (1996) 3871 [arXiv:hep-ph/9503445].
- [56] J. P. Saha, B. Misra, A. Kundu, *Phys. Rev.* **D81** (2010) 095011. [arXiv:1003.1384 [hep-ph]].

- [57] S. R. Coleman, E. J. Weinberg, *Phys. Rev.* **D7** (1973) 1888-1910.
- [58] T. Elliott, S. F. King, P. L. White, *Phys. Rev.* **D49** (1994) 2435-2456. [hep-ph/9308309].
- [59] S. W. Ham, T. Hur, P. Ko, S. K. Oh, *J. Phys. G* **G35** (2008) 095007. [arXiv:0801.2361 [hep-ph]].
- [60] [ALEPH and DELPHI and L3 and OPAL and SLD and LEP Electroweak Working Group and SLD Electroweak Group and SLD Heavy Flavour Group Collaborations], *Phys. Rept.* **427** (2006) 257-454. [hep-ex/0509008].
- [61] W. Porod, *Comput. Phys. Commun.* **153** (2003) 275-315. [hep-ph/0301101]. B. C. Allanach, *Comput. Phys. Commun.* **143** (2002) 305-331. [hep-ph/0104145]. C. Hugonie, G. Belanger, A. Pukhov, *JCAP* **0711** (2007) 009. [arXiv:0707.0628 [hep-ph]].
- [62] Wolfram Research, Inc., *Mathematica*, Version 7.0, Champaign, IL (2008).
- [63] N. Setzer, S. Spinner, *Phys. Rev.* **D71** (2005) 115010. [hep-ph/0503244].
- [64] M. Galassi et al, "GNU Scientific Library Reference Manual (3rd Ed.)", ISBN 0954612078.
- [65] W. Kilian, T. Ohl and J. Reuter, *Eur. Phys. J. C* **71** (2011) 1742 [arXiv:0708.4233 [hep-ph]]. M. Moretti, T. Ohl and J. Reuter, In *2nd ECFA/DESY Study 1998-2001* 1981-2009 [hep-ph/0102195].
- [66] J. A. Nelder, R. Mead, *Comput. J.* **7** (1965) 308-313.
- [67] S. Kirkpatrick, C. D. Gelatt, M. P. Vecchi, *Science* **220** (1983) 671-680.
- [68] T. D. Lee, C. -N. Yang, *Phys. Rev.* **87** (1952) 410-419.
- [69] G. P. Lepage, *J. Comput. Phys.* **27** (1978) 192.
- [70] O. Brein, *Comput. Phys. Commun.* **170** (2005) 42-48. [hep-ph/0407340].
- [71] J. Reuter, F. Braam, *AIP Conf. Proc.* **1200** (2010) 470-473. [arXiv:0909.3059 [hep-ph]]. J. M. Butterworth *et al.*, arXiv:1003.1643 [hep-ph].
- [72] N. D. Christensen and C. Duhr, *Comput. Phys. Commun.* **180** (2009) 1614 [arXiv:0806.4194 [hep-ph]].
- [73] N. D. Christensen, C. Duhr, B. Fuks, J. Reuter and C. Speckner, arXiv:1010.3251 [hep-ph].
- [74] M. S. Carena, M. Quiros and C. E. M. Wagner, *Nucl. Phys. B* **461** (1996) 407 [hep-ph/9508343].

-
- [75] J. P. Hall, S. F. King, R. Nevzorov, S. Pakvasa and M. Sher, arXiv:1012.5114 [hep-ph].
- [76] M. R. Whalley, D. Bourilkov and R. C. Group, hep-ph/0508110.
- [77] J. Pumplin, D. R. Stump, J. Huston, H. L. Lai, P. M. Nadolsky and W. K. Tung, JHEP **0207** (2002) 012 [hep-ph/0201195].
- [78] J. L. Rosner, Phys. Lett. B **221** (1989) 85.
- [79] T. P. Cheng and L. F. Li, Oxford, Uk: Clarendon (1984) 536 P. (Oxford Science Publications)
- [80] R. Cousins, J. Mumford and V. Valuev, CMS-NOTE-2005-022.
- [81] F. Braam, D. Wiesler, A. Knochel, J. Reuter, in preparation
- [82] T. Kaluza, In *O’Raifeartaigh, L.: The dawning of gauge theory* 53-58.

Danksagung

An dieser Stelle möchte ich mich herzlich bei allen bedanken, die mich während meiner Dissertation unterstützt haben. Insbesondere gilt mein Dank:

- Dr. Jürgen Reuter, für die freundliche Aufnahme in seine Arbeitsgruppe und die Betreuung der vorliegenden Arbeit.
- Prof. Dr. Jan Louis für die Begutachtung der Arbeit, sowie die Unterstützung bei der Vorbereitung der Verteidigung.
- Dr. Alexander Knochel und Daniel Wiesler, für die fruchtbare Zusammenarbeit, für die zahlreichen Diskussionen und Anregungen, sowie das Korrekturlesen dieser Arbeit.
- Meinen zum Teil ehemaligen Kollegen: Christoph Horst, Sebastian Schmidt, Felix Jörder und Anke Butenuth, für interessante Diskussionen und eine angenehme Arbeitsatmosphäre.
- Prof. Dr. Stefan Dittmaier und seiner gesamten Abteilung an der Universität Freiburg, für die freundliche Aufnahme nach dem Umzug der AG Reuter nach Hamburg. Insbesondere möchte ich Dr. Christian Speckner und Dr. Frank Siegert für die Unterstützung bei programmiertechnischen Problemen danken.
- Besonderer Dank gilt meiner Familie, meinem Freundeskreis und meiner Freundin, die mich in jeder Hinsicht in selbstverständlicher Weise unterstützen.